Mediators of Inflammation

Anti-Inflammatory Natural Products

Guest Editors: Yifu Yang, Lifei Hou, Abdelfattah El Ouaamari, and Lijun Xin

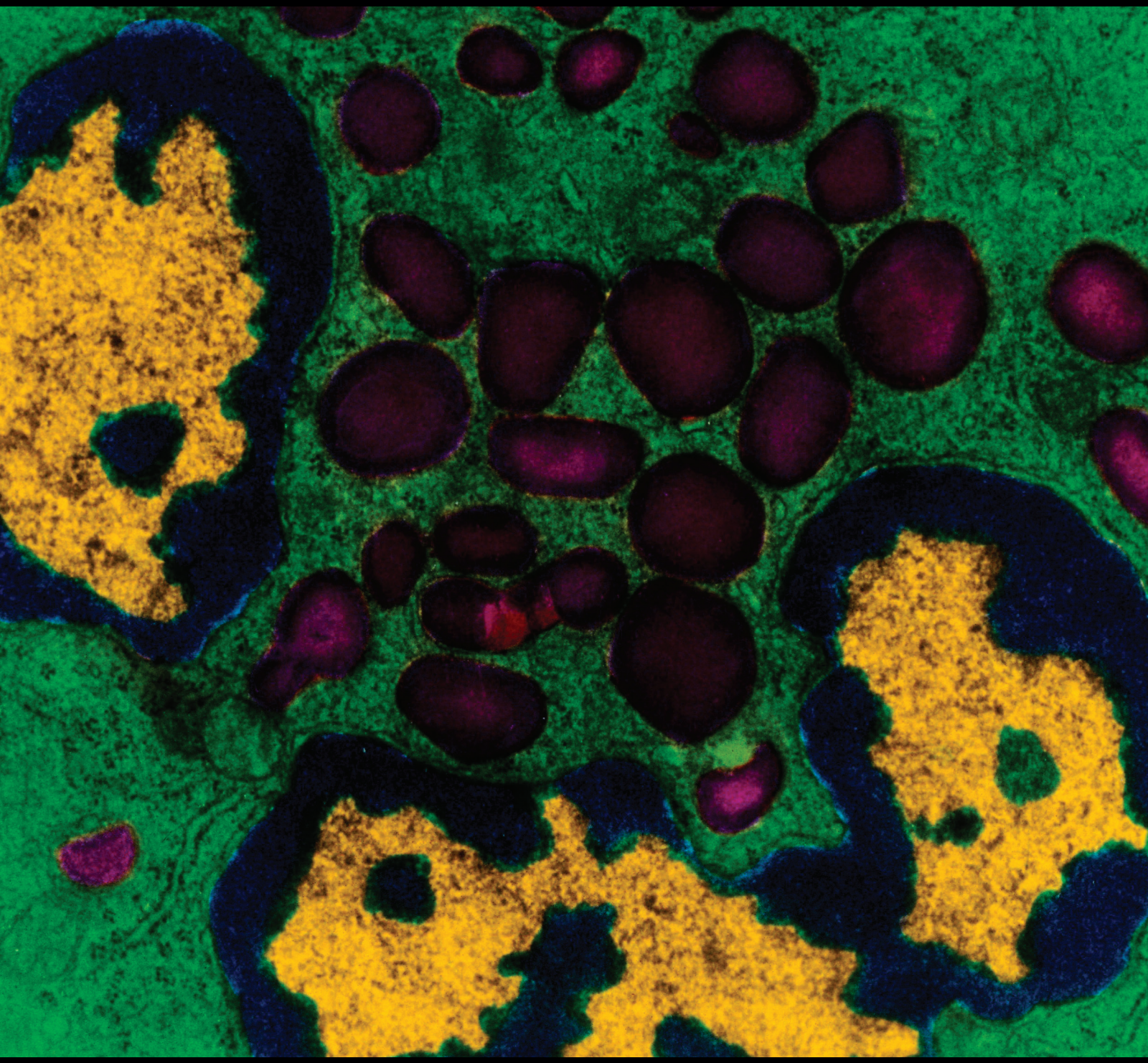

Anti-Inflammatory Natural Products

Anti-Inflammatory Natural Products

Guest Editors: Yifu Yang, Lifei Hou,
Abdelfattah El Ouaamari, and Lijun Xin

Editorial Board

Contents

Hindawi Publishing Corporation
Mediators of Inflammation
Volume 2015, Article ID 608613, 1 page
http://dx.doi.org/10.1155/2015/608613

Editorial

Anti-Inflammatory Natural Products

Yifu Yang,[1] Lifei Hou,[2] Abdelfattah El Ouaamari,[3] and Lijun Xin[4]

[1]*Laboratory of Immunology and Virology, Shanghai University of Traditional Chinese Medicine, Shanghai 201203, China*
[2]*Program in Cellular and Molecular Medicine, Boston Children's Hospital and Department of Pediatrics, Harvard Medical School, Boston, MA 02115, USA*
[3]*Joslin Diabetes Center, Harvard Medical School, Boston, MA 02115, USA*
[4]*Division of Infectious Diseases, Cincinnati Children's Hospital Medical Center, Cincinnati, OH 45229, USA*

Correspondence should be addressed to Yifu Yang; yangyifu@mail.shcnc.ac.cn

Received 22 March 2015; Accepted 22 March 2015

Inflammation is the first biological response of the immune system against infection or irritation. However, accumulating epidemiological and clinical study indicates that zealous acute inflammation or chronic inflammatory reaction is a significant risk factor to develop various human diseases. Controlling or modulating inflammation is therefore important to prevent or ameliorate certain diseases, such as organ transplantations, allergic diseases, and autoimmune diseases.

Natural products have played an important role throughout the world in treating and preventing human diseases for thousands of years, and, over the past few decades, great efforts have been made to explore modern preparations of natural products with higher efficacy and lower toxicity. Indeed, it is particularly impressive that most of the immunosuppressants are initially derived from natural products including mycophenolic acid (MPA), cyclosporin A (CsA), rapamycin, tacrolimus (FK506), and fingolimod (FTY720) (summarized in review [1]). In addition, several clinical trials carried out in the USA have already shown significant benefits of *T. wilfordii* extract in patients with rheumatoid arthritis (summarized in review [2]). Moreover, recent advances in chemistry and biology have introduced new technologies to synthesize or purify components from natural products and also improved the studies of the underlying mechanisms of action.

This special issue will introduce you to the valuable research reports on anti-inflammatory natural products, ranging from basic researches to exploring roles of natural products against inflammatory diseases. We hope this timely special issue will encourage the research and development of valuable natural products and finally lead to the development of novel therapeutic agents to provide better care to patients.

Yifu Yang
Lifei Hou
Abdelfattah El Ouaamari
Lijun Xin

References

[1] W. Tang and J. P. Zuo, "Immunosuppressant discovery from *Tripterygium wilfordii* Hook f: the novel triptolide analog (5R)-5-hydroxytriptolide (LLDT-8)," *Acta Pharmacologica Sinica*, vol. 33, no. 9, pp. 1112–1118, 2012.

[2] R. Graziose, M. A. Lila, and I. Raskin, "Merging traditional chinese medicine with modern drug discovery technologies to find novel drugs and functional foods," *Current Drug Discovery Technologies*, vol. 7, no. 1, pp. 2–12, 2010.

Hindawi Publishing Corporation
Mediators of Inflammation
Volume 2015, Article ID 380218, 11 pages
http://dx.doi.org/10.1155/2015/380218

Research Article

Punicalagin Induces Nrf2/HO-1 Expression via Upregulation of PI3K/AKT Pathway and Inhibits LPS-Induced Oxidative Stress in RAW264.7 Macrophages

Xiaolong Xu,[1] Hongquan Li,[2] Xiaolin Hou,[3] Deyin Li,[3] Shasha He,[1] Changrong Wan,[1] Peng Yin,[1] Mingjiang Liu,[1] Fenghua Liu,[3,4] and Jianqin Xu[1]

[1]*CAU-BUA TCVM Teaching and Researching Team, College of Veterinary Medicine, China Agricultural University (CAU), No. 2 West Yuanmingyuan Road, Beijing 100193, China*
[2]*College of Animal Science and Veterinary Medicine, Shanxi Agricultural University, Taigu, Shanxi 030801, China*
[3]*College of Animal Science and Technology, Beijing University of Agriculture (BUA), Beijing 102206, China*
[4]*Beijing Key Laboratory for Dairy Cow Nutrition, Beijing 102206, China*

Correspondence should be addressed to Fenghua Liu; liufenghua1209@126.com and Jianqin Xu; xujianqincau@126.com

Received 26 July 2014; Revised 12 October 2014; Accepted 17 October 2014

Academic Editor: Yi Fu Yang

Reactive oxygen species (ROS) and oxidative stress are thought to play a central role in potentiating macrophage activation, causing excessive inflammation, tissue damage, and sepsis. Recently, we have shown that punicalagin (PUN) exhibits anti-inflammatory activity in LPS-stimulated macrophages. However, the potential antioxidant effects of PUN in macrophages remain unclear. Revealing these effects will help understand the mechanism underlying its ability to inhibit excessive macrophage activation. Hemeoxygenase-1 (HO-1) exhibits antioxidant activity in macrophages. Therefore, we hypothesized that HO-1 is a potential target of PUN and tried to reveal its antioxidant mechanism. Here, PUN treatment increased HO-1 expression together with its upstream mediator nuclear factor-erythroid 2 p45-related factor 2 (Nrf2). However, specific inhibition of Nrf2 by brusatol (a specific Nrf2 inhibitor) dramatically blocked PUN-induced HO-1 expression. Previous research has demonstrated that the PI3K/Akt pathway plays a critical role in modulating Nrf2/HO-1 protein expression as an upstream signaling molecule. Here, LY294002, a specific PI3K/Akt inhibitor, suppressed PUN-induced HO-1 expression and led to ROS accumulation in macrophages. Furthermore, PUN inhibited LPS-induced oxidative stress in macrophages by reducing ROS and NO generation and increasing *superoxide dismutase (SOD) 1* mRNA expression. These findings provide new perspectives for novel therapeutic approaches using antioxidant medicines and compounds against oxidative stress and excessive inflammatory diseases including tissue damage, sepsis, and endotoxemic shock.

1. Introduction

Reactive oxygen species (ROS) play a vital role in LPS-triggered macrophage activation by regulating intracellular reduction-oxidation (redox) sensitive signaling pathways and nuclear transcription factors, such as nuclear factor-κB (NF-κB) and nuclear factor-erythroid 2 p45-related factor 2 (Nrf2) [1–3]. Overproduction of ROS in macrophages leads to excessive expression of cytokines and inflammatory factors, resulting in atheromatous plaques, acute inflammation, tissue injury, and sepsis [4]. However, most cell types have developed defensive mechanisms to counteract ROS generation [5, 6]. Hemeoxygenase-1 (HO-1), a member of the intracellular phase II enzyme family, is thought to play an essential role in maintaining cellular redox homeostasis against ROS generation and oxidative stress [7, 8]. HO-1, which is expressed in cells at a low level without stimulation, can be rapidly induced by various oxidative-inducing agents, including LPS [9], heme [10], hypoxia, and subsequent lethality [11]. In oxidative stress and inflammation conditions, enhancement of HO-1 expression plays an important role in cell protection [9, 11]. This important cytoprotective action in

response to various cellular stimuli makes it conceivable to target HO-1 induction as a promising therapeutic intervention in treating a variety of disorders related to oxidative stress and inflammation. Nrf2, an upstream transcription factor modulating phase II enzyme activity, interacts with the antioxidant response element (ARE) in the nucleus to induce ARE-dependent gene expression. Under physiological conditions, Nrf2 is sequestered by binding to Kelch-like ECH-associated protein 1 (Keap1). Upon oxidative stress, Nrf2 parts from Keap1 and translocates into the nucleus to induce the expression of HO-1 [12]. Suppression of Nrf2 by the specific Nrf2 inhibitor, brusatol, has been reported to attenuate the Nrf2-mediated defense mechanism and weaken its antioxidant ability, indicating the importance of Nrf2 in antioxidant activity [13].

Previous studies have suggested that phosphatidylinositol 3-kinase (PI3K)/Akt is a key survival signaling pathway that enhances cellular defense, making it a potential treatment target not only by promoting cell survival, but also by modulating Nrf2 as an upstream signaling molecule [14–17]. Crosstalk between the PI3K/Akt and Nrf2 signaling pathways has been reported to govern the cellular defense system against inflammatory and oxidative damages [14]. LY294002, a specific PI3K/Akt inhibitor, could significantly attenuate the PI3K/Akt-mediated cell defense mechanism by suppressing phosphorylation of Akt and thus inhibiting activation of Nrf2/HO-1 expression [18]. Therefore, the PI3K/Akt pathway plays a vital role in the Nrf2-mediated antioxidant response, making it a potential target for medical intervention.

Many polyphenols that scavenge free radicals have been identified and proposed as therapeutic agents to counteract oxidative stress-induced diseases [19]. Recently, pomegranate extract, composed of abundant tannins, has been reported to exhibit antioxidant, anti-inflammation, and lipase inhibitory activities [20–23]. Punicalagin (2,3-hexahydroxydiphenoyl-gallagyl-D-glucose; PUN) is the major polyphenol isolated from pomegranate (*Punica granatum L.*), but few studies have been carried out focusing on its bioactivities. Our previous research has shown that PUN inhibits LPS-induced mitogen-activated protein kinases (MAPKs) and NF-κB activation and thus suppresses overproduction of cytokines and inflammatory factors, including nitric oxide (NO), prostaglandin E2 (PGE2), interleukin- (IL-) 1β, IL-6, and tumor necrosis factor- (TNF-) α [24]. However, the antioxidant activity and mechanisms of PUN in macrophages remain unknown.

In this study, we investigated the PUN modulation of the Nrf2/HO-1 antioxidant signaling. Furthermore, we tried to uncover the molecular mechanism by which the PI3K/Akt pathway regulates the PUN-induced Nrf2/HO-1 activation and antioxidant activity. Moreover, we tried to reveal the underlying defense mechanism of PUN in LPS-stimulated macrophage oxidative stress.

2. Materials and Methods

2.1. Reagents. PUN (>98% HPLC purity) and brusatol were purchased from Tauto Biotech (Shanghai, China). LPS (*Escherichia coli* 055:B5) and insulin were purchased from Sigma-Aldrich Chemical (St. Louis, MO, USA). Fetal bovine serum (FBS), antibiotic-antimycotic, and TRIzol reagent were purchased from Gibco (Grand Island, NY, USA). Bicinchoninic acid (BCA) protein assay kit was purchased from Pierce (Rockford, IL, USA). Antibodies against GAPDH, Akt, p-Akt, Keap1, Nrf2 and HO-1, and LY294002 were purchased from Cell Signaling Technology (Danvers, MA, USA). The goat anti-mouse antibody was purchased from Li-cdr Odyssey (Lincoln, NE, USA). The probe, 2′,7′-dichlorodihydrofluorescein diacetate ($DCFH_2$-DA), was purchased from Invitrogen (Carlsbad, CA, USA). The nitrate assay kit was purchased from Beyotime (Haimen, China).

2.2. Cell Line. RAW264.7 cells were purchased from the American Type Culture Collection (Rockville, MD, USA). Cells were cultured in DMEM medium supplemented with 10% FBS and antibiotics (100 U/mL penicillin and 100 U/mL streptomycin) at 37°C in a humidified incubator with 5% CO_2.

2.3. NO Assay. The nitrite accumulated in the culture medium was measured as an indicator of NO production based on the Griess reaction. RAW264.7 cells, cultured in 96-well plates for 24 h, were treated with or without LPS (1 μg/mL) in the presence of various doses of PUN (25, 50, or 100 μM, 1 h prior to LPS treatment). After 24 h, culture supernatants were mixed with Griess reagent (equal volumes of 1% (w/v) sulfanilamide in 5% (v/v) phosphoric acid and 0.1% (w/v) naphthylethylenediamine-HCL) and incubated at room temperature for 10 min. Absorbance values were measured at 550 nm and NO concentration was calculated with reference to a standard curve of sodium nitrite.

2.4. Measurement of ROS Production. ROS production was detected by measuring intracellular ROS formation using the $DCFH_2$-DA probe. Briefly, RAW264.7 cells, cultured in 24-well plates for 24 h before the experiment, were pretreated with PUN (100 μM) for 1 h and then stimulated with LPS (1 μg/mL) for 12 h to induce ROS production. Cells were washed twice with PBS and then incubated with $DCFH_2$-DA probe (20 nM) for 15 min. Fluorescence staining was visualized using a fluorescence microscope (Olympus, IX71), and fluorescence assays were measured with a fluorescence microplate reader (Tecan, Sunrise) at excitation/emission 525/610 nm.

2.5. Western Blotting Analysis. RAW264.7 cells (1×10^6) cultured in tissue culture flasks for 24 h were treated with the desired agents. Cells were then harvested on ice, washed twice with ice-cold PBS, and suspended in 500 μL of lysis buffer supplemented with protease inhibitors (JianCheng, Nanjing, China). After 30 min incubation on ice, cell extracts were subjected to centrifugation (12,000 ×g) at 4°C for 15 min to get cell protein. Protein quantification was performed with a BCA protein assay kit. Proteins were separated by SDS-PAGE, electrotransferred to nitrocellulose membranes (Pierce), and then hybridized with the specific antibodies. Blots were normalized against GAPDH to correct for differences in protein loading. Densitometric values of immunoblot signals

were obtained from three separate experiments using Image J (National Institutes of Health, Bethesda, MD, USA).

2.6. Quantitative RT-PCR Analysis. RAW264.7 cells were preincubated in 6-well plates (1×10^6) and pretreated with PUN (25, 50, or 100 μM) 1 h prior to 1 μg/mL LPS treatment for 12 h in a 37°C and 5% CO_2 incubator. Total RNA was extracted using TRIzol reagent. The concentration and integrity of the RNA were measured at a 260/280 nm ratio. Quantitative PCR analysis was carried out using the DNA Engine Mx3000P fluorescence detection system (Agilent, Santa Clara, CA, USA) against a double-stranded DNA-specific fluorescent dye (Stratagene, La Jolla, CA, USA) according to optimized PCR protocols. *β-Actin* was amplified in parallel with the target genes and used as a normalization control. The PCR conditions were as follows: 95°C for 3 min, followed by 40 cycles of 95°C for 10 s, 60°C for 20 s, and 72°C for 60 s. Expression levels were determined using the relative threshold cycle (CT) method as described by the manufacturer (Stratagene). The PCR reaction system (25 μL in total) contained 12.5 μL of SYBR Green PCR mix (Stratagene), 0.375 μL of reference dye, 1 μL of each primer (both 10 μM), 1 μL of cDNA template, and 9.125 μL of DEPC-treated water. Quantitative real-time RT-PCR was performed using the following primers: *β-actin*, F: 5′-CCCATCTATGAGGGTTACGC-3′, R: 5′-TTTAATGTCACGCACGATTT C-3′; *SOD1*, F: 5′-CCACGTCCATCAGTATGGGG-3′, R: 5′-CGTCCTTTCCAGCAGTCACA-3′; *SOD2*, F: 5′-GTGTCTGTGGGAGTCCAAGG-3′, R: 5′-CCCCAGTCATAGTGCTGCAA-3′; *HO-1*, F: 5′-CACGCATATACCCGCTACCT-3′, R: 5′-CCAGAGTGTTCATTCGAGCA-3′; *Nrf2*, F: 5′-AACAGAACGGCCCTAAAGCA-3′, R: 5′-TGGGATTCACGCATAGGAGC-3′.

3. Statistical Analysis

The results were expressed as mean ± SEM and differences between mean values of normally distributed data were assessed by the one-way analysis of variance (ANOVA) followed by Duncan's test for multiple comparisons. P value of 0.05 or 0.01 was considered statistically significant.

4. Results

4.1. PUN Increases Nrf2/HO-1 Expression in RAW264.7 Cells. HO-1 expression was measured to determine whether PUN exhibits potential antioxidant activity by upregulating the intracellular phase II enzyme, HO-1, in RAW264.7 cells. Western blot analysis was performed to detect the expression of HO-1 induced by different concentrations of PUN and as a function of time. The results showed that PUN started to significantly increase HO-1 protein levels from 6 h in a time-dependent manner (Figure 1(a)). Furthermore, PUN enhanced HO-1 protein levels at doses of 50 to 200 μM in a dose-dependent manner (Figure 1(b)). To further characterize the molecular mechanism of PUN activity, Nrf2, a vital upstream signaling mediator of HO-1, was examined by Western blot analysis. The data demonstrated that 100 μM PUN treatment significantly increased Nrf2 expression from 4 h to 8 h in a time-dependent manner (Figure 1(c)). Also, an 8 h treatment with 50 to 200 μM PUN increased Nrf2 expression in a dose-dependent manner (Figure 1(d)). Keap1 functions as a suppressor of Nrf2 by retaining it in the cytoplasm and enhancing its proteasomal degradation via ubiquitination. Keap1 deficiency leads to Nrf2 isolation and translocation into the nucleus. However, in our study PUN treatment also increased Keap1 accumulation from 4 h to 12 h (100 μM) and at doses of 50 to 200 μM (8 h) (Figures 1(c) and 1(d)). RT-PCR results also showed that PUN could significantly increase the Nrf2 and HO-1 mRNA expression since 4 h treatment. However, we found that 24 h treatment still showed an enhancement in Nrf2 mRNA expression but not in Nrf2 protein expression, indicating that the inhibition effect of PUN on Keap1-Nrf2 could not last more than 24 h (Figure 1S available online at http://dx.doi.org/10.1155/2015/380218). Thus, we speculated that PUN increased Nrf2 accumulation and activation by inhibiting Keap1 ubiquitination of Nrf2 and/or the physical interaction, thereby preventing Nrf2 from being degraded. In the 12 h PUN treatment group, the Keap1 level significantly increased, while the Nrf2 level notably decreased, suggesting that the inhibitory effect of PUN (100 μM) on the Keap1-Nrf2 ubiquitination sustained no longer than 12 h, as Keap1 rapidly accumulated and degraded Nrf2 protein, keeping Nrf2 at a low concentration. Brusatol is a specific Nrf2 inhibitor, suppressing its translocation and preventing it from inducing ARE-mediated antioxidant genes, including *HO-1*. We used brusatol to block Nrf2 activity and found that the PUN-induced HO-1 accumulation was significantly attenuated (Figure 2), suggesting that PUN induced HO-1 upregulation via Nrf2-mediated signaling.

4.2. PI3K/Akt Regulates PUN-Induced HO-1 Expression in RAW264.7 Cells. Recent studies have demonstrated that the PI3K/Akt pathway acts as an important upstream regulator of HO-1 expression [25]; thus we investigated whether the PI3K/Akt pathway also plays a central role in the PUN-induced HO-1 expression. Western blot analysis showed that PUN treatment notably enhanced Akt phosphorylation after 2 h of treatment in a time-dependent manner, but not the total Akt protein level, suggesting that the PUN-induced HO-1 expression may be associated with the PI3K/Akt signaling pathway (Figure 3(a)). To further reveal the mechanism, we used LY294002, a specific PI3K/Akt inhibitor. The results showed that PUN treatment significantly increased HO-1 expression; however, inhibiting Akt phosphorylation by LY294002 significantly attenuated the PUN-induced HO-1 activation (Figure 3(b)). Therefore, we concluded that PI3K/Akt is essential for the PUN antioxidant activity by regulating PUN-induced HO-1 expression. LPS treatment triggers ROS generation in macrophages, so we used LPS to determine whether PI3K/Akt signaling regulates the ROS scavenging property of PUN. As expected, both fluorescence staining and assay values demonstrated that the PI3K/Akt pathway regulates the ability of PUN to scavenge ROS (Figure 4), which is in accordance with its effect on HO-1 expression.

4.3. Nrf2 Is Essential for PI3K/Akt-Mediated HO-1 Expression in PUN-Treated RAW264.7 Cells. The results showed that

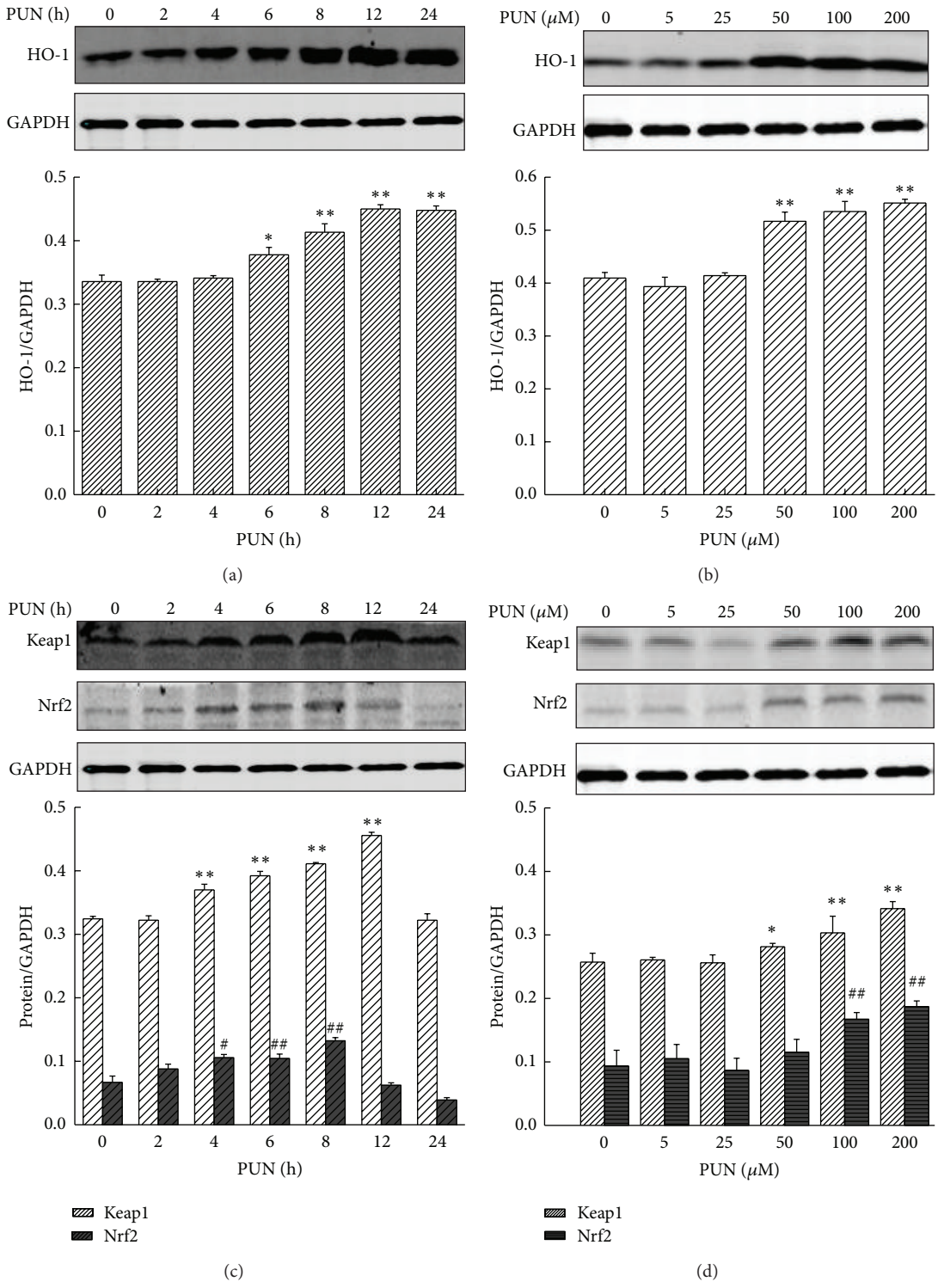

Figure 1: PUN increases Nrf2/HO-1 expression in RAW264.7 cells in time-dependent manner and dose-dependent manner. Cells were incubated at 37°C in a humidified incubator with 5% CO_2. (a) RAW264.7 cells were treated with 100 μM PUN for indicated durations (0, 2, 4, 6, 8, 12, and 24 h). The HO-1 protein expression was analyzed by Western blotting. (b) RAW264.7 cells were treated for 8 h with PUN at the indicated concerntrations (0, 5, 25, 50, 100, and 200 μM). The HO-1 protein expression was analyzed by Western blotting. (c) RAW264.7 cells were treated with 100 μM PUN for indicated durations (0, 2, 4, 6, 8, 12, and 24 h). The Nrf2 and Keap1 protein expression were analyzed by Western blotting. (d) RAW264.7 cells were treated for 8 h with PUN at the indicated concerntrations (0, 5, 25, 50, 100, and 200 μM). The Nrf2 and Keap1 protein expression were analyzed by Western blotting. Data represent the mean ± SEM of three independent experiments and differences between mean values were assessed by one-way ANOVA. $^{*}P < 0.05$, $^{**}P < 0.01$, $^{\#}P < 0.05$, and $^{\#\#}P < 0.01$ indicate significant differences compared with the control group of indicated proteins, respectively.

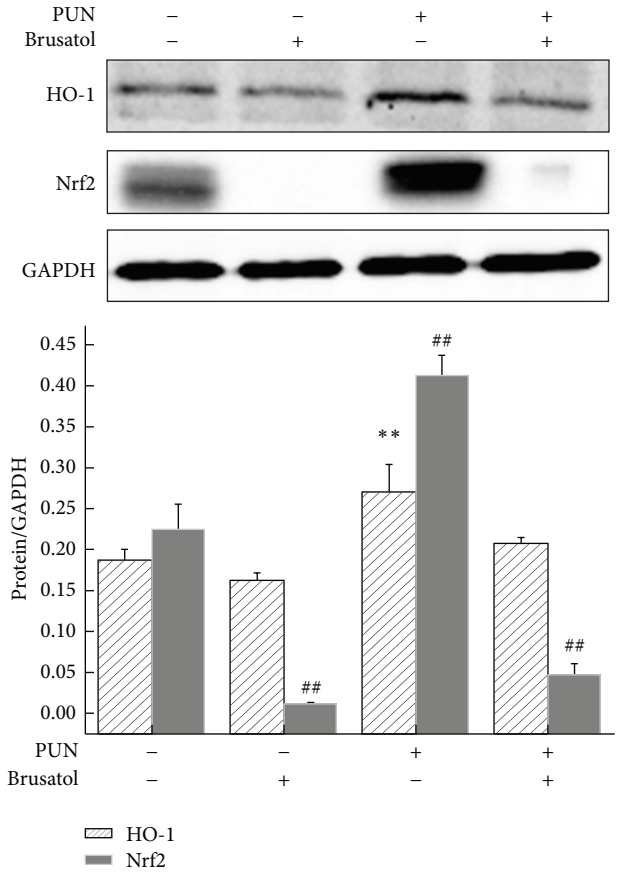

Figure 2: Inhibition of Nrf2 suppresses PUN induced HO-1 protein expression in RAW264.7 cells. Cells were treated for 8 h with 100 μM PUN in the presence or absence of 20 nM brusatol at 37°C in a humidified incubator with 5% CO_2. The HO-1 and Nrf2 protein expression were analyzed by Western blotting. Data represent the mean ± SEM of three independent experiments and differences between mean values were assessed by one-way ANOVA. $^{**}P < 0.01$ and $^{\#\#}P < 0.01$ indicate significant differences compared with the control group.

LY294002 inhibited the PUN-induced activation of Nrf2 (Figure 3(b)), indicating that Nrf2 may be a vital molecule in the PI3K/Akt-mediated HO-1 expression in PUN-treated cells. To further understand this mechanism, brusatol was used to suppress the Nrf2-mediated signaling pathway in the presence of PI3K/Akt mediators. We found that upregulation (insulin) or downregulation (LY294002) of PI3K/Akt in presence of PUN did not show a significant modulation effect on HO-1 expression when Nrf2 was blocked (Figure 5), indicating that Nrf2 plays a central role in the PI3K/Akt-regulated HO-1 expression in PUN-treated cells. Hence, we concluded that Nrf2 is downstream PI3K/Akt, but upstream HO-1 in the PUN-regulated antioxidant signaling pathway.

4.4. PUN Inhibits LPS-Induced Oxidative Stress in RAW264.7 Cells. When stimulated with LPS, the intracellular ROS level in macrophages increased rapidly, causing oxidative stress. We then tried to evaluate the antioxidant activity of PUN by examining ROS generation and *SOD1*/*SOD2* mRNA expression. LPS stimulation significantly increased the ROS level in macrophages, but pretreatment with PUN notably prevented the LPS-induced ROS generation. As a well-established ROS scavenger, N-acetyl cysteine (NAC) treatment also showed a significant inhibitory effect on the LPS-induced ROS overproduction. The inhibitory effect of 200 μM PUN and 50 μM NAC treatment was comparable (Figures 6(a) and 6(b)). RT-PCR analysis showed that LPS significantly reduced *SOD1* mRNA expression and enhanced *SOD2* mRNA expression. PUN pretreatment significantly reversed the reduction in *SOD1* mRNA caused by LPS but showed no effect on *SOD2* mRNA expression (Figure 6(c)). NO is another important free radical molecule and proinflammatory factor in LPS-stimulated macrophages. Because we revealed that the PI3K/Akt pathway is essential for PUN to scavenge intracellular ROS, we examined the role of PI3K/Akt in the reduction of NO production in PUN-treated cells. The results showed that PUN pretreatment notably decreased the LPS-induced NO overexpression in macrophages; however, upregulation or downregulation of PI3K/Akt did not affect the PUN-induced reduction in NO, suggesting that PUN inhibited the LPS-induced NO expression via another signaling pathway Figure 6(d).

5. Discussion

Pomegranate extracts have been reported to have many beneficial health effects, exhibiting antioxidant,

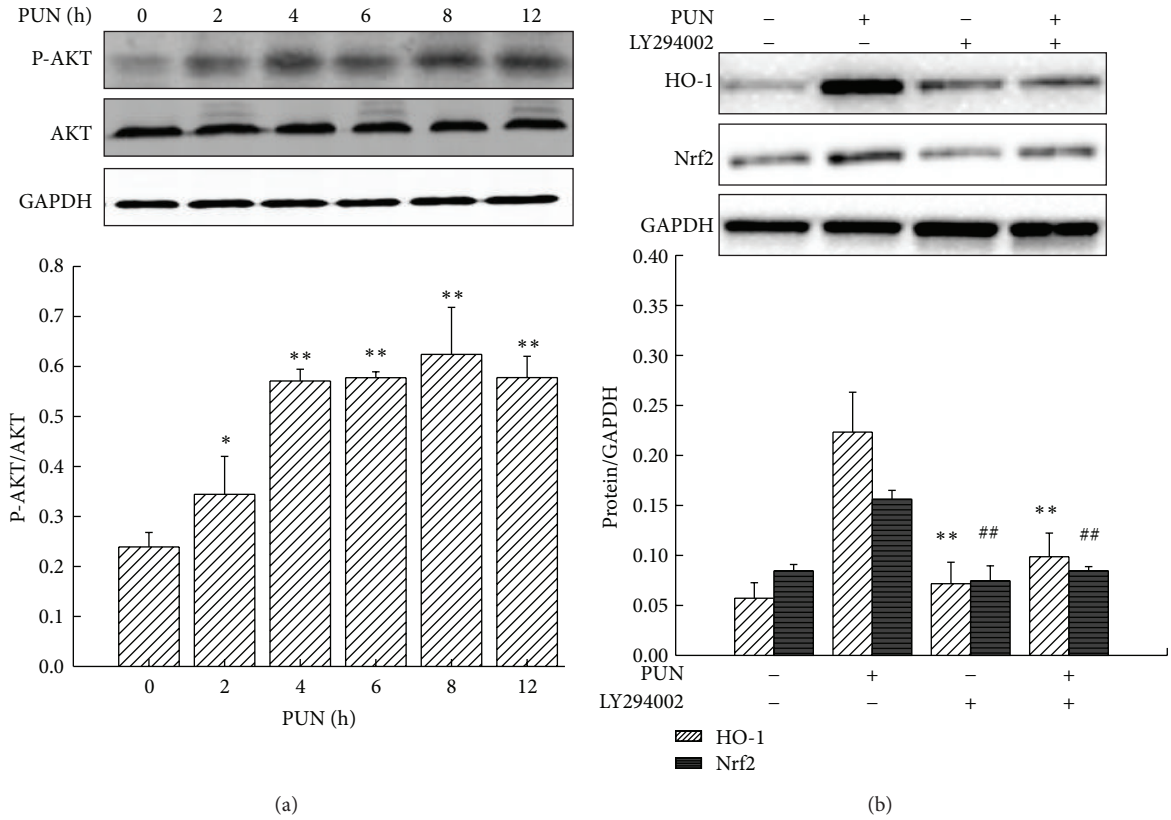

(a) (b)

Figure 3: PUN induced HO-1 protein expression via PI3K/Akt pathway. Cells were incubated at 37°C in a humidified incubator with 5% CO_2. (a) RAW264.7 cells were treated with 100 μM PUN for indicated durations (0, 2, 4, 6, 8, and 12 h). The Akt protein and Akt phosphorylation level were analyzed by Western blotting. (b) RAW264.7 cells were treated for 8 h with 100 μM PUN in the presence or absence of 20 μM LY294002. The HO-1 and Nrf2 proteins expression were analyzed by Western blotting. Data represent the mean ± SEM of three independent experiments and differences between mean values were assessed by one-way ANOVA. $^{**}P < 0.01$ and $^{\#\#}P < 0.01$ indicate significant differences compared with the PUN-treated group of indicated proteins, respectively.

anti-inflammation, antiproliferative, and DNA repair activities, which are generally attributed to the high polyphenol content [26–28]. The pomegranate husk is rich in polyphenols such as punicalagin (PUN), punicalin, gallagic acid, ellagic acid, and EA-glycosides [29]. PUN is a hydrolysable polyphenol in which gallagic acids are linked to a sugar moiety with a molecular weight of 1084 [30]. Previous studies have shown that PUN composes 85% of the total pomegranate tannins and accounts for more than 50% of the antioxidant activity of pomegranate juice [29, 31]. An increasing number of studies indicated that the bioactivities of pomegranate extracts are associated with PUN [32, 33]. Our recent study has demonstrates that PUN inhibits LPS-induced inflammatory factors and cytokine overexpression, including NO, PGE2, IL-1β, IL-6, and TNF-α, via suppression of toll-like receptor 4-mediated MAPKs and NF-κB activation in macrophages, which may contribute to the inhibition effect of pomegranate on inflammation [24]. Oxidative stress caused by LPS or other stimuli may trigger the activation of macrophages, leading to an excessive inflammatory process. However, as a polyphenol possessing most of the pomegranate's antioxidant activity, only limited studies have been carried out on the antioxidant property of PUN and its underlying mechanism in macrophages.

HO-1 can be stimulated by a variety of factors, including heme, hyperoxia, and ROS in most cell types, and studies have revealed that upregulation of HO-1 contributes to the cellular defense mechanism in response to stimuli [34]. LPS challenge rapidly increases the ROS level in macrophages, not only directly damaging DNA, but also inducing overproduction of inflammatory factors as well as cytokines, which may lead to severe tissue injury [35]. Macrophages are essential for recognizing and eliminating microbial pathogens, and thus the survival of macrophages may directly contribute to the host defense system. Furthermore, counteracting the overproduction of ROS is crucial for inhibiting excessive inflammation. Therefore, HO-1, which is important for protecting macrophages from ROS, has recently become a popular target for antioxidant medicine development [36–38]. The present study showed that PUN treatment markedly increased HO-1 protein level in macrophages in a time- and dose-dependent manner, indicating that PUN exhibited antioxidant activity by upregulating HO-1 expression.

Nrf2 is known as an upstream mediator of ARE-dependent phase II enzyme expression, including HO-1 [39–41]. Under quiescent conditions, Nrf2 is anchored in the inactive form to the cytoplasm through binding to Keap1, which in turn facilitates the ubiquitination and subsequent

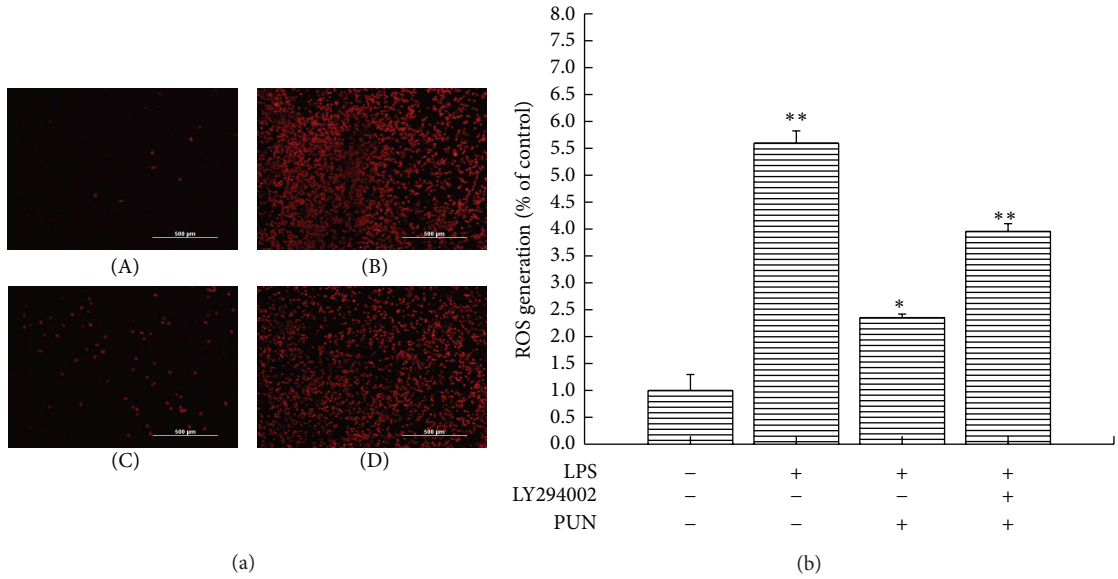

Figure 4: PI3K/Akt pathway regulates property of PUN on ROS scavenging. (a) ROS detection was performed using a fluorescence macroscopy. (A) RAW264.7 cells were cultured in DMEM for 12 h and then incubated with probe DCFH2DA for 15 min. (B) RAW264.7 cells were treated with 1 μg/mL LPS for 12 h and then incubated with probe DCFH2DA for 15 min. (C) RAW264.7 cells were pretreated with 100 μM PUN for 1 h and treated with 1 μg/mL LPS for 12 h and then incubated with probe DCFH2DA for 15 min. (D) RAW264.7 cells were pretreated with 100 μM PUN and 20 μM LY294002 for 1 h and treated with 1 μg/mL LPS for 12 h and then incubated with probe DCFH2DA for 15 min. (b) ROS production was measured by a fluorescence microplate reader. RAW264.7 cells were pretreated for 1 h with 100 μM PUN in the presence or absence of 20 μM LY294002 before treatment with 1 μg/mL LPS for 12 h and then incubated with probe DCFH2DA for 15 min. Data represent the mean ± SEM of three independent experiments and differences between mean values were assessed by one-way ANOVA. $^{*}P < 0.05$ and $^{**}P < 0.01$ indicate significant differences compared with the control group.

proteolysis of Nrf2 protein. The sequestration and further degradation of Nrf2 are mechanisms for the repressive effect of Keap1 and Nrf2. To investigate whether PUN upregulates HO-1 via enhancing Nrf2 accumulation and activation, protein was extracted and the Nrf2 protein level was examined by Western blot analysis. The results showed that PUN treatment significantly increased Nrf2 protein level in the nucleus from 4 h to 8 h and in a dose range of 50 μM to 200 μM, suggesting that PUN may regulate HO-1 expression by mediating Nrf2 signaling. We used brusatol, a specific Nrf2 inhibitor, to determine whether blocking Nrf2-mediated signaling attenuates PUN-induced HO-1 expression. As expected, we found that inhibition of Nrf2 markedly suppressed PUN-induced HO-1 expression. Therefore, we concluded that PUN exhibited antioxidant activity via upregulating Nrf2-mediated HO-1 expression. However, as shown in Figures 1(c) and 1(d), the protein level of Keap1 also increased by PUN treatment. As a CUL3-RBX1-dependent E3 ubiquitin ligase, Keap1 degrades Nrf2 by directly interacting with it and conjugating ubiquitin onto the N-terminal Neh2 domain of Nrf2 [42]. Thus, we hypothesized that PUN may also affect the interaction between Keap1 and Nrf2. Further research will be carried out in the future to examine this mechanism.

The PI3K/Akt signaling pathway is also involved in regulating HO-1 expression [43]. Therefore, we investigated the possibility that PI3K/Akt mediates PUN-induced HO-1 expression. As shown in Figure 3(a), PUN treatment notably increased the phosphorylation level of Akt protein, while no significant changes were found in the total Akt protein level, suggesting that enhancement of Akt protein phosphorylation may contribute to the PUN-induced HO-1 expression. To further identify the role of the PI3K/Akt pathway, LY294002, a specific PI3K/Akt inhibitor, was used to treat macrophages together with PUN. The results showed that inhibition of the PI3K/Akt signaling pathway markedly blocked HO-1 expression in the presence of PUN. Furthermore, we investigated whether PI3K/Akt plays an important role in ROS scavenging by PUN, in accordance with its regulation of HO-1 expression. Fluorescent probes showed that blocking PI3K/Akt signaling by LY294002 attenuated the ROS scavenging capability of PUN in LPS-induced oxidative stress in macrophages, and this may be related to the downregulation of HO-1 expression.

Because the PI3K/Akt and Nrf2 pathways are both implicated in the transcriptional regulation of the antioxidant enzyme HO-1 [44], we tried to reveal their underlying mechanisms in the PUN-induced HO-1 protein expression. The data demonstrated that inhibition of PI3K/Akt significantly suppressed Nrf2 protein expression induced by PUN. Then, we examined whether blocking Nrf2 inhibits the PI3K/Akt-mediated HO-1 expression in the presence of PUN. The results demonstrated that inhibition of Nrf2 suppressed the upregulation of HO-1 by PUN treatment in macrophages; however, neither LY294002 nor insulin had a significant effect when the Nrf2 signaling was blocked. Therefore, we concluded that the PI3K/Akt signaling pathway played a vital role in PUN-induced HO-1 expression by regulating Nrf2.

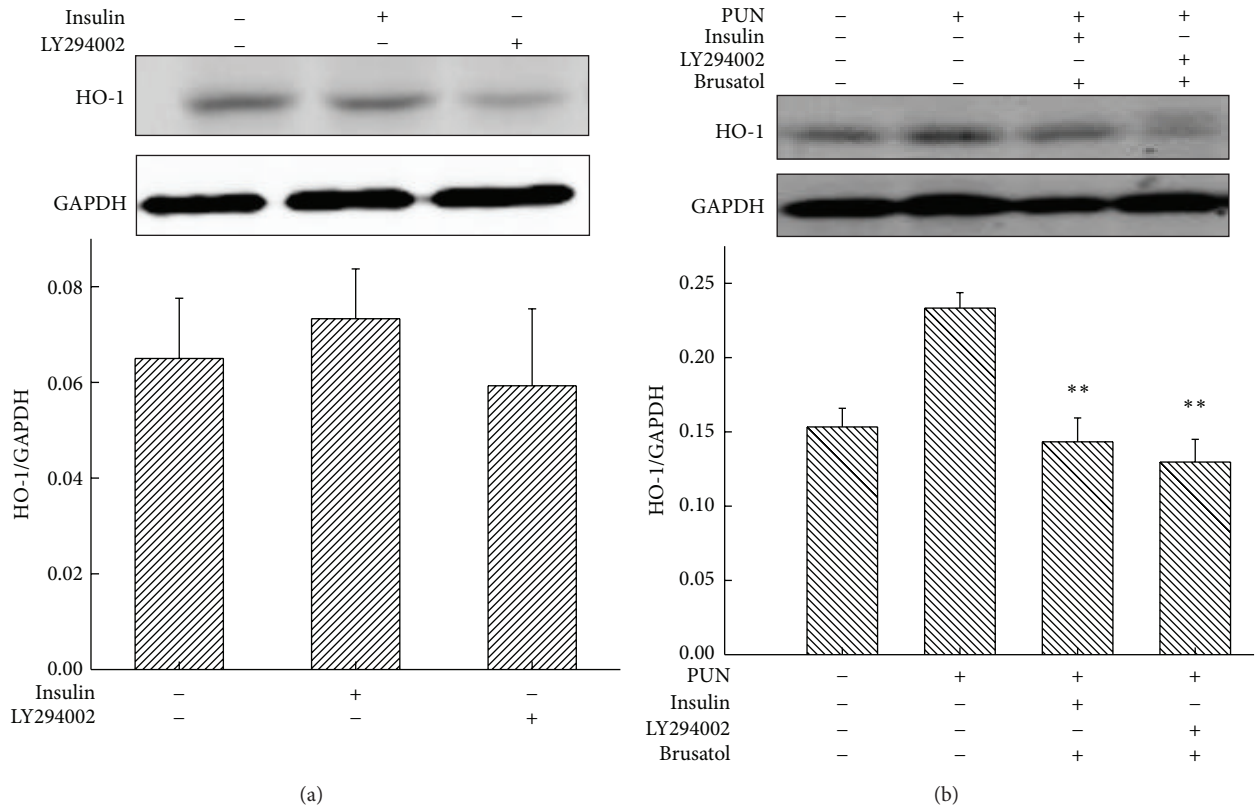

Figure 5: Blocking Nrf2 suppresses modulatory effect of PI3K/Akt pathway on PUN-induced HO-1 protein expression. RAW264.7 cells were treated for 8 h with 100 μM PUN in the presence or absence of indicated inhibitor (LY294002, 20 μM; brusatol, 10 nM) and inducer (insulin, 10 μM) at 37°C in a humidified incubator with 5% CO_2. The HO-1 protein expression was analyzed by Western blotting. Data represent the mean ± SEM of three independent experiments and differences between mean values were assessed by one-way ANOVA. $^{**}P < 0.01$ indicates significant differences compared with the PUN-treated group.

ROS overproduction plays a central role in LPS-induced macrophage activation, leading to an excessive inflammatory process. In this study, we assessed the inhibitory effect of PUN on ROS production. Compared with the control group, LPS treatment significantly increased ROS generation. However, pretreatment with PUN dramatically decreased ROS production. NAC, a well-established ROS scavenger, was used to treat macrophages as a positive control, and 50 μM NAC significantly decreased the LPS-induced ROS overproduction, to a similar extent as 200 μM PUN treatment. SOD, which catalyzes the dismutation of superoxide radical (O_2^-) to hydrogen peroxide (H_2O_2) and oxygen (O_2), is another kind of phase II enzyme mediated by Nrf2 that serves as a defense mechanism against oxidative damage [45]. SOD1 (Cu/Zn-SOD) locates primarily in the cytoplasm, and SOD2 (Mn-SOD), a structurally distinct protein, locates in the mitochondria [46]. Our results demonstrated that a 12 h LPS challenge significantly reduced the *SOD1* mRNA expression and increased *SOD2* mRNA expression in macrophages. However, PUN pretreatment only notably reversed the *SOD1* mRNA expression, with no effect on *SOD2* mRNA expression. NO is another important molecule regulated by the Nrf2-mediated pathway, whose excessive generation has been shown to result in oxidative stress and inflammation during an LPS challenge [37, 47]. Previous studies have indicated that the PI3K/Akt pathway is a potential target of medicines that exhibit an NO inhibition effect in LPS-induced macrophages [48, 49]. Hence, we investigated whether PI3K/Akt signaling also modulates the inhibition property of PUN on NO generation in macrophages. PUN treatment significantly weakened the LPS-induced NO overproduction. However, comparing LY294002 treatment with insulin treatment, we concluded that upregulation or downregulation of PI3K/Akt showed no significant changes in decreasing the LPS-induced NO expression in the presence of PUN, indicating that PI3K/Akt signaling was not involved in the inhibitory effect of PUN on NO expression in macrophages. Our previous study has revealed that PUN inhibits LPS-induced NO overproduction by suppressing MAPKs/NF-κB activation. In that study, we inferred that PUN inhibited NO expression through MAPKs signaling, but not through PI3K/Akt signaling. Thus, we concluded that PUN exhibited antioxidant properties, including scavenging ROS, potentiating *SOD1* expression, and inhibiting NO production.

Taken together, these results show that PUN enhances HO-1 expression by upregulating the Nrf2-mediated pathway in macrophages and that the PI3K/Akt pathway plays a central role in this mechanism. Our data also demonstrated

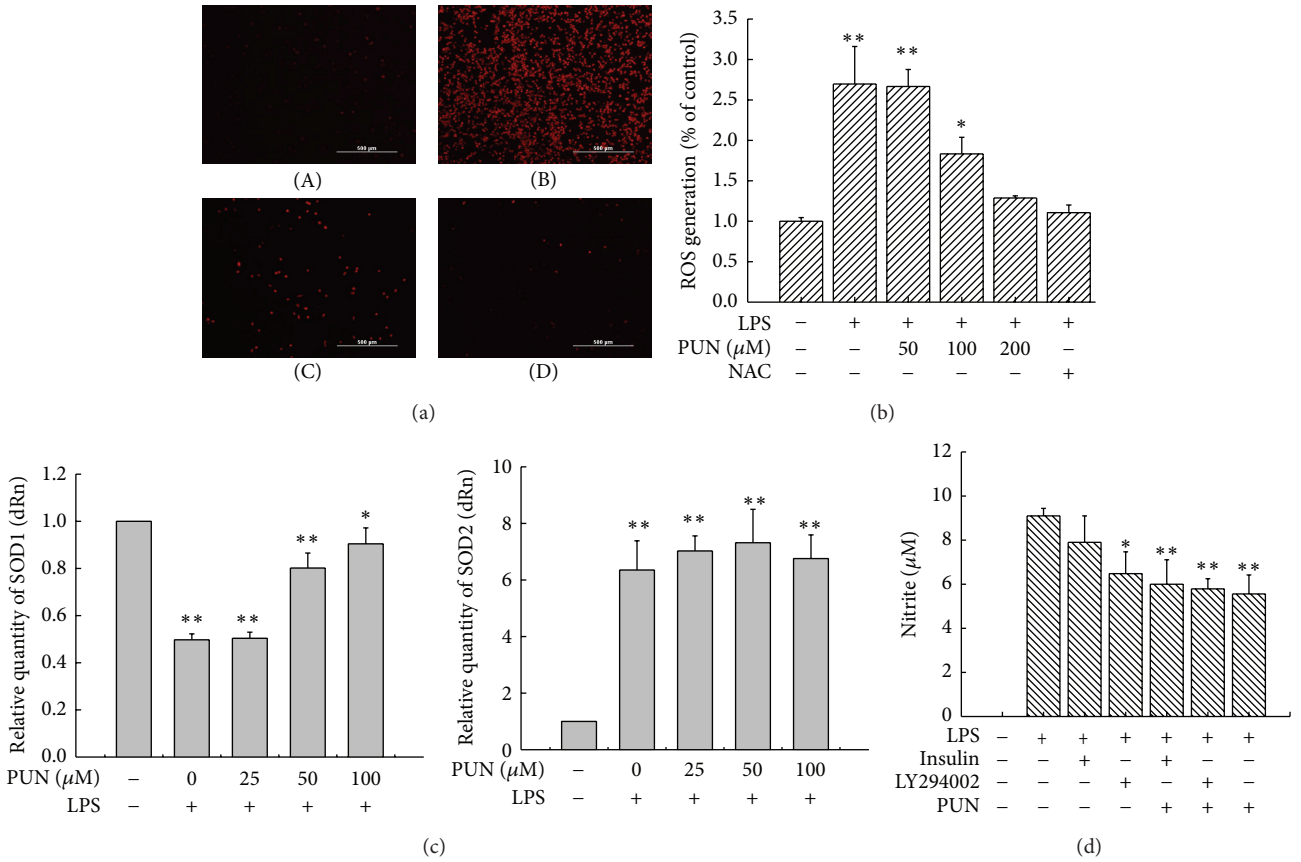

Figure 6: PUN inhibits LPS-induced oxidative stress. (a) PUN inhibits LPS-induced ROS generation. (A) RAW264.7 cells were cultured in DMEM for 12 h and then incubated with probe DCFH2DA for 15 min. (B) RAW264.7 cells were treated with 1 μg/mL LPS for 12 h and then incubated with probe DCFH2DA for 15 min. (C) RAW264.7 cells were pretreated with 100 μM PUN for 1 h before treatment with 1 μg/mL LPS for 12 h and then incubated with probe DCFH2DA for 15 min. (D) RAW264.7 cells were pretreated with 50 μM NAC for 1 h before treatment with 1 μg/mL LPS for 12 h and then incubated with probe DCFH2DA for 15 min. (b) ROS detection was performed by a fluorescence microplate reader. RAW264.7 cells were pretreated for 1 h with PUN at indicated doses (0, 50, 100, and 200 μM) in the presence or absence of 100 μM NAC and before treatment with 1 μg/mL LPS for 12 h and then incubated with probe DCFH2DA for 15 min. (c) PUN mediated SOD1 and SOD2 mRNA expression in LPS-treated RAW264.7 cells. Cells were pretreated with PUN (25, 50, and 100 μM) and then treated to 1 μg/mL LPS for 12 h; SOD1 and SOD2 mRNA expression were detected using RT-PCR. (d) PUN inhibits LPS-induced NO overproduction; RAW264.7 cells were pretreated for 1 h with or without 100 μM PUN in the presence or absence of indicated inhibitor (LY294002, 20 μM) and inducer (insulin, 10 μM) before treatment with 1 μg/mL LPS for 12 h. NO production in the supernatant was measured using Griess reaction. Data represent the mean ± SEM of three independent experiments and differences between mean values were assessed by one-way ANOVA. $^{*}P < 0.05$, $^{**}P < 0.01$, $^{\triangle}P < 0.05$, $^{\triangle\triangle}P < 0.01$, $^{\#}P < 0.05$, and $^{\#\#}P < 0.01$ indicate significant differences compared with the control group of indicated proteins, respectively.

that PUN exhibits considerable antioxidant properties in LPS-stimulated macrophages by inhibiting ROS generation and NO overproduction and by enhancing the *SOD1* mRNA expression. These findings provide new perspectives for novel therapeutic approaches using antioxidant medicines and compounds against oxidative stress and excessive inflammatory diseases including tissue damage, sepsis, and endotoxemic shock.

Conflict of Interests

The authors confirm that there is no conflict of interests.

Acknowledgments

This work was supported by grants from the National Twelve-Five Technological Supported Plan of China (no. 2011BAD34B01) and The Ministry of Agriculture, Public Service Sectors Agriculture Research Projects (no. 201003060-9/10).

References

[1] W.-J. Zhang, H. Wei, and B. Frei, "Genetic deficiency of NADPH oxidase does not diminish, but rather enhances, LPS-induced

acute inflammatory responses in vivo," *Free Radical Biology and Medicine*, vol. 46, no. 6, pp. 791–798, 2009.

[2] D. Menon, R. Coll, L. A. J. O'Neill et al., "Glutathione transferase Omega 1 is required for the LPS stimulated induction of NADPH Oxidase 1 and the production of reactive oxygen species in macrophages," *Free Radical Biology & Medicine*, 2014.

[3] Y. Emre, C. Hurtaud, T. Nübel, F. Criscuolo, D. Ricquier, and A.-M. Cassard-Doulcier, "Mitochondria contribute to LPS-induced MAPK activation via uncoupling protein UCP2 in macrophages," *Biochemical Journal*, vol. 402, no. 2, pp. 271–278, 2007.

[4] Z. Zhai, S. E. Gomez-Mejiba, M. S. Gimenez et al., "Free radical-operated proteotoxic stress in macrophages primed with lipopolysaccharide," *Free Radical Biology and Medicine*, vol. 53, no. 1, pp. 172–181, 2012.

[5] T. W. Kensler, N. Wakabayashi, and S. Biswal, "Cell survival responses to environmental stresses via the Keap1-Nrf2-ARE pathway," *Annual Review of Pharmacology and Toxicology*, vol. 47, pp. 89–116, 2007.

[6] Q. Ma, "Role of Nrf2 in oxidative stress and toxicity," *Annual Review of Pharmacology and Toxicology*, vol. 53, pp. 401–426, 2013.

[7] K.-J. Min, J. T. Lee, E.-H. Joe, and T. K. Kwon, "An IκBα phosphorylation inhibitor induces heme oxygenase-1(HO-1) expression through the activation of reactive oxygen species (ROS)-Nrf2-ARE signaling and ROS-PI3K/Akt signaling in an NF-κB-independent mechanism," *Cellular Signalling*, vol. 23, no. 9, pp. 1505–1513, 2011.

[8] S. W. Ryter and A. M. K. Choi, "Heme oxygenase-1: redox regulation of a stress protein in lung and cell culture models," *Antioxidants and Redox Signaling*, vol. 7, no. 1-2, pp. 80–91, 2005.

[9] S. W. Chung, X. Liu, A. A. Macias, R. M. Baron, and M. A. Perrella, "Heme oxygenase-1-derived carbon monoxide enhances the host defense response to microbial sepsis in mice," *Journal of Clinical Investigation*, vol. 118, no. 1, pp. 239–247, 2008.

[10] N. G. Abraham and A. Kappas, "Heme oxygenase and the cardiovascular-renal system," *Free Radical Biology and Medicine*, vol. 39, no. 1, pp. 1–25, 2005.

[11] S. W. Ryter, J. Alam, and A. M. K. Choi, "Heme oxygenase-1/carbon monoxide: from basic science to therapeutic applications," *Physiological Reviews*, vol. 86, no. 2, pp. 583–650, 2006.

[12] J. A. Johnson, D. A. Johnson, A. D. Kraft et al., "The Nrf2-ARE pathway: an indicator and modulator of oxidative stress in neurodegeneration," *Annals of the New York Academy of Sciences*, vol. 1147, pp. 61–69, 2008.

[13] D. Ren, N. F. Villeneuve, T. Jiang et al., "Brusatol enhances the efficacy of chemotherapy by inhibiting the Nrf2-mediated defense mechanism," *Proceedings of the National Academy of Sciences of the United States of America*, vol. 108, no. 4, pp. 1433–1438, 2011.

[14] K. Nakaso, H. Yano, Y. Fukuhara, T. Takeshima, K. Wada-Isoe, and K. Nakashima, "PI3K is a key molecule in the Nrf2-mediated regulation of antioxidative proteins by hemin in human neuroblastoma cells," *FEBS Letters*, vol. 546, no. 2-3, pp. 181–184, 2003.

[15] H. Qi, Y. Han, and J. Rong, "Potential roles of PI3K/Akt and Nrf2-Keap1 pathways in regulating hormesis of Z-ligustilide in PC12 cells against oxygen and glucose deprivation," *Neuropharmacology*, vol. 62, no. 4, pp. 1659–1670, 2012.

[16] L. C. Cantley, "The phosphoinositide 3-kinase pathway," *Science*, vol. 296, no. 5573, pp. 1655–1657, 2002.

[17] A. Brunet, S. R. Datta, and M. E. Greenberg, "Transcription-dependent and -independent control of neuronal survival by the PI3K-Akt signaling pathway," *Current Opinion in Neurobiology*, vol. 11, no. 3, pp. 297–305, 2001.

[18] X. Meng, M. Wang, X. Wang et al., " Suppression of NADPH oxidase- and mitochondrion-derived superoxide by Notoginsenoside R1 protects against cerebral ischemia-reperfusion injury through estrogen receptor-dependent activation of Akt/Nrf2 pathways," *Free Radical Research*, 2014.

[19] P. Vitaglione, F. Morisco, N. Caporaso, and V. Fogliano, "Dietary antioxidant compounds and liver health," *Critical Reviews in Food Science and Nutrition*, vol. 44, no. 7-8, pp. 575–586, 2004.

[20] V. Tapias, J. R. Cannon, and J. T. Greenamyre, "Pomegranate juice exacerbates oxidative stress and nigrostriatal degeneration in Parkinson's disease," *Neurobiology of Aging*, vol. 35, no. 5, pp. 1162–1176, 2014.

[21] M. Spilmont, L. Leotoing, M. J. Davicco et al., "Pomegranate and its derivatives can improve bone health through decreased inflammation and oxidative stress in an animal model of postmenopausal osteoporosis," *European Journal of Nutrition*, vol. 53, no. 5, pp. 1155–1164, 2014.

[22] V. M. Adhami, I. A. Siddiqui, D. N. Syed, R. K. Lall, and H. Mukhtar, "Oral infusion of pomegranate fruit extract inhibits prostate carcinogenesis in the TRAMP model," *Carcinogenesis*, vol. 33, no. 3, pp. 644–651, 2012.

[23] N. Khan, F. Afaq, M.-H. Kweon, K. Kim, and H. Mukhtar, "Oral consumption of pomegranate fruit extract inhibits growth and progression of primary lung tumors in mice," *Cancer Research*, vol. 67, no. 7, pp. 3475–3482, 2007.

[24] X. Xu, P. Yin, C. Wan et al., "Punicalagin Inhibits Inflammation in LPS-Induced RAW264.7 Macrophages via the Suppression of TLR4-Mediated MAPKs and NF-κB Activation," *Inflammation*, vol. 37, no. 3, pp. 956–965, 2014.

[25] D. Qi, C. Ouyang, Y. Wang et al., "HO-1 attenuates hippocampal neurons injury via the activation of BDNF-TrkB-PI3K/ Akt signaling pathway in stroke," *Brain Research*, vol. 1577, pp. 69–76, 2014.

[26] N. P. Seeram, L. S. Adams, S. M. Henning et al., "In vitro antiproliferative, apoptotic and antioxidant activities of punicalagin, ellagic acid and a total pomegranate tannin extract are enhanced in combination with other polyphenols as found in pomegranate juice," *Journal of Nutritional Biochemistry*, vol. 16, no. 6, pp. 360–367, 2005.

[27] A. Bishayee, D. Bhatia, R. J. Thoppil, A. S. Darvesh, E. Nevo, and E. P. Lansky, "Pomegranate-mediated chemoprevention of experimental hepatocarcinogenesis involves Nrf2-regulated antioxidant mechanisms," *Carcinogenesis*, vol. 32, no. 6, pp. 888–896, 2011.

[28] E. P. Lansky and R. A. Newman, "*Punica granatum* (pomegranate) and its potential for prevention and treatment of inflammation and cancer," *Journal of Ethnopharmacology*, vol. 109, no. 2, pp. 177–206, 2007.

[29] T. Ismail, P. Sestili, and S. Akhtar, "Pomegranate peel and fruit extracts: a review of potential anti-inflammatory and anti-infective effects," *Journal of Ethnopharmacology*, vol. 143, no. 2, pp. 397–405, 2012.

[30] F. Aqil, M. V. Vadhanam, and R. C. Gupta, "Enhanced activity of punicalagin delivered via polymeric implants against benzo[*a*]pyrene-induced DNA adducts," *Mutation Research/Genetic Toxicology and Environmental Mutagenesis*, vol. 743, no. 1-2, pp. 59–66, 2012.

[31] M. I. Gil, F. A. Tomas-Barberan, B. Hess-Pierce, D. M. Holcroft, and A. A. Kader, "Antioxidant activity of pomegranate juice and its relationship with phenolic composition and processing," *Journal of Agricultural and Food Chemistry*, vol. 48, no. 10, pp. 4581–4589, 2000.

[32] B. Chen, M. G. Tuuli, M. S. Longtine et al., "Pomegranate juice and punicalagin attenuate oxidative stress and apoptosis in human placenta and in human placental trophoblasts," *American Journal of Physiology: Endocrinology and Metabolism*, vol. 302, no. 9, pp. E1142–E1152, 2012.

[33] F. Aqil, R. Munagala, M. V. Vadhanam et al., "Anti-proliferative activity and protection against oxidative DNA damage by punicalagin isolated from pomegranate husk," *Food Research International*, vol. 49, no. 1, pp. 345–353, 2012.

[34] A. Paine, B. Eiz-Vesper, R. Blasczyk, and S. Immenschuh, "Signaling to heme oxygenase-1 and its anti-inflammatory therapeutic potential," *Biochemical Pharmacology*, vol. 80, no. 12, pp. 1895–1903, 2010.

[35] B. Zhang, J. Hirahashi, X. Cullere, and T. N. Mayadas, "Elucidation of molecular events leading to neutrophil apoptosis following phagocytosis: cross-talk between caspase 8, reactive oxygen species, and MAPK/ERK activation," *Journal of Biological Chemistry*, vol. 278, no. 31, pp. 28443–28454, 2003.

[36] S. E. Lee, S. I. Jeong, H. Yang et al., "Extract of Salvia miltiorrhiza (Danshen) induces Nrf2-mediated heme oxygenase-1 expression as a cytoprotective action in RAW 264.7 macrophages," *Journal of Ethnopharmacology*, vol. 139, no. 2, pp. 541–548, 2012.

[37] I. S. Choi, E.-Y. Choi, J.-Y. Jin, H. R. Park, J.-I. Choi, and S.-J. Kim, "Kaempferol inhibits *P. intermedia* lipopolysaccharide-induced production of nitric oxide through translational regulation in murine macrophages: critical role of heme oxygenase-1-mediated ROS reduction," *Journal of Periodontology*, vol. 84, no. 4, pp. 545–555, 2013.

[38] J.-S. Wang, F.-M. Ho, H.-C. Kang, W.-W. Lin, and K.-C. Huang, "Celecoxib induces heme oxygenase-1 expression in macrophages and vascular smooth muscle cells via ROS-dependent signaling pathway," *Naunyn-Schmiedeberg's Archives of Pharmacology*, vol. 383, no. 2, pp. 159–168, 2011.

[39] J. Alam, D. Stewart, C. Touchard, S. Boinapally, A. M. K. Choi, and J. L. Cook, "Nrf2, a Cap'n'Collar transcription factor, regulates induction of the heme oxygenase-1 gene," *Journal of Biological Chemistry*, vol. 274, no. 37, pp. 26071–26078, 1999.

[40] S. Braun, C. Hanselmann, M. G. Gassmann et al., "Nrf2 transcription factor, a novel target of keratinocyte growth factor action which regulates gene expression and inflammation in the healing skin wound," *Molecular and Cellular Biology*, vol. 22, no. 15, pp. 5492–5505, 2002.

[41] H.-Y. Cho, S. P. Reddy, and S. R. Kleeberger, "Nrf2 defends the lung from oxidative stress," *Antioxidants and Redox Signaling*, vol. 8, no. 1-2, pp. 76–87, 2006.

[42] D. F. Lee, H. P. Kuo, M. Liu et al., "KEAP1 E3 ligase-mediated downregulation of NF-κB signaling by targeting IKKβ," *Molecular Cell*, vol. 36, no. 1, pp. 131–140, 2009.

[43] R. G. Jayasooriya, K.-T. Lee, H. J. Lee, Y. H. Choi, J. W. Jeong, and G. Y. Kim, "Anti-inflammatory effects of β-hydroxyisovalerylshikonin in BV2 microglia are mediated through suppression of the PI3K/Akt/NF-kB pathway and activation of the Nrf2/HO-1 pathway," *Food and Chemical Toxicology*, vol. 65, pp. 82–89, 2014.

[44] D. Martin, A. I. Rojo, M. Salinas et al., "Regulation of heme oxygenase-1 expression through the phosphatidylinositol 3-kinase/Akt pathway and the Nrf2 transcription factor in response to the antioxidant phytochemical carnosol," *The Journal of Biological Chemistry*, vol. 279, no. 10, pp. 8919–8929, 2004.

[45] Z. Zhang, W. Cui, G. Li et al., "Baicalein protects against 6-OHDA-induced neurotoxicity through activation of Keap1/Nrf2/HO-1 and involving PKCα and PI3K/AKT signaling pathways," *Journal of Agricultural and Food Chemistry*, vol. 60, no. 33, pp. 8171–8182, 2012.

[46] J. Wuerges, J.-W. Lee, Y.-I. Yim, H.-S. Yim, S.-O. Kang, and K. D. Carugo, "Crystal structure of nickel-containing superoxide dismutase reveals another type of active site," *Proceedings of the National Academy of Sciences of the United States of America*, vol. 101, no. 23, pp. 8569–8574, 2004.

[47] T. Itoh, M. Koketsu, N. Yokota, S. Touho, M. Ando, and Y. Tsukamasa, "Reduced scytonemin isolated from Nostoc commune suppresses LPS/IFNγ-induced NO production in murine macrophage RAW264 cells by inducing hemeoxygenase-1 expression via the Nrf2/ARE pathway," *Food and Chemical Toxicology*, vol. 69, pp. 330–338, 2014.

[48] J.-H. Kim, G.-Y. Park, S. Y. Bang, S. Y. Park, S.-K. Bae, and Y. Kim, "Crocin suppresses LPS-stimulated expression of inducible nitric oxide synthase by upregulation of heme oxygenase-1 via calcium/calmodulin-dependent protein kinase 4," *Mediators of Inflammation*, vol. 2014, Article ID 728709, 14 pages, 2014.

[49] E. Y. Gohar, S. M. El-Gowilly, H. M. El-Gowelli, M. A. El-Demellawy, and M. M. El-Mas, "PI3K/Akt-independent NOS/HO activation accounts for the facilitatory effect of nicotine on acetylcholine renal vasodilations: modulation by ovarian hormones," *PLoS ONE*, vol. 9, no. 4, Article ID e95079, 2014.

Hindawi Publishing Corporation
Mediators of Inflammation
Volume 2015, Article ID 563713, 7 pages
http://dx.doi.org/10.1155/2015/563713

Research Article

Percentages of CD4+CD161+ and CD4−CD8−CD161+ T Cells in the Synovial Fluid Are Correlated with Disease Activity in Rheumatoid Arthritis

Jinlin Miao,[1] Kui Zhang,[1] Feng Qiu,[2] Tingting Li,[3] Minghua Lv,[1] Na Guo,[1,4] Qing Han,[1] and Ping Zhu[1]

[1]*Department of Clinical Immunology, Xijing Hospital, Fourth Military Medical University, Xi'an 710032, China*
[2]*Department of Neurology, Chinese Navy General Hospital, Beijing 100048, China*
[3]*Department of Geriatric Gastroenterology, Chinese People's Liberation Army General Hospital, Beijing 100853, China*
[4]*Institute of Basic Medical Science, Xi'an Medical University, Xi'an 710032, China*

Correspondence should be addressed to Ping Zhu; zhuping@fmmu.edu.cn

Received 17 October 2014; Accepted 1 December 2014

Academic Editor: Lifei Hou

Objective. CD161 has been identified as a marker of human IL-17-producing T cells that are implicated in the pathogenesis of rheumatoid arthritis (RA). This study aimed to investigate the potential link between the percentage of CD161+ T cells and disease activity in RA patients. *Methods*. Peripheral blood (PB) from 54 RA patients and 21 healthy controls was evaluated. Paired synovial fluid (SF) ($n = 17$) was analyzed. CD161 expression levels on CD4+, CD8+, and CD4−CD8− T cells were assessed by flow cytometry. *Results*. The percentage of CD4+CD161+ T cells in RA SF was higher than RA PB, and it was positively correlated with DAS28, erythrocyte sedimentation rate (ESR), and C-reactive protein (CRP). CD4−CD8−CD161+ T cell percentage was decreased in RA PB and was further reduced in RA SF, and its level in SF was inversely correlated with DAS28, ESR, and CRP. However, CD8+CD161+ T cell percentage was neither changed in RA PB and SF nor correlated with disease activity indices. *Conclusion*. An increased CD4+CD161+ T cell percentage and a decreased CD4−CD8−CD161+ T cell percentage are present in RA SF and are associated with disease activity, and the accumulation of CD4+CD161+ T cells in SF may contribute to the local inflammation of RA.

1. Introduction

Rheumatoid arthritis (RA) is a systemic inflammatory disease characterized by joint inflammation of synovial tissue eventually leading to joint damage and functional disability. Multiple innate and adaptive effector cells, including macrophages, neutrophils, fibroblasts, B cells, and T cells, play important roles in the pathogenesis of RA [1]. T helper-type 17 (Th17) cells, a distinct subset of Th cells producing interleukin-(IL-) 17 in humans, may be involved in the pathogenesis of autoimmune and chronic inflammatory disorders, including RA [2, 3]. Numerous clinical studies including our data have demonstrated that the percentage of Th17 cells in RA patients was elevated and positively correlated with the degree of local and systemic disease activity [4–6]. Moreover, IL-17, the characteristic cytokine of Th17 cells, was implicated in the pathogenesis of RA [7]. IL-17A is a proinflammatory cytokine expressed in synovial membrane cultures of RA patients [8] and synovial tissue IL-17 is associated with more rapid joint damage progression in synergy with tumor necrosis factor-(TNF-) α [9]. An enhanced expression of IL-17 has also been observed in the synovial fluid of RA patients [8, 10], and IL-17 has become a new therapeutic target for mouse RA models and human RA [11].

CD161 is the human equivalent of mouse NK cell receptor P1A and constitutes a type II transmembrane glycoprotein with characteristics of the C-type lectin superfamily [12]. CD161 was one of the most upregulated genes in human Th17 cells compared to Th1 or Th2 cells and its expression is induced by RAR-related orphan receptor C (RORC), the Th17 lineage transcription factor [13, 14]. In addition, human Th17 cells exclusively originate from CD4+CD161+

naive T cell progenitors, and CD161 is a novel surface marker for Th17 cells [13, 14]. Moreover, Maggi et al. provided evidence that CD161 is a marker of all human IL-17-producing T cell subsets, including CD3+CD4+CD8−, CD3+CD4−CD8+, and CD3+CD4−CD8− cells [14]. It has been reported that circulating CD4+CD161+ T cells are increased in seropositive arthralgia patients but decreased in newly diagnosed RA patients [15]. Furthermore, this study showed that CD4+CD161+ T cells were enriched in synovial fluid (SF), while CD8+CD161+ T cells were not accumulated in SF of RA patients [15]. In fact, we have previously demonstrated that RA patients seemed to have higher percentages of circulating CD161+ cells in CD4+ T cells than healthy controls, but the difference did not reach statistical significance [16]. However, little was known about the percentages of CD161 expressing T cell subsets (including CD3+CD4+, CD3+CD8+, and CD3+CD4−CD8− cells) in blood and the local site of inflammation of RA patients and their potential link to disease activity.

Therefore, we explored the percentages of CD161 expressing T cell subsets in PB and SF of RA patients and assessed their correlations with the degree of disease activity.

2. Materials and Methods

2.1. Patients. Samples of peripheral blood (PB) were obtained from 54 RA patients and from 21 age- and sex-matched healthy controls. And synovial fluid (SF) samples were obtained from the knee joints of 17 patients with active RA. All patients fulfilled the 1987 revised criteria of the American College of Rheumatology [17]. Disease activity was assessed by the 28-joint disease activity score (DAS28) on the day of sample collection. Erythrocyte sedimentation rate (ESR) and C-reactive protein (CRP) were determined on the day of sample collection in the clinical laboratory. The study conforms to the recommendations of the Declaration of Helsinki. The Ethics Committee of Xijing Hospital approved this study, and the informed consent from all subjects was obtained.

2.2. Preparation of Mononuclear Cells. SF samples were treated with 20 μg/mL hyaluronidase (Sigma-Aldrich, St. Louis, MO, USA) for 30 min at 37°C, and cells were then washed twice with phosphate-buffered saline. SF mononuclear cells (SFMCs) and PB mononuclear cells (PBMCs) were isolated from sodium heparinized whole blood and SF cell suspension samples using Ficoll-Paque density gradient centrifugation (GE Healthcare, Pittsburgh, PA, USA) by standard procedures.

2.3. Flow Cytometric Analysis of T Cell Surface Markers. The phenotypes of lymphocytes in PB and SF were determined using flow cytometry. Briefly, PBMCs and SFMCs were stained with the following fluorochrome conjugated monoclonal antibodies: fluorescein isothiocyanate- (FITC-) conjugated CD3 (SK7), peridinin chlorophyll protein- (PerCP-) conjugated CD4 (SK3), allophycocyanin- (APC-) conjugated CD8 (SK1), phycoerythrin- (PE-) conjugated CD161 (DX12), and isotype-matched control IgG antibodies (all from BD Biosciences, San Diego, CA, USA) for 30 min at room temperature, according to the manufacturer's instructions. Stained cells were analyzed using FACSCalibur flow cytometer (BD Biosciences), and data analysis was performed with Cell Quest software (BD Biosciences).

2.4. Statistical Analysis. Differences between groups were determined using the nonparametric Mann-Whitney test. Paired samples were compared using a Wilcoxon matched pairs signed rank sum test. Correlations were evaluated by nonparametric Spearman's correlation analysis. Data analyses were performed using GraphPad Prism version 5.0 (GraphPad Software, San Diego, CA, USA). For all tests, a two-sided P value less than 0.05 was considered significant.

3. Results

3.1. Subject Basic Characteristics. Clinical characteristics of RA patients and healthy controls are illustrated in Table 1. Fifty-four patients with RA and 21 healthy controls (HC) were recruited, and synovial fluid (SF) samples were obtained from 17 active RA patients. There was no significant difference in age and gender between the three groups. In addition, disease duration, positive rate of RF and anti-CCP antibodies, and proportion of patients previously using medications were comparable between the group of total RA patients and the group of those patients with collected SF. In addition, ESR levels tended to be increased in RA patients with collected SF ($P = 0.052$), and CRP and DAS28 levels were significantly higher in RA patients with collected SF than in total RA patients ($P = 0.032$ and $P = 0.017$, resp.).

3.2. Percentage of Circulating CD161+ T Cells in RA Patients and Healthy Controls. First, we assessed circulating CD3+ T cell subsets expressing the IL-17 producing cells marker CD161 in RA patients and HC, and representative examples of flow cytometric dot-plots are shown in Figure 1(a). The percentage of circulating CD4+CD161+ (22.19, 18.41–29.44%) (median, interquartile range) and CD8+CD161+ cells (19.90, 16.26–29.74%) in RA patients was not different from HC (20.34, 18.35–22.58%, and 19.27, 17.19–24.27%; $P = 0.122$ and $P = 0.675$, resp.) (Figures 1(b) and 1(c)), while the percentage of CD4−CD8−CD161+ cells was significantly lower in RA patients (65.22, 53.92–72.81%) than in HC (77.54, 73.92–82.14%; $P < 0.001$) (Figure 1(d)).

3.3. Percentage of CD161+ T Cells at the Site of Inflammation in RA. CD161 may function as an adhesion molecule and is involved in transendothelial migration [18, 19]. Then, the relative percentages of CD161 expression T cells in SF from patients with RA were assessed. The percentage of CD4+CD161+ cells in the RA SF was significantly increased (36.71, 34.99–43.18%) as compared to HC PB ($P < 0.001$), total RA PB ($P < 0.001$), and paired RA PB (25.43, 20.33–30.04%; $P < 0.001$) (Figures 1(b) and 2(a)), while a significantly lower percentage of CD4−CD8−CD161+ cells was observed in the RA SF (35.50, 31.49–40.45%) than in HC PB ($P < 0.001$),

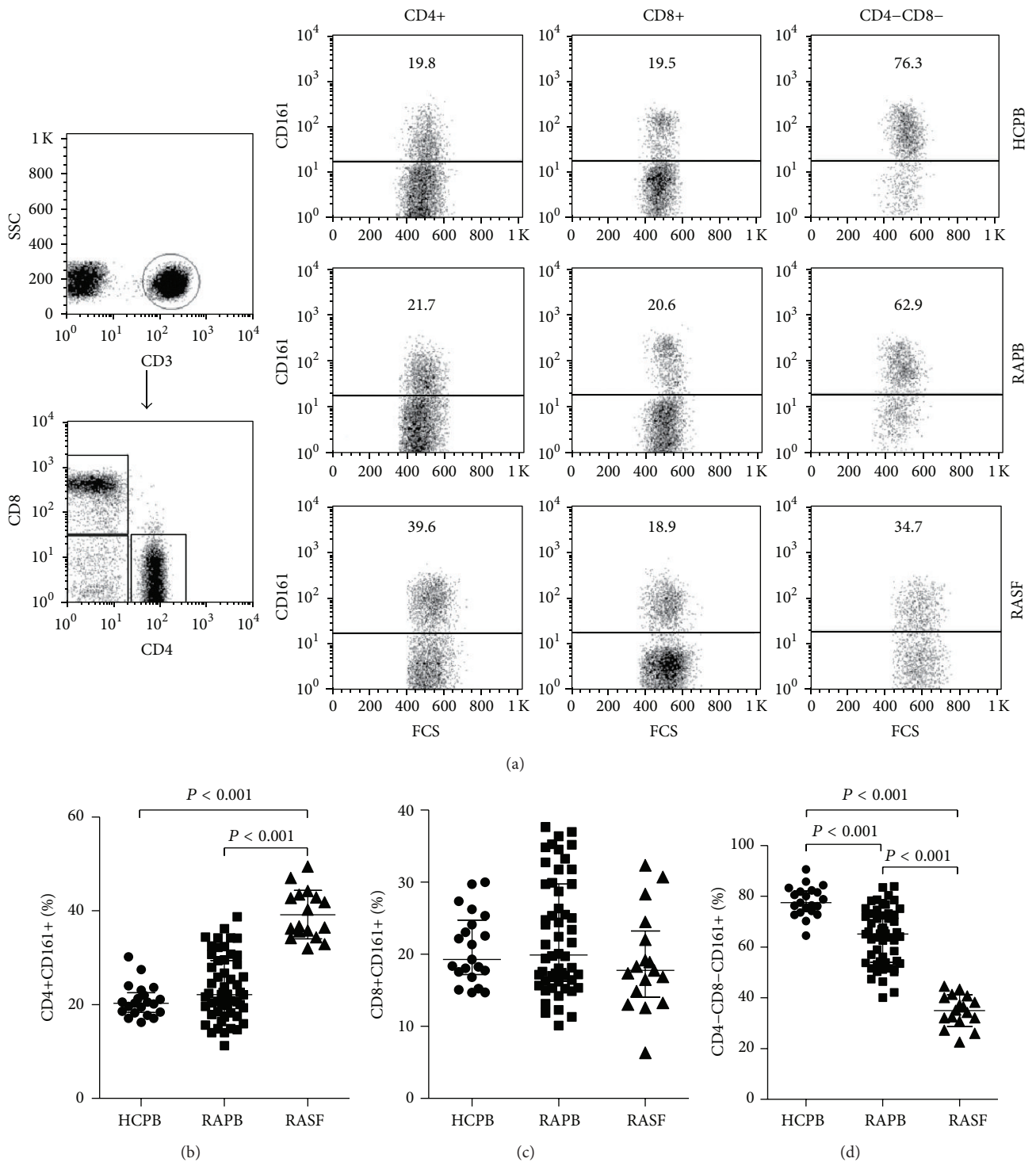

Figure 1: Presence of CD161+ T cell subsets in RA patients and HC. (a) Flow cytometric dot-plots show gating strategy: CD3+ T cells were gated using side scatter profile and the expression of CD3; then CD4+, CD8+, and CD4−CD8− T cells were gated based on their expression of CD4 and CD8, and the CD161 expression levels in these T cell subsets were analyzed from representative HC peripheral blood (PB), RA PB, and RA synovial fluid (SF). Percentages of CD4+CD161+ (b), CD8+CD161+ (c), and CD4−CD8−CD161+ T cells (d) in HC PB, RA PB, and RA SF. Horizontal line indicates median value. *P* values were assessed by Mann-Whitney *U* test.

Table 1: Characteristics of rheumatoid arthritis (RA) patients and healthy controls (HC).

Characteristics	HC	RA	SF RA
Number of patients	21	54	17
Age in years, median (IQR)	45.0 (34.0–53.0)	46.5 (36.5–54.8)	47.0 (42.0–54.5)
Female sex, *n* (%)	15 (71.4)	40 (74.1)	13 (76.5)
Disease duration, mo, median (IQR)	na	66.0 (11.8–115.5)	60.0 (19.0–102.0)
Rheumatoid factor positive, *n* (%)	na	38 (70.4%)	12 (70.6%)
Anti-CCP positive, *n* (%)	na	40 (74.1%)	14 (82.4%)
ESR, mm/hour, median (IQR)	na	26.5 (14.8–54.0)	54.0 (25.5–72.0)
CRP, mg/dL, median (IQR)	na	0.6 (0.3–3.6)	3.1 (0.5–5.7)*
DAS28, median (IQR)	na	4.5 (2.6–5.7)	5.4 (4.5–6.1)*
Systemic steroids, *n* (%)	na	7 (13.0)	2 (11.8)
NSAIDs, *n* (%)	na	8 (14.8)	3 (17.6)
DMARDs (excluding anti-TNF), *n* (%)	na	43 (79.6)	13 (76.5)
Anti-TNF-α therapy, *n* (%)	na	8 (14.8)	3 (17.6)

Values are presented as median (interquartile range) or number (percentage). SF, synovial fluid; IQR, interquartile range; Anti-CCP, anticyclic citrullinated peptide antibodies; ESR, erythrocyte sedimentation rate; CRP, C-reactive protein; DAS28, 28-joint disease activity score; NSAIDs, nonsteroidal anti-inflammatory drugs; DMARDs, disease-modifying antirheumatic drugs; TNF-α, tumor necrosis factor-α; na, not applicable. *$P < 0.05$ compared to RA patients.

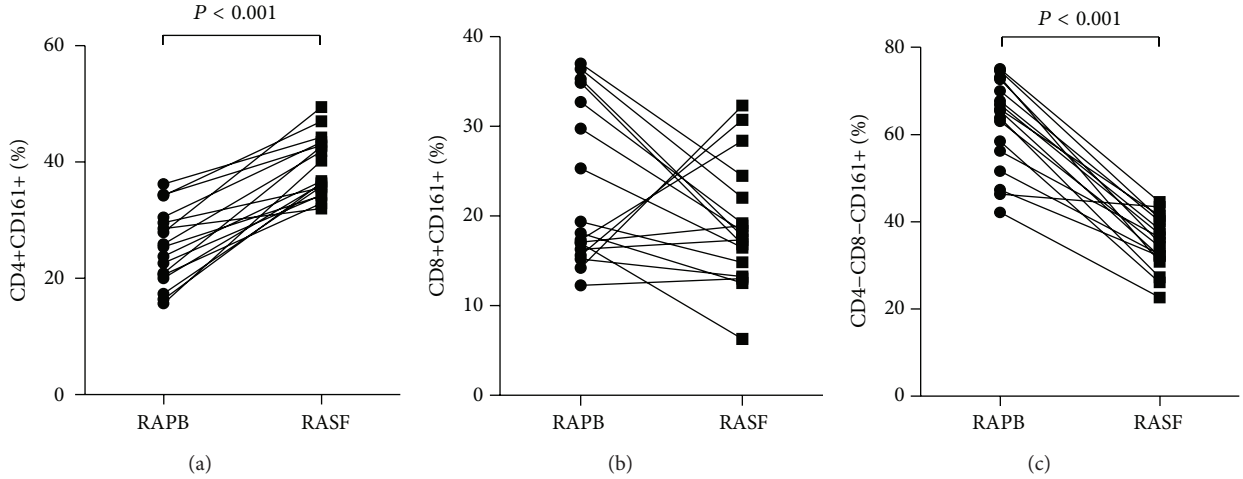

Figure 2: The percentages of CD4+CD161+ (a), CD8+CD161+ (b), and CD4−CD8−CD161+ T cells (c) in paired RA PB and SF samples are shown. *P* values were assessed by Wilcoxon matched pairs signed rank sum test.

total RA PB ($P < 0.001$), and paired PB (65.41, 53.91–71.36%; $P < 0.001$) (Figures 1(d) and 2(c)). However, there were no significant differences in the percentage of CD8+CD161+ T cells among HC PB, total RA PB, RA SF (17.75, 14.06–23.27%) and paired PB (18.12, 15.96–33.80%) (all $P > 0.05$) (Figures 1(c) and 2(b)).

3.4. Correlations of CD161+ T Cells with Disease Activity in RA Patients. Then, we assessed if the presence of CD161+ T cells in SF was correlated with systemic markers of disease activity (Table 2). The percentage of CD4+CD161+ cells in SF was positively correlated with DAS28 ($r = 0.689$, $P = 0.002$), ESR ($r = 0.569$, $P = 0.017$), and CRP levels ($r = 0.679$, $P = 0.003$). In contrast, the percentage of CD4−CD8−CD161+ cells in SF was correlated inversely with DAS28 ($r = -0.671$, $P = 0.003$), ESR ($r = -0.632$, $P = 0.007$), and CRP levels ($r = -0.663$, $P = 0.004$). However, no correlations were present between percentages of CD8+CD161+ cells in SF and DAS28 ($r = 0.137$, $P = 0.599$), ESR ($r = -0.199$, $P = 0.445$), and CRP levels ($r = 0.074$, $P = 0.779$). Additionally, there were no correlations between systemic markers of disease activity and CD161+ T cells in PB (all $P > 0.05$) (Table 2).

4. Discussion

Ample previous studies have indicated that Th17 cells and IL-17 critically contribute to the pathogenesis of RA [2–11]. Furthermore, not only CD4+ cells but also CD8+ and CD4−CD8− T cells that produce IL-17 express the CD161 on their surface, CD161 thus is considered a marker of all IL-17-producing T cells [14]. Moreover, it has been reported that the expression of CD161 is maintained in the life cycle of

Table 2: Correlations between percentages of CD161+ T cell subsets in RA synovial fluid (SF) and peripheral blood (PB) and DAS28, ESR, and CRP.

	DAS28		ESR		CRP	
	r	*P*	*r*	*P*	*r*	*P*
SF						
CD4+CD161+	0.689	**0.002**	0.569	**0.017**	0.679	**0.003**
CD8+CD161+	0.137	0.599	−0.199	0.445	−0.074	0.779
CD4−CD8−CD161+	−0.671	**0.003**	−0.632	**0.007**	−0.663	**0.004**
PB						
CD4+CD161+	0.224	0.103	0.099	0.477	0.137	0.324
CD8+CD161+	0.106	0.445	0.044	0.752	0.167	0.227
CD4−CD8−CD161+	−0.191	0.166	−0.104	0.453	−0.125	0.367

human IL-17-producing T cells [13, 14, 18]. Therefore, CD161 expression may represent a way to detect IL-17-producing T cell ancestry in circulating and tissue infiltrating T cells.

We hypothesized that CD161 expressing T cells representing IL-17-producing T cells act on the pathogenesis of RA, and the levels of CD161 expression T cells in circulation or at inflammatory sites may be regulated prior to or after the development of inflammatory arthritis. Therefore, we assessed the percentage of circulating CD161 expression T cells in HC and RA patients first. Our results showed that the percentage of circulating CD4+CD161+ cells was not different from HC, as we previously reported [16]. However, conflicting data have been reported in a recent study which showed that patients with newly diagnosed RA had decreased levels of CD4+CD161+ cells [20]. Some of this variation may be due to the study cohort. The previous study recruited patients with newly diagnosed RA (with a mean duration of preceding symptoms of 10.2 months), while our cohort had a median disease duration of 66 months and thus may be more consistent with patients with established disease. In addition, this variation may be explained by treatment effects, as most of patients in our study were treated with DMARDs (Table 1), while the patients in the previous study were treatment-naïve [20].

CD161 may function as an adhesion molecule and thereby facilitates extravasation and tissue localization [18, 19]. And a recent study reported that CD161 is a receptor expressed on different T cell subsets and may be involved in the pathogenesis of a given disease [21]. Hence, we investigated the performance of CD161 expressing T cells from the synovial fluid of RA patients as representative cells from the RA inflammatory site. Indeed, synovial fluid from active RA patients was found to be enriched in CD4+CD161+ T cells, which is in agreement with the data of a recent study [20]. Moreover, the percentage of CD4+CD161+ cells was positively correlated with DAS28, ESR, and CRP levels in SF of RA patients. These findings suggest that extravasation and migration of CD4+CD161+ T cells to the joints may be facilitated by CD161 mediated adhesion [19] and indicate that CD4+CD161+ T cells, as Th17 precursor cells, may play a pathogenic role at the local site of inflammation in RA. Moreover, the proportions of CD4+CD161+ T cells in SF might reflect the degree of disease activity in RA patients. Thus, we believe that further studies are needed to assess whether the CD4+CD161+ population was associated with joint damage progression, such as cartilage damage and bone erosion.

Meanwhile, levels of CD8+CD161+ cells and CD4−CD8−CD161+ cells in PB and SF were also examined in this study. Similar to a previous study [22], our data showed that the percentage of circulating CD8+CD161+ T cells in RA patients was not different from HC. In addition, no differences were observed between RA SF and paired RA PB or total RA PB of CD8+CD161+ T cells. Furthermore, there was no correlation between CD8+CD161+ T cell percentage and disease activity in SF or PB of RA. This could be due to the relatively limited number of patients, but an intrinsic phenomenon is possible as well.

As reported in the literature, upon activation of the T cell receptor, a small number of CD3+ T cells that are CD4 and CD8 double negative have the capacity to produce IL-17 [23]. Furthermore, IL-17-producing cells were only found in the CD161+ cell fraction of CD4−CD8− cells, and CD4−CD8− T cells have the highest mRNA expression of RORC and IL-23R when compared to CD4+ and CD8+ T cells [14]. In addition, IL-17-producing CD4−CD8− T cells were expanded and involved in the pathogenesis of kidney damage and salivary gland damage in patients with systemic lupus erythematosus and Sjögren's syndrome [24, 25]. However, we demonstrated that the percentage of circulating CD4−CD8−CD161+ cells, representing IL-17-producing CD4−CD8− T cell ancestry cells, was significantly decreased in RA patients when compared to HC. To our surprise, there was no correlation between circulating CD4−CD8−CD161+ cell percentage and the disease activity indices of RA. Furthermore, CD4−CD8−CD161+ cell percentage in RA SF was further decreased as compared to paired RA PB and total RA PB, and this reduction in SF was negatively correlated with DAS28, ESR, and CRP levels in RA patients. These findings suggest that the pathogenesis of RA may differ from that of other rheumatic diseases, and further investigations are needed to determine the mechanism for decreased CD4−CD8−CD161+ cell percentage and the performance of IL-17-producing CD4−CD8− T cells in RA patients. In addition, these results indicate that CD4+CD161+ and CD4−CD8−CD161+ T cells in the joint fluid may be considered as local parameters

of joint inflammation, whereas CRP and ESR levels were regarded as systemic parameters of inflammation. More importantly, these data point towards a potentially important role for CD4+CD161+ and CD4−CD8−CD161+ T cells as regulators of joint inflammation and RA pathogenesis.

5. Conclusion

In conclusion, our results demonstrated that an increased percentage of CD4+CD161+ T cells and a decreased percentage of CD4−CD8−CD161+ T cells are present in SF of RA patients and correlate well with disease activity indices, and thus, may be involved in the local inflammation and clinical outcome of RA. These data suggest that CD4+CD161+ and CD4−CD8−CD161+ T cell levels in SF may reflect the degree of disease activity and joint inflammation in RA patients. Further studies are required to clarify the pathogenetic role of CD4+CD161+ and CD4−CD8−CD161+ T cells and investigate the mechanism for their change in RA.

Disclosure

Jinlin Miao, Kui Zhang, Feng Qiu, and Tingting Li are joint first authors.

Conflict of Interests

The authors declare that there is no conflict of interests regarding the publication of this paper.

Acknowledgments

This work was supported by grants from the Key Program of the National Natural Science Foundation of China (no. 81030058) and the National Natural Science Foundation of China (no. 81401338). This research was approved by Ethical Standards Committee of Xijing Hospital.

References

[1] I. B. McInnes and G. Schett, "The pathogenesis of rheumatoid arthritis," *The New England Journal of Medicine*, vol. 365, no. 23, pp. 2205–2219, 2011.

[2] H. Park, Z. Li, X. O. Yang et al., "A distinct lineage of CD4 T cells regulates tissue inflammation by producing interleukin 17," *Nature Immunology*, vol. 6, no. 11, pp. 1133–1141, 2005.

[3] F. Annunziato, L. Cosmi, F. Liotta, E. Maggi, and S. Romagnani, "Type 17 T helper cells-origins, features and possible roles in rheumatic disease," *Nature Reviews Rheumatology*, vol. 5, no. 6, pp. 325–331, 2009.

[4] H. Shen, J. C. Goodall, and J. S. Hill Gaston, "Frequency and phenotype of peripheral blood Th17 cells in ankylosing spondylitis and rheumatoid arthritis," *Arthritis and Rheumatism*, vol. 60, no. 6, pp. 1647–1656, 2009.

[5] D. Y. Chen, Y. M. Chen, H. H. Chen et al., "Increasing levels of circulating Th17 cells and interleukin-17 in rheumatoid arthritis patients with an inadequate response to anti-TNF-α therapy," *Arthritis Research & Therapy*, vol. 13, no. 4, article R126, 2011.

[6] J. Miao, K. Zhang, M. Lv et al., "Circulating Th17 and Th1 cells expressing CD161 are associated with disease activity in rheumatoid arthritis," *Scandinavian Journal of Rheumatology*, vol. 43, no. 3, pp. 194–201, 2014.

[7] S. Sarkar and D. A. Fox, "Targeting il-17 and th17 cells in rheumatoid arthritis," *Rheumatic Disease Clinics of North America*, vol. 36, no. 2, pp. 345–366, 2010.

[8] M. Chabaud, J. M. Durand, N. Buchs et al., "Human interleukin-17: a T cell-derived proinflammatory cytokine produced by the rheumatoid synovium," *Arthritis and Rheumatism*, vol. 42, no. 5, pp. 963–970, 1999.

[9] B. W. Kirkham, M. N. Lassere, J. P. Edmonds et al., "Synovial membrane cytokine expression is predictive of joint damage progression in rheumatoid arthritis: a two-year prospective study (the DAMAGE study cohort)," *Arthritis and Rheumatism*, vol. 54, no. 4, pp. 1122–1131, 2006.

[10] M. Ziolkowska, A. Koc, G. Luszczykiewicz et al., "High levels of IL-17 in rheumatoid arthritis patients: IL-15 triggers in vitro IL-17 production via cyclosporin A-sensitive mechanism," *The Journal of Immunology*, vol. 164, no. 5, pp. 2832–2838, 2000.

[11] W. Hueber, D. D. Patel, T. Dryja et al., "Effects of AIN457, a fully human antibody to interleukin-17A, on psoriasis, rheumatoid arthritis, and uveitis," *Science Translational Medicine*, vol. 2, no. 52, pp. 52r–72r, 2010.

[12] L. L. Lanier, C. Chang, and J. H. Phillips, "Human NKR-P1A: a disulfide-linked homodimer of the C-type lectin superfamily expressed by a subset of NK and T lymphocytes," *The Journal of Immunology*, vol. 153, no. 6, pp. 2417–2428, 1994.

[13] L. Cosmi, R. De Palma, V. Santarlasci et al., "Human interleukin 17-producing cells originate from a CD161+CD4+ T cell precursor," *Journal of Experimental Medicine*, vol. 205, no. 8, pp. 1903–1916, 2008.

[14] L. Maggi, V. Santarlasci, M. Capone et al., "CD161 is a marker of all human IL-17-producing T-cell subsets and is induced by RORC," *European Journal of Immunology*, vol. 40, no. 8, pp. 2174–2181, 2010.

[15] P. Chalan, B. J. Kroesen, K. S. M. van der Geest et al., "Circulating CD4+CD161+ T lymphocytes are increased in seropositive arthralgia patients but decreased in patients with newly diagnosed rheumatoid arthritis," *PLoS ONE*, vol. 8, no. 11, Article ID e79370, 2013.

[16] J. Miao, J. Geng, K. Zhang et al., "Frequencies of circulating IL-17-producing CD4+CD161+ T cells and CD4+CD161+ T cells correlate with disease activity in rheumatoid arthritis," *Modern Rheumatology*, vol. 24, no. 2, pp. 265–570, 2014.

[17] F. C. Arnett, S. M. Edworthy, D. A. Bloch et al., "The American Rheumatism Association 1987 revised criteria for the classification of rheumatoid arthritis," *Arthritis and Rheumatism*, vol. 31, no. 3, pp. 315–324, 1988.

[18] M. A. Kleinschek, K. Boniface, S. Sadekova et al., "Circulating and gut-resident human Th17 cells express CD161 and promote intestinal inflammation," *Journal of Experimental Medicine*, vol. 206, no. 3, pp. 525–534, 2009.

[19] A. Poggi, P. Costa, M. R. Zocchi, and L. Moretta, "Phenotypic and functional analysis of CD4+ NKRP1A+ human T lymphocytes. Direct evidence that the NKRP1A molecule is involved in transendothelial migration," *European Journal of Immunology*, vol. 27, no. 9, pp. 2345–2350, 1997.

[20] P. Chalan, B. J. Kroesen, K. S. M. van der Geest et al., "Circulating CD4+CD161+ T lymphocytes are increased in seropositive arthralgia patients but decreased in patients with

newly diagnosed rheumatoid arthritis," *PLoS ONE*, vol. 8, no. 11, Article ID e79370, 2013.

[21] A. Poggi, P. Canevali, M. Contatore, and G. Ciprandi, "Higher frequencies of CD161+ circulating T lymphocytes in allergic rhinitis patients compared to healthy donors," *International Archives of Allergy and Immunology*, vol. 158, no. 2, pp. 151–156, 2012.

[22] A. Mitsuo, S. Morimoto, Y. Nakiri et al., "Decreased CD161+CD8+ T cells in the peripheral blood of patients suffering from rheumatic diseases," *Rheumatology*, vol. 45, no. 12, pp. 1477–1484, 2006.

[23] J. C. Crispín and G. C. Tsokos, "Human TCR-$\alpha\beta$+ CD4− CD8− T cells can derive from CD8+ T cells and display an inflammatory effector phenotype," *The Journal of Immunology*, vol. 183, no. 7, pp. 4675–4681, 2009.

[24] J. C. Crispín, M. Oukka, G. Bayliss et al., "Expanded double negative T cells in patients with systemic lupus erythematosus produce IL-17 and infiltrate the kidneys," *Journal of Immunology*, vol. 181, no. 12, pp. 8761–8766, 2008.

[25] A. Alunno, O. Bistoni, E. Bartoloni et al., "IL-17-producing CD4-CD8- T cells are expanded in the peripheral blood, infiltrate salivary glands and are resistant to corticosteroids in patients with primary Sjögren's syndrome," *Annals of the Rheumatic Diseases*, vol. 72, no. 2, pp. 286–292, 2013.

Hindawi Publishing Corporation
Mediators of Inflammation
Volume 2015, Article ID 918089, 9 pages
http://dx.doi.org/10.1155/2015/918089

Research Article

The Combination of N-Acetyl Cysteine, Alpha-Lipoic Acid, and Bromelain Shows High Anti-Inflammatory Properties in Novel *In Vivo* and *In Vitro* Models of Endometriosis

C. Agostinis,[1] S. Zorzet,[2] R. De Leo,[1] G. Zauli,[1] F. De Seta,[1,3] and R. Bulla[2]

[1]*Institute for Maternal and Child Health, IRCCS Burlo Garofolo, 34137 Trieste, Italy*
[2]*Department of Life Sciences, University of Trieste, Via Valerio 28, 34127 Trieste, Italy*
[3]*Department of Medical, Surgical and Health Sciences, University of Trieste, Ospedale di Cattinara, Strada di Fiume 447, 34149 Trieste, Italy*

Correspondence should be addressed to R. Bulla; rbulla@units.it

Received 4 August 2014; Accepted 3 October 2014

Academic Editor: Lifei Hou

To evaluate the efficacy of an association of N-acetyl cystein, alpha-lipoic acid, and bromelain (NAC/LA/Br) in the treatment of endometriosis we set up a new *in vivo* murine model. We explored the anti-inflammatory and proapoptotic effect of this combination on human endometriotic endothelial cells (EECs) and on endothelial cells isolated from normal uterus (UtMECs). We implanted fragments of human endometriotic cysts intraperitoneally into SCID mice to evaluate the efficacy of NAC/LA/Br treatment. UtMECs and EECs, untreated or treated with NAC/LA/Br, were activated with the proinflammatory stimulus TNF-α and their response in terms of VCAM1 expression was evaluated. The proapoptotic effect of higher doses of NAC/LA/Br on UtMECs and EECs was measured with a fluorogenic substrate for activated caspases 3 and 7. The preincubation of EECs with NAC/LA/Br prior to cell stimulation with TNF-α prevents the upregulation of the expression of the inflammatory "marker" VCAM1. Furthermore NAC/LA/Br were able to induce EEC, but not UtMEC, apoptosis. Finally, the novel mouse model allowed us to demonstrate that mice treated with NAC/LA/Br presented a lower number of cysts, smaller in size, compared to untreated mice. Our findings suggest that these dietary supplements may have potential therapeutic uses in the treatment of chronic inflammatory diseases like endometriosis.

1. Introduction

Endometriosis (EM) is a chronic estrogen-dependent disorder characterized by the presence of endometrium-like tissue outside the uterine cavity. It is associated with dysmenorrhea, dyspareunia, noncyclic pelvic pain, subfertility, and infertility [1]. This frequent gynaecological disease affects 10–15% of women in reproductive age [2]. It is well accepted that a blood supply is essential for the survival of endometriotic implants and the development of EM, as blood is crucial for providing nutrients and growth factors and for promoting recruitment of inflammatory cells to the endometriotic lesions, as described by Groothuis [3]. Endometriotic lesions are highly vascularized, and it is now widely accepted that the formation of new blood vessels at implantation sites plays a key role in the growth of endometriotic cells [4]. Furthermore, eutopic endometrium from women with EM has greater angiogenic potential than eutopic endometrium from healthy subjects [5]. Since the growth of newly formed blood vessels is of pivotal importance in the development of EM, the inhibition of angiogenesis may offer an opportunity for treatment [6–8]. In this respect, it is noteworthy that vascular endothelium is known to play a critical role in regulation of inflammatory processes [9] and that cell adhesion molecules such as vascular cell adhesion molecule-1 (VCAM1), as well as proinflammatory cytokines, play key roles in the pathogenesis of EM [10].

EM can be treated by excising peritoneal implants, deep nodules, and ovarian cysts. Although lesion eradication is

considered a fertility-enhancing procedure, the benefit on reproductive performance is moderate [11]. Surgical removal of ectopic lesions represents the first line of intervention for the treatment of EM but is characterized by a relevant percentage of recurrences [12]. In addition, a variety of medical hormonal therapies, that all aimed to reduce the levels of circulating estrogens, are currently available [13]. However, these treatments are often unsatisfactory and cannot be used over long periods of time, due to the occurrence of severe adverse effects [14]. Therefore, new and improved therapeutic solutions that can efficiently reduce lesions with limited side effects and no interference with the patient's fertility are definitely desirable. In this respect, it has been recently shown that N-acetyl cysteine (NAC) effectively treats ovarian endometriosis. In terms of reduction in cysts size, the data reported by Porpora et al. are even more favorable than those granted by the currently adopted hormonal treatments, with the further advantages of fertility preservation and of the virtual absence of undesired side effects [15].

On these bases, the aim of this study was to investigate the effects of an association of NAC, alpha-lipoic acid (LA), and bromelain (Br) *in vivo* after establishing a novel model of EM based on the injection of human endometrial tissue in the peritoneum of SCID mice. In addition, the of NAC/LA/Br combination was analyzed *in vitro* on microvascular endothelial cells isolated from human endometriotic tissues (EECs) as well as in microvascular endothelial cells isolated from human endometrium (UtMECs).

2. Materials and Methods

2.1. Preparation of the Compound Mixture. All components of the mixture were purchased from Sigma-Aldrich (Milan, Italy) and solutions were sterilized by 0.22 μm filtration. Stock concentrations were 10 mg/mL in H_2O for NAC, 5 mg/mL in absolute ethanol for LA, and Br 1 mg/mL in PBS for Br. NAC and LA solutions were stored at 4°C while Br at −20°C until use. All reagents were tested for sterility and LPS. For cell culture studies, the three drugs were combined in complete cell culture medium at a final concentration of 1000 μg/mL NAC + 500 μg/mL LA + 50 μg/mL Br. In these conditions, the solution did not form visible precipitates and pH was stable (measured with pH-Meter BASIC20+, CRISON INSTRUMENT). To choose the optimal concentrations for the *in vitro* studies, we have referred to the concentrations of NAC, LA, and Br, proportionally to those present in the new dietary supplement Naxend (Pizeta Pharma, Perugia, Italy; 72.72% NAC, 24.24% LA and 3.03% Br), considering also their bioavailability, the absorption, and the peak plasma of each compound.

2.2. Human Tissues. The Maternal-Children's Hospital (RC 08/13, IRCCS "Burlo Garofolo," Trieste, Italy) approved this study, and following informed consent, endometriosis specimens were obtained from women undergoing laparoscopy to remove endometrial cysts and endometrial tissue was fertile women undergoing hysterectomy for leiomyomatosis in the midproliferative and midsecretory phase defined according to Noyes criteria [16].

2.3. Animals. Female SCID mice (4–6 weeks of age) were purchased from Charles River (Milan, Italy) and maintained under pathogen-free conditions. All the experimental procedures involving animals were done in compliance with the guidelines of the European (86/609/EEC) and the Italian (D.L.116/92) laws and were approved by both the Italian Ministry of Health and the Administration of the University Animal House.

2.4. Animal Model and Ex Vivo Analysis of Cysts. Endometriotic tissue from three peritoneal cysts was collected in sterile PBS and then suspended as coarse fragments, loaded in 3 mL syringes, and standardized with respect to volume and weight. A volume of 0.5 mL of cyst suspension approximately equal to 0.4 g of wet tissue was injected by 16 ga needle intraperitoneally into SCID mice (Charles River). Hormonal therapy with 17-β-estradiol-3-benzoate (Sigma-Aldrich, 30 μg/kg i.m.) was initiated at the time of cyst tissue injection and at 3-day intervals thereafter. The day after injection mice were divided randomly in two groups and we administered only to the first one NAC 250 mg/kg/die, LA 125 mg/kg/die, and Br 12,5 mg/kg/die *per os*. Twenty-one days following injection, the animals were killed and implanted endometriotic lesions in treated ($n = 7$) or untreated mice ($n = 9$) were identified, counted, resected, and collected in formalin 10%.

Endometriotic lesions excised from SCID mice were fixed in 10% buffered formalin and paraffin embedded. Four-micrometers-thick sections were stained with Diff-Quick (Biomap, Milan, Italy) staining (following the manufacturer instructions) and examined for the presence and distribution of vessels and glands. For immunohistochemical analysis, the slides were microwaved three times in Tris-HCl/EDTA (ethylenediamine tetraacetic acid) pH 9.0 buffer (Dako) for 5 min, brought to RT, and washed in PBS. After neutralization of the endogenous peroxidase with H_2O_2 for 10 min, the sections were first incubated with protein block (Dako) for 10 min and then with the primary antibodies for 1 h at RT (polyclonal rabbit anti-human vWF from Dako). The bound antibodies were revealed using the horseradish peroxidase- (HRP-) conjugated anti-rabbit IgG antibodies (Sigma-Aldrich) and diaminobenzidine (DAB) as substrate (Dako). Slides were evaluated under Leica DM3000 microscope (Leica, Wetzlar, Germany) and the pictures were collected using a Leica DFC320 digital camera (Leica).

2.5. Immunofluorescent Staining. Endometriotic tissue fragments approximately 1 cm^3 were embedded in OCT (BioOptica, Milan, Italy), snap-frozen in liquid nitrogen, and kept at −80°C until use. Cryostat sections of about 6 μm were air dried, fixed in acetone, and either used immediately or kept at −80°C. Binding of mouse anti-human cytokeratin 8/18 (CK8/18) or mouse anti-human vWF (Dako, Milan, Italy) was detected by incubating the sections with goat anti-mouse IgG Cy3-conjugated secondary antibodies 30 min at RT, and then the nuclei were stained blue with DAPI (4′,6-diamidino-2-phenylindole, Sigma-Aldrich) 1 μg/mL.

2.6. Cell Isolation and Culture. UtMECs and EECs were isolated and characterized as previously described by Bulla et al. [17]. Both ECs were positively selected with Dynabeads M-450 (Life Technologies, Milan, Italy) coated with *Ulex europaeus* 1 lectin (Sigma-Aldrich), seeded on 12,5 cm^2 flask precoated with 2 $\mu g/cm^2$ fibronectin (Roche, Milan, Italy), and maintained in serum-free endothelial basal medium (Life Technologies, Monza, Italy) supplemented with 20 ng/mL bFGF (basic Fibroblast Growth Factor), 10 ng/mL EGF (Epidermal Growth Factor), 10% FCS (all from Life Technologies), and 10% human serum and incubated at 37°C, 5% CO_2. The purity of the resulting EC populations was more than 98% as verified by staining with antibodies to VWF, CD105, VE cadherin (Dako, Milano, Italy), and CD31/PECAM-1 kindly provided by M. R. Zocchi (San Raffaele Hospital, Milan, Italy).

2.7. Immunofluorescence on Endothelial Cells. ECs were plated in 8-chamber culture slides (BD Biosciences Discovery Labware, Milan, Italy) coated with 2 $\mu g/cm^2$ fibronectin (Roche) and incubated at 37°C in CO_2 enriched atmosphere. When cells grew to confluence, they were fixed and permeabilized with FIX & PERM cell permeabilization kit (Società Italiana Chimici, Rome, Italy). Then cells were incubated with primary mAb, (cloneF8/86) mouse anti-human vWF (Dako), or mouse anti-human CD31 (Immunotools, Germany) for 1 h at room temperature (RT) followed by FITC-conjugated goat anti-mouse IgG for 1 h at RT. Images were acquired with Leica DM3000 microscope (Leica) and the pictures were collected using a Leica DFC320 digital camera (Leica).

2.8. Cytofluorimetric Analysis. ECs were detached from culture flasks with 5 mM EDTA at 37°C and a total number of 5 $\times 10^5$ were fixed with FIX & PERM cell permeabilization kit (Società Italiana Chimici) and incubated in permeabilization solution in ice for 30′ with mAb (clone 9) mouse anti-human vimentin (Sigma-Aldrich), mAb (cloneF8/86) mouse anti-human vWF, or mAb (cloneV9) mouse anti-human CK8/18. The binding of primary antibodies was detected by incubation with FITC-conjugated goat anti-mouse IgG. The membrane antigens were detected on unfixed cells, using monoclonal anti-human CD31, CD45, CD34, and CD105 directly FITC-conjugated, all purchased from Immunotools (Germany). The cells were fixed with 1% paraformaldehyde (Sigma-Aldrich) and analyzed for fluorescence with a FACScalibur instrument (BD Falcon, Milan, Italy) using CellQuest software.

2.9. Whole Cell VCAM1 ELISA. Both types of cells were grown to the confluence in 96-well plates and incubated with drugs (concentration of NAC 10 μg/mL, LA 9 μg/mL, and Br 2 μg/mL), alone or in association, for 48 h 37°C 5% CO_2. Successively the cells were stimulated overnight with TNF-α (100 ng/mL), washed with Dulbecco's PBS added with 2% BSA (Bovine Serum Albumine, fraction V, Sigma-Aldrich) and $CaCl_2$-$MgCl_2$ 0,7 mM (Sigma-Aldrich), and then incubated with mouse mAb anti-human VCAM1 (Sigma-Aldrich) 5 μg/mL for 90 min at RT. The binding of primary antibody was reveled incubating the cells with a polyclonal anti-mouse IgG conjugated with alkaline phosphatase. The enzymatic reaction was developed with PNPP (p-nitrophenyl phosphate) (Sigma-Aldrich; 1 mg/mL) as substrate and read kinetically at 405 nm using a Titertek Multiskan ELISA reader (Flow Labs, Milano, Italy).

2.10. Apoptosis Assay. Both types of cells were grown to 80% of confluence in 96-well plates and incubated with the compounds, alone or in association, for 72 h 37°C. After then cells were incubated with 5 μM of CellEvent Caspase-3/7 Green Detection Reagent (Life Technologies), a fluorogenic substrate for activated caspases 3 and 7. The reagent consists of a four amino acid peptide (DEVD) conjugated to a nucleic acid binding dye. This cell-permeant substrate is intrinsically nonfluorescent, because the DEVD peptide inhibits the ability of the dye to bind to DNA. After activation of caspase-3 or caspase-7 in apoptotic cells, the DEVD peptide is cleaved, enabling the dye to bind to DNA and produce a bright, fluorogenic response with an absorption/emission maxima of ~502/530 nm. The fluorescence data were acquired with TECAN Infinite200 and normalized for total protein present in each well. For the protein quantitation the cells were then lysed with NaOH 1 M and evaluated by Bradford assay as previously reported [18].

3. Statistical Analysis

For each set of experiments, values are reported as means ± SE. The results were evaluated by using the Mann-Whitney test. Statistical significance was defined as $P < 0.05$.

4. Results

4.1. Establishment of a Relevant In Vivo Model for EM and Efficacy of the NAC/LA/Br Combination in Decreasing the Number of Cysts Formation In Vivo. The primary aim of our study was the evaluation of the effect of NAC/LA/Br in a relevant model of EM. For this purpose, we set up a new mouse model, modifying the animal model described by Awwad and colleagues [19] and by Grummer and colleagues [20]. Specifically, we used human endometriotic tissue obtained from ovarian cysts instead of normal human endometrium to create the endometriotic lesions into the peritoneal cavity of SCID mice. Endometriotic tissue from three peritoneal cysts was injected in the peritoneal cavity of SCID mice. Hormonal therapy with 17-β-estradiol-3-benzoate was initiated at the time of injection and at intervals of 3 days thereafter. Twenty-one days following injection, the animals were killed and implanted endometriotic lesions were identified, analyzed, and characterized. This protocol provided an implantation rate of 100% and the dimension and the histology of these cysts were evaluated. Excised explants revealed the presence of EM-like features upon histologic examination, that is, stroma and endometrial glands. All the implants showed a well restructured columnar and/or cuboidal glandular epithelium with cytogenetic stroma. A nascent capillary network was present at the interface between the implant and the underlying murine tissue. The presence of new

vessels, indicated with black arrows in Figure 1(a), was confirmed by immunohistochemistry, staining the sections with anti-vWF polyclonal antibodies (Figure 1(b)). For these *in vivo* experiments, we treated the animals daily with NAC (250 mg/kg), LA (125 mg/kg), and Br (12,5 mg/kg) provided in the animals' water bottles, a *per os* administration that mimics human dosing [21]. To choose the optimal concentrations of NAC, LA, and Br, we have referred to the concentrations of NAC, LA, and Br, proportionally to those present in the new dietary supplement Naxend (Pizeta Pharma, Perugia, Italy; 72.72% NAC, 24.24% LA, and 3.03% Br).

As shown in Figure 1(c), all control group animals developed at least 1 cyst, with up to 4 in some control animals. In 4 mice treated with the NAC/LA/Br combination, no cyst was visible and in 3 mice only 1 cyst was present. The number of cysts developing in treated compared to untreated animals was significantly ($P < 0.05$) lower (Figure 1(d)). It is also noteworthy that the cysts present in the untreated animal were larger than those in the treated mice.

4.2. Isolation and Characterization of Endometriotic Endothelial Cells (EECs) and Evaluation of Their In Vitro Response to the NAC/LA/Br Combination. Since endothelial cells play a significant role in the development of endometriotic lesions [4], as also confirmed in our animal model, we next developed a new protocol for the isolation and culture of endothelial cells from human endometriotic ovarian cysts. For this purpose, the presence and the density of the vessels inside human endometriotic cysts were initially analyzed by immunofluorescence on sections of human endometriotic tissues. The sections were stained with mAb anti-human vWF, a classical endothelial cell marker, and with CK8/18, in order to evidence the presence of endometriotic glands. Figure 2 clearly shows the presence of several vessels inside the cysts and the presence of one representative gland. These samples were then used to isolate the endothelial cells. The isolated endothelial cells cultured on fibronectin easily reach confluence within few days. The morphology of cultured EECs stained with mAb anti-CD31, another typical marker of endothelial cells, is shown in Figure 3. We then characterized EECs by cytofluorimetric analysis in order to evaluate the purity of these cells and to exclude the presence of contaminating cells. 100% of these cells were positive for classical endothelial cell markers (CD31, CD105, vWF, and vimentin) and 80% were positive for CD34, a marker for newly formed vessels (Figure 3). Cultured EECs were devoid of expression of the epithelial marker CK8/18 and leukocyte marker CD45. Consistent results were obtained for EEC populations derived from five different patients.

4.3. NAC/LA/Br Exerts Anti-Inflammatory Effect Reducing the Expression of VCAM1 in TNF-α Stimulated EECs. In next group of experiments, EECs from 5 distinct patients were grown to confluence and then stimulated with 100 ng/mL of the proinflammatory cytokine TNF-α in order to upregulate the expression of the adhesion molecule VCAM1 [22], which represent a proinflammatory marker. We compared the total amount of VCAM1 by ELISA on EECs untreated, EECs stimulated for 12 hours with TNF-α, and cells treated with TNF-α previously preincubated for 72 hours with NAC, LA, and Br, (NAC 10 μg/mL, AL 9 μg/mL, and Br 2 μg/mL) used alone or in association. No reduction in VCAM1 expression was observed in cells treated with individual drugs (Figure 4(a)). Only the drug combination exerted a statistically ($P < 0.05$) significant although incomplete decrease of VCAM1 levels as compared to TNF-α-treated cultures. For comparison, we have used endothelial cells isolated from normal human endometrium from women undergoing hysterectomy (UtMECs) [17]. As shown in Figure 4(b), the downregulation of VCAM1 in TNF-α-treated UtMECs was complete in the presence of the combination of NAC + Br + LA (MIX). The addition of NAC/LA/Br to the endothelial cell culture media did not alter the medium pH and no effect to the cell viability was observed for ECs treated with the same concentrations of compounds as assessed by trypan blue staining (data not shown).

4.4. NAC/LA/Br Combination Selectively Exerts Proapoptotic Activity on EECs. In order to evaluate whether besides the anti-inflammatory activity the NAC, LA, and Br mixture might also affect endothelial cell viability, EECs were plated on 8-chamber culture slides, grown to 80% confluence, and incubated for 72 h with NAC, LA, and Br (NAC 20 μg/mL, AL 18 μg/mL, and Br 4 μg/mL) used alone or in combination. As shown in Figures 5(a)-5(b), EECs incubated with the mixture of compounds showed a decreased number of viable cells as compared to untreated cultures. Based on these results, we then investigated the ability of NAC/LA/Br to induce apoptosis. Both EECs and UtMECs were incubated with a fluorogenic substrate for activated caspases 3 and 7 and the fluorescence values obtained were normalized for total protein present in each well. As shown in Figure 5(c), treatment of the cells with the NAC/LA/Br mixture, at these higher concentrations, was able to induce a statistically significant ($P < 0.05$) increase of apoptosis of EECs. In fact, the induction of caspase activity induced by the drug combination was comparable to that of positive control (H_2O_2). Of note, the NAC/LA/Br mixture was totally ineffective in UtMECs (Figure 5(d)).

5. Discussion

Most recent guidelines for the treatment of endometriosis-associated symptoms recommend to surgically treat endometriosis, as this is effective for reducing endometriosis-associated pain for those in whom medical treatment has failed [23]. Medical treatments for EM are usually aimed at reducing the production of endogenous estrogens or inducing endometrial differentiation with progestins. The pain associated with endometriosis is usually treated initially with oral contraceptive agents or non-steroidal anti-inflammatory drugs, because these agents have fewer side effects and are less expensive than other treatment options. GnRH agonists, as well as other agents such as danazol or progestational agents,

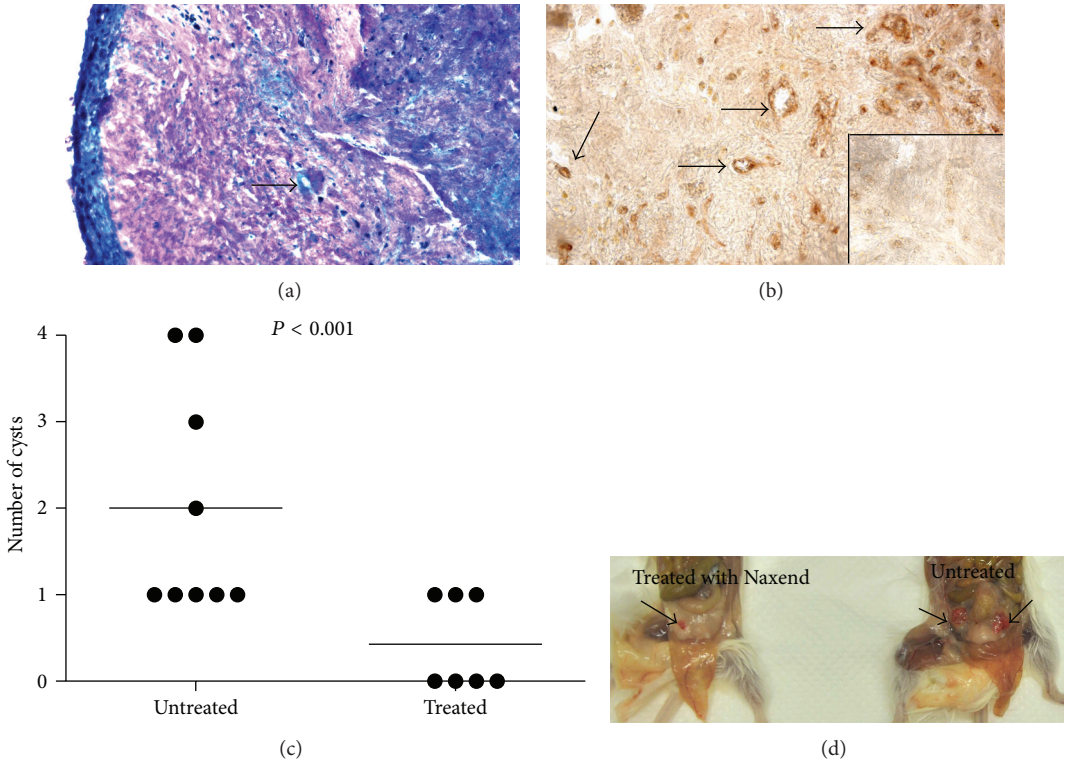

Figure 1: NAC/LA/Br reduces the number and the dimension of cysts in a new *in vivo* model of EM. (a) Histochemical analysis of an endometriotic lesion in mice with Diff-Quick staining. Original Magnification 100x. (b) Immunohistochemical analysis of a cyst excised from the peritoneum of mice. Sections were stained with rabbit anti-vWF followed by a secondary antibody to rabbit IgG HRP conjugated and revealed with DAB. The inset showed the staining obtained with only secondary antibody. Original Magnification 100x. (c) Number of cysts counted in untreated mice ($n = 9$) or treated with NAC 250 mg/kg/die, AL 125 mg/kg/die, and Br 12,5 mg/kg/die ($n = 7$). Mann-Whitney test $P < 0.001$. (d) Representative image of the different morphological appearance of cysts in treated or untreated SCID mice.

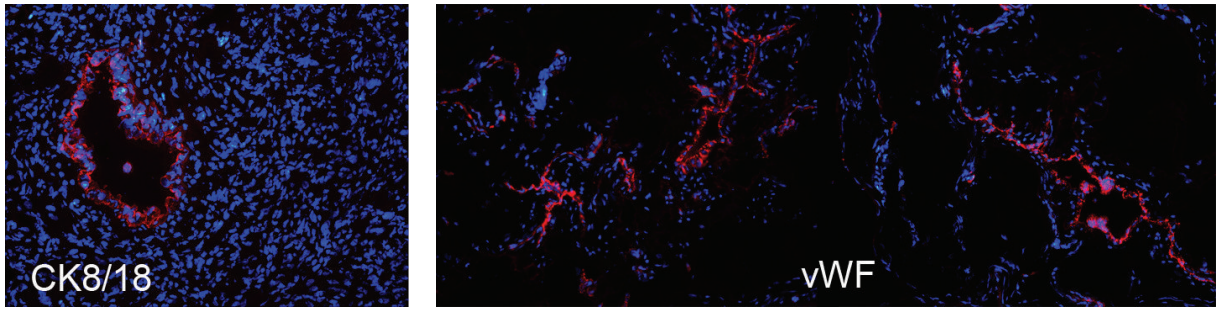

Figure 2: Immunofluorescence analysis of human endometriotic cysts. The frozen sections were stained with mAb anti-human vWF to highlight the vessels or with mAb anti-human CK 8/18 to show the glands. The binding of mouse monoclonal antibodies was revealed by the incubation with goat anti-mouse IgG Cy3-conjugated secondary antibodies. Nuclei were stained in blue by DAPI: original magnification 100x.

and, recently, aromatase inhibitors are usually reserved for use if the first-line agents fail to provide an acceptable degree of relief. These agents represent standard therapies for EM but are associated with long-term side effects [14]. Although currently available medical therapies are not curative *per se*, they are important for pain suppression and lesion regression. Thus, efforts are still being focused on the improvement and promotion of new treatments with higher efficacy and fewer side effects. A high number of medications have been tested in preclinical models of endometriosis due to their theoretical capacity of disrupting important pathophysiologic pathways of the disease, such as inflammatory response, angiogenesis and cell survival, proliferation, migration, adhesion, and invasion. TNF-α blockers, nuclear factor kB inhibitors, antiangiogenic agents, statins, antioxidants, immune-modulators, flavonoids, histone deacetylase

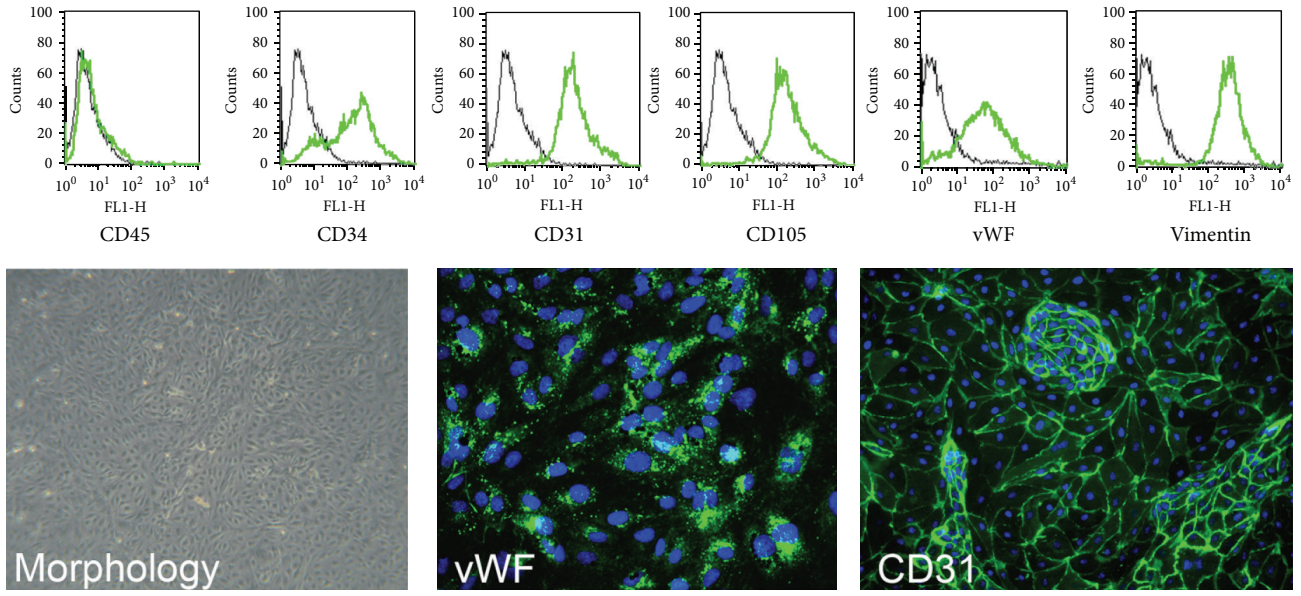

Figure 3: Characterization of the purity of endothelial cells isolated from endometriotic tissue. (A) EECs were characterized by cytofluorimetric analysis for the expression of CD45, CD34, CD31, CD105, vWF, and vimentin, and the expression of these markers (green lines) was compared with correlated control antibodies (black lines). The expression of vWF and CD31 was confirmed by immunofluorescence, on EECs grown to confluence in 8-chamber culture slides. After fixation and permeabilization the cells were stained with mAb anti-human CD31 or anti-vWF. The binding of mouse monoclonal antibodies was revealed by the incubation with goat anti-mouse IgG FITC-conjugated secondary antibodies. Nuclei were stained in blue by DAPI: original magnification 200x.

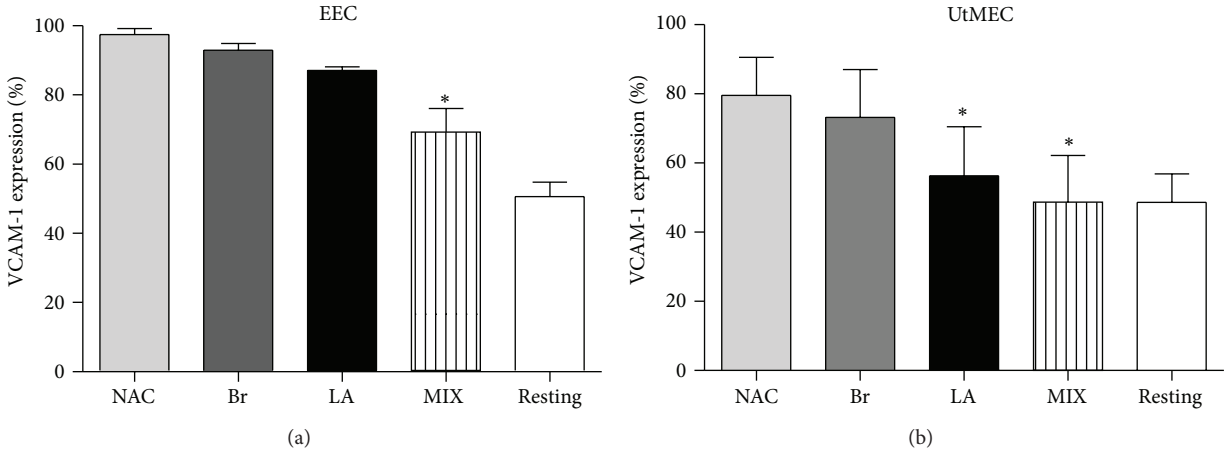

Figure 4: Anti-inflammatory effect of NAC/LA/Br on ECs: analysis of VCAM1 expression. Five different populations of endometriotic endothelial cells (EECs) and 5 different populations of uterine microvascular endothelial cell (UtMECs) were isolated, as described by Bulla et al. [17] with some modifications. ECs were grown to confluence in a 96-well plate and then incubated with NAC 10 μg/mL, AL 9 μg/mL, and Br 2 μg/mL, alone or in association (MIX). Successively the cells were stimulated overnight with TNF-α (100 ng/mL) and incubated with anti-human VCAM1. The binding of primary antibody was revealed incubating the cells with a goat anti-mouse IgG conjugated with alkaline phosphatase. The 100% of VCAM1 expression is referred to the TNF-α-treated cells. Data are expressed as mean ± SE of results from five experiments each performed in triplicate. $^{*}P < 0.05$ with respect to the untreated (Mann-Whitney test).

inhibitors, matrix metalloproteinase inhibitors, metformin, novel modulators of sex steroids expression, and apoptotic agents were all effective *in vitro* and/or in animal models. Most of these agents did not reach the clinical setting, mainly because of the high risk of adverse effects [24].

An alternative approach for treatment of EM is represented by anti-inflammatory compounds [11]. In particular, Pittaluga and colleagues [25] and Onalan et al. [26] recently demonstrated the efficacy of NAC in two different *in vivo* models of EM. No data are available on the use of LA

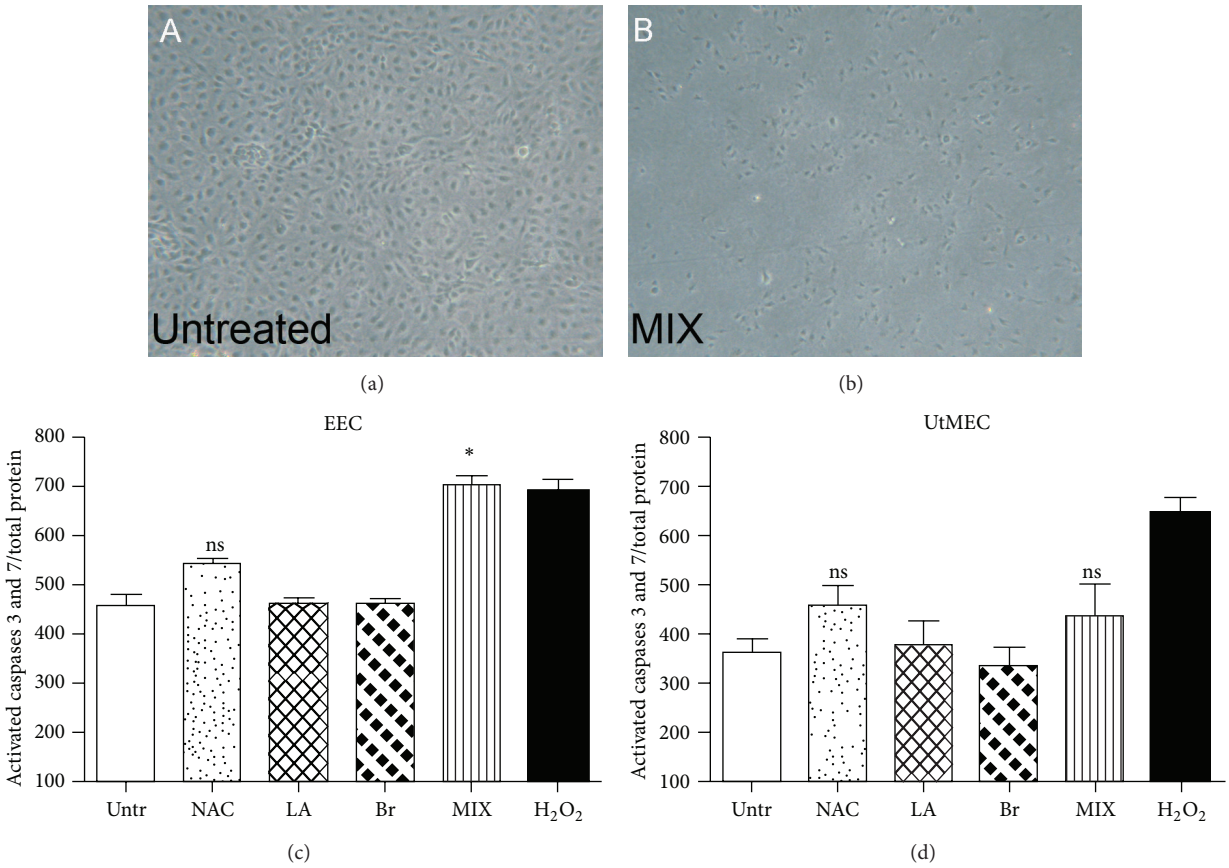

Figure 5: Evaluation of the proapoptotic effect of NAC/LA/Br on ECs. (a), (b) Morphologic appearance of EECs untreated (a) or incubated with NAC 20 μg/mL, AL 18 μg/mL, and Br 4 μg/mL in association (MIX) (b). (c), (d) Both types of cells were grown to 80% of confluence in 96-well plates and incubated with NAC 20 μg/mL, AL 18 μg/mL, and Br 4 μg/mL, alone or in association (MIX), for 72 h 37°C. The cells were then incubated with 5 μM of CellEvent Caspase-3/7 Green Detection Reagent (Life Technologies), a fluorogenic substrate for activated caspases 3 and 7. The fluorescence data were normalized for the total protein present in each well. Data are expressed as mean ± SE of results from three experiments each performed in triplicate. $^*P < 0.05$ with respect to the untreated (Mann-Whitney test).

and Br for the treatment of EM but they are currently in clinical use for the treatment of inflammatory diseases [27, 28]. Endometriotic lesions are highly vascularized, and it is now widely accepted that the formation of new blood vessels in implanted places plays a key role in the growth of endometriotic cells [4]. The growth of newly formed blood vessels is of pivotal importance in the development of EM, so inhibition of angiogenesis may offer a new opportunity for treatment [29]. Therefore, in this study we have proposed an innovative *in vitro* model to study the efficacy of a new treatment for EM, based on the analysis of endometriotic endothelial cell response, in consideration of the key role of endothelial cells in controlling inflammation and angiogenesis. A first important achievement of our study was the establishment of a novel mouse model based on the intraperitoneal injection of endometriotic human tissue in SCID mice. In analogous models available in the literature, fragments of human endometriotic cysts were surgically fixed to the peritoneal wall [20]. The benefit of our model is that our procedures reduce animal suffering and animal losses. The fact that all treated animals developed at least one cyst is a profoundly beneficial aspect of this model. Immunohistochemical observations indicated that the tissue excised from murine peritoneum developed several new vessels, indicating that the cysts had a morphological organization similar to human cysts with new blood vessel formations. Thanks to the development of this mouse model we have been able to demonstrate the effectiveness of NAC/LA/Br *in vivo* with the result that treated mice presented a lower number of cysts, which were also smaller in size than those in untreated mice.

A second important finding of our study was the successful isolation of pure endothelial cells from human endometriotic lesions. Using these cells to set up an *in vitro* model that exploits the endothelial cells is preferable, since many differences exist between endothelial cells isolated from different sites [30]. Our results indicated that when used alone the three studied compounds are able to induce only a modest or null inhibition of TNF-α activation of VCAM1 and a strong inhibition when used in combination, suggesting the presence of an additive effect of the three compounds. In line with our current data previous findings obtained on hypertensive patients (with type 2 diabetes) treated with NAC

experienced reduction of C-reactive protein, intracellular adhesion molecule, and vascular cell adhesion molecule [31]. In addition, Tisato et al. documented that LA significantly decreased the baseline levels of PDGF, RANTES, and CXCL10 expression and counteracted TNF-α-induced NF-B and p38/MAPK activation in endothelial cells from chronic venous disease patients [27]. A second important finding of our study was the ability of NAC/LA/Br to promote apoptosis in EEC. In this respect, it should be underlined that the *in vitro* behavior of UtMECs was different as these cells were totally unaffected by the NAC/LA/Br combination in terms of apoptosis induction. These findings underline the importance not only of tissue-specificity but also of pathological specificity of endothelial cells. This might explain the partial discrepancies of our current data with those of Cai et al. [32] and Mohr and Desser [33] which, respectively, indicated that Br inhibits endothelial cell invasion and angiogenesis, while Larghero et al. [34] demonstrated that LA induced apoptosis through the production of the proapoptotic TNF-alpha-related apoptosis-inducing ligand (TRAIL) cytokine in endothelial cells [34].

6. Conclusions

In conclusion, we have adopted an improved *in vivo* model of EM, which reduces animal suffering by nonsurgical implantation of tissue from human cysts. Moreover, EECs are a unique, human-derived, easily available, *in vitro* model of EM that may advance study of the inflammatory process and the role of angiogenesis in endometriosis. Thanks to these models, we could demonstrate that NAC/LA/Br is an effective treatment for EM that may have potential therapeutic uses in the prevention and treatment of patients. It would be interesting in a further study to compare the effect of NAC/LA/Br with standard therapies and to evaluate if the use of NAC/LA/Br in combination with standard therapies may lead to the improvement of the standard medical treatment for EM.

Conflict of Interests

The authors declared that they have no conflict of interests regarding the publication of this paper.

Authors' Contribution

C. Agostinis and S. Zorzet contributed equally to this work. F. De Seta and R. Bulla share senior authorship.

Acknowledgments

The contribution of Stefania Consenti e Francesca Gelleni is gratefully acknowledged. This work was supported by Grants from the Ministry of Health (Ricerca Finalizzata RC41/08 e RC 01/09), Fondazione Casali to R. Bulla, and by a generous/liberal donation from PiZeta Pharma S.p.A, Perugia, Italy.

References

[1] N. Berlanda, P. Vercellini, E. Somigliana, M. P. Frattaruolo, L. Buggio, and U. Gattei, "Role of surgery in endometriosis-associated subfertility," *Seminars in Reproductive Medicine*, vol. 31, no. 2, pp. 133–143, 2013.

[2] P. Vercellini, L. Fedele, G. Aimi, G. Pietropaolo, D. Consonni, and P. G. Crosignani, "Association between endometriosis stage, lesion type, patient characteristics and severity of pelvic pain symptoms: a multivariate analysis of over 1000 patients," *Human Reproduction*, vol. 22, no. 1, pp. 266–271, 2007.

[3] P. G. Groothuis, "Angiogenesis and vascular remodelling in female reproductive organs," *Angiogenesis*, vol. 8, no. 2, pp. 87–88, 2005.

[4] Q.-Y. Jiang and R.-J. Wu, "Growth mechanisms of endometriotic cells in implanted places: a review," *Gynecological Endocrinology*, vol. 28, no. 7, pp. 562–567, 2012.

[5] S. E. Hur, J. Y. Lee, H.-S. Moon, and H. W. Chung, "Angiopoietin-1, angiopoietin-2 and Tie-2 expression in eutopic endometrium in advanced endometriosis," *Molecular Human Reproduction*, vol. 12, no. 7, pp. 421–426, 2006.

[6] K. Schweppe, "Histological and electron-microscopy studies on endometriosis," *Hormone Research*, vol. 32, no. 1, pp. 106–109, 1989.

[7] G. Hudelist, J. Keckstein, K. Czerwenka et al., "Estrogen receptor β and matrix metalloproteinase 1 are coexpressed in uterine endometrium and endometriotic lesions of patients with endometriosis," *Fertility and Sterility*, vol. 84, no. 2, pp. 1249–1256, 2005.

[8] J. Meola, J. C. Rosa e Silva, D. B. Dentillo et al., "Differentially expressed genes in eutopic and ectopic endometrium of women with endometriosis," *Fertility and Sterility*, vol. 93, no. 6, pp. 1750–1773, 2010.

[9] A. Mantovani, F. Bussolino, and E. Dejana, "Cytokine regulation of endothelial cell function," *The FASEB Journal*, vol. 6, no. 8, pp. 2591–2599, 1992.

[10] R. O. Burney and L. C. Giudice, "Pathogenesis and pathophysiology of endometriosis," *Fertility and Sterility*, vol. 98, no. 3, pp. 511–519, 2012.

[11] P. Crosignani, D. Olive, A. Bergqvist, and A. Luciano, "Advances in the management of endometriosis: an update for clinicians," *Human Reproduction Update*, vol. 12, no. 2, pp. 179–189, 2006.

[12] M. G. Porpora, D. Pallante, A. Ferro, B. Crisafi, F. Bellati, and P. Benedetti Panici, "Pain and ovarian endometrioma recurrence after laparoscopic treatment of endometriosis: a long-term prospective study," *Fertility and Sterility*, vol. 93, no. 3, pp. 716–721, 2010.

[13] R. W. Kistner, "Conservative management of endometriosis," *The Lancet*, vol. 79, no. 5, pp. 179–183, 1959.

[14] V. M. Rice, "Conventionalmedical therapies for endometriosis," in *Annals of the New York Academy of Sciences*, pp. 343–352, 2002.

[15] M. G. Porpora, R. Brunelli, G. Costa et al., "A promise in the treatment of endometriosis: an observational cohort study on ovarian endometrioma reduction by N-acetylcysteine," *Evidence-based Complementary and Alternative Medicine*, vol. 2013, Article ID 240702, 7 pages, 2013.

[16] R. W. Noyes, A. T. Hertig, and J. Rock, "Dating the endometrial biopsy," *American Journal of Obstetrics and Gynecology*, vol. 122, no. 2, pp. 262–263, 1975.

[17] R. Bulla, C. Agostinis, F. Bossi et al., "Decidual endothelial cells express surface-bound C1q as a molecular bridge between

endovascular trophoblast and decidual endothelium," *Molecular Immunology*, vol. 45, no. 9, pp. 2629–2640, 2008.

[18] P. Spessotto, R. Bulla, C. Danussi et al., "EMILIN1 represents a major stromal element determining human trophoblast invasion of the uterine wall," *Journal of Cell Science*, vol. 119, part 21, pp. 4574–4584, 2006.

[19] J. T. Awwad, R. A. Sayegh, X. J. Tao, T. Hassan, S. T. Awwad, and K. Isaacson, "The SCID mouse: an experimental model for endometriosis," *Human Reproduction*, vol. 14, no. 12, pp. 3107–3111, 1999.

[20] R. Grummer, F. Schwarzer, K. Bainczyk et al., "Peritoneal endometriosis: validation of an in-vivo model," *Human Reproduction*, vol. 16, no. 8, pp. 1736–1743, 2001.

[21] A. A. Bachmanov, D. R. Reed, G. K. Beauchamp, and M. G. Tordoff, "Food intake, water intake, and drinking spout side preference of 28 mouse strains," *Behavior Genetics*, vol. 32, no. 6, pp. 435–443, 2002.

[22] L. Osborn, C. Hession, R. Tizard et al., "Direct expression cloning of vascular cell adhesion molecule 1, a cytokine-induced endothelial protein that binds to lymphocytes," *Cell*, vol. 59, no. 6, pp. 1203–1211, 1989.

[23] G. A. J. Dunselman, N. Vermeulen, C. Becker et al., "ESHRE guideline: management of women with endometriosis," *Human Reproduction*, vol. 29, no. 3, pp. 400–412, 2014.

[24] S. R. Soares, A. Martínez-Varea, J. J. Hidalgo-Mora, and A. Pellicer, "Pharmacologic therapies in endometriosis: a systematic review," *Fertility and Sterility*, vol. 98, no. 3, pp. 529–555, 2012.

[25] E. Pittaluga, G. Costa, E. Krasnowska et al., "More than antioxidant: N-acetyl-L-cysteine in a murine model of endometriosis," *Fertility and Sterility*, vol. 94, no. 7, pp. 2905–2908, 2010.

[26] G. Onalan, C. Gulumser, B. Mulayim, A. Dagdeviren, and H. Zeyneloglu, "Effects of amifostine on endometriosis, comparison with N-acetyl cysteine, and leuprolide as a new treatment alternative: a randomized controlled trial," *Archives of Gynecology and Obstetrics*, vol. 289, no. 1, pp. 193–200, 2014.

[27] V. Tisato, G. Zauli, E. Rimondi et al., "Inhibitory effect of natural anti-inflammatory compounds on cytokines released by chronic venous disease patient-derived endothelial cells," *Mediators of Inflammation*, vol. 2013, Article ID 423407, 13 pages, 2013.

[28] S. Müller, R. März, M. Schmolz, B. Drewelow, K. Eschmann, and P. Meiser, "Placebo-controlled randomized clinical trial on the immunomodulating activities of low- and high-dose bromelain after oral administration—new evidence on the antiinflammatory mode of action of bromelain," *Phytotherapy Research*, vol. 27, no. 2, pp. 199–204, 2013.

[29] D. Djokovic and C. Calhaz-Jorge, "Angiogenesis as a therapeutic target in endometriosis," *Acta Médica Portuguesa*, vol. 27, no. 4, pp. 489–497, 2014.

[30] W. C. Aird, "Phenotypic heterogeneity of the endothelium: II. Representative vascular beds," *Circulation Research*, vol. 100, no. 2, pp. 174–190, 2007.

[31] V. Cherubini, M. Cantarini, E. Ravaglia, and E. Bartolotta, "Incidence of IDDM in the Marche Region, Italy," *Diabetes Care*, vol. 17, no. 5, pp. 432–435, 1994.

[32] T. Cai, G. Fassina, M. Morini et al., "N-acetylcysteine inhibits endothelial cell invasion and angiogenesis," *Laboratory Investigation*, vol. 79, no. 9, pp. 1151–1159, 1999.

[33] T. Mohr and L. Desser, "Plant proteolytic enzyme papain abrogates angiogenic activation of human umbilical vein endothelial cells (HUVEC) in vitro," *BMC Complementary and Alternative Medicine*, vol. 13, article 231, 2013.

[34] P. Larghero, R. Venè, S. Minghelli et al., "Biological assays and genomic analysis reveal lipoic acid modulation of endothelial cell behavior and gene expression," *Carcinogenesis*, vol. 28, no. 5, pp. 1008–1020, 2007.

Hindawi Publishing Corporation
Mediators of Inflammation
Volume 2015, Article ID 626934, 6 pages
http://dx.doi.org/10.1155/2015/626934

Research Article

The Evaluation of Plasma and Leukocytic IL-37 Expression in Early Inflammation in Patients with Acute ST-Segment Elevation Myocardial Infarction after PCI

Xin Wang,[1] Xiangna Cai,[2] Lan Chen,[1] Duanmin Xu,[1] and Jilin Li[1]

[1]*Department of Cardiology, First Affiliated Hospital of Shantou University Medical College, No. 57, Changping Road, Shantou, Guangdong 515041, China*
[2]*Department of Plastic Surgery, First Affiliated Hospital of Shantou University Medical College, No. 57, Changping Road, Shantou, Guangdong 515041, China*

Correspondence should be addressed to Jilin Li; lijilin@126.com

Received 16 August 2014; Accepted 3 October 2014

Academic Editor: Yi Fu Yang

Objective. Acute ST-segment elevation myocardial infarction (ASTEMI) is accompanied by increased expression of inflammation and decreased expression of anti-inflammation. IL-37 was found to be involved in the atherosclerosis-related diseases and increased in acute coronary syndrome. However, the level of IL-37 in blood plasma and leukocytes from patients with ASTEMI after percutaneous coronary intervention (PCI) has not been explored. *Methods*. We collected peripheral venous blood from consented patients at 12 h, 24 h, and 48 h after PCI and healthy volunteers. Plasma IL-37, IL-18, IL-18-binding protein (BP), and high sensitive C reaction protein (hs-CRP) were quantified by ELISA and leukocytic IL-37 and ICAM-1 by immunoblotting. *Results*. Plasma IL-37, IL-18, and IL-18 BP expression decreased compared to those in healthy volunteers while hs-CRP level was high. Both leukocytic IL-37 and ICAM-1 were highest expressed at 12 h point but significantly decreased at 48 h point. *Conclusion*. These findings suggest L-37 does not play an important role in the systematic inflammatory response but may be involved in leukocytic inflammation in ASTEMI after PCI.

1. Introduction

Despite modern reperfusion strategies have been well accepted around the world, acute myocardial infarction (AMI) still remains a leading cause of death worldwide. This suggests that AMI patients still need more understanding of potential pathophysiology for recurrent events of treatment especially in the early post-ACS period. So far, the systemic inflammatory response after AMI has been well described and may play an important role in series of events after AMI. Both circulating inflammatory markers, such as interleukin- (IL-) 6 and high sensitive C reaction protein (hs-CRP), as well as circulating inflammatory cells, including leukocytes and inflammatory monocytes, are elevated acutely after an AMI event in a temporal pattern that corresponds to elevated event rates and is predictive of recurrent events [1].

Anti-inflammation strategy is a good option of improving treatment for patients after AMI. Anti-inflammatory cytokines such as IL-10 are involved in the events of early AMI. The ratio of IL-18/IL-10 is found as an indicator for prognosis of AMI [2, 3]. IL-37 is a recently found anti-inflammatory cytokine in the IL-1 ligand family and proved as a fundamental inhibitor of innate immunity [4]. IL-37 was elevated in some inflammatory diseases such as inflammatory bowel disease, atopic dermatitis, rheumatoid arthritis, and systemic lupus erythematosus [5–8], indicating IL-37 may have potential protective effect on inflammatory diseases. IL-37 is found to be increased in patients with acute coronary syndrome [9] but not investigated in patients after percutaneous coronary intervention (PCI).

Additionally, IL-37 is normally expressed at low levels in peripheral blood mononuclear cells (PBMCs), mainly

monocytes, and dendritic cells (DCs) [9], which is rapidly upregulated in the inflammatory context after AMI. IL-37 effectively suppresses the activation of macrophage and DCs [10], and therefore IL-37 may conversely inhibit the production of inflammatory cytokines in PBMCs and DCs after AMI. Given that IL-37 may be associated with the development of atherosclerosis, we hypothesize that IL-37 may play a potential role in the inflammation response including plasma and leukocytes in AMI patients after PCI.

So IL-37, as a new anti-inflammatory cytokine, may suppress immune responses and inflammation [11]. Inflammation is an important step after AMI. Understanding of IL-37 expression helps us further to explore that role and effect of IL-37 in AMI situation. Since it is also reported that a complex of the IL-37 and IL-18-binding protein reduces IL-18 activity [12], we wanted to explore (1) the expression of plasma and leukocytic IL-37 in early period after AMI; (2) the possible relationship between plasma IL-37, IL-18, and IL-18BP; and (3) the possible inhibitory effect of IL-37 on ICAM-1 in leukocytes.

2. Methods

2.1. Materials. β-Actin antibody was purchased from Santa Cruz Biotechnology (Dallas, Texas, USA), and HRP-conjugated rabbit anti-human IgG was purchased from Jackson ImmunoResearch (West Grove, PA, USA); ICAM-1 and IL-18 antibody were purchased from Abcam (Cambridge, MA, USA). IL-37 was purchased from Adipogen AG, Liestal, Switzerland, IL-18 from MBL, Nagoya, Japan, IL-18BP from RayBiotech, Norcross GA, USA, and hs-CRP from Elisa Biotech (Shanghai, China).

2.2. Patients Population. From October, 2013, to April, 2014, a total of 112 cases of healthy volunteers (56) and patients (56) with ASTEMI agreed to participate in this test. STEMI was defined as chest pain suggestive of myocardial ischemia for at least 30 minutes before hospital admission and the electrocardiogram (ECG) with new ST-segment elevation in 2 or more contiguous leads of 0.2 mV or more in leads V2 to V3 and/or 0.1 mV or more in other leads. The exclusion criteria were as follows: (1) patients presenting with STEMI after 12 hours from symptom onset; (2) patients presenting with vasospastic angina (as determined by the resolution of ST-segment elevation and relief of symptoms after an IV administration of nitroglycerin); (3) patients over 75 years old; (4) recent (<1 week) systemic or local inflammation disease; (5) organ (liver, kidney) dysfunction; (6) cardiogenic shock.

Emergency PCI procedure must be carried out on all patients within 2 hours. All patients will receive 300 mg aspirin and a loading dose of 600 mg clopidogrel before the procedure. Unfractionated heparin will be administered intravenously in boluses to maintain an activated clotting time of >250 seconds during the procedure. Administration of glycoprotein IIb/IIIa inhibitors will be based on the physicians' discretion. PCI will be performed according to current international guidelines. The goals of the procedure are to achieve optimal angiographic efficacy of PCI at the infarct-related artery and minimize the risk of procedure-related complications. A full range of commercially available guiding catheters, balloon catheters, and guide wires will be readily available. All patients included in this trial will be treated according to the current American College of Cardiology (ACC)/American Heart Association (AHA) guidelines regarding poststenting management, which specify treatment with at least 100 mg of aspirin daily and 75 mg clopidogrel daily for at least 12 months after PCI. Angiotensin converting enzyme inhibitors and β-blockers will be administrated after PCI if no limitation exists.

2.3. Leukocytes and Blood Plasma Isolation. Blood collection from consented healthy volunteers and patients was approved by the Human Ethics Committee of First Affiliated Hospital of Shantou University Medical College. An approximate volume of 3 mL peripheral venous blood was collected from all patients at different time point (12 h, 24 h, and 48 h) after PCI procedure into the procoagulation tube and ethylenediaminetetra acetic acid (EDTA)-K2 anticoagulation tube separately. Sample collection from healthy volunteers was obtained in the morning. Plasma was isolated from blood sample in procoagulation tube after centrifugation at the speed of 3,000 rpm, 15 min. Leukocyte was isolated from blood sample in EDTA-K2 tube using erythrocyte lysis buffer (Qiagen, Hilden, Germany) and then collected after centrifugation at the speed of 2000 r/min, 10 min. Leukocytic protein was stored at −80°C for immunoblotting.

2.4. Immunoblotting. Immunoblotting was used to detect leukocytic IL-37 and ICAM-1. Samples were separated on 10% SDS-polyacrylamide gels and transferred onto nitrocellulose membranes. Membranes were blocked for 1 h at room temperature with 5% dry milk in TPBS (PBS containing 0.1% Tween 20) and then incubated with the appropriate primary antibodies (ICAM-1 antibody was diluted into 1 : 1000, IL-37 1 : 500, and β-blocker 1 : 1000) overnight at 4°C. After washing with TPBS, membranes were incubated with horseradish peroxidase- (HRP-) linked secondary antibodies (1 : 5000 dilution with TPBS containing 5% dry milk) at room temperature for 1 h. Bands were developed using ECL and exposed on X-ray films. Band density was analyzed using NIH ImageJ software.

2.5. Elisa. Plasma hs-CRP, IL-18, IL-18BP, and IL-37 were quantified by ELISA kits. Plasma hs-CRP was just detected at 12 h point, while IL-18, IL-18BP, and IL-37 were detected at 12 h, 24 h, and 48 h point. Recombinant cytokines were used to construct standard curves. Absorbance of standards and samples was determined spectrophotometrically at 450 nm using a microplate reader (KHB labsystem wallscan k3, Thermo Scientific, Finland). Results were plotted against the standard curve. The assays were carried out according to the protocols provided by the manufacturer.

2.6. Statistic Analysis. Data are expressed as mean ± standard error of mean (SEM). Analysis of variance (ANOVA) was

Table 1: Baseline characteristics of healthy volunteers and patients with ASTEMI after PCI.

	Patients ($n = 56$)	Healthy populations ($n = 56$)	P value
Age (years)	56.5 ± 1.82	56.7 ± 2.22	0.532
Male gender	46	40	0.605
WBC (∗10E9/L)	9.48 ± 0.62	8.65 ± 0.45	0.876
Hs-CRP (mg/L)	24.98 ± 3.33		
Cardiovascular risk factors			
Hypertension	28		
Diabetes mellitus	16		
Hypercholesterolemia	30		
Smoking history	30		
Ischemic time (min)			
Mean	385		
Median	245		
Number of diseased vessels			
1	24		
2	23		
3	6		
Infarct-related artery			
LAD	34		
LCX	3		
RCA	19		

WBC: white blood cells; LAD: left anterior descending artery; LCX: left circumflex artery; RCA: right coronary.

Table 2: Plasma IL-37, IL-18, and IL-18BP expression decreased in 48 h after PCI procedure.

Group	Patients ($n = 56$)			Healthy ($n = 56$)
	12 h	24 h	48 h	
IL-37 (pg/mL)	82.8 ± 14.79*	82.2 ± 9.28*	84.4 ± 13.35*	120.6 ± 2.67
IL-18 (pg/mL)	46.9 ± 5.06*	44.2 ± 5.28*	43.1 ± 4.60*	91.0 ± 2.80
IL-18BP (pg/mL)	231.9 ± 22.06*	261.5 ± 24.18*	234.6 ± 19.53*	461.9 ± 62.06

Plasma IL-37, IL-18, and IL-18BP from healthy volunteers and patients at different time point were qualified by Elisa kit. Lower expression of both IL-37, IL-18, and IL-18BP was in patients compared to those in healthy volunteers (*$P < 0.05$). No difference of change in all plasma cytokines was expressed at different time point in the patients with ASTEMI after PCI.

performed, and differences were considered significant when $P < 0.05$, as verified by Fisher post hoc test.

3. Results

3.1. Baseline Characteristics. Baseline clinical characteristics on the basis of age, gender, and leukocyte count between healthy volunteers and patients with STEMI are presented in Table 1. Mean age, gender disturbance, and leukocyte count were balanced between the groups. Most patients have 2 or more cardiovascular risk factors, while few patients have single parameter (2 have only hypertension, 2 only diabetes, 4 only hypercholesterolemia, and 4 only smoking history). Most patients have one or two diseased arteries, while 3 cases have 3 diseased ones. And most patients were occluded in LAD or RCA, while only 3 cases were infarcted in LCX. Plasma hs-CRP was elevated and indicated high inflammation situation after AMI with PCI.

3.2. Plasma IL-37, IL-18, and IL-18BP Decreased at Early Period. We tested plasma IL-37, IL-18, and IL-18BP expression at different time points (12 h, 24 h, and 48 h after PCI) in patients with STEMI with Elisa kit (Table 2). Both IL-37, IL-18, and IL-18BP expression were balanced but decreased at all time points in patients if compared to those in healthy volunteers ($P < 0.05$). We then test IL-37 and ICAM-1 expression in leukocytes to check cellular inflammation and anti-inflammation after PCI.

3.3. Leukocytic IL-37 and ICAM-1 Expression Change. Leukocyte is an important cell involved in inflammatory response after AMI and expressed IL-37 under inflammation [4]. We analyzed cellular IL-37 and ICAM-1 protein expression with immunoblotting. We found that both cellular IL-37 and ICAM-1 protein were highest expressed at 12 h point but significantly decreased at 48 h point (Figure 1, $P < 0.05$).

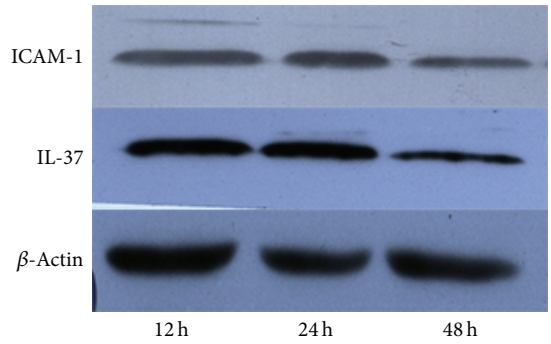

Figure 1: Leukocytic IL-37 and ICAM-1 expression change at early period. Leukocytic IL-37 and ICAM-1 protein expression were detected with immunoblotting. Both leukocytic IL-37 and ICAM-1 protein were highest expressed at 12 h point but significantly decreased at 48 h point ($P < 0.05$, $n = 48$).

4. Discussion

In this study, we demonstrated the expression of plasma IL-37 and leukocytic IL-37 in STEMI patients after PCI in early period. We found that plasma IL-37 did not increase and leukocytic IL-37 went down while plasma hs-CRP is high which indicates high inflammation response in the first 2 days after PCI. Plasma IL-18, which was found to be inhibited by IL-37, was also not increased under this situation.

STEMI is usually associated with inflammation and develops into severe complications. It is proved that inflammation is involved in atherosclerostic plaque formation and rupture, coronary thrombosis, and myocardial necrosis and repair after myocardial infarction [13–15]. Anti-inflammation strategy may be good for myocardial prognosis, but some anti-inflammatory cytokines such as IL-10 reduced in ACS patients, reflecting the imbalance in systemic cytokine response following an ACS [2, 16]. IL-37 is already proved as an anti-inflammatory cytokine and reported to be elevated in ACS patients [9], but we found that it decreased in patients after PCI in our study. This may be because PCI treatment could inhibit systematic IL-37 expression. Hereby, we found that systematic plasma IL-37 and leukocytic IL-37 decreased in the early period. In vivo expression of human IL-37 in mice reduces local and systemic inflammation in ConA-induced hepatitis and LPS challenge [17]. Therefore, IL-37 reduction may fail to inhibit systematic inflammation in patients with ASTEMI after PCI.

Not only hs-CRP but also IL-18 had been proved to be good indicators for prognosis for patients [18–20]. IL-18 is enhanced in STEMI situation [21–23], and the expression change of IL-18 is not reported before in patients after PCI. We found that IL-18 is decreased in the patients with PCI compared to that in healthy volunteers. A complex of the IL-37 and IL-18-binding protein reduces IL-18 activity [12]; but plasma IL-37, IL-18 and IL-18BP were increased in patients with ACS [9]. We wanted to test whether there is any relationship between changes of IL-18 and IL-37 in STEMI after PCI. The synchronous reduction of systematic IL-37 and IL-18 could not reveal the inhibitory effect of IL-37 on IL-18. The reduction of systematic IL-18 after PCI is not due to enhanced anti-inflammatory response. The ratio of IL-18/IL-10 was found to be an independent predictor of adverse events in patients with ACS [2, 3]. To decrease IL-18 and increase IL-10 are helpful for the recovery of patients with ACS [2]. The potential predictor effect of the ratio of IL-18/IL-37 on adverse events could be explored in the future. And to change the imbalance between inflammation and anti-inflammation is still meaningful. Although inflammatory markers such as CRP predict future cardiovascular events in ACS patients, when all inflammatory mediators are taken into account in a prospective analysis of risk, markers reflecting anti-inflammatory mechanisms may be better prognostic markers [18]. Furthermore, elevated level of plasma IL-37, IL-18, and IL-18BP had no correlation with the severity of the coronary artery stenosis [9], and decreased level of those was not related with that in our study.

Leukocyte is an important inflammatory cell in STEMI patients and is involved in myocardial necrosis and repair after STEMI [24]. Circulating monocytes could express high level of proinflammatory cytokines, TNF-alpha, and IL-6, as well as anti-inflammatory cytokine IL-10 [25]. ICAM-1 induces the interaction between leukocytes and endothelial cells [26], which is involved in the myocardial remodeling. We isolated circulating leukocytes and found reduction of both ICAM-1 and IL-37 in early period, indicating a balance of inflammatory and anti-inflammatory response in circulating leukocytes. We can suggest that ICAM-1 expression decreased because of IL-37, which is better to be confirmed by isolated leukocyte culture. Different from the systematic imbalance, the changes of IL-37 and ICAM-1 indicated a balance of inflammation and anti-inflammation on leukocytes. Leukocytes include several types including neutrophils, lymphocytes, and monocytes, so we cannot acutely tell which subtype has only or more IL-37 expression. We think neutrophils, most percentage of leukocytes, may be a potential good target to explore IL-37 expression and change in the future.

In this study, our baseline is healthy volunteers without some cardiovascular risk factors except age and gender. There is no report about systematic IL-37 expression in healthy volunteers before. We found that it is lower in the STEMI than that in the healthy, which may be because anti-inflammatory response is inhibited [2, 16]. Compared to other studies about anti-inflammatory cytokines, we can suggest that this is due to the inhibitory effect of anti-inflammatory response in ACS. Enhancing anti-inflammatory effect in STEMI may help to repair myocardial damage [27, 28]. How to increase IL-37 expression may be helpful and it is interesting to investigate that in future study. Furthermore, sample size is not too much in our study; we can investigate expression difference in different subgroup if we have more samples.

5. Conclusion

In conclusion, our study firstly demonstrates that systematic IL-37 expression was decreased in STEMI with PCI situation and on decline in leukocytes after PCI. These suggest that IL-37 does not play an important role in the systematic inflammatory response but may be involved in leukocytic

inflammation in ASTEMI after PCI. More studies should be investigated for that.

Abbreviations

ACS: Acute coronary syndrome
AMI: Acute myocardial infarction
DC: Dendritic cell
Hs-CRP: High sensitive C reaction protein
ICAM-1: Intercellular adhesion molecule-1
IL: Interleukin
LPS: Lipopolysaccharide
PBMC: Peripheral blood mononuclear cell
PCI: Percutance coronary intervention.

Conflict of Interests

The authors declare that there is no conflict of interests regarding the publication of this paper.

Authors' Contribution

Jilin Li is involved in experimental design, acquisition, and analysis of data and drafted the paper. Lan Chen, Xiangna Cai, and Xin Wang participated in the experiment and the acquisition and analysis of data. Xiangna Cai and Duanmin Xu were involved in drafting the paper. All authors read and approved the final paper. Xiangna Cai equally contributed to this paper as co-first authors.

Acknowledgments

This work was supported in part by National Nature Science Foundation of China 81300123 and by College Students' Innovation and Entrepreneurship Training Program of Guangdong Province 1056013093.

References

[1] J. T. Willerson and P. M. Ridker, "Inflammation as a cardiovascular risk factor," *Circulation*, vol. 109, no. 21, supplement 1, pp. II2–II10, 2004.

[2] G. K. Chalikias, D. N. Tziakas, J. C. Kaski et al., "Interleukin-18: interleukin-10 ratio and in-hospital adverse events in patients with acute coronary syndrome," *Atherosclerosis*, vol. 182, no. 1, pp. 135–143, 2005.

[3] G. K. Chalikias, D. N. Tziakas, J. C. Kaski et al., "Interleukin-18/interleukin-10 ratio is an independent predictor of recurrent coronary events during a 1-year follow-up in patients with acute coronary syndrome," *International Journal of Cardiology*, vol. 117, no. 3, pp. 333–339, 2007.

[4] M. F. Nold, C. A. Nold-Petry, J. A. Zepp, B. E. Palmer, P. Bufler, and C. A. Dinarello, "IL-37 is a fundamental inhibitor of innate immunity," *Nature Immunology*, vol. 11, no. 11, pp. 1014–1022, 2010.

[5] H. Imaeda, K. Takahashi, T. Fujimoto et al., "Epithelial expression of interleukin-37b in inflammatory bowel disease," *Clinical and Experimental Immunology*, vol. 172, no. 3, pp. 410–416, 2013.

[6] H. Fujita, Y. Inoue, K. Seto, N. Komitsu, and M. Aihara, "Interleukin-37 is elevated in subjects with atopic dermatitis," *Journal of Dermatological Science*, vol. 69, no. 2, pp. 173–175, 2013.

[7] B. Pei, S. Xu, T. Liu, F. Pan, J. Xu, and C. Ding, "Associations of the IL-1F7 gene polymorphisms with rheumatoid arthritis in Chinese Han population," *International Journal of Immunogenetics*, vol. 40, no. 3, pp. 199–203, 2013.

[8] L. Song, F. Qiu, Y. Fan et al., "Glucocorticoid regulates interleukin-37 in systemic lupus erythematosus," *Journal of Clinical Immunology*, vol. 33, no. 1, pp. 111–117, 2013.

[9] Q. Ji, Q. Zeng, and Y. Huang, "Elevated plasma IL-37, IL-18, and IL-18BP concentrations in patients with acute coronary syndrome," *Mediators of Inflammation*, 2014.

[10] B. W. Wu, Q. T. Zeng, K. Meng, and Q. W. Ji, "The potential role of IL-37 in atherosclerosis," *Die Pharmazie*, vol. 68, no. 11, pp. 857–860, 2013.

[11] S. Tetè, D. Tripodi, M. Rosati et al., "IL-37 (IL-1F7) the newest anti-inflammatory cytokine which suppresses immune responses and inflammation," *International Journal of Immunopathology and Pharmacology*, vol. 25, no. 1, pp. 31–38, 2012.

[12] P. Bufler, T. Azam, F. Gamboni-Robertson et al., "A complex of the IL-1 homologue IL-1F7b and IL-18-binding protein reduces IL-18 activity," *Proceedings of the National Academy of Sciences of the United States of America*, vol. 99, no. 21, pp. 13723–13728, 2002.

[13] J. F. Bentzon, F. Otsuka, R. Virmani, and E. Falk, "Mechanisms of plaque formation and rupture," *Circulation Research*, vol. 114, no. 12, pp. 1852–1866, 2014.

[14] I. Burazor and A. Vojdani, "Chronic exposure to oral pathogens and autoimmune reactivity in acute coronary atherothrombosis," *Autoimmune Diseases*, vol. 2014, Article ID 613157, 8 pages, 2014.

[15] N. G. Frangogiannis, "The inflammatory response in myocardial injury, repair, and remodelling," *Nature Reviews Cardiology*, vol. 11, no. 5, pp. 255–265, 2014.

[16] A. L. Pasqui, M. di Renzo, G. Bova et al., "Pro-inflammatory/anti-inflammatory cytokine imbalance in acute coronary syndromes," *Clinical and Experimental Medicine*, vol. 6, no. 1, pp. 38–44, 2006.

[17] A.-M. Bulau, M. Fink, C. Maucksch et al., "In vivo expression of interleukin-37 reduces local and systemic inflammation in concanavalin A-induced hepatitis," *TheScientificWorldJournal*, vol. 11, pp. 2480–2490, 2011.

[18] D. N. Tziakas, G. K. Chalikias, J. C. Kaski et al., "Inflammatory and anti-inflammatory variable clusters and risk prediction in acute coronary syndrome patients: a factor analysis approach," *Atherosclerosis*, vol. 193, no. 1, pp. 196–203, 2007.

[19] M. Hartford, O. Wiklund, L. M. Hultén et al., "Interleukin-18 as a predictor of future events in patients with acute coronary syndromes," *Arteriosclerosis, Thrombosis, and Vascular Biology*, vol. 30, no. 10, pp. 2039–2046, 2010.

[20] L. Kubková, J. Špinar, M. Pávková Goldbergová, J. Jarkovský, and J. Pařenica, "Inflammatory response and C-reactive protein value in patient with acute coronary syndrome," *Vnitrni Lekarstvi*, vol. 59, no. 11, pp. 981–988, 2013.

[21] T. C. T. M. van der Pouw Kraan, F. J. P. Bernink, C. Yildirim et al., "Systemic toll-like receptor and interleukin-18 pathway activation in patients with acute ST elevation myocardial infarction," *Journal of Molecular and Cellular Cardiology*, vol. 67, pp. 94–102, 2014.

[22] H. O. El-Mesallamy, N. M. Hamdy, A. K. El-Etriby, and E. F. Wasfey, "Plasma granzyme B in ST elevation myocardial

infarction versus non-ST elevation acute coronary syndrome: comparisons with IL-18 and fractalkine," *Mediators of Inflammation*, vol. 2013, Article ID 343268, 8 pages, 2013.

[23] N. D. Brunetti, I. Munno, P. L. Pellegrino et al., "Inflammatory cytokines imbalance in the very early phase of acute coronary syndrome: correlations with angiographic findings and in-hospital events," *Inflammation*, vol. 34, no. 1, pp. 58–66, 2011.

[24] J.-C. Tardif, J.-F. Tanguay, S. S. Wright et al., "Effects of the P-selectin antagonist inclacumab on myocardial damage after percutaneous coronary intervention for non-ST-segment elevation myocardial infarction: results of the SELECT-ACS trial," *Journal of the American College of Cardiology*, vol. 61, no. 20, pp. 2048–2055, 2013.

[25] C. del Fresno, L. Soler-Rangel, A. Soares-Schanoski et al., "Inflammatory responses associated with acute coronary syndrome up-regulate IRAK-M and induce endotoxin tolerance in circulating monocytes," *Journal of Endotoxin Research*, vol. 13, no. 1, pp. 39–52, 2007.

[26] L. C. Dieterich, H. Huang, S. Massena, N. Golenhofen, M. Phillipson, and A. Dimberg, "αb-crystallin/HspB5 regulates endothelial-leukocyte interactions by enhancing NF-κB-induced up-regulation of adhesion molecules ICAM-1, VCAM-1 and E-selectin," *Angiogenesis*, vol. 16, no. 4, pp. 975–983, 2013.

[27] A. Baruch, N. Van Bruggen, J. B. Kim, and J. E. Lehrer-Graiwer, "Anti-inflammatory strategies for plaque stabilization after acute coronary syndromes topical collection on vascular biology," *Current Atherosclerosis Reports*, vol. 15, no. 6, article 327, 2013.

[28] I. M. Seropian, S. Toldo, B. W. van Tassell, and A. Abbate, "Anti-inflammatory strategies for ventricular remodeling following St-segment elevation acute myocardial infarction," *Journal of the American College of Cardiology*, vol. 63, no. 16, pp. 1593–1603, 2014.

Hindawi Publishing Corporation
Mediators of Inflammation
Volume 2015, Article ID 419106, 9 pages
http://dx.doi.org/10.1155/2015/419106

Research Article

Ginkgo biloba Extract Improves Insulin Signaling and Attenuates Inflammation in Retroperitoneal Adipose Tissue Depot of Obese Rats

Bruna Kelly Sousa Hirata,[1] Renata Mancini Banin,[1] Ana Paula Segantine Dornellas,[2] Iracema Senna de Andrade,[2] Juliane Costa Silva Zemdegs,[2] Luciana Chagas Caperuto,[1] Lila Missae Oyama,[2] Eliane Beraldi Ribeiro,[2] and Monica Marques Telles[1]

[1] *Departamento de Ciências Biológicas, Universidade Federal de São Paulo (UNIFESP), Rua Arthur Riedel, 275 Eldorado, 09972-270 Diadema, SP, Brazil*
[2] *Departamento de Fisiologia, Disciplina de Fisiologia da Nutrição, Universidade Federal de São Paulo (UNIFESP), Rua Botucatu, 862 Vila Clementino, São Paulo, SP, Brazil*

Correspondence should be addressed to Monica Marques Telles; mmtelles@unifesp.br

Received 21 October 2014; Revised 16 December 2014; Accepted 17 December 2014

Academic Editor: Yi Fu Yang

Due to the high incidence and severity of obesity and its related disorders, it is highly desirable to develop new strategies to treat or even to prevent its development. We have previously described that *Ginkgo biloba* extract (GbE) improved insulin resistance and reduced body weight gain of obese rats. In the present study we aimed to evaluate the effect of GbE on both inflammatory cascade and insulin signaling in retroperitoneal fat depot of diet-induced obese rats. Rats were fed with high fat diet for 2 months and thereafter treated for 14 days with 500 mg/kg of GbE. Rats were then euthanized and samples from retroperitoneal fat depot were used for western blotting, RT-PCR, and ELISA experiments. The GbE treatment promoted a significant reduction on both food/energy intake and body weight gain in comparison to the nontreated obese rats. In addition, a significant increase of both Adipo R1 and IL-10 gene expressions and IR and Akt phosphorylation was also observed, while NF-κB p65 phosphorylation and TNF-α levels were significantly reduced. Our data suggest that GbE might have potential as a therapy to treat obesity-related metabolic diseases, with special interest to treat obese subjects resistant to adhere to a nutritional education program.

1. Introduction

The incidence of both obesity and overweight has been dramatically increasing around the world. In 2008, 35% of worldwide population was overweight while 11% was obese [1]. In addition, it has been estimated that obesity will achieve one-third of the population in 2030 [2]. This perspective is particularly worrying since obesity is related to chronic comorbidities, such as insulin resistance, type 2 diabetes (T2D), subclinical inflammation, and others [3].

It has been suggested that consumption of high-fat diet is directly involved in the obesity pathogenesis since it affects either central control of food intake and peripheral metabolism, resulting in increased body weight gain, insulin resistance, and other metabolic disturbances [4, 5]. Thus, we have previously demonstrated that prolonged hyperlipidic diet ingestion promoted in rats a significant increase of body adiposity, triacylglycerol, and glucose plasma levels with a concomitant loss of insulin sensitivity [6].

Insulin resistance is a chronic condition in which the hormone insulin fails to activate its own signaling cascade, resulting in hyperglycemia. It has been highly correlated to visceral adiposity excess and increased white adipose tissue (WAT) expression of cytokines, such as tumor necrosis factor-alpha (TNF-α) and interleukin-6 (IL-6) [3, 7]. Furthermore, high-fat diet intake has been pointed as an important

risk factor for insulin resistance, since it both impairs insulin signaling pathway and stimulates inflammation, via Toll-like receptors signaling cascade [5, 7, 8].

Taking into account that most of hypoglycemiants present undesirable side effects [9–12] and due to the severity of insulin resistance progression it is highly desirable to discover new drugs and treatment methods. It has been proposed that *Ginkgo biloba* extract (GbE) might have positive effects on hyperglycemia. This plant extract mainly contains around 24% flavonoid glycosides and 6% terpenoids, including A, B, C, M, J, P, and Q ginkgolides [13].

We have previously described that prolonged GbE treatment significantly reduced food intake and body adiposity, prevented against hyperglycemia and dyslipidemia, while it increased insulin sensitivity evaluated by ITT (insulin tolerance test) in obese rats fed with lard-enriched hyperlipidic diet [6]. In agreement to our previous findings, other studies proposed that GbE intake improved glycaemic profile of both healthy and T2D patients [14, 15]. In addition, a reduction on glucose elevation stimulated by oral administration of saccharin agents in rats was demonstrated [16].

The data above suggest beneficial effects of GbE on insulin resistance and obesity-related disorders. However, it is highly important to better describe the mechanisms by which GbE improves insulin action. In this context, the present study aimed to evaluate if a 14-day oral GbE treatment alters retroperitoneal WAT depot insulin and Toll-like receptors signaling cascades of diet-induced obese rats, a model of insulin resistance.

2. Materials and Methods

2.1. Animals. The Committee on Animal Research Ethics of the Universidade Federal de São Paulo approved all procedures for the care of the animals used in this study (Process number: 271359). All efforts were made to minimize suffering. Male Wistar rats from CEDEME (São Paulo, Brazil) were housed 4 per cage and maintained in controlled conditions of light (12 : 12-h light/dark, lights on at 6 am) and temperature (23°C ± 1°C), with free access to food and water.

2-month-old rats were fed a highly fat-enriched diet which was prepared by adding 40% (w/w) standard chow plus 28% (w/w) lard, 2% (w/w) soy oil, 10% (w/w) sucrose, 20% (w/w) casein, in order to obtain the protein content of the control diet, and butylated hydroxytoluene in the amount of 0.02% (w/w) of the additional oil. This provided 19.5% of energy as carbohydrate, 23.2% as protein, and 57.3% as fat. Table 1 shows the macronutrient and fatty acid compositions of the diet.

After 8 weeks, animals were divided into two groups, according to the phytotherapy treatment described below.

2.2. Phytotherapy Treatment. *Ginkgo biloba* extract (GbE) was obtained from Southern Anhui Dapeng (China) and contained 26.12% of flavone glycosides, 6.86% of terpenoids, 2.20% of ginkgolide A, 1.11% of ginkgolide B, 1.05% of ginkgolide C, and 2.50% of bilobalide.

Table 1: Macronutrients and fatty acid compositions of high fat diet.

	High fat diet
Humidity (%)	1.1
Lipid (%)	31.6
Protein (%)	27.0
Carbohydrate (%)	27.5
Total food fiber (%)	8.6
Mineral residue fixed (%)	4.2
Sodium chloride (%)	0.2
Calculated energy (Kcal/g)	5.0

Phytotherapy treatment was performed for a 14-day period. The obese animals were divided in two groups: O+V (Obese + Vehicle) and O+Gb (Obese + *Ginkgo biloba*). The O+Gb group was daily gavaged with 500 mg/kg of GbE [17, 18] diluted in 1 mL of 0.9% saline (vehicle) while the O+V was gavaged with 1 mL of vehicle.

2.3. Body Weight Gain, Accumulated Food, and Energy Intake. During the phytotherapy treatment period, 24-h food intake and body weight were daily measured. The evaluation of food intake was calculated by the difference between the amount of meal offered and the remnant after 24 hours.

Body weight gain was calculated by the difference between final weight (last day of treatment) and initial weight (first day of treatment). Accumulated food and energy intakes were measured by the mean of the first 13 days of treatment. In the last day of treatment rats were kept overnight fasted.

2.4. Retroperitoneal Adipose Tissue and Serum Parameters. Rats were anesthetized with sodium thiopental (80 mg/Kg of body wt, intraperitoneal) and decapitated after a 10-hour fasting period. Retroperitoneal white adipose tissue depot was removed and homogenized in 1.0 mL of lysis buffer (100 mM Tris, pH 7.5, 10 mM EDTA, and 0,1 mg/mL aprotinin; 2 mM PMSF; 10 mM sodium orthovanadate; 100 mM sodium fluoride; 10 mM sodium pyrophosphate; and 10% TritonX-100). Levels of proinflammatory cytokine TNF-α and anti-inflammatory cytokine IL-10 were measured by ELISA kit (R&D Systems).

Portal vein blood was also collected for the measurement of adiponectin by Milliplex MAP (Millipore).

2.5. Western Blotting. Rats were deeply anesthetized with sodium thiopental (80 mg/Kg of body wt, intraperitoneal). The abdominal cavity was opened and negative control samples (O+V− and O+Gb−) were obtained from the left side retroperitoneal fat depot. After the collection, samples were immediately inserted into a vial containing 3.0 mL of lysis buffer (100 mM Tris, pH 7.5, 10 mM EDTA, and 0.1 mg/mL aprotinin; 2 mM PMSF; 10 mM sodium orthovanadate; 100 mM sodium fluoride; 10 mM sodium pyrophosphate; and 10% TritonX-100), homogenized, and centrifuged at 16000 g for 40 minutes at 4°C. Then, the portal vein was exposed and 10^{-5} M of insulin was injected intravenously (i.v.). Right side retroperitoneal fat depot was removed 90 seconds after the

i.v. insulin injection (positive samples: O+V+ and O+Gb+) following the same protocol described above [19, 20]. Total protein was quantified by BCA kit (BioRad) and samples were used for both immunoprecipitation and total extract evaluations.

To reduce the risk of nonspecific antibody binding, we evaluated the IR phosphorylation levels after immunoprecipitation with antibody against IR. To perform immunoprecipitation experiments, samples were overnight incubated with 10 μL primary antibody anti-IR (insulin Rβ sc-711) and proteins were precipitated by Protein A Sepharose (GE). After all, proteins were separated on 10% SDS-PAGE. Proteins were then transferred to nitrocellulose membranes by wet transfer apparatus (Bio-Rad). The membranes were preincubated for 1 hour in blocking buffer (5% bovine serum albumin [BSA], 1 M Tris, pH 7.5, 5 M NaCl, and 0.02% Tween-20). Membranes were overnight incubated at 4°C with the primary antibody against p-Tyr (Cell Signaling 8954). All membranes were then incubated with specific horseradish peroxidase-conjugated anti-rabbit IgG antibody (Cell Signaling 7074) followed by chemiluminescence detection (Amersham Biosciences). Since all samples were immunoprecipitated with IR antibody, we considered that bands with molecular weight of 95 kDa were related to the phosphorylated form of IR. In addition, IR levels were used as internal standards since all the other proteins were removed by the immunoprecipitation method.

To perform the total extract experiments, after the protein quantification, total proteins were then separated on 8% SDS-PAGE. Proteins were transferred by semidry transfer apparatus (Bio-Rad).

All membranes were overnight incubated at 4°C with the primary antibody against phospho-Akt (Cell Signaling Ser 473–9271); Akt (Cell Signaling 9272), phospho-NF-κB p65 (Cell Signaling Ser 536–3033), NF-κB p65 (Cell Signaling 6956), MyD88 (Cell Signaling 4283), TLR4 (SC 293072), and β-tubulin (Cell Signaling 2146). All membranes were then incubated with specific horseradish peroxidase-conjugated anti mouse/rabbit IgG antibody (Cell Signaling 7076; Cell Signaling 7074, resp.) followed by chemiluminescence detection (Amersham Biosciences). β-tubulin (Cell Signaling 2146) level was used as an internal standard.

Quantitative analysis was performed with Scion Image software (Scion Corporation, Frederick, MD, USA). In all experiments, at least one sample from each group was analyzed simultaneously and the results were expressed as percentage change relative to the basal levels.

2.6. RNA Extraction and Quantitative Real-Time Polymerase Chain Reaction (qPCR). In order to evaluate the gene expression of Adipo R1, Adipo R2, and IL-10, additional groups (O+V and O+Gb) of five rats each were performed. For total RNA extraction, two hundred mg of frozen retroperitoneal adipose tissue from each sample were homogenized by adding 1 mL of Trizol reagent (Invitrogen, USA). The samples were centrifuged at 16.000 g for 15 min at 4°C and the aqueous phase was removed and mixed with 0.5 mL of isopropyl alcohol. After centrifugation at 16.000 g for 10 min at 4°C, the pellet was washed with 1 mL of 75% ethanol and then dissolved in 20 μL DEPC-Treated water (Ambion, USA).

Table 2: Retroperitoneal fat depot cytokine levels (ρg/μg of protein).

Cytokine	O + V	O + Gb
IL-10	0.47 ± 0.09	0.33 ± 0.03
IL-6	0.57 ± 0.09	0.55 ± 0.08
TNF-α	0.47 ± 0.07	0.30 ± 0.02*

*$P < 0.05$ versus O + V.

One microgram of RNA was reverse transcribed to cDNA using the High-Capacity cDNA kit (Applied Biosystems). Gene expression was evaluated by real-time qPCR using the Taqman PCR Assays. Primers and probe catalog numbers were Adipo R1 (Rn01483784_m1), Adipo R2 (Rn01463173_m1), IL-10 (Rn00563409_m1), and Actin b (Rn00667869_m1).

Reactions were performed in 96-well plates and carried out in triplicate. Amplification conditions consisted of 40 cycles of 50°C/2 min, 95°C/10 min, 95°C/15 s, and 60°C/1 min. The method $2^{-\Delta\Delta Ct}$ was used to evaluate the relative quantification of amplification products.

2.7. Statistics. Statistical analysis was performed using PASW Statistics version 19 (SPSS Inc, Chicago, IL, USA) with the level of statistical significance set at $P < 0.05$. Comparisons among two groups were performed by Student's t test.

3. Results

3.1. Food Intake and Body Adiposity in Response to Phytotherapy Treatment. Accumulated food intake during the first 13 days of phytotherapy treatment is illustrated in Figure 1(a). It is interesting to note that O+Gb group ingested 6.3% less than O+V group ($P = 0.031$). In relation to energy intake, it can be observed at Figure 1(b) that O+Gb also presented a significant reduction of 6.3% in comparison to O+V ($P = 0.031$).

The effect of GbE on body weight gain is presented in Figure 1(c). It can be seen that the O+Gb group had a significant reduction of 62% ($P = 0.013$) in comparison to O+V group.

3.2. Cytokine Levels and Gene Expression. Table 2 presents the results of retroperitoneal fat depot cytokine levels. A decrease of 36% ($P = 0.014$) on TNF-α was observed in the O+Gb in comparison to the O+V group. The levels of IL-10 and IL-6 were similar in both groups.

Figure 2 depicts the effect of GbE on retroperitoneal fat depot gene expression of Adipo R1, Adipo R2, and IL-10. It can be observed in Figures 2(a) and 2(c) that the GbE treatment promoted a significant increase on gene expression of both Adipo R1 (33%; $P = 0.013$) and IL-10 (70%; $P = 0.040$), in comparison to the O+V group. However, no differences were observed in gene expression of Adipo R2 in response to GbE treatment (Figure 2(b)).

3.3. Fasting Serum Adiponectin Levels. In relation to adipnectin serum levels, no differences were observed among

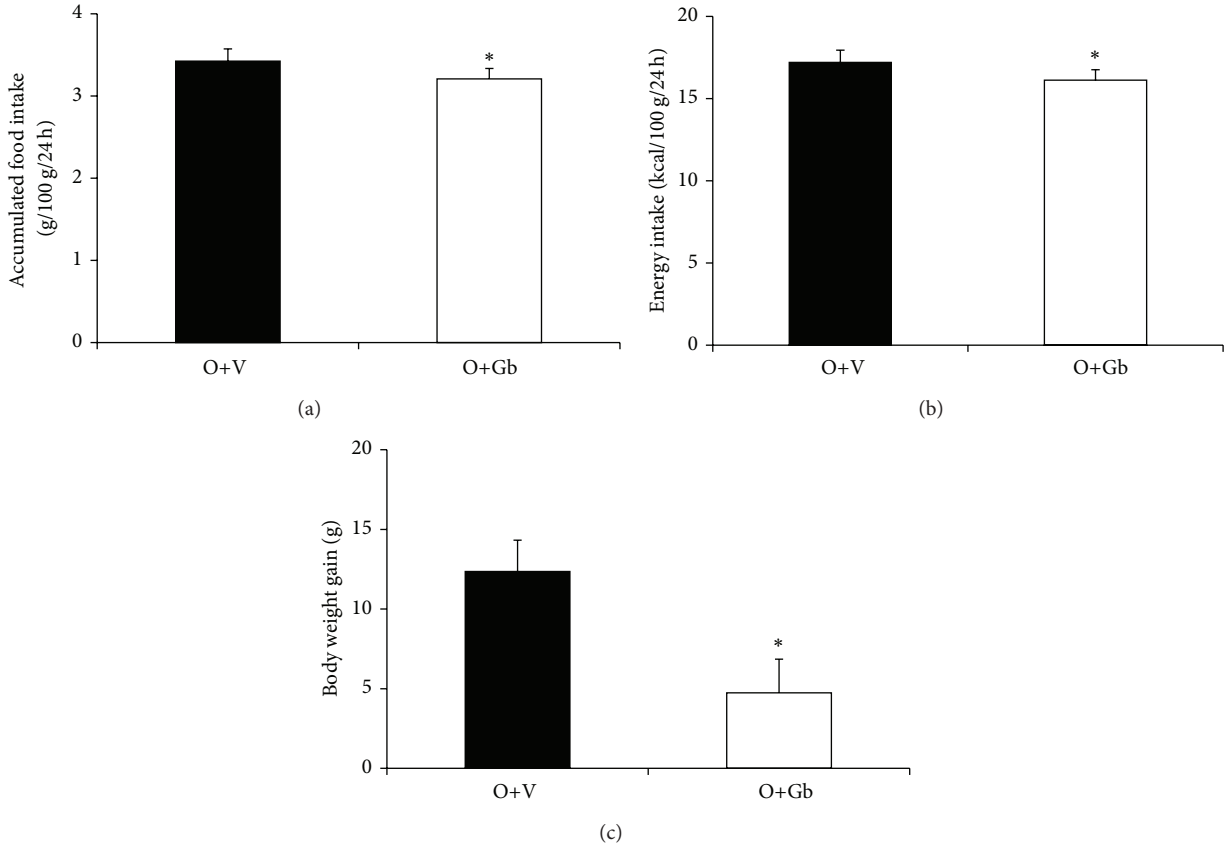

Figure 1: Food intake and body weight gain in response to EGb treatment. (a) Accumulated food intake (g/100 g/24 h), (b) energy intake (Kcal/100 g/24 h), and (c) body weight gain (g) of O+V ($n = 17$) and O+Gb ($n = 15$) groups during the phytotherapy treatment. $^{*}P < 0.05$ versus O+V.

O+V group (14.74 ± 0.92 μg/mL) and O+Gb group (12.96 ± 1.16 μg/mL).

3.4. IR and AKT Phosphorylation Levels. In Figure 3(a) it can be observed that insulin-induced IR phosphorylation (O+V+) was impaired by the ingestion of high-fat diet, since no differences were observed in relation to basal levels (O+V−). However, it can be seen in Figure 3(b) that prolonged administration of GbE promoted a significant 2.81-fold increase ($P = 0.004$) on insulin-induced IR phosphorylation (O+Gb+) in relation to basal levels (O+Gb−).

Figure 4 illustrates that Akt phosphorylation was also stimulated by the GbE treatment. The GbE treatment promoted a significant 0.67-fold increase ($P = 0.039$) on Akt phosphorylation levels in comparison to basal levels (O+Gb+ versus O+Gb−) (Figure 4(b)) whilst no effect was observed in nontreated obese rats after insulin infusion (O+V+ versus O+V−) (Figure 4(a)).

3.5. Inflammatory Signaling Pathway. It can be seen in Figure 5 that GbE treatment did not modify the total protein levels of TLR4, MyD88, and NF-κB p65 ($P = 0.900$; $P = 0.982$; $P = 0.163$, resp.) in retroperitoneal fat depot. Yet, the GbE treatment did significantly reduce the phosphorylation of NF-κB p65 by 60% in comparison to the nontreated obese rats ($P = 0.004$).

4. Discussion

It has been considered that prolonged fat intake is the main predisposing risk factor for the development of obesity [21, 22]. High fat intake also impairs insulin action by reducing glucose uptake and both IR and Akt phosphorylation in brown and white adipose tissues [5, 6, 23]. Due to the risks involved in the obesity and insulin resistance establishment, it is highly desirable to develop new strategies to treat obesity and its related disorders.

In our previous study it was demonstrated that prolonged treatment with GbE promoted a significant visceral adiposity loss, improvement of insulin sensitivity, reduction of dyslipidemia, and stimulation of insulin signaling cascade in gastrocnemius muscle [6]. Taking into consideration the promising results obtained in our previous study, the present one was aimed to further evaluate the beneficial effects of GbE on obesity-related insulin resistance, focusing now on both insulin and inflammatory cascades of retroperitoneal fat depot, an insulin-dependent tissue.

Similar to our previous study [6], the present data has demonstrated that GbE treatment significantly has decreased

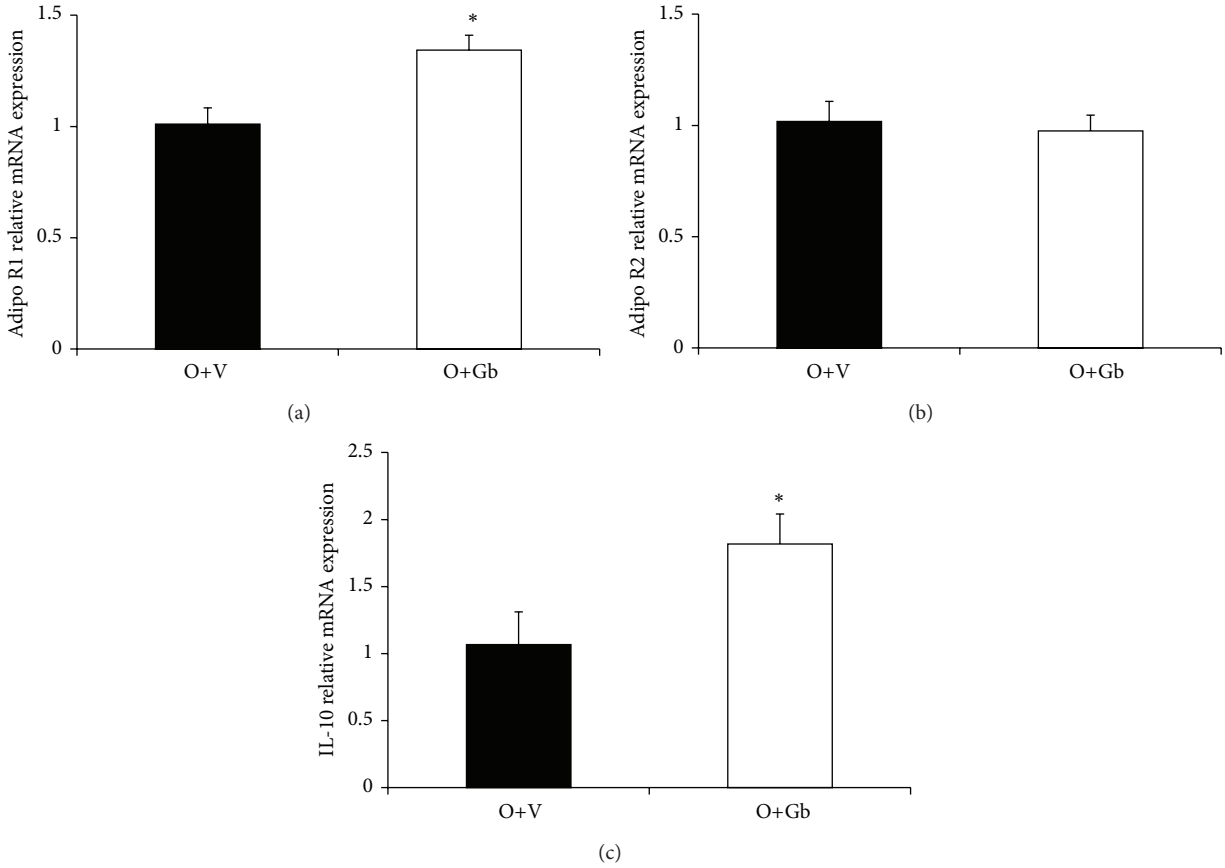

Figure 2: Effect of GbE on retroperitoneal fat depot gene expression of Adipo R1, Adipo R2, and IL-10. Gene expression in retroperitoneal WAT depot of O+V ($n = 5$) and O+Gb ($n = 5$) groups evaluated by Real Time PCR. $^{*}P < 0.05$ versus O+V.

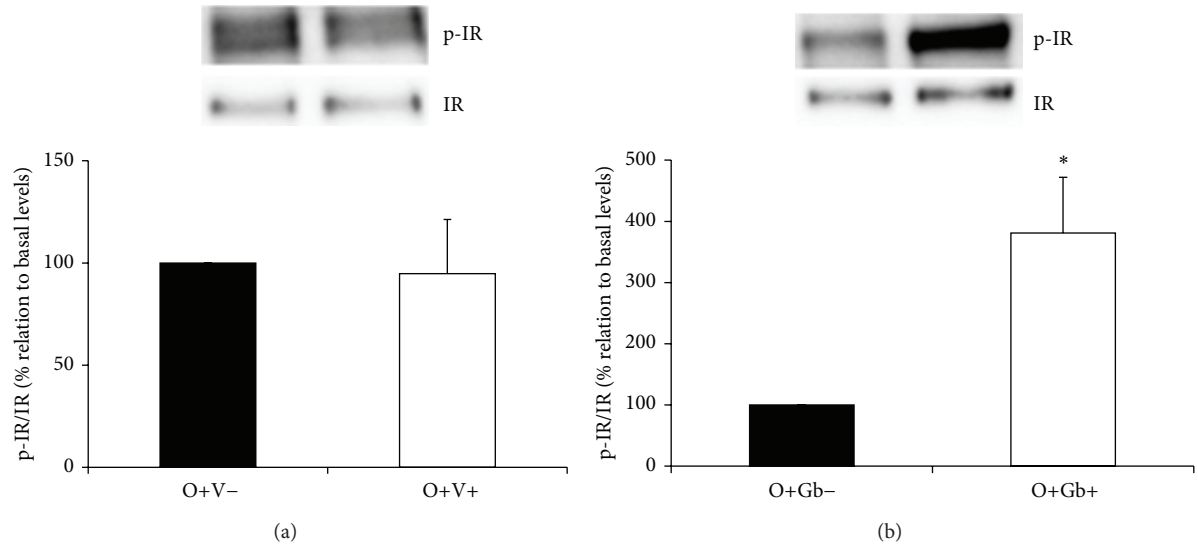

Figure 3: Effect of GbE on IR phosphorylation levels of retroperitoneal fat depot: insulin-induced IR phosphorylation levels in retroperitoneal WAT depot of groups: (a) O+V− ($n = 10$) and O+V+ ($n = 9$); (b) O+Gb− ($n = 9$) and O+Gb+ ($n = 9$) evaluated by western blotting. $^{*}P < 0.05$ versus basal levels.

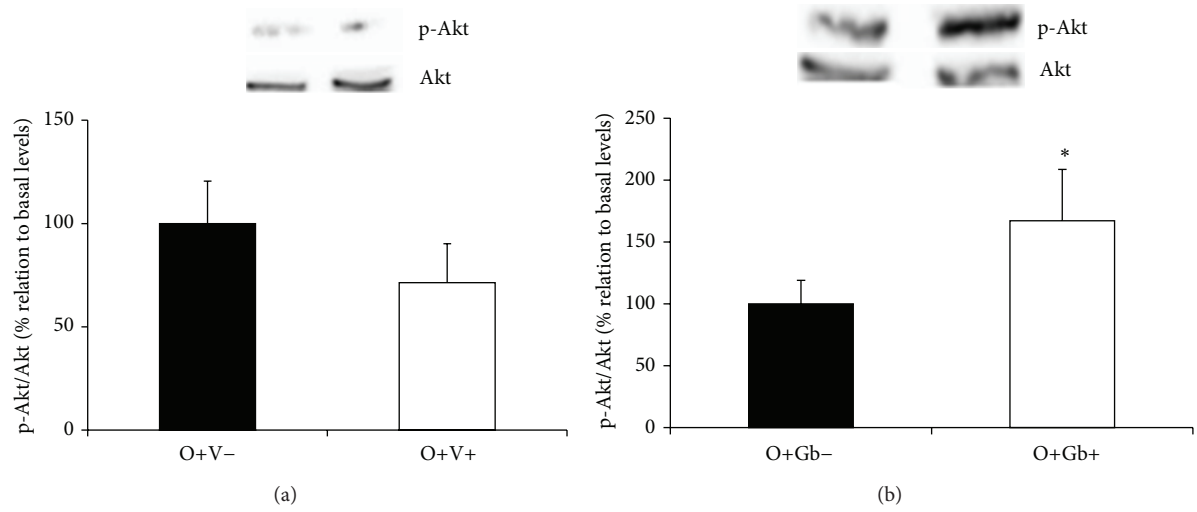

Figure 4: Effect of GbE on Akt phosphorylation levels of retroperitoneal fat depot: insulin-induced Akt phosphorylation levels in retroperitoneal WAT depot of groups: (a) O+V− ($n = 8$) and O+V+ ($n = 9$); (b) O+Gb− ($n = 8$) and O+Gb+ ($n = 7$) evaluated by western blotting. $^{*}P < 0.05$ versus basal levels.

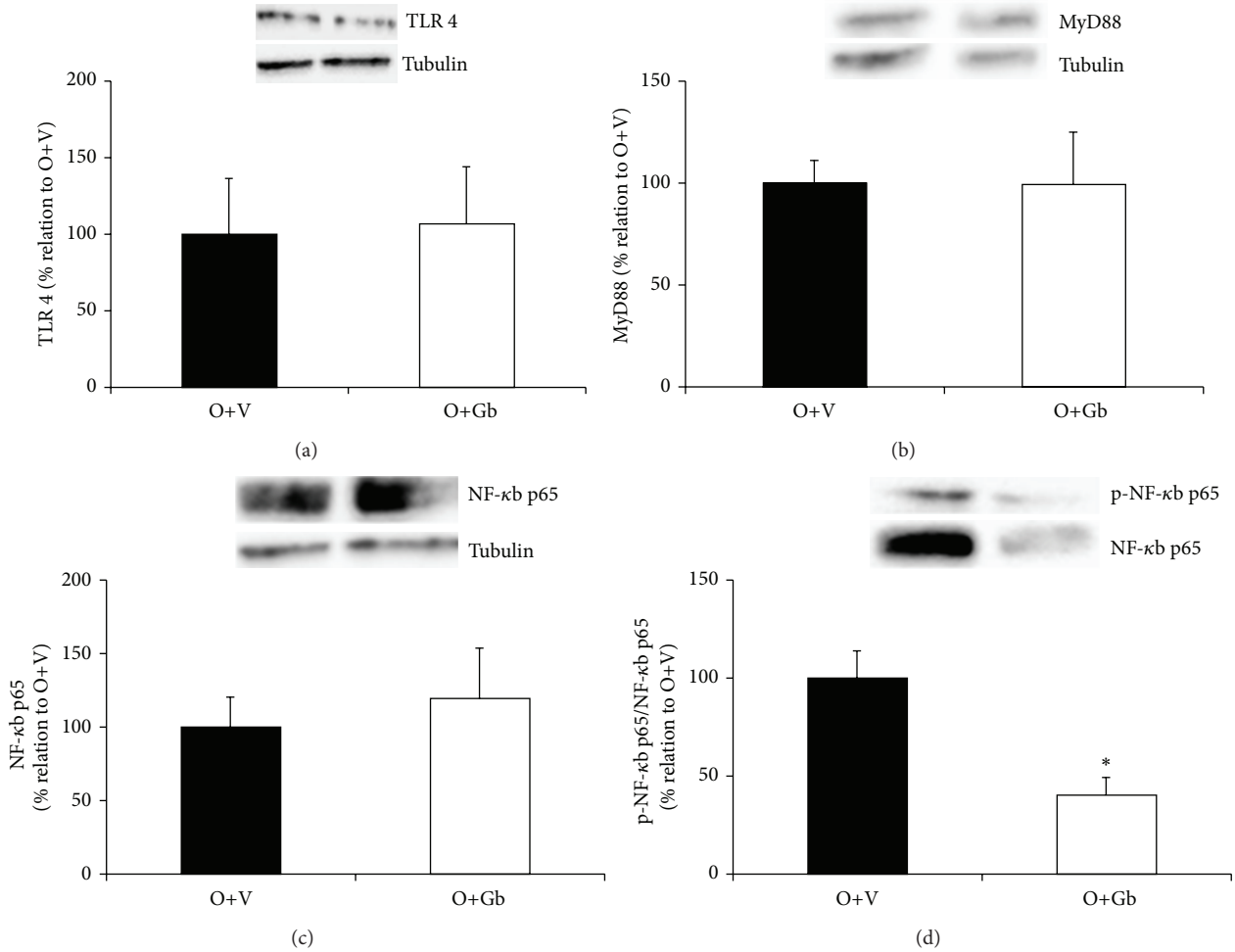

Figure 5: Effect of GbE on inflammatory signaling pathway: total protein levels of TLR4 (O+V $n = 6$; O+Gb $n = 6$), MyD88 (O+V $n = 13$; O+Gb $n = 9$), NF-κB p65 (O+V $n = 5$; O+Gb $n = 4$), and phosphorylation of NF-κB p65 (O+V $n = 10$; O+Gb $n = 8$) in retroperitoneal WAT depot evaluated by western blotting. $^{*}P < 0.05$ versus O+V.

food/energy intake and, in addition, it has also reduced the body weight gain of diet-induced obese rats. Data on literature are scarce to demonstrate such effect. However, some studies demonstrated a potent anti-inflammatory effect of GbE (24–26) especially via reduction of LPS-induced inflammatory cytokines or inhibition of the Toll-like receptors pathway (27–30). Since obesity is related to hypothalamic inflammation (31–35), it is possible that the treatment with GbE might have promoted a positive anti-inflammatory effect on hypothalamus, increasing anorexigenic peptides levels and/or reducing the orexigenic ones resulting in appetite suppression and weight loss. Additional studies are necessary to better comprehend the mechanisms involved in the GbE-induced appetite suppression of obese rats.

In the nontreated obese group insulin failed to stimulate the phosphorylation of both IR and Akt in retroperitoneal fat depot indicating that high fat intake impairs insulin signaling. Interestingly, in the obese group treated with GbE, the phosphorylation of both IR and Akt was significantly increased by 281% and 67%, respectively. It is noteworthy that the beneficial effects of GbE were observed in rats that remained fed with high fat diet, suggesting that it might be efficient to treat the development of obesity-related insulin resistance.

Previous study of our laboratory showed that GbE improved insulin sensitivity evaluated by the insulin tolerance test while it did significantly improve insulin-induced Akt phosphorylation and IRS-1 levels with a concomitant reduction on PTP-1B levels in gastrocnemius muscle [6]. In addition, other studies have shown that GbE reduces glycaemia and improves glucose intolerance [16, 24]. Besides, GbE stimulated both pancreatic beta-cells function and insulin production in healthy subjects with normal glucose tolerance, while it significantly reduced the glycated hemoglobin levels of T2D patients after a 3-month period of treatment [14, 15].

It is well described that adiponectin—an adipokyne expressed inversely to body adiposity—improves insulin signaling and reduces inflammation especially via Adipo R1 receptor [25, 26]. We failed to demonstrate an effect of GbE on the adiponectin serum levels. However, the present study has demonstrated a significant increase on the adiponectin receptor, Adipo R1, gene expression in retroperitoneal fat depot while no effect was observed on the Adipo R2, indicating that GbE might improve the signaling of adiponectin. In agreement with our data, Liu et al. [27] revealed that the GbE fraction isoginkgetin enhances adiponectin secretion *in vitro*, suggesting a positive effect of GbE on the adiponectin antidiabetic action. In addition, Rasmussen et al. [25] described that the weight loss observed in obese subjects submitted to a hypocaloric diet was associated with an increase in Adipo R1 mRNA levels. Yamaguchi et al. [26] demonstrated that the binding of adiponectin to the Adipo R1 receptor, but not to Adipo R2, in macrophages was responsible for the inhibition of TLR signaling pathway mediated by the suppression of NF-κB. In view of the above considerations, it is possible that the increased expression of Adipo R1 herein demonstrated might have contributed for the stimulatory effect of GbE on insulin signaling.

Another important factor involved in the pathogenesis of insulin resistance is the low grade inflammation present in obese subjects [28]. It has been shown that, in this condition, the proinflammatory adipokine TNF-α is increased while a reduction can be observed in the levels of the anti-inflammatory IL-10, resulting in the impairment of insulin sensitivity and glucose uptake [29].

Despite the fact that, in the present study GbE failed to alter TLR4, MyD88, and NF-κB p65 proteins expression, it has significantly reduced the phosphorylation of NF-κB p65 in retroperitoneal fat depot, indicating an inhibitory effect on this inflammatory pathway. In fact, Yoshikawa et al. [30] described GbE as a potent anti-inflammatory agent. The majority of GbE anti-inflammatory effects were observed by LPS induction while the effect of GbE on the obesity-related inflammation has remained unclear. Thus, the present study is the first to demonstrate a beneficial role of GbE in such condition.

The present data have also shown that GbE reduced TNF-α levels while IL-10 and IL-6 levels were not modified in retroperitoneal adipose tissue. Besides, our results have also demonstrated an increase on the anti-inflammatory cytokine IL-10 gene expression in retroperitoneal fat depot. It is possible that the GbE treatment duration was not sufficient to affect the other cytokine levels rather than TNF-α. In addition, it is well known that the white adipose tissue presents a depot-specific response to different stimuli [31, 32]. It allows to speculate that other fat depots rather than the retroperitoneal one might present altered levels of IL-6 and IL-10 in response to GbE treatment.

It is known that increased plasma IL-10 levels are associated with visceral reduction [33]. Furthermore, IL-10 improves insulin sensitivity and glucose transport, thereby having a protective role against obesity-induced insulin resistance [29, 34]. In addition, the low IL-10 production capacity presented in pathological conditions such as obesity is associated with the development of metabolic syndrome and T2D [35]. In this context, it is possible that, in a more prolonged treatment period, the stimulatory effect of GbE on IL-10 gene expression herein demonstrated might also lead to an increase on IL-10 tissue levels, contributing to the beneficial effects of GbE on insulin signaling cascade already observed after 14 days of treatment.

An inhibitory effect of GbE on TNF-α levels on other tissues, such as brain and lungs, has been described [36, 37]. We consider that the anti-inflammatory effect of GbE via reduction of TNF-α retroperitoneal fat depot levels might soften the harmful effects of the prolonged consumption of high fat diets, resulting in the stimulation of the insulin signaling pathway.

5. Conclusions

The data presented above showed that GbE markedly stimulated the insulin signaling cascade, since it promoted the insulin-induced phosphorylation of both IR and Akt in retroperitoneal fat depot. Nevertheless, our results indicate that the inhibitory effect of GbE on both NF-κB p65 phosphorylation and TNF-α levels might have contributed to

the stimulation of the insulin signaling. Summing up, the results herein presented suggest a potential use of GbE to treat obesity-related insulin resistance. These results are especially interesting taking into consideration the high number of obese people resistant to perform diet therapy. However, additional studies are necessary to better comprehend the effects of GbE on obesity-related disorders.

Conflict of Interests

The authors declare that there is no conflict of interests regarding the publication of this paper.

Acknowledgments

The authors gratefully acknowledge the valuable support given by Janilda de Pina Pereira, Mauro Cardoso Pereira, Valter Tadeu Boldarine, and Viviane da Silva Julio. This research was supported by grants from the Brazilian agencies: FAPESP (Fundação de Amparo à Pesquisa do Estado de São Paulo) and CAPES (Coordenação de Aperfeiçoamento de Pessoal de Nível Superior).

References

[1] "World Health Organization database," http://www.who.int/gho/ncd/risk_factors/overweight/en/.

[2] M. Knaapen, R. S. Kootte, E. G. Zoetendal et al., "Obesity, non-alcoholic fatty liver disease, and atherothrombosis: a role for the intestinal microbiota?" *Clinical Microbiology and Infection*, vol. 19, no. 4, pp. 331–337, 2013.

[3] A. Federico, E. D'Aiuto, F. Borriello et al., "Fat: a matter of disturbance for the immune system," *World Journal of Gastroenterology*, vol. 16, no. 38, pp. 4762–4772, 2010.

[4] T. Jiang, Z. Wang, G. Proctor et al., "Diet-induced obesity in C57BL/6J mice causes increased renal lipid accumulation and glomerulosclerosis via a sterol regulatory element-binding protein-1c-dependent pathway," *Journal of Biological Chemistry*, vol. 280, no. 37, pp. 32317–32325, 2005.

[5] R. Buettner, J. Schölmerich, and L. C. Bollheimer, "High-fat diets: modeling the metabolic disorders of human obesity in rodents," *Obesity*, vol. 15, no. 4, pp. 798–808, 2007.

[6] R. M. Banin, B. K. S. Hirata, I. S. Andrade et al., "Beneficial effects of *Ginkgo biloba* extract on insulin signaling cascade, dyslipidemia, and body adiposity of diet-induced obese rats," *Brazilian Journal of Medical and Biological Research*, vol. 47, no. 9, pp. 780–788, 2014.

[7] V. Z. Rocha and E. J. Folco, "Inflammatory concepts of obesity," *International Journal of Inflammation*, vol. 2011, Article ID 529061, 14 pages, 2011.

[8] J.-F. Tanti and J. Jager, "Cellular mechanisms of insulin resistance: role of stress-regulated serine kinases and insulin receptor substrates (IRS) serine phosphorylation," *Current Opinion in Pharmacology*, vol. 9, no. 6, pp. 753–762, 2009.

[9] L. Azoulay, V. Schneider-Lindner, S. Dell'Aniello, K. B. Filion, and S. Suissa, "Thiazolidinediones and the risk of incident strokes in patients with type 2 diabetes: a nested case-control study," *Pharmacoepidemiology and Drug Safety*, vol. 19, no. 4, pp. 343–350, 2010.

[10] A. Vanasse, A. C. Carpentier, J. Courteau, and S. Asghari, "Stroke and cardiovascular morbidity and mortality associated with rosiglitazone use in elderly diabetic patients," *Diabetes and Vascular Disease Research*, vol. 6, no. 2, pp. 87–93, 2009.

[11] D. J. Graham, R. Ouellet-Hellstrom, T. E. Macurdy et al., "Risk of acute myocardial infarction, stroke, heart failure, and death in elderly medicare patients treated with rosiglitazone or pioglitazone," *Journal of the American Medical Association*, vol. 304, no. 4, pp. 411–418, 2010.

[12] J. Cuypers, C. Mathieu, and K. Benhalima, "SGLT2-inhibitors: a novel class for the treatment of type 2 diabetes introduction of SGLT2-inhibitors in clinical practice," *Acta Clinica Belgica*, vol. 68, no. 4, pp. 287–293, 2013.

[13] Z. Zeng, J. Zhu, L. Chen, W. Wen, and R. Yu, "Biosynthesis pathways of ginkgolides," *Pharmacognosy Reviews*, vol. 7, no. 13, pp. 47–52, 2013.

[14] G. B. Kudolo, "The effect of 3-month ingestion of *Ginkgo biloba* extract on pancreatic β-cell function in response to glucose loading in normal glucose tolerant individuals," *Journal of Clinical Pharmacology*, vol. 40, no. 6, pp. 647–654, 2000.

[15] G. B. Kudolo, W. Wang, M. Javors, and J. Blodgett, "The effect of the ingestion of *Ginkgo biloba* extract (EGb 761) on the pharmacokinetics of metformin in non-diabetic and type 2 diabetic subjects—a double blind placebo-controlled, crossover study," *Clinical Nutrition*, vol. 25, no. 4, pp. 606–616, 2006.

[16] S. Tanaka, L.-K. Han, Y.-N. Zheng, and H. Okuda, "Effects of the flavonoid fraction from *Ginkgo biloba* extract on the postprandial blood glucose elevation in rats," *Yakugaku Zasshi*, vol. 124, no. 9, pp. 605–611, 2004.

[17] D. R. Oliveira, P. F. Sanada, F. A. C. Saragossa et al., "Neuromodulatory property of standardized extract *Ginkgo biloba* L. (EGb 761) on memory: behavioral and molecular evidence," *Brain Research*, vol. 1269, pp. 68–89, 2009.

[18] D. R. Oliveira, P. F. Sanada, A. C. S. Filho, G. M. S. Conceição, J. M. Cerutti, and S. M. Cerutti, "Long-term treatment with standardized extract of *Ginkgo biloba* L. enhances the conditioned suppression of licking in rats by the modulation of neuronal and glial cell function in the dorsal hippocampus and central amygdala," *Neuroscience*, vol. 235, pp. 70–86, 2013.

[19] R. Zanuto, M. A. Siqueira-Filho, L. C. Caperuto et al., "Melatonin improves insulin sensitivity independently of weight loss in old obese rats," *Journal of Pineal Research*, vol. 55, no. 2, pp. 156–165, 2013.

[20] L. C. Caperuto, G. F. Anhê, A. M. Amanso et al., "Distinct regulation of IRS proteins in adipose tissue from obese aged and dexamethasone-treated rats," *Endocrine*, vol. 29, no. 3, pp. 391–398, 2006.

[21] A. L. Hoefel, F. Hansen, P. D. Rosa et al., "The effects of hypercaloric diets on glucose homeostasis in the rat: influence of saturated and monounsaturated dietary lipids," *Cell Biochemistry and Function*, vol. 29, no. 7, pp. 569–576, 2011.

[22] Y. Yang, L. Zhou, Y. Gu et al., "Diet chickpeas reverse visceral adiposity, dyslipidaemia and insulin resistance in rats induced by a chronic high-fat diet," *British Journal of Nutrition*, vol. 98, no. 4, pp. 720–726, 2007.

[23] M. Stumvoll, B. J. Goldstein, and T. W. van Haeften, "Type 2 diabetes: principles of pathogenesis and therapy," *The Lancet*, vol. 365, no. 9467, pp. 1333–1346, 2005.

[24] L. Zhou, Q. Meng, T. Qian, and Z. Yang, "Ginkgo biloba extract enhances glucose tolerance in hyperinsulinism-induced hepatic cells," *Journal of Natural Medicines*, vol. 65, no. 1, pp. 50–56, 2011.

[25] M. S. Rasmussen, A. S. Lihn, S. B. Pedersen, J. M. Bruun, and B. Richelsen, "Adiponectin receptors in human adipose tissue: effects of obesity, weight loss, and fat depots," *Obesity*, vol. 14, no. 1, pp. 28–35, 2006.

[26] N. Yamaguchi, J. G. M. Argueta, Y. Masuhiro et al., "Adiponectin inhibits Toll-like receptor family-induced signaling," *FEBS Letters*, vol. 579, no. 30, pp. 6821–6826, 2005.

[27] G. Liu, M. Grifman, J. Macdonald, P. Moller, F. Wong-Staal, and Q.-X. Li, "Isoginkgetin enhances adiponectin secretion from differentiated adiposarcoma cells via a novel pathway involving AMP-activated protein kinase," *Journal of Endocrinology*, vol. 194, no. 3, pp. 569–578, 2007.

[28] U. J. Jung and M. S. Choi, "Obesity and its metabolic complications: the role of adipokines and the relationship between obesity, inflammation, insulin resistance, dyslipidemia and nonalcoholic fatty liver disease," *International Journal of Molecular Sciences*, vol. 15, no. 4, pp. 6184–6223, 2014.

[29] K. Makki, P. Froguel, and I. Wolowczuk, "Adipose tissue in obesity-related inflammation and insulin resistance: cells, cytokines, and chemokines," *ISRN Inflammation*, vol. 2013, Article ID 139239, 12 pages, 2013.

[30] T. Yoshikawa, Y. Naito, and M. Kondo, "*Ginkgo biloba* leaf extract: review of biological actions and clinical applications," *Antioxidants and Redox Signaling*, vol. 1, no. 4, pp. 469–480, 1999.

[31] M. M. Telles, T. G. da Silva, R. L. H. Watanabe et al., "Lateral hypothalamic serotonin is not stimulated during central leptin hypophagia," *Regulatory Peptides*, vol. 184, pp. 75–80, 2013.

[32] A. S. Yamashita, F. S. Lira, J. C. Rosa et al., "Depot-specific modulation of adipokine levels in rat adipose tissue by diet-induced obesity: the effect of aerobic training and energy restriction," *Cytokine*, vol. 52, no. 3, pp. 168–174, 2010.

[33] G. Formoso, M. Taraborrelli, M. T. Guagnano et al., "Correction: magnetic resonance imaging determined visceral fat reduction associates with enhanced IL-10 plasma levels in calorie restricted obese subjects," *PLoS ONE*, vol. 8, no. 9, 2013.

[34] S. Tateya, F. Kim, and Y. Tamori, "Recent advances in obesity-induced inflammation and insulin resistance," *Frontiers in Endocrinology*, vol. 4, 2013.

[35] E. van Exel, J. Gussekloo, A. J. M. de Craen, M. Frölich, A. B.-V. D. Wiel, and R. G. J. Westendorp, "Low production capacity of interleukin-10 associates with the metabolic syndrome and type 2 diabetes: the Leiden 85-plus study," *Diabetes*, vol. 51, no. 4, pp. 1088–1092, 2002.

[36] Y.-Y. Hu, M. Huang, X.-Q. Dong, Q.-P. Xu, W.-H. Yu, and Z.-Y. Zhang, "Ginkgolide B reduces neuronal cell apoptosis in the hemorrhagic rat brain: possible involvement of Toll-like receptor 4/nuclear factor-kappa B pathway," *Journal of Ethnopharmacology*, vol. 137, no. 3, pp. 1462–1468, 2011.

[37] N. A. E. Boghdady, "Antioxidant and antiapoptotic effects of proanthocyanidin and *Ginkgo biloba* extract against doxorubicin-induced cardiac injury in rats," *Cell Biochemistry and Function*, vol. 31, no. 4, pp. 344–351, 2013.

Hindawi Publishing Corporation
Mediators of Inflammation
Volume 2015, Article ID 435713, 7 pages
http://dx.doi.org/10.1155/2015/435713

Review Article

Anti-Inflammatory and Immunoregulatory Functions of Artemisinin and Its Derivatives

Chenchen Shi,[1] Haipeng Li,[2] Yifu Yang,[1] and Lifei Hou[3]

[1]*Laboratory of Immunology and Virology, Shanghai University of Traditional Chinese Medicine, Shanghai, China*
[2]*Department of Orthopedics, Beijing Army General Hospital, Beijing, China*
[3]*Program in Cellular and Molecular Medicine, Boston Children's Hospital and Department of Pediatrics, Harvard Medical School, Boston, MA 02115, USA*

Correspondence should be addressed to Yifu Yang; yangyifu@mail.shcnc.ac.cn and Lifei Hou; lifei.hou@childrens.harvard.edu

Received 14 December 2014; Revised 26 February 2015; Accepted 2 March 2015

Academic Editor: Elisabetta Buommino

Artemisinin and its derivatives are widely used in the world as the first-line antimalarial drug. Recently, growing evidences reveal that artemisinin and its derivatives also possess potent anti-inflammatory and immunoregulatory properties. Meanwhile, researchers around the world are still exploring the unknown bioactivities of artemisinin derivatives. In this review, we provide a comprehensive discussion on recent advances of artemisinin derivatives affecting inflammation and autoimmunity, the underlying molecular mechanisms, and also drug development of artemisinins beyond antimalarial functions.

1. Introduction

Artemisinin was isolated from *Artemisia annua* L. in 1972 by Chinese researchers. At the end of 1975, its unique chemical structure was elucidated, as a sesquiterpene lactone bearing a peroxy group, quite different from that of all known antimalarial drugs (reviewed in [1]). Artemisinin and its derivatives are currently considered the most effective drug in treating cerebral malaria and chloroquine resistant falciparum malaria [2, 3]. It is also recognized as the "best hope for the treatment of malaria" by the World Health Organization because of its effectiveness, nonresistant characteristics, and minimal side effects [2, 3]. The active metabolite of artemisinin is dihydroartemisinin (DHA). Currently, artemisinin derivatives used in clinical treatment include DHA, artemether, artesunate, and arteether. In addition to their excellent antimalarial effects, the clinical and experimental studies also suggested that artemisinin and its derivatives possess potent immune-suppressive abilities to treat autoimmune and allergic diseases. Recently, scientists from Shanghai Institute of Materia Medica (SIMM, CAS) designed a series of novel artemisinin derivatives with lower toxicity, higher bioavailability, and potent immunosuppressive activity. In this paper, we will review the progress of the anti-inflammation and immunoregulatory studies of artemisinin family compounds including both commercial available and newly synthesized ones including 3-(12-β-artemisininoxy) phenoxyl succinic acid (SM735) [4], 1-(12-β-dihydroartemisinoxy)-2-hydroxy-3-tert-butylaminopropane maleate (SM905) [5–7], ethyl 2-[4-(12-β-artemisininoxy)] phenoxylpropionate (SM933) [8], and 2′-aminoarteether (β) maleate (SM934) [9–12] (chemical structures were shown in Figure 1). Of note, the SM934 is recently approved by the China Food and Drug Administration for clinical trial as novel therapeutic agent to treat systemic lupus erythematosus (SLE).

2. Antimalarial Mechanism of Artemisinin

Artemisinin is a sesquiterpene lactone containing peroxide bridge. Studies have shown that peroxide bridge plays an essential role in antimalarial pathways for artemisinin. The damage or absence of such peroxide bridge will reduce or even diminish the antimalarial effect. In contrast, leaving peroxide bridge untouched, antimalarial effect of artemisinin remains, no matter how the sesquiterpene was chemically modified [13, 14].

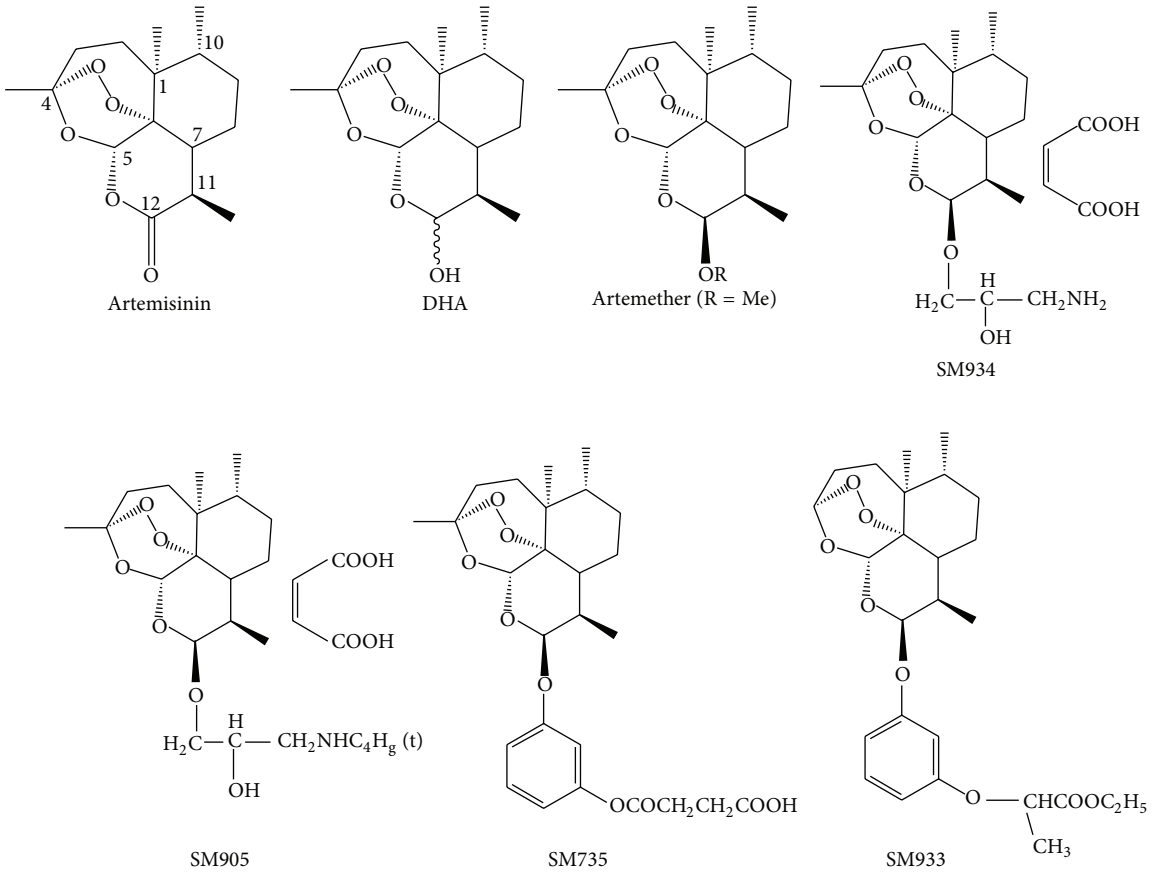

Figure 1: Chemical structure of artemisinin and its derivatives.

To date, it is broadly accepted that artemisinin exerts antimalarial effects through the following molecular mechanisms: Heme or free iron will break the peroxide bridge, which results in the degradation of the molecular structure of artemisinin to form the nucleophilic radical metabolites with the center of C_4. Consequently, the free radicals, acting as an alkylating agent, will attack macromolecular bearing electrophilic groups or centers, which eventually leads to parasitic death [14, 15]. Actually, the red blood cells have high level of oxidative stress once they are infected with *Plasmodium*. Meanwhile, the intracellular free radicals and lipid peroxidation level will dramatically increase due to oxidative stress. As a result, parasite-infected red blood cells will increase their susceptibility to artemisinin. Accordingly, *in vivo*, artemisinin is effective in killing parasite-infected red blood cells at nM levels; in sharp contrast, artemisinin only shows marginal effects on resting red blood cells, even with the concentration as high as mM levels [16, 17].

3. Anti-Inflammation and Immunoregulatory Effect of Artemisinin

3.1. In Vitro Immunosuppressive Activity. T cells play pivotal role in acquired immune reaction, which includes three fundamental steps [18, 19]. First, TCR cross-linking drives T cells from G0 to G1 transition and subsequent secretion of T cell growth factor IL-2 and expression of high-affinity receptor IL-2Rα chain (CD25). Second, through autocrine/paracrine proliferative loop, IL-2 induces clone expansion and maintains survival of activated T cells. Third, after successful clearance of the pathogen, the stimulus for cytokines production is lost and activated T cells thus will undergo apoptosis. However, in autoimmune diseases, due to the persistence of autoantigen, autoreactive T cells will be activated and survive better. Autoreactive T cell proliferation is involved in the pathogenesis of various autoimmune diseases, such as rheumatoid arthritis (RA) and multiple sclerosis (MS) [20, 21]. Artemether is a potent antimalarial drug [1]. In 2007, Wang et al. found artemether significantly suppressed the proliferation and IL-2 and interferon-γ (IFN-γ) production of T cells triggered by TCR engagement [22]. Artemether significantly inhibited TCR engagement-triggered MAPKs signaling pathway including phosphorylation of ERK1/2, Jnk, and P38. Authors further dissected that artemether majorly affected the function of T cells, rather than the antigen-presenting cells (APCs) to exert the immunosuppressive effects.

In recent years, by inserting new groups to the parent structure of artemisinin, Li from SIMM synthesized a series of artemisinin derivatives with higher water solubility and lower toxicity [23–25]. The new compounds were screened for *in vitro* immunosuppressive activity, majorly focused on suppressing T cell activation. SM735, one of artemisinin

derivatives developed by Li group, substantially inhibited the proliferation and IFN-γ production of mitogen Con A-stimulated splenocytes [4]. It also significantly suppressed the IL-12, IFN-γ, and IL-6 productions from LPS-stimulated splenocytes. SM934 and SM905 were recently synthesized derivatives by Li group in SIMM [23, 25]. Similar to SM735, the studies in Zuo group in SIMM found SM905 possessed potent immunoregulatory properties [5–7].

However, SM934 is quite distinct [11]. Similar to SM905 and artemether, *in vitro*, SM934 significantly inhibited the proliferation and IFN-γ production of splenocytes or purified CD4+ T cells induced by mixed lymphocyte reaction (MLR) or TCR cross-linking. In sharp contrast to all of SM905, SM735, and artemether, SM934 exerted no influence on IL-2 production and CD25 upregulation of T cells but could remarkably suppress IL-2-mediated proliferation and survival of activated T cells, which might be the consequence of blocking IL-2-induced phosphorylation of Akt. In addition, through combined staining of CD69 and annexin V, SM934 was found to preferentially promote activated T cells into early apoptosis, leaving resting T cells untouched.

Moreover, there are also studies suggesting that artemisinin derivatives will bind to calmodulin to inhibit phosphodiesterase activity, which causes the increase of intracellular cAMP level, and thus to exert the immunosuppressive activity [26, 27].

3.2. Artemisinin Derivatives Treat Rheumatoid Arthritis. Collagen-induced arthritis (CIA) is a classic murine model of human rheumatoid arthritis. In CIA model, SM905 could dramatically prevent or treat arthritis, which was manifested by significantly reduced incidence, joint synovial injury, and inflammatory factors secretion [7]. In addition, oral treatment of SM905 skewed the T cell subset from pathogenic Th17 to protective Th2 subset in CIA model. SM905 treatment increased IL-4 production from T cells and suppressed the RORγt mRNA expression and IL-17 production from T cells.

K/BxN mice spontaneously develop an autoimmune arthritis disease with many clinical, histopathological, and immunological features of the human rheumatoid arthritis. Breakdown of T and B cells tolerance leads to the production of high-titer autoantibodies against glucose-6-phosphate isomerase (GPI), which can directly induce joint pathology. Given the well-studied disease mechanisms and clearly defined roles of various immune cells, K/BxN mice have been an informative model to investigate therapeutic agents targeting antibody-mediated autoimmune diseases. A recent study by Hou et al. demonstrated that artemisinin analog artesunate remarkably ameliorated the arthritis in K/BxN mouse [28]. Artesunate treatment prevented the arthritis development in young K/BxN mice by inhibiting germinal center formation and production of autoantibodies. In adult K/BxN mice with established arthritis, artesunate treatment rapidly diminished germinal center B cells in a few days. However, artesunate did not affect the follicular helper T cells (Tfh). In contrast to the spontaneous K/BxN model, artesunate treatment exerted minor influence on K/BxN serum transfer induced arthritis, suggesting that artesunate has minor effects on inflammatory responses downstream of antibody production. Thus, authors demonstrated that highly proliferative GC B cells were the most sensitive cellular targets to artesunate treatment. Besides, in rat model of Freund's complete adjuvant-induced arthritis, artesunate was found to produce dose-dependent reduction in joint inflammation and improvement in functional parameters, including stair climbing ability, motility, and suppression of mechanical allodynia [29, 30].

In addition to the animal model, artemisinin derivatives also showed promising effects on human rheumatoid arthritis. *In vitro*, artesunate could significantly inhibit IL-1β, IL-6, and IL-8 production from synovial cells of RA patients, when stimulated with TNF-α. Further studies demonstrated that artesunate inhibited Akt phosphorylation and IκB degradation by blocking PI3K/Akt signaling pathway downstream of TNF-α [30, 31].

3.3. Artemisinin Derivatives Treat Systemic Lupus Erythematosus. Systemic lupus erythematosus (SLE) is a chronic autoimmune disease characterized by abnormal accumulation of autoreactive T lymphocytes and production of autoantibody against self-antigen, which result in the development of immune complex-mediated glomerulonephritis and renal failure. Female MRL/lpr mice and NZBW/F1 mice were two well-established murine models for lupus study and represent human lupus disease closely [32]. Hou et al. showed SM934 is able to significantly prolong the lifespan and limit the glomerulonephritis in the MRL/lpr mice by inhibiting both Th1 and Th17 responses [10]. The therapeutic properties of SM934 were characterized by suppressing the serum level of pathogenic cytokines interferon-γ (IFN-γ) and interleukin-10 (IL-10), reducing the secretion and deposition of pathogenic anti-dsDNA IgG autoantibodies in serum and kidneys, and ameliorating the renal injury. SM934 treatment also rectified the abnormal lymphocyte development including reduced double negative T cells (DN T) and elevated conventional single positive T cells and B cells in the spleen. In addition, SM934 treatment reduced the proportion of $CD4^+CD44^+CD62L^-$ Teff in spleens. Further investigations revealed that SM934 treatment significantly suppressed the excessive activation of STAT1, STAT3, and STAT5 in lupus.

In NZB/W F1 mice, the *fas* gene is intact, which makes the pathogenesis of NZB/W F1 mice largely different from that of MRL/lpr mice [33]. However, SM934 also exerts comprehensive therapeutic effects on NZB/W F1 mice both in short-term and long-term treatment [9]. Similarly to MRL/lpr mice, SM934 treatment could significantly increase Treg percentage and suppress the Th1 and Th17 responses in NZB/W F1 mice. Clinical improvement was accompanied with decreased Th1-related anti-dsDNA IgG2a and IgG3 Abs and serum IL-17 and increased Th2-related anti-dsDNA IgG1 Ab, serum IL-10, and IL-4. Furthermore, the therapeutic effects of SM934 on NZB/W F1 mice were tightly linked to enhancing IL-10 production from macrophages, which was absent in MRL/lpr mice.

In another mouse model of lupus BXSB, dihydroartemisinin was found to significantly improve lupus nephritis,

reduce serum TNFα level, and suppress TNFα production from peritoneal macrophages [34].

3.4. Artemisinin Derivatives Treat Multiple Sclerosis. Multiple sclerosis (MS) is a class of autoimmune disease occurring in the central nervous system, which was mediated by both of Th17- and Th1-type T cells. The main symptom of patients with MS was progressive paralysis. Experimental allergic encephalomyelitis (EAE) is a well-established murine model to study the pathogenesis of MS and for drug screening. Several artemisinin derivatives were reported to treat EAE including SM933, SM934, and dihydroartemisinin (DHA) with different mechanisms [8, 12, 35]. In 2007, SM933 was reported to possess unique anti-inflammatory properties through regulation of signaling pathways, leading to amelioration of EAE [35]. The anti-inflammatory properties of SM933 were characterized by a regulatory mechanism involving the NFκB and the Rig-G/JAB1 signaling pathways. Regulation of the Rig-G/JAB1 pathway by SM933 led to altered cell cycle activity of encephalitogenic T cells as a result of its selective effect on activated, but not resting, T cells.

In contrast to SM933, both SM934 and DHA were demonstrated to treat EAE majorly through regulating the balance between effector T cells and regulatory T cells. Zhao et al. found that administration of DHA significantly decreased effector CD4 T cells but increased Tregs in EAE mice [8]. Their study argued that DHA reciprocally regulates effector T cell and regulatory T cell generation through modulating mTOR pathway. On top of DHA work, through both BrdU incorporation strategy and *in vitro* Treg differentiation assays, Zuo group in SIMM further revealed that SM934 treatment could directly promote the expansion of Treg cells *in vivo* and *in vitro* [12].

3.5. Artemisinin Derivatives Treat Allergic Diseases. Allergy is an acquired hypersensitivity reaction of the immune system mediated by cross-linking of allergen-specific IgE with high-affinity IgE receptors, leading to immediate mast cell degranulation. Allergic disorders have substantially different pathogenesis with autoimmune diseases. However, artemisinin derivatives were also reported to be therapeutic against the allergic diseases [36–38]. Several studies by Wong group demonstrated that artesunate ameliorates experimental allergic airway inflammation probably via negative regulation of PI3K/Akt pathway and blocking IgE-induced mast cell degranulation. A recent study also reported that artesunate could suppress the proliferation of airway smooth muscle, which further strengthened the reasonability for artesunate to treat allergic airway disorders.

4. Structure-Activity Relationship

It is broadly accepted that artemisinin exerts antimalarial effects through the following molecular mechanisms: Heme or free iron will break the peroxide bridge, which results in the degradation of the molecular structure of artemisinin to form the nucleophilic radical metabolites. Consequently, the free radicals, acting as an alkylating agent, will attack macromolecular bearing electrophilic groups or centers, which eventually leads to cell damage [17]. One elegant study showed that artemisinin inhibits endoplasmic reticulum Ca^{2+}-ATPase (SERCA), resulting in calcium to accumulate in the cytoplasm [39]. The high concentration of cytoplasmic calcium activates a secondary influx of calcium into the cell, which induces the apoptosis. Thapsigargin (TG), a specific inhibitor of SERCA, could induce intracellular calcium accumulation and leads to cell apoptosis. TG is structurally similar to artemisinin, which allows it to antagonize the inhibition of artemisinin activities on SERCA *in vitro*. There are further evidences showing that TG and artemisinin have the same binding site [17]. Sequence alignments of the thapsigargin-binding pocket of mammalian SERCAs and from different *Plasmodium* spp. show several amino acids that differ among SERCAs. Further structural biology study demonstrated that a single amino acid (Leu263) in transmembrane segment 3 of SERCAs can determine susceptibility to artemisinin. Introduction of a residue in *Plasmodium vivax* SERCA (PvSERCA) increased sensitivity to artemisinins by threefold, whereas introduction of a residue in *Plasmodium berghei* SERCA (PbSERCA) decreased sensitivity by threefold [39, 40].

Although peroxide bridge plays a necessary role in the biological activity of artemisinin, finding in stereochemistry indicates that the binding site of artemisinin and SERCA does not include the peroxide bridge [41]. We hypothesize that peroxide bridge might act as a "catalyst" for artemisinin to inhibit SERCA. According to stereochemistry and transitional state theory, when the peroxide bridge is intact, the spatial configuration of artemisinin is relatively rigid, and the sesquiterpene lactone structure might not be able to flexibly rotate and fold. In this case, artemisinin has relatively lower affinity to SERCA. However, once the peroxide bridge has been reduced by divalent iron ion and broken, the sesquiterpene lactone part will be released and will be flexible and will bind to SERCA with high affinity. As a result, the inhibitory effect of artemisinin against SERCA is enhanced.

Studies have found that, in parasites-infected red blood cells and activated lymphocytes, the divalent iron ion level is significantly higher than the resting state/cells. In this case, the opportunity for peroxide bridge to be broken is largely increased, which consequently makes the activated cells, rather than the resting cells, much more vulnerable to artemisinin. In conclusion, the peroxide bridge is a unique structure and is essential for the biological activity of artemisinin. Furthermore, since mammalian SERCAs are not susceptible to inhibition by artemisinins [39], the biochemical mechanism and molecular target of artemisinin to exert immunosuppressive function still need to be further studied.

5. Summary and Future Outlook

Artemisinin and its derivatives are potent antimalarial agents with high efficacy and low toxicity. Besides the outstanding antimalarial activity, artemisinin and its derivatives also possess immunosuppressive activities and are experimentally

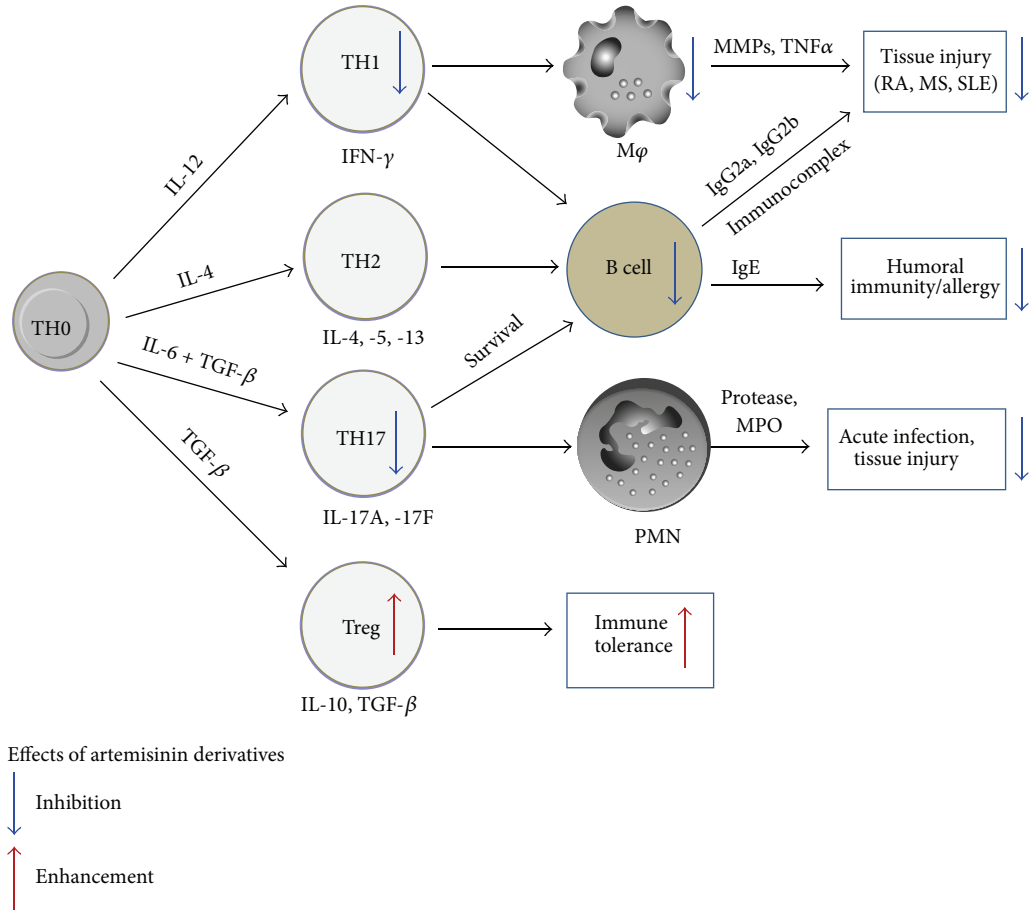

Figure 2: Schematic of artemisinin derivatives affecting immune and inflammation.

used to treat autoimmune diseases, such as SLE, RA, and CIA. In this paper, we summarized the recent progress of artemisinin derivatives in treating autoimmune and allergic disorders. We conclude that artemisinin derivatives perform immunosuppressive functions primarily through inhibiting pathogenic T cell activation, suppressing B cells activation and antibody production, and expanding regulatory T cells (impact of artemisinins and derivatives on different immune cells is shown in Figure 2). We deem that, as anti-inflammatory agents, artemisinin derivatives possess more advantages to act on multiple checkpoints within the immune signaling cascade, with selectivity for activated pathogenic T cells, to create a synergistic treatment effect on disease activity. Thus, these new artemisinin derivatives may be a kind of promising candidates to treat inflammation and autoimmune disorders.

Abbreviations

DHA: Dihydroartemisinin
SM735: 3-(12-β-Artemisininoxy) phenoxyl succinic acid
SM905: 1-(12-β-Dihydroartemisinoxy)-2-hydroxy-3-tert-butylaminopropane maleate
SM933: Ethyl 2-[4-(12-β-artemisininoxy)] phenoxylpropionate
SM934: 2′-Aminoarteether (β) maleate
SLE: Systemic lupus erythematosus
RA: Rheumatoid arthritis
MS: Multiple sclerosis
EAE: Experimental allergic encephalomyelitis
CIA: Collagen-induced arthritis
MOG: Myelin oligodendrocyte glycoprotein
SERCA: Endoplasmic reticulum Ca^{2+}-ATPase
TCR: T cell receptor
STAT: Signal transducer and activator of transcription
CD: Cluster of differentiation
Th: T helper
IL: Interleukin
IFN: Interferon
ConA: Concanavalin A
SERCA: Endoplasmic reticulum Ca^{2+}-ATPase
Treg: Regulatory T cell
TNF: Tumor necrosis factor
TG: Thapsigargin.

Conflict of Interests

The authors have no conflict of interests.

Authors' Contribution

Chenchen Shi and Haipeng Li contribute equally.

References

[1] Y. Li, "Qinghaosu (artemisinin): chemistry and pharmacology," *Acta Pharmacologica Sinica*, vol. 33, no. 9, pp. 1141–1146, 2012.

[2] N. J. White, "Qinghaosu (artemisinin): the price of success," *Science*, vol. 320, no. 5874, pp. 330–334, 2008.

[3] M. B. van Hensbroek, E. Onyiorah, S. Jaffar et al., "A trial of artemether or quinine in children with cerebral malaria," *The New England Journal of Medicine*, vol. 335, no. 2, pp. 69–75, 1996.

[4] W. L. Zhou, J. M. Wu, Q. L. Wu et al., "A novel artemisinin derivative, 3-(12-beta-artemisininoxy) phenoxyl succinic acid (SM735), mediates immunosuppressive effects in vitro and in vivo," *Acta Pharmacologica Sinica*, vol. 26, no. 11, pp. 1352–1358, 2005.

[5] J.-X. Wang, L.-F. Hou, Y. Yang, W. Tang, Y. Li, and J.-P. Zuo, "SM905, an artemisinin derivative, inhibited NO and pro-inflammatory cytokine production by suppressing MAPK and NF-B pathways in RAW 264.7 macrophages," *Acta Pharmacologica Sinica*, vol. 30, no. 10, pp. 1428–1435, 2009.

[6] J.-X. Wang, W. Tang, Z.-S. Yang et al., "Suppressive effect of a novel water-soluble artemisinin derivative SM905 on T cell activation and proliferation *in vitro* and *in vivo*," *European Journal of Pharmacology*, vol. 564, no. 1–3, pp. 211–218, 2007.

[7] J.-X. Wang, W. Tang, R. Zhou et al., "The new water-soluble artemisinin derivative SM905 ameliorates collagen-induced arthritis by suppression of inflammatory and Th17 responses," *British Journal of Pharmacology*, vol. 153, no. 6, pp. 1303–1310, 2008.

[8] Y. G. Zhao, Y. Wang, Z. Guo et al., "Dihydroartemisinin ameliorates inflammatory disease by its reciprocal effects on Th and regulatory T cell function via modulating the mammalian target of rapamycin pathway," *Journal of Immunology*, vol. 189, no. 9, pp. 4417–4425, 2012.

[9] L.-F. Hou, S.-J. He, X. Li et al., "Sm934 treated lupus-prone NZB×NZW F_1 mice by enhancing macrophage interleukin-10 production and suppressing pathogenic T cell development," *PLoS ONE*, vol. 7, no. 2, Article ID e32424, 2012.

[10] L.-F. Hou, S.-J. He, X. Li et al., "Oral administration of artemisinin analog SM934 ameliorates lupus syndromes in MRL/lpr mice by inhibiting Th1 and Th17 cell responses," *Arthritis and Rheumatism*, vol. 63, no. 8, pp. 2445–2455, 2011.

[11] L.-F. Hou, S.-J. He, J.-X. Wang et al., "SM934, a water-soluble derivative of arteminisin, exerts immunosuppressive functions *in vitro* and *in vivo*," *International Immunopharmacology*, vol. 9, no. 13-14, pp. 1509–1517, 2009.

[12] X. Li, T.-T. Li, X.-H. Zhang et al., "Artemisinin analogue SM934 ameliorates murine experimental autoimmune encephalomyelitis through enhancing the expansion and functions of regulatory T cell," *PLoS ONE*, vol. 8, no. 8, Article ID e74108, 2013.

[13] P. L. Olliaro, R. K. Haynes, B. Meunier, and Y. Yuthavong, "Possible modes of action of the artemisinin-type compounds," *Trends in Parasitology*, vol. 17, no. 3, pp. 122–126, 2001.

[14] J. L. Vennerstrom, S. Arbe-Barnes, R. Brun et al., "Identification of an antimalarial synthetic trioxolane drug development candidate," *Nature*, vol. 430, no. 7002, pp. 900–904, 2004.

[15] A. Robert, F. Benoit-Vical, C. Claparols, and B. Meunier, "The antimalarial drug artemisinin alkylates heme in infected mice," *Proceedings of the National Academy of Sciences of the United States of America*, vol. 102, no. 38, pp. 13676–13680, 2005.

[16] A. E. Mercer, J. L. Maggs, X.-M. Sun et al., "Evidence for the involvement of carbon-centered radicals in the induction of apoptotic cell death by artemisinin compounds," *The Journal of Biological Chemistry*, vol. 282, no. 13, pp. 9372–9382, 2007.

[17] J. Golenser, J. H. Waknine, M. Krugliak, N. H. Hunt, and G. E. Grau, "Current perspectives on the mechanism of action of artemisinins," *International Journal for Parasitology*, vol. 36, no. 14, pp. 1427–1441, 2006.

[18] J. Alberola-Ila, S. Takaki, J. D. Kerner, and R. M. Perlmutter, "Differential signaling by lymphocyte antigen receptors," *Annual Review of Immunology*, vol. 15, pp. 125–154, 1997.

[19] N. C. Lea, S. J. Orr, K. Stoeber et al., "Commitment point during $G_0 \rightarrow G_1$ that controls entry into the cell cycle," *Molecular and Cellular Biology*, vol. 23, no. 7, pp. 2351–2361, 2003.

[20] A. VanderBorght, P. Geusens, J. Raus, and P. Stinissen, "The autoimmune pathogenesis of rheumatoid arthritis: role of autoreactive T cells and new immunotherapies," *Seminars in Arthritis and Rheumatism*, vol. 31, no. 3, pp. 160–175, 2001.

[21] C. J. Hedegaard, M. Krakauer, K. Bendtzen, H. Lund, F. Sellebjerg, and C. H. Nielsen, "T helper cell type 1 (Th1), Th2 and Th17 responses to myelin basic protein and disease activity in multiple sclerosis," *Immunology*, vol. 125, no. 2, pp. 161–169, 2008.

[22] J.-X. Wang, W. Tang, L.-P. Shi et al., "Investigation of the immunosuppressive activity of artemether on T-cell activation and proliferation," *British Journal of Pharmacology*, vol. 150, no. 5, pp. 652–661, 2007.

[23] Z.-S. Yang, J.-X. Wang, Y. Zhou, J.-P. Zuo, and Y. Li, "Synthesis and immunosuppressive activity of new artemisinin derivatives. Part 2: 2-[12(beta or alpha)-dihydroartemisinoxymethyl(or 1'-ethyl)]phenoxyl propionic acids and esters," *Bioorganic and Medicinal Chemistry*, vol. 14, no. 23, pp. 8043–8049, 2006.

[24] Z.-S. Yang, W.-L. Zhou, Y. Sui et al., "Synthesis and immunosuppressive activity of new artemisinin derivatives. 1. [12(β or α)-dihydroartemisininoxy]phen(ox)yl aliphatic acids and esters," *Journal of Medicinal Chemistry*, vol. 48, no. 14, pp. 4608–4617, 2005.

[25] J.-X. Zhang, J.-X. Wang, Y. Zhang et al., "Synthesis and immunosuppressive activity of new artemisinin derivatives containing polyethylene glycol group," *Yaoxue Xuebao*, vol. 41, no. 1, pp. 65–70, 2006.

[26] S. Noori, Z. M. Hassan, B. Rezaei, A. Rustaiyan, Z. Habibi, and F. Fallahian, "Artemisinin can inhibit the calmodulin-mediated activation of phosphodiesterase in comparison with Cyclosporin A," *International Immunopharmacology*, vol. 8, no. 13-14, pp. 1744–1747, 2008.

[27] S. Noori, Z. M. Hassan, M. Taghikhani, B. Rezaei, and Z. Habibi, "Dihydroartemisinin can inhibit calmodulin, calmodulin-dependent phosphodiesterase activity and stimulate cellular immune responses," *International Immunopharmacology*, vol. 10, no. 2, pp. 213–217, 2010.

[28] L. Hou, K. E. Block, H. Huang, and J. Zhang, "Artesunate abolishes germinal center B cells and inhibits autoimmune arthritis," *PLoS ONE*, vol. 9, no. 8, Article ID e104762, 2014.

[29] B. Guruprasad, P. Chaudhary, T. Choedon, and V. L. Kumar, "Artesunate ameliorates functional limitations in Freund's complete adjuvant-induced monoarthritis in rat by maintaining oxidative homeostasis and inhibiting COX-2 expression," *Inflammation*, 2014.

[30] Y. He, J. Fan, H. Lin et al., "The anti-malaria agent artesunate inhibits expression of vascular endothelial growth factor and hypoxia-inducible factor-1α in human rheumatoid arthritis fibroblast-like synoviocyte," *Rheumatology International*, vol. 31, no. 1, pp. 53–60, 2011.

[31] H. Xu, Y. He, X. Yang et al., "Anti-malarial agent artesunate inhibits TNF-α-induced production of proinflammatory cytokines via inhibition of NF-κB and PI3 kinase/Akt signal pathway in human rheumatoid arthritis fibroblast-like synoviocytes," *Rheumatology*, vol. 46, no. 6, pp. 920–926, 2007.

[32] A. N. Theofilopoulos and F. J. Dixon, "Murine models of systemic lupus erythematosus," *Advances in Immunology*, vol. 37, pp. 269–390, 1985.

[33] B. Andrews, R. A. Eisenberg, A. N. Theofilopoulos et al., "Spontaneous murine lupus-like syndromes. Clinical and immunopathological manifestations in several strains," *The Journal of Experimental Medicine*, vol. 148, no. 5, pp. 1198–1215, 1978.

[34] W.-D. Li, Y.-J. Dong, Y.-Y. Tu, and Z.-B. Lin, "*Dihydroarteannuin ameliorates* lupus symptom of BXSB mice by inhibiting production of TNF-alpha and blocking the signaling pathway NF-kappa B translocation," *International Immunopharmacology*, vol. 6, no. 8, pp. 1243–1250, 2006.

[35] Z. Wang, J. Qiu, T. B. Guo et al., "Anti-inflammatory properties and regulatory mechanism of a novel derivative of artemisinin in experimental autoimmune encephalomyelitis," *The Journal of Immunology*, vol. 179, no. 9, pp. 5958–5965, 2007.

[36] C. Cheng, W. E. Ho, F. Y. Goh et al., "Anti-malarial drug artesunate attenuates experimental allergic asthma via inhibition of the phosphoinositide 3-kinase/Akt pathway," *PLoS ONE*, vol. 6, no. 6, Article ID e20932, 2011.

[37] C. Cheng, D. S. W. Ng, T. K. Chan et al., "Anti-allergic action of anti-malarial drug artesunate in experimental mast cell-mediated anaphylactic models," *Allergy*, vol. 68, no. 2, pp. 195–203, 2013.

[38] S. S. L. Tan, B. Ong, C. Cheng et al., "The antimalarial drug artesunate inhibits primary human cultured airway smooth muscle cell proliferation," *The American Journal of Respiratory Cell and Molecular Biology*, vol. 50, no. 2, pp. 451–458, 2014.

[39] U. Eckstein-Ludwig, R. J. Webb, I. D. A. van Goethem et al., "Artemisinins target the SERCA of *Plasmodium falciparum*," *Nature*, vol. 424, no. 6951, pp. 957–961, 2003.

[40] A.-C. Uhlemann, A. Cameron, U. Eckstein-Ludwig et al., "A single amino acid residue can determine the sensitivity of SERCAs to artemisinins," *Nature Structural and Molecular Biology*, vol. 12, no. 7, pp. 628–629, 2005.

[41] M. Jung, H. Kim, Y. N. Ki, and T. N. Kyoung, "Three-dimensional structure of Plasmodium falciparum Ca^{2+}-ATPase(PfATP6) and docking of artemisinin derivatives to PfATP6," *Bioorganic and Medicinal Chemistry Letters*, vol. 15, no. 12, pp. 2994–2997, 2005.

Hindawi Publishing Corporation
Mediators of Inflammation
Volume 2015, Article ID 274314, 11 pages
http://dx.doi.org/10.1155/2015/274314

Research Article

Astragaloside IV Inhibits NF-κB Activation and Inflammatory Gene Expression in LPS-Treated Mice

Wei-Jian Zhang and Balz Frei

Linus Pauling Institute and Department of Biochemistry and Biophysics, Oregon State University, 307 Linus Pauling Science Center, Corvallis, OR 97331, USA

Correspondence should be addressed to Wei-Jian Zhang; weijian.zhang@oregonstate.edu

Received 16 December 2014; Revised 27 February 2015; Accepted 28 February 2015

Academic Editor: Yi Fu Yang

In this study we investigated the role of astragaloside IV (AS-IV), one of the major active constituents purified from the Chinese medicinal herb *Astragalus membranaceus*, in LPS-induced acute inflammatory responses in mice *in vivo* and examined possible underlying mechanisms. Mice were assigned to four groups: vehicle-treated control animals; AS-IV-treated animals (10 mg/kg b.w. AS-IV daily i.p. injection for 6 days); LPS-treated animals; and AS-IV plus LPS-treated animals. We found that AS-IV treatment significantly inhibited LPS-induced increases in serum levels of MCP-1 and TNF by 82% and 49%, respectively. AS-IV also inhibited LPS-induced upregulation of inflammatory gene expression in different organs. Lung mRNA levels of cellular adhesion molecules, MCP-1, TNFα, IL-6, and TLR4 were significantly attenuated, and lung neutrophil infiltration and activation were strongly inhibited, as reflected by decreased myeloperoxidase content, when the mice were pretreated with AS-IV. Similar results were observed in heart, aorta, kidney, and liver. Furthermore, AS-IV significantly suppressed LPS-induced NF-κB and AP-1 DNA-binding activities in lung and heart. In conclusion, our data provide new *in vivo* evidence that AS-IV effectively inhibits LPS-induced acute inflammatory responses by modulating NF-κB and AP-1 signaling pathways. Our results suggest that AS-IV may be useful for the prevention or treatment of inflammatory diseases.

1. Introduction

Endothelial cells are a primary target of inflammatory responses, and their injury can lead to vasculopathy and organ dysfunction [1]. The bacterial endotoxin LPS directly elicits several acute inflammatory responses in endothelial cells, including production of cellular adhesion molecules, such as E-selectin, vascular cell adhesion molecule-1 (VCAM-1), and intercellular adhesion molecule-1 (ICAM-1), and other proinflammatory mediators, such as TNFα, IL-6, and monocyte chemoattractant protein-1 (MCP-1). Together, these proinflammatory mediators elicit leukocyte adhesion to the vasculature and transmigration into the underlying tissue, causing endothelial injury and dysfunction associated with sepsis [1]. Although these proinflammatory mediators are required for an adequate host-defense response, their dysregulation can lead to refractory hypotension, cardiovascular hyporeactivity, intravascular coagulation, multiple organ failure, and death [2, 3].

The regulation of inflammatory gene transcription has been shown to be controlled by specific signaling pathways and transcription factors, such as NF-κB and AP-1 [4, 5]. In particular, the NF-κB pathway affects host defense against infectious agents by upregulating inflammatory genes that cause acute neutrophilic inflammation and the systemic inflammatory response syndrome [5]. Under normal condition, NF-κB is located in the cytoplasm in an inactive form in association with its inhibitor, IκB. In response to stimulation, for example, by LPS, IκB is phosphorylated by IκB kinase. Following phosphorylation, IκB is ubiquitinated and degraded, allowing NF-κB to translocate to the nucleus, bind to DNA promoter regions, and induce inflammatory gene transcription. Various agents that block NF-κB signaling have been shown to decrease expression of proinflammatory

mediators [6–9]. Thus, the inhibition of NF-κB activation is expected to be protective in pathological inflammatory states.

Astragalus membranaceus is one of the most widely used Chinese medicinal herbs for the treatment of many diseases, including cardiovascular disease, nephritis, hepatitis, and diabetes [10]. It also has been available in Europe and the US for many years as a food supplement. Evidence from pharmacological research and clinical practice suggests that *Astragalus* possesses a wide spectrum of activities, including immunomodulation [11, 12], cardiovascular protection [13–15], anti-inflammatory effects [16–18], hepatoprotection [19, 20], antidiabetes [21], anticancer [22], and neuroprotection [23].

The biologically active constituents of *Astragalus* roots represent three classes of chemical compounds: saponins, polysaccharides, and flavonoids [24]. By chemical degradation and ^{13}C nuclear magnetic resonance examination, the structure of astragaloside IV (AS-IV) was determined as 3-O-β-D-xylopyranosyl-6-O-β-D-glucopyranosyl-cycloastragenol ($C_{41}H_{68}O_{14}$; MW = 784.9) [25]. As one of the major active constituents of *Astragalus*, AS-IV is used as the characteristic marker for quality evaluation of *Astragalus* in the Chinese Pharmacopeia and has been shown to exert potent cardioprotective and anti-inflammatory effects [6, 10, 26–30]. We have previously shown that AS-IV inhibits LPS- and TNFα-induced adhesion molecule expression and NF-κB activation in cultured human endothelial cells [6]. However, *in vivo* evidence supporting such activity is currently lacking. Therefore, in this study we investigated whether AS-IV can inhibit LPS-induced acute inflammatory responses in experimental mice.

2. Materials and Methods

2.1. Animals and Experimental Procedures. Female C57BL/6J mice, 12 weeks old and weighing 20–22 g, were purchased from Jackson Laboratory (Bar Harbor, ME) and housed in specific pathogen-free conditions and a temperature- and humidity-controlled environment (12-h light/dark cycle) with unlimited access to tap water and Purina 5001 chow diet (Harlan Teklad, Madison, WI). The investigation conformed to the *Guide for the Care and Use of Laboratory Animals* by NIH, and all animal procedures were reviewed and approved by the Oregon State University Institutional Animal Care and Use Committee.

AS-IV was purchased from Quality Phytochemicals LLC (Edison, NJ), and a stock solution was prepared with propylene glycol (Sigma Aldrich, St. Louis, MO) and further diluted with Hank's buffered saline solution (HBSS). LPS (serotype 055:B5 from *Escherichia coli,* Sigma Aldrich) stock solution was prepared in HBSS. Mice were randomly assigned to 4 groups as follows: (i) control animals received daily i.p. injection of the vehicle propylene glycol with HBSS for 6 days followed by a single i.p. HBSS injection; (ii) AS-IV-treated animals received 10 mg/kg b.w. AS-IV daily i.p. for 6 days followed by a single i.p. HBSS injection; (iii) LPS-treated animals received daily i.p. injection of propylene glycol with HBSS for 6 days followed by a single i.p. injection of 0.5 μg/g b.w. LPS; and (iv) AS-IV plus LPS-treated animals received AS-IV daily i.p. for 6 days followed by single i.p. injection of LPS. Animals were sacrificed 3 hours after HBSS or LPS injection. Based on our previous observations, the 3-h time point and LPS dose of 0.5 μg/g b.w. were chosen [31]. In some studies, mice were randomly assigned to receive i.p. injection of LPS and sacrificed after 1, 3, 8, or 24 h. Each group consisted of 4 to 5 animals. After sacrifice, blood and tissues were collected for further analysis.

2.2. Serum Inflammatory Mediators. Serum concentrations of MCP-1, TNFα, sVCAM-1, and sICAM-1 were measured by quantitative colorimetric sandwich ELISA (R&D Systems, Minneapolis, MN). The sensitivity of the assays is 2 pg/mL for MCP-1, 5 pg/mL for TNFα, and 30 pg/mL for sVCAM-1 and sICAM-1.

2.3. Tissue mRNA Levels of Inflammatory Mediators. Total RNA was isolated from different organs using TRIzol Reagent (Life Technologies, Foster City, CA). cDNA synthesis was performed using the high capacity cDNA archive kit (Life Technologies). mRNA levels of *VCAM-1, ICAM-1, E-selectin, P-selectin, MCP-1, TNFα, IL-6*, myeloperoxidase *(MPO)*, Toll-like receptor-4 *(TLR4)*, and glyceraldehyde-3-phosphate dehydrogenase *(GAPDH)* were quantitated by real-time qPCR. All primers and probes were purchased as kits (Assays on Demand, Life Technologies). The assays are supplied as a 20x mixture of PCR primers and TaqMan minor groove binder 6-FAM dye-labeled probes with a nonfluorescent quencher at the 3′ end. TaqMan quantitative PCR (40 cycles at 95°C for 15 sec and 60°C for 1 min) was performed using TaqMan Universal PCR Master Mix (Life Technologies) in 96-well plates with an ABI Prism 7500 Sequence Detection System (Life Technologies). To obtain relative quantification, two standard curves were constructed in each plate with one target gene and the internal control *GAPDH* gene. Standard curves were generated by plotting the threshold cycle number values against the log of the amount of input cDNA and used to quantify the expression of the target genes and *GAPDH* gene in the same sample. After normalization to internal *GAPDH* in each sample, results were expressed as percentage of GAPDH or fold of control.

2.4. Lung Protein Concentration of Myeloperoxidase. A part of the right lung lobe was homogenized, and the cytosolic fraction of lung tissue homogenate was prepared using nuclear extract kits (Active Motif, Carlsbad, CA). Lung cytosolic MPO was quantified using the MPO enzyme-linked immunosorbent assay kit (Hycult Biotechnology, Plymouth Meeting, PA) according to the manufacturer's instructions. The lung MPO concentration of each sample was normalized with cytosolic protein concentration and expressed as ng MPO/mg tissue protein.

2.5. Nuclear Transcription Factors. Nuclear extracts were prepared from lung and heart using nuclear extract kits (Active Motif). For analysis of nuclear transcription factor activation, ELISA-based assays (Active Motif) were used to determine the DNA-binding activity of NF-κB (p65) and AP-1 (c-fos).

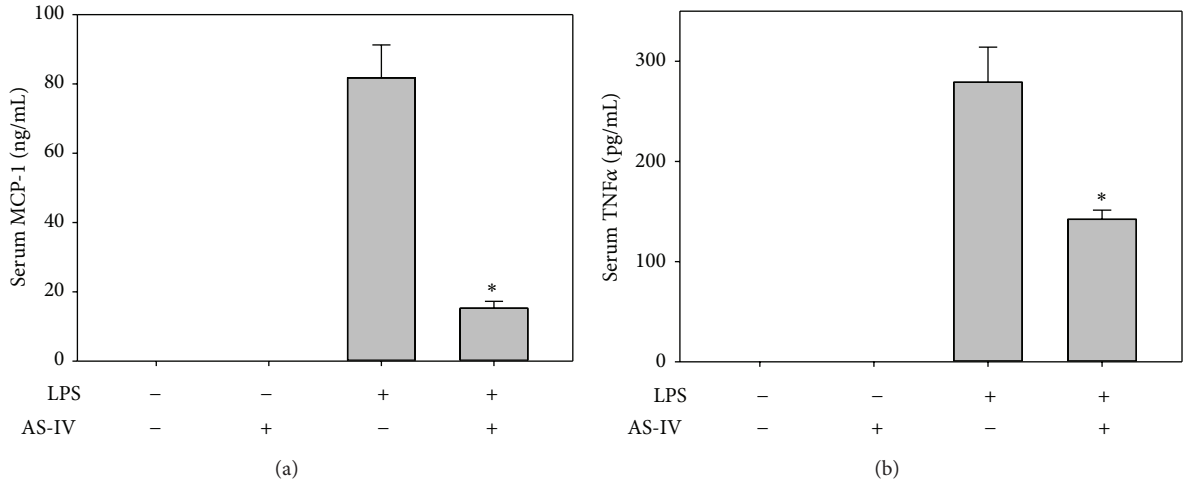

Figure 1: AS-IV inhibits LPS-induced increases in serum MCP-1 and TNFα in mice. Mice were randomly assigned to 4 groups as follows: (i) control animals received daily i.p. injection of the vehicle HBSS for 6 days followed by a single i.p. HBSS injection; (ii) AS-IV-treated animals received 10 mg/kg b.w. AS-IV daily i.p. for 6 days followed by a single i.p. HBSS injection; (iii) LPS-treated animals received daily i.p. injection of vehicle HBSS for 6 days followed by a single i.p. injection of 0.5 μg/g b.w. LPS; and (iv) AS-IV plus LPS-treated animals received AS-IV daily i.p. for 6 days followed by single i.p. injection of LPS. Three hours after the HBSS or LPS injection, the animals were sacrificed and blood was collected. Serum MCP-1 (a) and TNFα (b) were measured by ELISA. Data shown are mean values ± SEM of five animals per group. $^*P < 0.05$ compared to animals treated with LPS only.

The specificity of binding was confirmed by competition with either wild-type or mutant oligonucleotides.

2.6. Statistical Analysis. The data were calculated as means ± SEM and analyzed by ANOVA with Fisher PLSD post hoc test. Statistical significance was set at $P < 0.05$.

3. Results and Discussion

The pathophysiology of acute inflammation triggered by the bacterial endotoxin LPS is characterized by the production of multiple proinflammatory cytokines and chemokines, expression of adhesion molecules, and infiltration of neutrophils and monocytes into inflamed tissues. Because of the complexity of the pathology of septic shock, major efforts have focused on identifying novel anti-inflammatory drugs that prevent the proinflammatory process at the early stage of gene expression of key inflammatory mediators [32].

We have previously shown that AS-IV inhibits LPS- and TNFα-induced adhesion molecule expression and consequent adherence of monocytes by modulating NF-κB signaling pathway in cultured human endothelial cells [6]. We now provide new evidence showing that AS-IV exhibits strong anti-inflammatory activities *in vivo* by attenuating LPS-induced acute inflammatory responses through inhibition of NF-κB- and AP-1-mediated inflammatory signaling pathways in mice.

3.1. AS-IV Inhibits LPS-Induced Increases in Serum MCP-1 and TNFα in Mice. Treatment of mice with AS-IV for 6 days had no effect on body weight changes compared to HBSS-treated control animals. The mean body weight was 20.8 ± 0.6 g before and 20.8 ± 0.5 g after 6-day AS-IV treatment. In control animals, the mean body weight was 20.2 ± 0.3 g before and 19.9 ± 0.4 g after 6-day HBSS treatment. We first investigated the effect of AS-IV on LPS-induced systemic inflammatory responses by determining serum levels of MCP-1, TNFα, and the soluble cellular adhesion molecules, sVCAM-1 and sICAM-1. Treatment of mice with AS-IV alone for 6 days had no effect on serum levels of these inflammatory mediators compared to HBSS-treated control animals. As expected, 3 hours after LPS injection, significant increases in the serum levels of MCP-1 and TNFα were observed (Figure 1). Interestingly, pretreatment of animals with AS-IV significantly inhibited LPS-induced increases in serum MCP-1 (Figure 1(a)) and TNFα (Figure 1(b)) by 82% and 49%, respectively. Specifically, MCP-1 levels were 15.2 ± 2.0 ng/mL in mice treated with AS-IV plus LPS, compared to 81.8 ± 9.5 ng/mL in animals treated with LPS only; TNFα levels were 142 ± 9 pg/mL and 279 ± 35 pg/mL, respectively ($P < 0.05$, $n = 5$). However, AS-IV did not inhibit the LPS-induced increases in serum sVCAM-1 and sICAM-1 concentrations (data not shown).

3.2. AS-IV Inhibits LPS-Induced Upregulation of Inflammatory Gene Expression in Mouse Lung and Other Tissues. To investigate whether AS-IV inhibits LPS-induced acute inflammatory responses in mouse organs, we assessed gene expression of inflammatory mediators in lung, heart, aorta, kidney, and liver of LPS-exposed mice, using real-time qPCR analysis. Treatment of mice with AS-IV alone did not affect gene expression of cellular adhesion molecules and proinflammatory mediators (Figures 2–6). As expected, treatment of mice with LPS for 3 hours strongly upregulated inflammatory gene expression in all tissues examined (Figures 2–6). Pretreatment of mice with AS-IV significantly inhibited

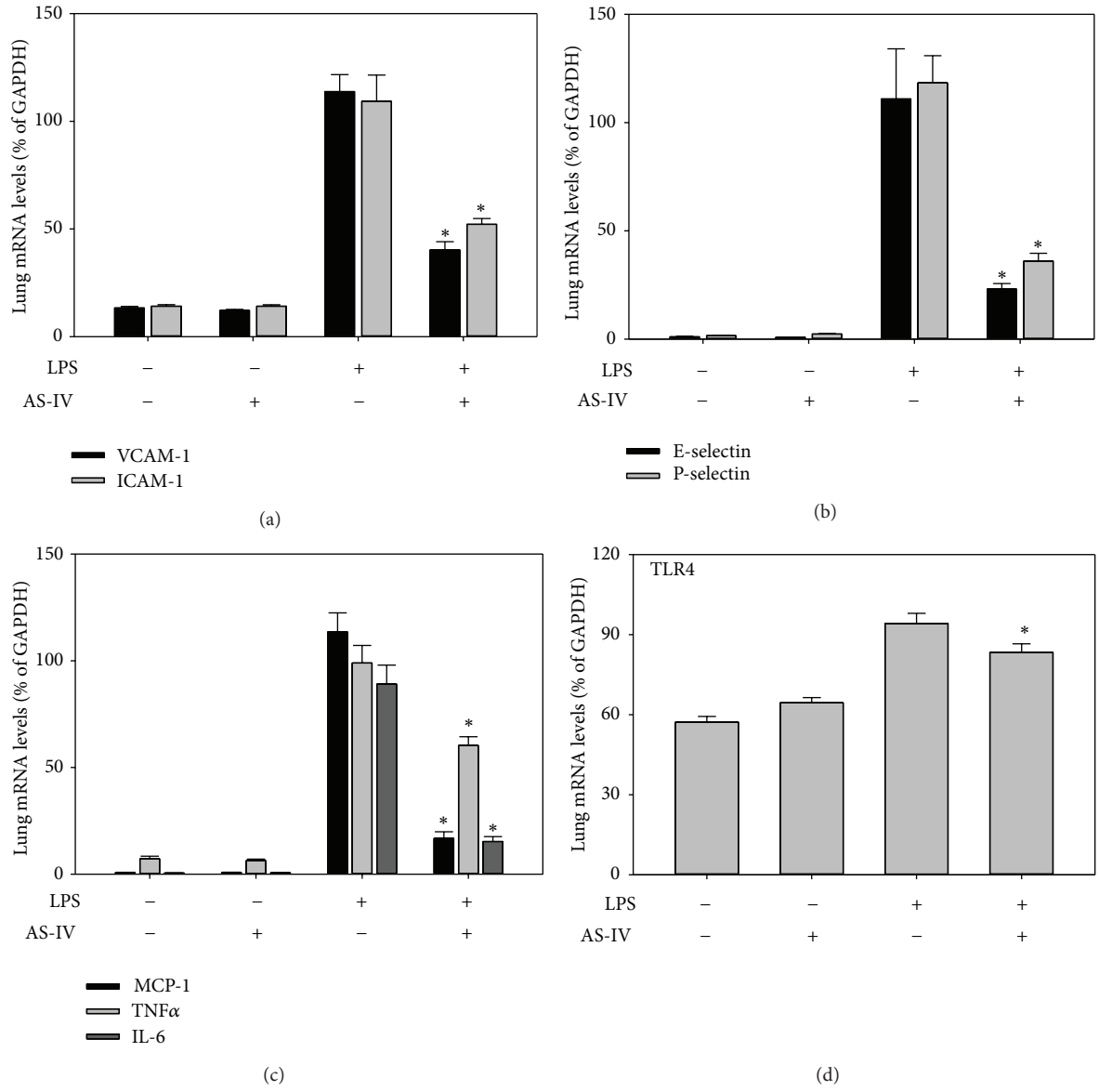

Figure 2: AS-IV inhibits LPS-induced inflammatory gene expression in mouse lung. Mice were randomly assigned to 4 groups as follows: (i) control animals received daily i.p. injection of the vehicle HBSS for 6 days followed by a single i.p. HBSS injection; (ii) AS-IV-treated animals received 10 mg/kg b.w. AS-IV daily i.p. for 6 days followed by a single i.p. HBSS injection; (iii) LPS-treated animals received daily i.p. injection of vehicle HBSS for 6 days followed by a single i.p. injection of 0.5 μg/g b.w. LPS; and (iv) AS-IV plus LPS-treated animals received AS-IV daily i.p. for 6 days followed by single i.p. injection of LPS. Three hours after the HBSS or LPS injection, the animals were sacrificed and tissues were collected. Total RNA was isolated from lung. Inflammatory gene expression was quantified using real-time quantitative PCR. After normalization to the internal control gene GAPDH, the results for each target gene were expressed as percentage of GAPDH. Data shown are means ± SEM of 5 animals per group. $^*P < 0.05$ compared to animals treated with LPS only.

the LPS-induced increase in lung mRNA levels of adhesion molecules: *VACM-1* by 73%, *ICAM-1* by 60%, *E-selectin* by 79%, and *P-selectin* by 71% and other proinflammatory mediators: *MCP-1* by 85%, *TNFα* by 42%, *IL-6* by 83%, and *TLR4* by 30% ($P < 0.05$, $n = 5$) (Figure 2). Similar inhibitory effects of AS-IV were also observed in heart (Figure 4), aorta (Figure 5), kidney (Figure 6), and liver (data not shown).

3.3. AS-IV Inhibits LPS-Induced Neutrophil Infiltration and Activation in Lung. As polymorphonuclear neutrophils (PMN) and other phagocytic cells, such as monocyte-macrophages, play critical roles in acute inflammation and tissue injury, we assessed lung myeloperoxidase (MPO), a well-documented PMN-specific biomarker [31, 33, 34], after LPS challenge. MPO is rapidly released when PMN are activated, which triggers transcriptional upregulation of mRNA and new protein synthesis of MPO. Therefore, upregulation of *MPO* mRNA levels also reflects PMN activation during acute lung inflammatory responses [31, 33]. As shown in Figure 3(a), lung *MPO* mRNA was at very low

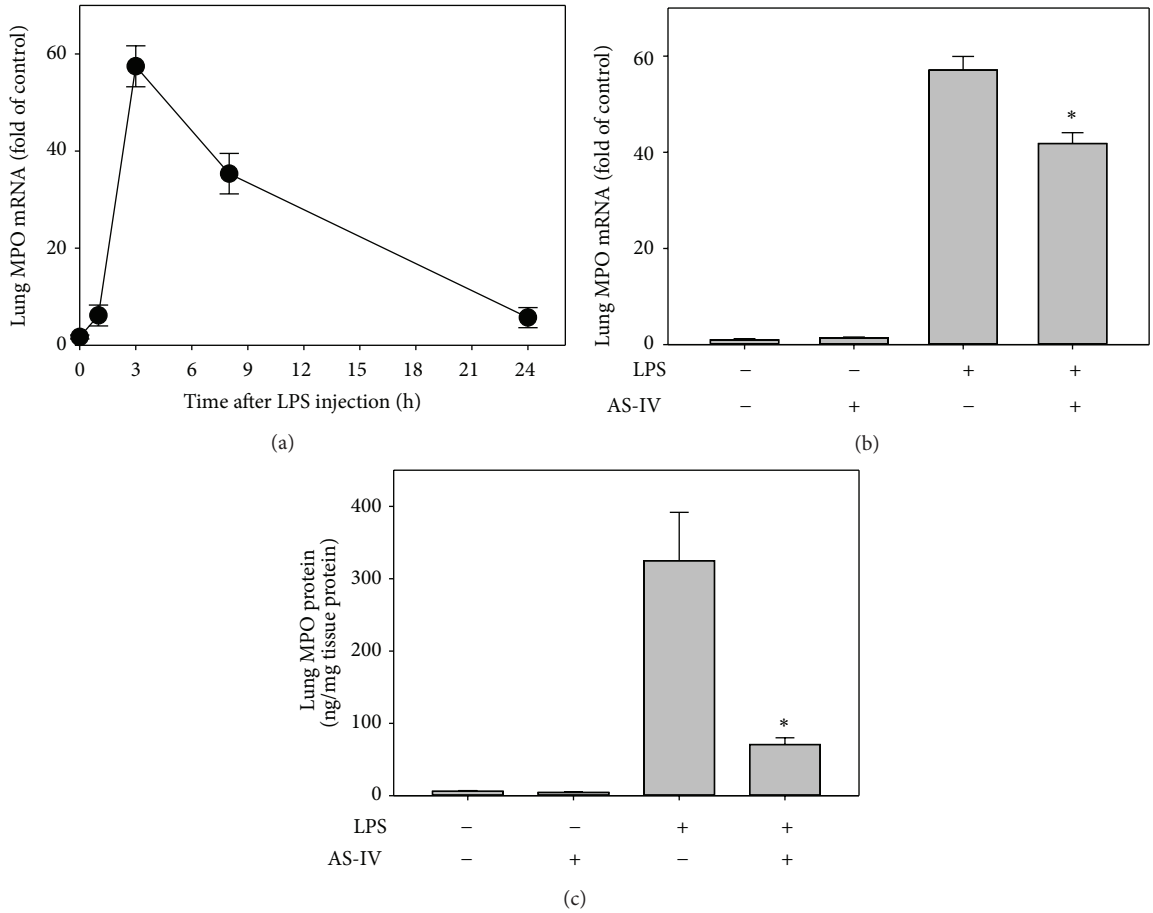

Figure 3: AS-IV inhibits LPS-induced gene and protein expression of myeloperoxidase (MPO) in mouse lung. For panel (a), mice were randomly assigned to receive i.p. injection of LPS and sacrificed after 1, 3, 8, or 24 h. For panels (b) and (c), mice were treated as described in the legend of Figure 2. Total RNA and cytosolic protein were isolated from lung. Lung *MPO* gene expression was quantified as described in the legend of Figure 2. Lung MPO protein was determined using an ELISA kit as described in detail in Section 2. The mRNA data are shown as fold of control after normalization to the internal control gene GAPDH. Data shown are means ± SEM of 4 to 5 animals per group. $^{*}P < 0.05$ compared to animals treated with LPS only.

levels in control animals; however, LPS treatment induced time-dependent upregulation of lung *MPO* gene expression, which peaked at 3 h and remained elevated for up to 8 h and then declined after 24 h. These data indicate infiltration and activation of interstitial PMN in the lungs of LPS-treated mice in a time-dependent manner, which is consistent with our previous results showing that TNFα treatment induced increases in MPO mRNA and protein levels, enzyme activity, and morphological accumulation of PMN in mouse lung tissues [33]. However, pretreatment of mice with AS-IV significantly inhibited the LPS-induced increase in *MPO* mRNA level by 27% ($P < 0.05$, $n = 5$) (Figure 3(b)). This was further confirmed by the lung MPO protein level, which increased from 6 ± 1 ng/mg tissue protein in control animals to 325 ± 67 ng/mg tissue protein in LPS-treated animals and significantly reduced by AS-IV treatment by 80% to 71 ± 9 ng/mg tissue protein ($P < 0.05$, $n = 5$) (Figure 3(c)). As the lung is the main target for activated PMN during acute inflammation [31, 33, 34], these data support the notion that AS-IV inhibits PMN infiltration/recruitment to the lung and subsequent tissue damage during LPS-induced acute inflammatory responses.

3.4. AS-IV Inhibits LPS-Induced NF-κB and AP-1 DNA-Binding Activity in Mouse Lung and Heart. It is well recognized that NF-κB plays a prominent role in LPS-induced transcriptional regulation of most inflammatory genes that contribute to the development of septic shock, multiple organ failure, and death [5, 32]. Of clinical relevance, NF-κB activation was increased in patients with acute inflammation and sepsis and correlated with clinical severity and mortality [35]. To investigate possible signaling pathways mediating the inhibitory effect of AS-IV on LPS-induced inflammatory gene transcription, we assessed the nuclear content of the NF-κB subunit, p65, and the AP-1 subunit, c-fos, as indicators of nuclear translocation and activation of these transcription factors. The DNA-binding activity of NF-κB (p65) and AP-1 (c-fos) was detectable at low levels in lung and heart tissues of control and AS-IV-only-treated animals. AS-IV alone did not cause NF-κB or AP-1 activation in either lung

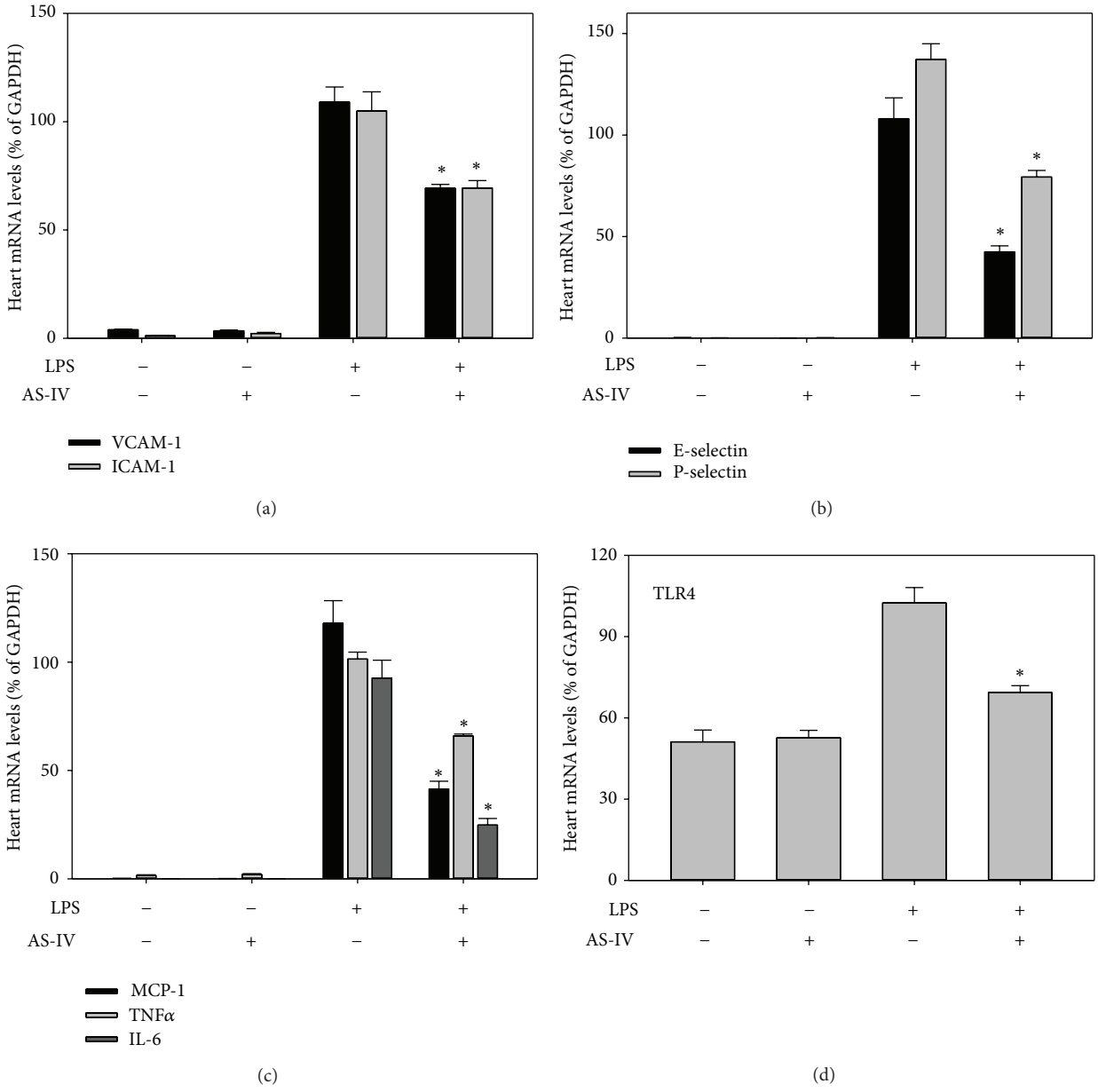

Figure 4: AS-IV inhibits LPS-induced inflammatory gene expression in mouse heart. Mice were treated as described in the legend of Figure 2. Total RNA was isolated from heart, and inflammatory gene expression was quantified as described in the legend of Figure 2. Data shown are means ± SEM of 5 animals per group. $^{*}P < 0.05$ compared to animals treated with LPS only.

or heart (Figure 7). LPS markedly increased NF-κB activity in lung and heart by 15.8- and 11.5-fold, respectively; AS-IV treatment significantly suppressed LPS-induced activation of NF-κB by 42% and 54%, respectively ($P < 0.05$, $n = 5$) (Figure 7(a)). LPS also strongly increased AP-1 activation by 9.6- and 25.3-fold, respectively, while AS-IV treatment significantly diminished LPS-induced AP-1 activity by 41% and 49%, respectively, in both lung and heart ($P < 0.05$, $n = 5$) (Figure 7(b)).

Our data provide new evidence that the inhibitory effect of AS-IV on LPS-induced inflammatory gene expression is mainly through modulating NF-κB and AP-1 DNA-binding activity. These data indicate that the ability of AS-IV to suppress the NF-κB and AP-1 pathways is the major underlying mechanism contributing to its anti-inflammatory potential *in vivo*. It is well documented that the "classic" TLR4 pathway plays a major role in LPS signaling during sepsis [36]. TLR4 recognizes LPS from Gram-negative bacteria and mediates the innate immune response by activating IκB kinase (IKK) and mitogen-activated protein kinase kinases (MKK), which in turn activate NF-κB and AP-1, respectively [5, 36]. Our results further show that AS-IV inhibits LPS-induced *TLR4* gene expression in lung and heart by 30% and 65%, respectively (Figures 2 and 4), which is consistent with its inhibitory

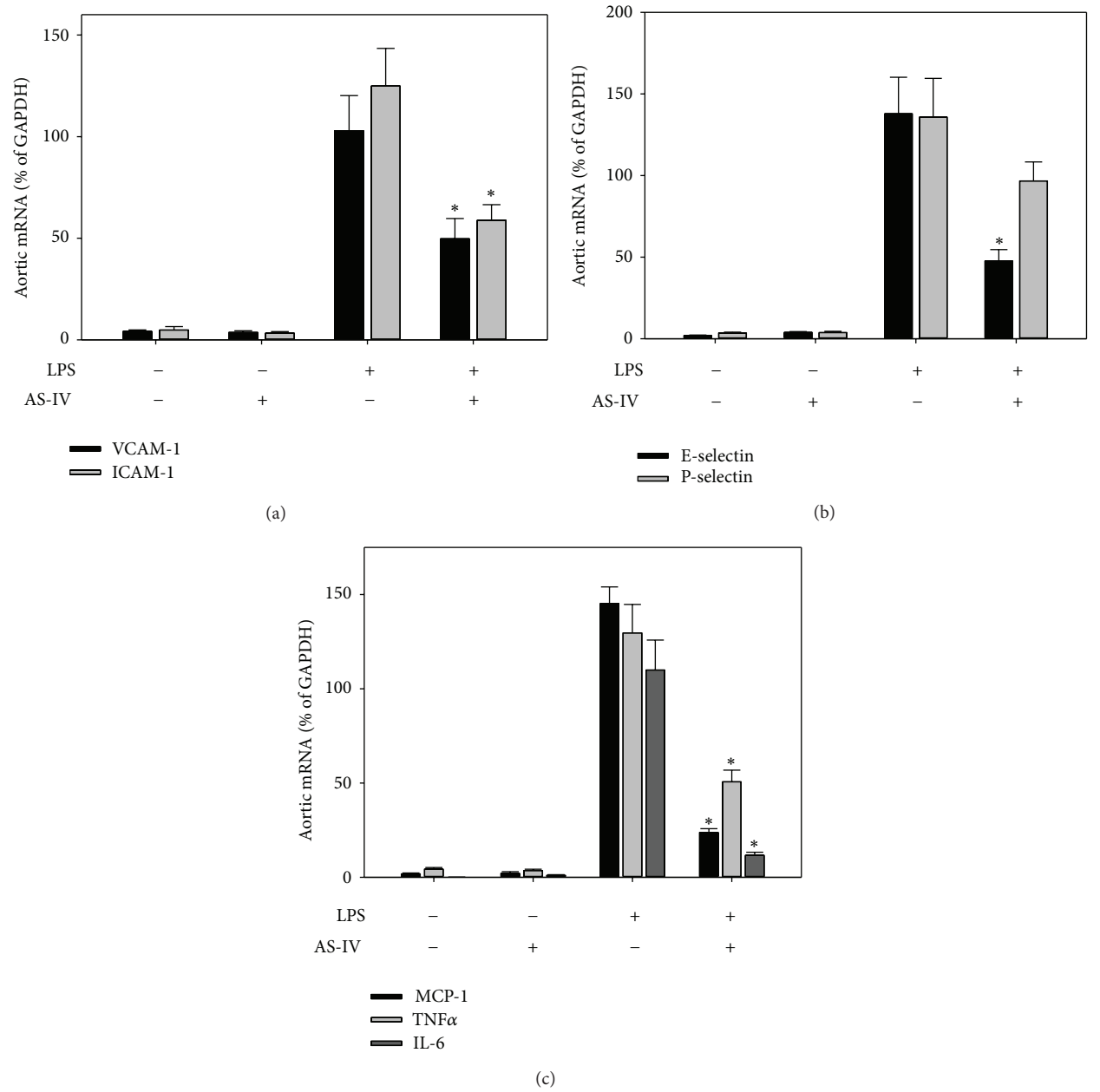

Figure 5: AS-IV inhibits LPS-induced inflammatory gene expression in mouse aorta. Mice were treated as described in the legend of Figure 2. Total RNA was isolated from aorta, and inflammatory gene expression was quantified as described in the legend of Figure 2. Data shown are means ± SEM of 5 animals per group. $^{*}P < 0.05$ compared to animals treated with LPS only.

effects on NF-κB and AP-1 activation in the same tissues. These data suggest that the inhibition of *TLR4* expression might be one of the mechanisms by which AS-IV affects the upstream targets of these pathways. Some *in vitro* studies have shown that AS-IV activates the PI3K/Akt pathway [29], which is known to negatively regulate LPS-induced acute inflammatory responses by modulating the NF-κB and AP-1 pathways [9, 37, 38]. Therefore, PI3K/Akt activation may be one of the underlying mechanisms for the anti-inflammatory activity of AS-IV. Further, as a novel antioxidant [39, 40], AS-IV may modulate LPS-induced formation of reactive oxygen species and subsequent activation of the redox-sensitive NF-κB and AP-1 pathways at different levels [40]. However, all these mechanisms observed *in vitro* need to be further investigated *in vivo*.

A limitation of our study is that we had to apply AS-IV by i.p. injection because it is poorly bioavailable. Previous studies on dogs and rats have found that only 7.4% and 3.7%, respectively, of orally supplemented AS-IV were absorbed [41, 42]. This is mainly due to AS-IV's low fat solubility and low transmittance in the small intestine [43]. In fact, in Chinese medicine AS-IV is clinically used as intravenous

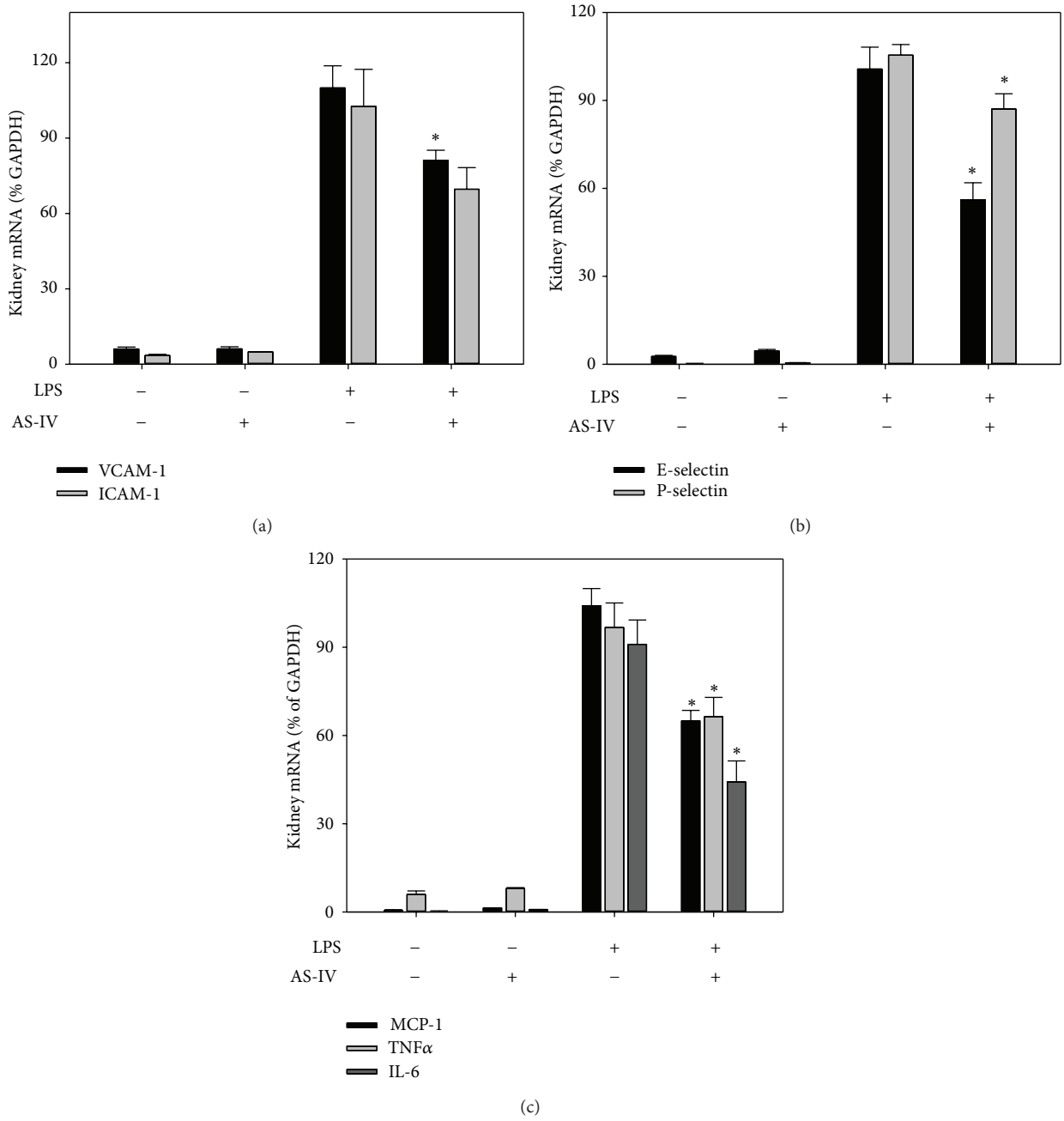

Figure 6: AS-IV inhibits LPS-induced inflammatory gene expression in mouse kidney. Mice were treated as described in the legend of Figure 2. Total RNA was isolated from kidney, and inflammatory gene expression was quantified as described in the legend of Figure 2. Data shown are means ± SEM of 5 animals per group. $^{*}P < 0.05$ compared to animals treated with LPS only.

(i.v.) therapy. Upon i.v. injection of AS-IV at 0.75 mg/kg in rats and 0.5 mg/kg in dogs, the maximum plasma concentrations reached were 3.79 μg/mL and 4.39 μg/mL, respectively, and the elimination half-life ($t_{1/2}$) was 98 min and 60 min, respectively [44, 45]. The highest concentration was found in lung and liver tissues (2.8–2.9 μg/g) after i.v. injection of 1.5 mg/kg AS-IV, whereas heart, muscle, skin, and kidney contained moderate amounts (0.16–1.0 μg/g) [45]. As *Astragalus* and AS-IV are now widely used in Chinese medicine and are also available in Europe and the US as dietary supplements, chemical modifications to improve the absolute bioavailability of AS-IV while maintaining its biological activity could be a focus of future research.

4. Conclusion

In conclusion, our data provide new evidence that AS-IV inhibits LPS-induced acute inflammatory responses *in vivo* by modulating the NF-κB and AP-1 signaling pathways. Our results might lead to the identification of AS-IV as a natural

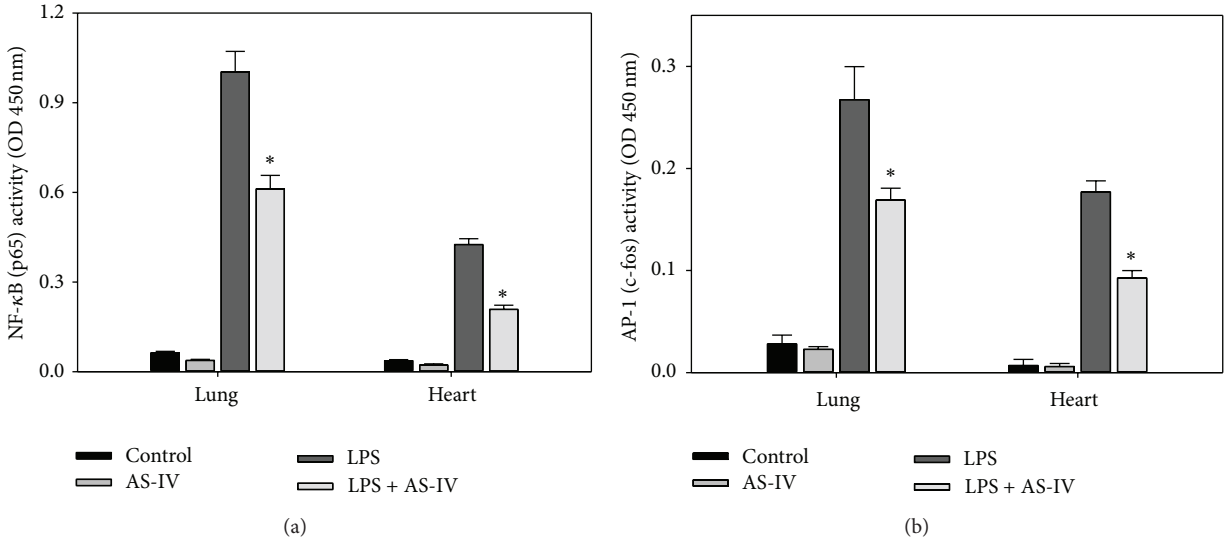

Figure 7: AS-IV inhibits LPS-induced NF-κB (a) and AP-1 (b) DNA-binding activity in mouse lung and heart. Mice were treated as described in the legend of Figure 2. Nuclear extracts were isolated from lung and heart. DNA-binding activity of NF-κB (p65) and AP-1 (c-fos) was quantified by ELISA. Data shown are means ± SEM of 5 animals per group. $^{*}P < 0.05$ compared to animals treated with LPS only.

compound or chemically derived drug that may be useful for the prevention or treatment of inflammatory diseases. We believe that the molecular basis for its therapeutic efficacy is intriguing and warrants further investigation.

Abbreviations

AP-1:	Activator protein-1
AS-IV:	Astragaloside IV
b.w.:	Body weight
GAPDH:	Glyceraldehyde-3-phosphate dehydrogenase
ICAM-1:	Intercellular adhesion molecule-1
i.p.:	Intraperitoneal
i.v.:	Intravenous
IKK:	IκB kinase
IL:	Interleukin
LPS:	Lipopolysaccharide
MCP-1:	Monocyte chemoattractant protein-1
MPO:	Myeloperoxidase
NF-κB:	Nuclear factor κB
PMN:	Polymorphonuclear neutrophils
Redox:	Reduction-oxidation
ROS:	Reactive oxygen species
sICAM-1:	Soluble intercellular adhesion molecule-1
sVCAM-1:	Soluble vascular cell adhesion molecule-1
TLR4:	Toll-like receptor-4
TNFα:	Tumor necrosis factor α
VCAM-1:	Vascular cell adhesion molecule-1.

Disclaimer

The content of this work is solely the responsibility of the authors and does not necessarily represent the official views of the NIH.

Conflict of Interests

The authors declare that they have no conflict of interests.

Authors' Contribution

Wei-Jian Zhang designed and performed experiments; Wei-Jian Zhang and Balz Frei analyzed data and wrote and approved the final paper.

Acknowledgments

This work was supported by NCCAM Center of Excellence Grant P01 AT002034 from the National Institutes of Health. The authors thank Stephen Lawson for carefully proofreading the paper.

References

[1] W. C. Aird, "The role of the endothelium in severe sepsis and multiple organ dysfunction syndrome," *Blood*, vol. 101, no. 10, pp. 3765–3777, 2003.

[2] J. E. Parrillo, "Pathogenetic mechanisms of septic shock," *The New England Journal of Medicine*, vol. 328, no. 20, pp. 1471–1477, 1993.

[3] D. G. Remick, "Pathophysiology of sepsis," *The American Journal of Pathology*, vol. 170, no. 5, pp. 1435–1444, 2007.

[4] T. Collins, M. A. Read, A. S. Neish, M. Z. Whitley, D. Thanos, and T. Maniatis, "Transcriptional regulation of endothelial cell adhesion molecules: NF-κB and cytokine-inducible enhancers," *The FASEB Journal*, vol. 9, no. 10, pp. 899–909, 1995.

[5] S. F. Liu and A. B. Malik, "NF-κB activation as a pathological mechanism of septic shock and inflammation," *American Journal of Physiology: Lung Cellular and Molecular Physiology*, vol. 290, no. 4, pp. L622–L645, 2006.

[6] W.-J. Zhang, P. Hufnagl, B. R. Binder, and J. Wojta, "Antiinflammatory activity of astragaloside IV is mediated by inhibition of NF-κB activation and adhesion molecule expression," *Thrombosis and Haemostasis*, vol. 90, no. 5, pp. 904–914, 2003.

[7] C. Weber, W. Erl, A. Pietsch, M. Strobel, H. W. L. Ziegler-Heitbrock, and P. C. Weber, "Antioxidants inhibit monocyte adhesion by suppressing nuclear factor-κB mobilization and induction of vascular cell adhesion molecule-1 in endothelial cells stimulated to generate radicals," *Arteriosclerosis and Thrombosis*, vol. 14, no. 10, pp. 1665–1673, 1994.

[8] W.-J. Zhang and B. Frei, "α-Lipoic acid inhibits TNF-α-induced NF-κB activation and adhesion molecule expression in human aortic endothelial cells," *The FASEB Journal*, vol. 15, no. 13, pp. 2423–2432, 2001.

[9] W. J. Zhang, H. Wei, T. Hagen, and B. Frei, "α-Lipoic acid attenuates LPS-induced inflammatory responses by activating the phosphoinositide 3-kinase/Akt signaling pathway," *Proceedings of the National Academy of Sciences of the United States of America*, vol. 104, no. 10, pp. 4077–4082, 2007.

[10] C. Chu, L.-W. Qi, E.-H. Liu, B. Li, W. Gao, and P. Li, "Radix astragali (Astragalus): latest advancements and trends in chemistry, analysis, pharmacology and pharmacokinetics," *Current Organic Chemistry*, vol. 14, no. 16, pp. 1792–1807, 2010.

[11] W. C. S. Cho and K. N. Leung, "*In vitro* and *in vivo* immunomodulating and immunorestorative effects of *Astragalus membranaceus*," *Journal of Ethnopharmacology*, vol. 113, no. 1, pp. 132–141, 2007.

[12] K. L. Denzler, R. Waters, B. L. Jacobs, Y. Rochon, and J. O. Langland, "Regulation of inflammatory gene expression in PBMCs by immunostimulatory botanicals," *PloS ONE*, vol. 5, no. 9, Article ID e12561, 2010.

[13] X. J. Chen, Z.-P. Bian, S. Lu et al., "Cardiac protective effect of Astragalus on viral myocarditis mice: comparison with Perindopril," *The American Journal of Chinese Medicine*, vol. 34, no. 3, pp. 493–502, 2006.

[14] X.-L. Xu, H. Ji, S.-Y. Gu, Q. Shao, Q.-J. Huang, and Y.-P. Cheng, "Cardioprotective effects of Astragali Radix against isoproterenol-induced myocardial injury in rats and its possible mechanism," *Phytotherapy Research*, vol. 22, no. 3, pp. 389–394, 2008.

[15] S. Fu, J. Zhang, F. Menniti-Ippolito et al., "Huangqi injection (a traditional chinese patent medicine) for chronic heart failure: a systematic review," *PLoS ONE*, vol. 6, no. 5, Article ID e19604, 2011.

[16] M. Ryu, E. H. Kim, M. Chun et al., "Astragali Radix elicits anti-inflammation via activation of MKP-1, concomitant with attenuation of p38 and Erk," *Journal of Ethnopharmacology*, vol. 115, no. 2, pp. 184–193, 2008.

[17] X.-H. Gao, X.-X. Xu, R. Pan et al., "Saponin fraction from *Astragalus membranaceus* roots protects mice against polymicrobial sepsis induced by cecal ligation and puncture by inhibiting inflammation and upregulating protein C pathway," *Journal of Natural Medicines*, vol. 63, no. 4, pp. 421–429, 2009.

[18] J. B. Jiang, J. D. Qiu, L. H. Yang, J. P. He, G. W. Smith, and H. Q. Li, "Therapeutic effects of astragalus polysaccharides on inflammation and synovial apoptosis in rats with adjuvant-induced arthritis," *International Journal of Rheumatic Diseases*, vol. 13, no. 4, pp. 396–405, 2010.

[19] S.-Y. Gui, W. Wei, H. Wang et al., "Effects and mechanisms of crude astragalosides fraction on liver fibrosis in rats," *Journal of Ethnopharmacology*, vol. 103, no. 2, pp. 154–159, 2006.

[20] S. Wang, J. Li, H. Huang et al., "Anti-hepatitis B virus activities of astragaloside IV isolated from *Radix Astragali*," *Biological and Pharmaceutical Bulletin*, vol. 32, no. 1, pp. 132–135, 2009.

[21] M. Li, W. Wang, J. Xue, Y. Gu, and S. Lin, "Meta-analysis of the clinical value of Astragalus membranaceus in diabetic nephropathy," *Journal of Ethnopharmacology*, vol. 133, no. 2, pp. 412–419, 2011.

[22] W. C. S. Cho and K. N. Leung, "*In vitro* and *in vivo* anti-tumor effects of *Astragalus membranaceus*," *Cancer Letters*, vol. 252, no. 1, pp. 43–54, 2007.

[23] C. Tohda, T. Tamura, S. Matsuyama, and K. Komatsu, "Promotion of axonal maturation and prevention of memory loss in mice by extracts of Astragalus mongholicus," *British Journal of Pharmacology*, vol. 149, no. 5, pp. 532–541, 2006.

[24] J.-Z. Song, H. H. W. Yiu, C.-F. Qiao, Q.-B. Han, and H.-X. Xu, "Chemical comparison and classification of Radix Astragali by determination of isoflavonoids and astragalosides," *Journal of Pharmaceutical and Biomedical Analysis*, vol. 47, no. 2, pp. 399–406, 2008.

[25] I. Kitagawa, H. K. Wang, M. Saito, A. Takagi, and M. Yoshikawa, "Saponin and sapogenol. XXXV. Chemical constituents of astragali radix, the root of Astragalus membranaceus Bunge. 2. Astragalosides I, II, and IV, acetylastragaloside I and isoastragaloside I and II," *Chemical and Pharmaceutical Bulletin*, vol. 31, no. 2, pp. 698–708, 1983.

[26] W.-D. Zhang, C. Zhang, X. H. Wang et al., "Astragaloside IV from *Astragalus membranaceus* shows cardioprotection during myocardial ischemia *in vivo* and *in vitro*," *Planta Medica*, vol. 72, no. 1, pp. 4–8, 2006.

[27] X.-L. Xu, H. Ji, S.-Y. Gu, Q. Shao, Q.-J. Huang, and Y.-P. Cheng, "Modification of alterations in cardiac function and sarcoplasmic reticulum by astragaloside IV in myocardial injury *in vivo*," *European Journal of Pharmacology*, vol. 568, no. 1–3, pp. 203–212, 2007.

[28] W. J. Zhang, J. Wojta, and B. R. Binder, "Regulation of the fibrinolytic potential of cultured human umbilical vein endothelial cells: astragaloside IV downregulates plasminogen activator inhibitor-1 and upregulates tissue-type plasminogen activator expression," *Journal of Vascular Research*, vol. 34, no. 4, pp. 273–280, 1997.

[29] L. Zhang, Q. Liu, L. Lu, X. Zhao, X. Gao, and Y. Wang, "Astragaloside IV stimulates angiogenesis and increases hypoxia-inducible factor-1α accumulation via phosphatidylinositol 3-kinase/akt pathway," *Journal of Pharmacology and Experimental Therapeutics*, vol. 338, no. 2, pp. 485–491, 2011.

[30] J. Zhao, P. Yang, F. Li et al., "Therapeutic effects of astragaloside IV on myocardial injuries: multi-target identification and network analysis," *PLoS ONE*, vol. 7, no. 9, Article ID e44938, 2012.

[31] W. J. Zhang, H. Wei, and B. Frei, "Genetic deficiency of NADPH oxidase does not diminish, but rather enhances, LPS-induced acute inflammatory responses in vivo," *Free Radical Biology and Medicine*, vol. 46, no. 6, pp. 791–798, 2009.

[32] S. S. Awad, "State-of-the-art therapy for severe sepsis and multisystem organ dysfunction," *The American Journal of Surgery*, vol. 186, supplement 1, no. 5, pp. 23S–30S, 2003.

[33] W.-J. Zhang, H. Wei, Y.-T. Tien, and B. Frei, "Genetic ablation of phagocytic NADPH oxidase in mice limits TNFα-induced inflammation in the lungs but not other tissues," *Free Radical Biology and Medicine*, vol. 50, no. 11, pp. 1517–1525, 2011.

[34] J. E. Juskewitch, J. L. Platt, B. E. Knudsen, K. L. Knutson, G. J. Brunn, and J. P. Grande, "Disparate roles of marrow- and parenchymal cell-derived TLR4 signaling in murine LPS-induced systemic inflammation," *Scientific Reports*, vol. 2, article 918, 2012.

[35] H. Böhrer, F. Qiu, T. Zimmermann et al., "Role of NFκB in the mortality of sepsis," *The Journal of Clinical Investigation*, vol. 100, no. 5, pp. 972–985, 1997.

[36] E. M. Pålsson-McDermott and L. A. J. O'Neill, "Signal transduction by the lipopolysaccharide receptor, Toll-like receptor-4," *Immunology*, vol. 113, no. 2, pp. 153–162, 2004.

[37] G. Schabbauer, M. Tencati, B. Pedersen, R. Pawlinski, and N. Mackman, "PI3K-Akt pathway suppresses coagulation and inflammation in endotoxemic mice," *Arteriosclerosis, Thrombosis, and Vascular Biology*, vol. 24, no. 10, pp. 1963–1969, 2004.

[38] D. L. Williams, C. Li, T. Ha et al., "Modulation of the phosphoinositide 3-kinase pathway alters innate resistance to polymicrobial sepsis," *Journal of Immunology*, vol. 172, no. 1, pp. 449–456, 2004.

[39] D. Gui, Y. Guo, F. Wang et al., "Astragaloside IV, a novel antioxidant, prevents glucose-induced podocyte apoptosis in vitro and in vivo," *PLoS ONE*, vol. 7, no. 6, Article ID e39824, 2012.

[40] Y. He, M. Du, Y. Gao et al., "Astragaloside IV attenuates experimental autoimmune encephalomyelitis of mice by counteracting oxidative stress at multiple levels," *PLoS ONE*, vol. 8, no. 10, Article ID e76495, 2013.

[41] Q. Zhang, L.-L. Zhu, G.-G. Chen, and Y. Du, "Pharmacokinetics of astragaloside*iv* in beagle dogs," *European Journal of Drug Metabolism and Pharmacokinetics*, vol. 32, no. 2, pp. 75–79, 2007.

[42] Y. Du, Q. Zhang, G. G. Chen, P. Wei, and C. Y. Tu, "Pharmacokinetics of Astragaloside IV in rats by liquid chromatography coupled with tandem mass spectrometry," *European Journal of Drug Metabolism and Pharmacokinetics*, vol. 30, no. 4, pp. 269–273, 2005.

[43] C. R. Huang, G. J. Wang, X. L. Wu et al., "Absorption enhancement study of astragaloside IV based on its transport mechanism in Caco-2 cells," *European Journal of Drug Metabolism and Pharmacokinetics*, vol. 31, no. 1, pp. 5–10, 2006.

[44] Y. Gu, G. Wang, G. Pan, J. P. Fawcett, J. A, and J. Sun, "Transport and bioavailability studies of astragaloside IV, an active ingredient in Radix astragali," *Basic and Clinical Pharmacology and Toxicology*, vol. 95, no. 6, pp. 295–298, 2004.

[45] W. D. Zhang, C. Zhang, R.-H. Liu et al., "Preclinical pharmacokinetics and tissue distribution of a natural cardioprotective agent astragaloside IV in rats and dogs," *Life Sciences*, vol. 79, no. 8, pp. 808–815, 2006.

Hindawi Publishing Corporation
Mediators of Inflammation
Volume 2015, Article ID 463530, 9 pages
http://dx.doi.org/10.1155/2015/463530

Research Article

Inhibitory Effect of Methyleugenol on IgE-Mediated Allergic Inflammation in RBL-2H3 Cells

Feng Tang,[1,2] Feilong Chen,[1,2] Xiao Ling,[1,2] Yao Huang,[1,2] Xiaomei Zheng,[1,2] Qingfa Tang,[1,2] and Xiaomei Tan[1,2]

[1] *School of Traditional Chinese Medical Sciences, Southern Medical University, Guangzhou 510515, China*
[2] *Guangdong Province Key Laboratory of Chinese Medicine Pharmaceutics, Southern Medical University, Guangzhou 510515, China*

Correspondence should be addressed to Qingfa Tang; tangqf96@163.com and Xiaomei Tan; tanxm_smu@163.com

Received 23 December 2014; Revised 16 February 2015; Accepted 18 February 2015

Academic Editor: Lifei Hou

Allergic diseases, such as asthma and allergic rhinitis, are common. Therefore, the discovery of therapeutic drugs for these conditions is essential. Methyleugenol (ME) is a natural compound with antiallergic, antianaphylactic, antinociceptive, and anti-inflammatory effects. This study examined the antiallergic effect of ME on IgE-mediated inflammatory responses and its antiallergy mechanism in the mast cell line, RBL-2H3. We found that ME significantly inhibited the release of β-hexosaminidase, tumor necrosis factor- (TNF-) α, and interleukin- (IL-) 4, and was not cytotoxic at the tested concentrations (0–100 μM). Additionally, ME markedly reduced the production of the proinflammatory lipid mediators prostaglandin E_2 (PGE_2), prostaglandin D_2 (PGD_2), leukotriene B_4 (LTB_4), and leukotriene C_4 (LTC_4). We further evaluated the effect of ME on the early stages of the FcεRI cascade. ME significantly inhibited Syk phosphorylation and expression but had no effect on Lyn. Furthermore, it suppressed ERK1/2, p38, and JNK phosphorylation, which is implicated in proinflammatory cytokine expression. ME also decreased cytosolic phospholipase A_2 ($cPLA_2$) and 5-lipoxygenase (5-LO) phosphorylation and cyclooxygenase-2 (COX-2) expression. These results suggest that ME inhibits allergic response by suppressing the activation of Syk, ERK1/2, p38, JNK, $cPLA_2$, and 5-LO. Furthermore, the strong inhibition of COX-2 expression may also contribute to the antiallergic action of ME. Our study provides further information about the biological functions of ME.

1. Introduction

Allergic airway diseases, such as asthma and allergic rhinitis, are common diseases caused by hypersensitivity of the immune system. Approximately 10–20% of the world population is affected by allergies, with the number of allergy patients increasing annually [1, 2]. Most allergy patients are genetically predisposed to produce IgE. Mast cells are a key player in early allergic response, which typically occurs within minutes of exposure to an appropriate antigen, and other biological responses, including inflammatory disorders [3]. These cells are critical effector cells in IgE-dependent immediate hypersensitivity reactions [4]. Mast cell degranulation can initiate an acute inflammatory response and contribute to the progression of chronic diseases [5]. When an IgE-antigen binds with FcεRI, the receptor is activated, and a variety of biologically active mediators are released, causing allergic reactions, including the release of β-hexosaminidase, a common degranulation marker, histamine, arachidonic acid metabolites, and inflammatory cytokines [6]. Importantly, arachidonic acid metabolites, including prostaglandins and leukotrienes, mediate acute and chronic allergic reactions [7, 8]. RBL-2H3 cells are a mast cell line that originated from rat basophilic leukemia and have been widely used to study IgE-FcεRI interactions and degranulation. Furthermore, RBL-2H3 cells are a useful model for *in vitro* screening of antiallergy drug candidates.

The MAP kinase cascade is an important signaling pathway that regulates the differentiation, activation, proliferation, degranulation, and migration of immune cells, including mast cells [9]. MAPK signaling molecules are divided into three groups: extracellular signal-regulated kinase (ERK) 1/2, p38 MAPK, and c-JunNH2-terminal kinase (JNK) 1/2. Erk1/2

is an essential signal in the production of interleukin- (IL-) 5, tumor necrosis factor- (TNF-) α, IL-3, and IL-13 in mast cells [10]. p38 MAP kinase stimulates IL-4 production in bone marrow mast cells (BMMCs) [11]. Additionally, the activation of JNK is also responsible, at least partially, for the expression and production of several cytokines, including TNF-α, IL-2, and IL-6 in mast cells [12, 13].

Methyleugenol (ME,1-allyl-3,4-dimethoxybenzene) is an analog of the phenolic compound eugenol, and it is found in essential oils, including basil, anise, clove, lemon grass, and laurel leaf oils. In East Asia, ME is found in the essential oil fraction of *Asiasari radix* (Xixin in Chinese). It is used as a flavoring substance in dietary products, including cookies, ice cream, and nonalcoholic beverages, and is found in cosmetics, shampoos, soaps, fragrances, and herbal products in Europe, the USA, and other countries [14]. Previous work indicates that ME exerts antiallergic [15], antispasmodic [16], antinociceptive [14], and anti-inflammatory [17] effects. It was reported that ME inhibited passive cutaneous anaphylaxis (PCA) in rats, release of 5-lipoxygenase (5-LO) from RBL-1 cells and leukotriene D_4 (LTD_4) induced constriction of guinea pig ileum. ME also inhibited compound 48/80-induced systemic anaphylaxis and antidinitrophenyl IgE-induced local anaphylaxis in mice [18]. However, the effects of ME on allergic response in IgE-activated RBL-2H3 cells and its antiallergic mechanism remain unknown.

In this study, we investigated the antiallergic effects of ME in IgE-activated RBL-2H3 cells. Furthermore, we evaluated the mechanisms responsible for the antiallergic effects of ME.

2. Materials and Methods

2.1. Reagents. ME was purchased from the National Institute for Food and Drug Control (Beijing, China; purity, ≥99.5%). Dulbecco's minimum essential medium (DMEM), penicillin, streptomycin, and fetal bovine serum (FBS) were purchased from GIBCO (Grand Island, NY, USA). 4-[3-(4-Iodophenyl)-2-4(4-nitrophenyl)-2H-5-tetrazolio]-1,3-benzene disulfonate (WST-1) was obtained from Dojindo (Kumamoto, Japan). Specific antibodies against phospho-Lyn, Lyn, phospho-Syk, Syk, phospho-ERK1/2, ERK1/2, phospho-p38, p38, phospho-JNK, JNK, cytosolic phospholipase A_2 ($cPLA_2$), phospho-$cPLA_2$, cyclooxygenase-2 (COX-2), and β-actin were purchased from Cell Signaling Technology (Beverly, MA, USA). Specific antibodies against phospho-5-lipoxygenase (5-LO) and 5-LO, and enzyme immunoassay (EIA) kits for prostaglandin E_2 (PGE_2), prostaglandin D_2 (PGD_2), leukotriene B_4 (LTB_4), and leukotriene C_4 (LTC_4) were purchased from Cayman Chemical (Ann Arbor, MI, USA). The enzyme-linked immunosorbent assay (ELISA) kits for TNF-α and IL-4 were obtained from Bangyi Technologies Inc. (Shanghai, China). Dinitrophenyl- (DNP-) IgE was obtained from Sigma-Aldrich (St. Louis, MO, USA), and DNP-bovine serum albumin (BSA) was obtained from Biosearch Technologies Inc. (Novato, CA, USA). All other chemicals were of analytical grade and were purchased from Sigma-Aldrich.

2.2. Cell Culture. RBL-2H3 cells were purchased from the Type Culture Collection of the Chinese Academy of Sciences (Shanghai, China). Cells were cultured in DMEM medium supplemented with 10% FBS and antibiotics (100 U/mL penicillin and 100 μg/mL streptomycin) at 37°C in a humidified 5% CO_2 atmosphere.

2.3. Cytotoxicity Assay. Cell respiration served as an indicator of cell viability and was determined by measuring the mitochondrial-dependent reduction of WST-1 to water-soluble tetrazolium salt [19]. Briefly, RBL-2H3 cells were seeded onto a 96-well plate (1×10^4 cells/well) in DMEM with 10% FBS at 37°C overnight. The cells were washed and incubated with DNP-IgE (10 μg/mL) for 24 h. The IgE-sensitized cells were incubated with ME (0–100 μM) for 1 h and stimulated with DNP-BSA (100 ng/mL) for 4 h. WST-1 reagent (10 μL) was added, and the mixture was further incubated for 1 h. Cell viability was determined by measuring the difference in absorbance at a wavelength of 450 nm.

2.4. β-Hexosaminidase Release Activity. RBL-2H3 cells were incubated in a 24-well plate (2×10^5 cells/well) at 37°C overnight. The cells were washed with 1× PBS and incubated with DNP-IgE (10 μg/mL) for 24 h. The IgE-sensitized cells were incubated with ME (0–100 μM) for 1 h, followed by 4 h incubation with DNP-BSA (100 ng/mL). To measure β-hexosaminidase activity, the culture medium was centrifuged (17,000 ×g, 10 min) at 4°C. The supernatant (25 μL) was mixed with 10 mM poly-N-acetyl glucosamine (p-NAG; 50 μL) in 0.1 M sodium citrate buffer (pH 4.5) in a 96-well plate and incubated for 1 h at 37°C. The reaction was terminated by stop buffer (0.1 M Na_2CO_3 buffer, pH 10.0). The β-hexosaminidase activity was determined by measuring the difference in absorbance at 405 nm. Data were displayed as the mean ± standard deviation (SD) of triplicate experiments.

2.5. ELISA. To measure the TNF-α and IL-4 concentrations in the culture media, all samples were centrifuged (17,000 ×g, 10 min) at 4°C and stored at −80°C until analysis. The TNF-α and IL-4 concentrations were measured using ELISA kits according to the manufacturer's instructions. Data were displayed as the mean ± SD of triplicate experiments.

2.6. EIA. To determine the PGE_2, PGD_2, LTB_4, and LTC_4 concentrations in the culture media, all samples were centrifuged (17,000 ×g for 10 min) at 4°C, and the supernatant was stored at −80°C until analysis. The PGE_2, PGD_2, LTB_4, and LTC_4 concentrations were measured with EIA kits according to the manufacturer's instructions. Data were displayed as the mean ± SD of triplicate experiments.

2.7. Western Blot Analysis. RBL-2H3 cells were seeded onto a 6-well plate (5×10^5 cells/well) in DMEM with 10% FBS at 37°C overnight. The cells were washed and incubated with DNP-IgE (10 μg/mL) for 24 h. The cells were then incubated in ME (0–100 μM) for 1 h and stimulated with DNP-BSA (100 ng/mL) for 4 h. The harvested cells were lysed, and the target protein was resuspended in protein lysis buffer.

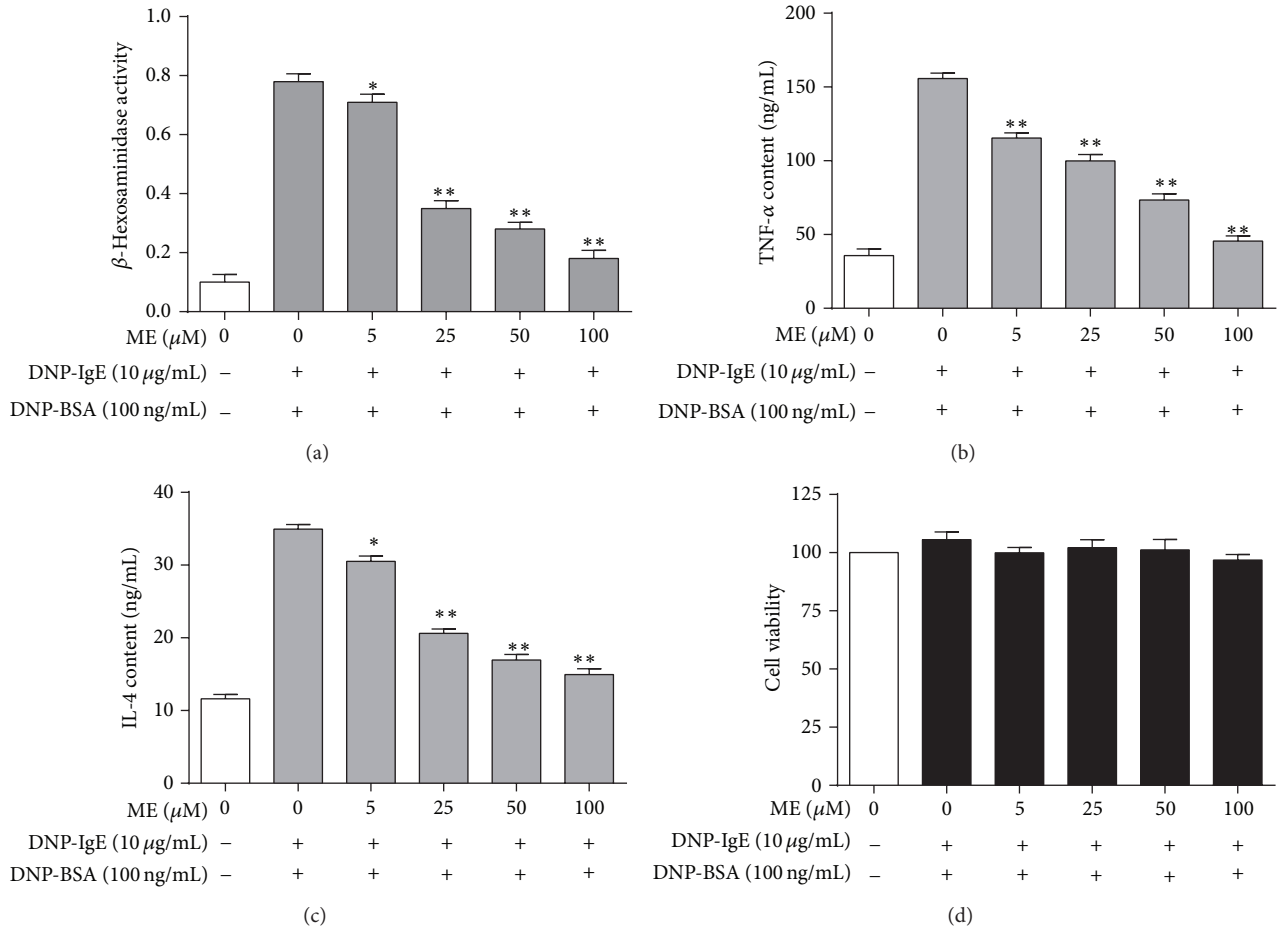

Figure 1: Effect of ME on activity of β-hexosaminidase and level of TNF-α, IL-4 released in IgE-activated RBL-2H3 cells. RBL-2H3 cells were seeded on a 24-well plate in DMEM with 10% FBS at 37°C overnight, and then the cells were washed and further incubated with DNP-IgE for 24 h. The cells were incubated with ME (0–100 μM) for 1 h and then stimulated by DNP-BSA (100 ng/mL) for 4 h. β-Hexosaminidase activity (a) and TNF-α level (b) and IL-4 level (c) were determined as described in Section 2. RBL-2H3 cells were seeded on a 96-well plate (2.5×10^4 cells/well) in DMEM with 10% FBS at 37°C overnight, and then the cells were washed and further incubated with DNP-IgE for 24 h. The cells were incubated with ME (0–100 μM) for 1 h, simultaneously treated with DNP-BSA (100 ng/mL) and WST-1 reagent (10 μL), and then incubated for 4 h. Cell viability (d) was determined as described in Section 2. Data represent the mean ± SD of three independent experiments and differences between mean values were assessed by one-way ANOVA. $^*P < 0.05$, $^{**}P < 0.01$ indicate significant differences compared with the DNP-BSA-treated group.

The cell lysates were separated by sodium dodecyl sulfate-polyacrylamide gel electrophoresis (SDS-PAGE) and transferred to polyvinylidene fluoride (PVDF) membranes. The membranes were then incubated with a 1 : 1,000 dilution of specific antibodies against phospho-Lyn, Lyn, phospho-Syk, Syk, phospho-ERK1/2, ERK1/2, phospho-p38, p38, phospho-JNK, JNK, phospho-cPLA$_2$, cPLA$_2$, COX-2, and β-actin and antibodies against phospho-5-LO and 5-LO. The blots were washed with TBS-T and incubated in a 1 : 5,000 dilution of horseradish peroxidase-conjugated IgG secondary antibodies. The proteins on the membranes were detected using a chemiluminescent reaction, and the membranes were exposed to Hyperfilm ECL. The target protein concentrations were compared to the control concentrations, and the results for each protein were expressed as a density ratio based on a protein standard size marker. The density of each band was determined using ImageJ software.

2.8. Statistical Analysis. The results were expressed as mean ± standard deviation (SD) and differences between mean values of normally distributed data were assessed by the one-way analysis of variance (ANOVA) followed by Duncan's test for multiple comparisons. P values of 0.05 or 0.01 were considered statistically significant.

3. Results

3.1. Inhibitory Effect of ME on IgE-Mediated Allergic Response in RBL-2H3 Cells. To determine the optimal concentrations of ME for our study, we assessed the cytotoxicity of ME and antigen (DNP-BSA) cotreatment. We treated the RBL-2H3 mast cells with ME concentrations ranging from 1 to 100 μM in subsequent experiments. The IgE-sensitized RBL-2H3 cells were exposed to ME at various concentrations (0–100 μM) for 1 h and stimulated with

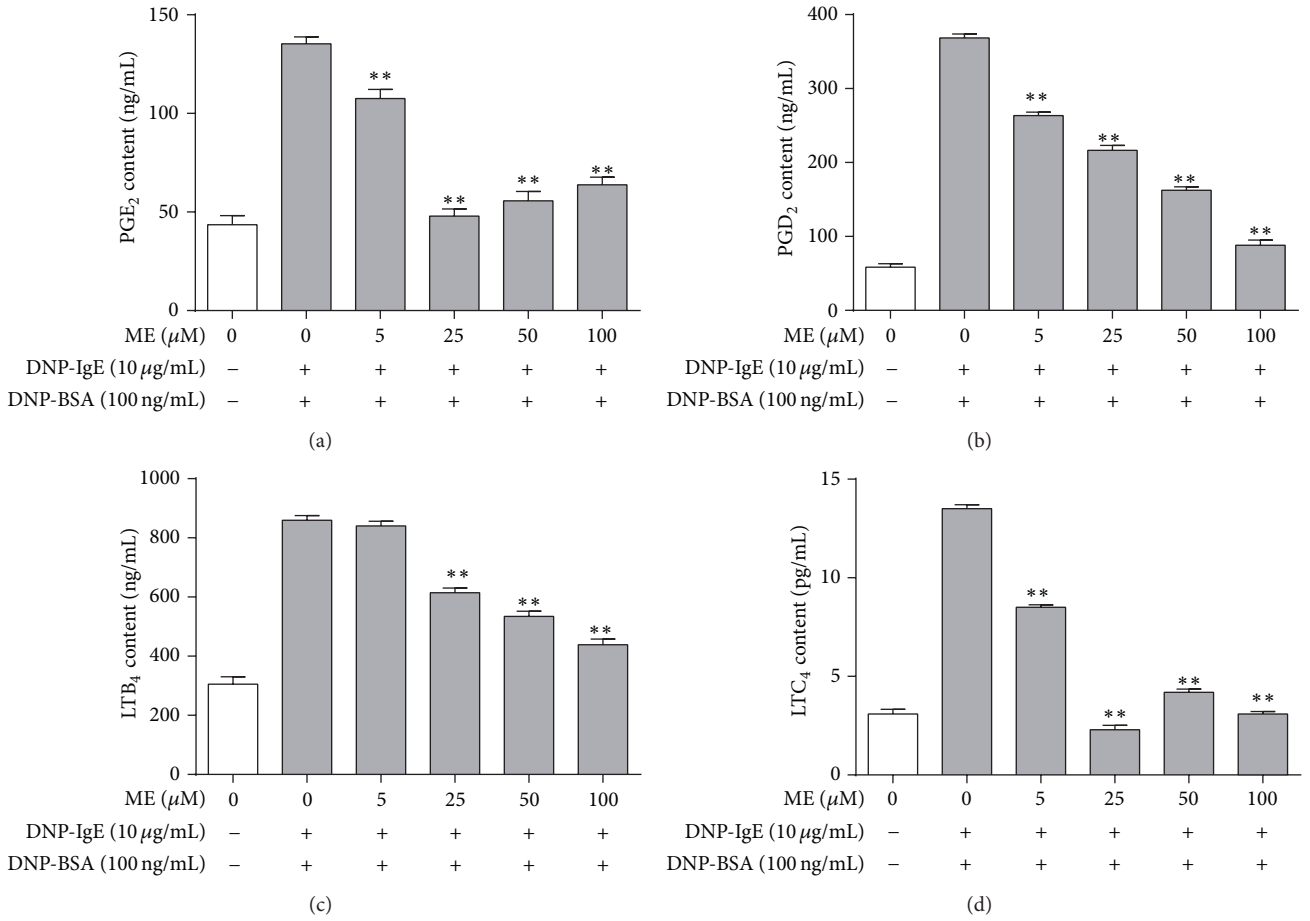

Figure 2: Effect of ME on formation of PGE_2, PGD_2, LTB_4, and LTC_4 in IgE-activated RBL-2H3 cells. RBL-2H3 cells were seeded on a 24-well plate in DMEM with 10% FBS at 37°C overnight, and then the cells were washed and further incubated with DNP-IgE for 24 h. The cells were incubated with ME (0–100 μM) for 1 h and then stimulated by DNP-BSA for 4 h. The amounts of PGE_2 (a), PGD_2 (b), LTB_4 (c), and LTC_4 (d) were determined as described in Section 2. Data represent the mean ± SD of three independent experiments and differences between mean values were assessed by one-way ANOVA. $^{*}P < 0.05$, $^{**}P < 0.01$ indicate significant differences compared with the DNP-BSA-treated group.

100 ng/mL DNP-BSA for 4 h for the β-hexosaminidase assay. ME markedly inhibited the release of β-hexosaminidase (Figure 1(a)), which is a general biomarker of degranulation and a hallmark characteristic of allergic reactions caused by allergen exposure. Additionally, the release of TNF-α and IL-4, two proinflammatory cytokines, from RBL-2H3 cells was markedly suppressed by ME in a dose-dependent manner (Figures 1(b) and 1(c)). ME treatment (0–100 μM) for 24 h produced no significant cytotoxic effect (Figure 1(d)).

3.2. Inhibitory Effects of ME on the Formation of Proinflammatory Lipid Mediators. We next examined the effect of ME on the formation of PGE_2, PGD_2, LTB_4, and LTC_4, which are proinflammatory lipid mediators that regulate allergic response [20–23] produced via arachidonate signaling downstream of IgE-mediated FcεRI activation [24]. RBL-2H3 cells were preincubated with ME (0–100 μM) prior to antigen challenge, and the formation of PGE_2, PGD_2, LTB_4, and LTC_4 was measured by EIA assay. As shown in Figure 2, ME markedly inhibited the formation of PGE_2, PGD_2, and LTC_4 and suppressed LTB_4 formation to a lesser extent. Collectively, these results suggest that ME suppresses allergic inflammation induced by PGE_2, PGD_2, LTB_4, and LTC_4. This indicates that ME directly inhibits an enzyme involved in prostaglandin and leukotriene biosynthesis.

3.3. Regulatory Effects of ME on Enzymes Associated with the Arachidonate Cascade. We additionally investigated the antiallergic effects of ME on the activation of enzymes in the arachidonate cascade. Arachidonate cascade activation has been implicated in FcεRI receptor activation in IgE-activated mast cells [22]. Therefore, we hypothesized that ME, which showed antiallergic effects, would affect $cPLA_2$, 5-LO, or COX-2 activation (Figure 3). When the IgE-sensitized RBL-2H3 cells were exposed to ME at various concentrations for 1 h prior to antigen stimulation, phosphorylation of $cPLA_2$, the rate-limiting step of the arachidonate cascade, was diminished. Similarly, ME suppressed 5-LO phosphorylation, the rate-limiting step of leukotriene biosynthesis, and inhibited COX-2 expression, which catalyzes the rate-limiting step of prostaglandin biosynthesis. These findings indicate that ME

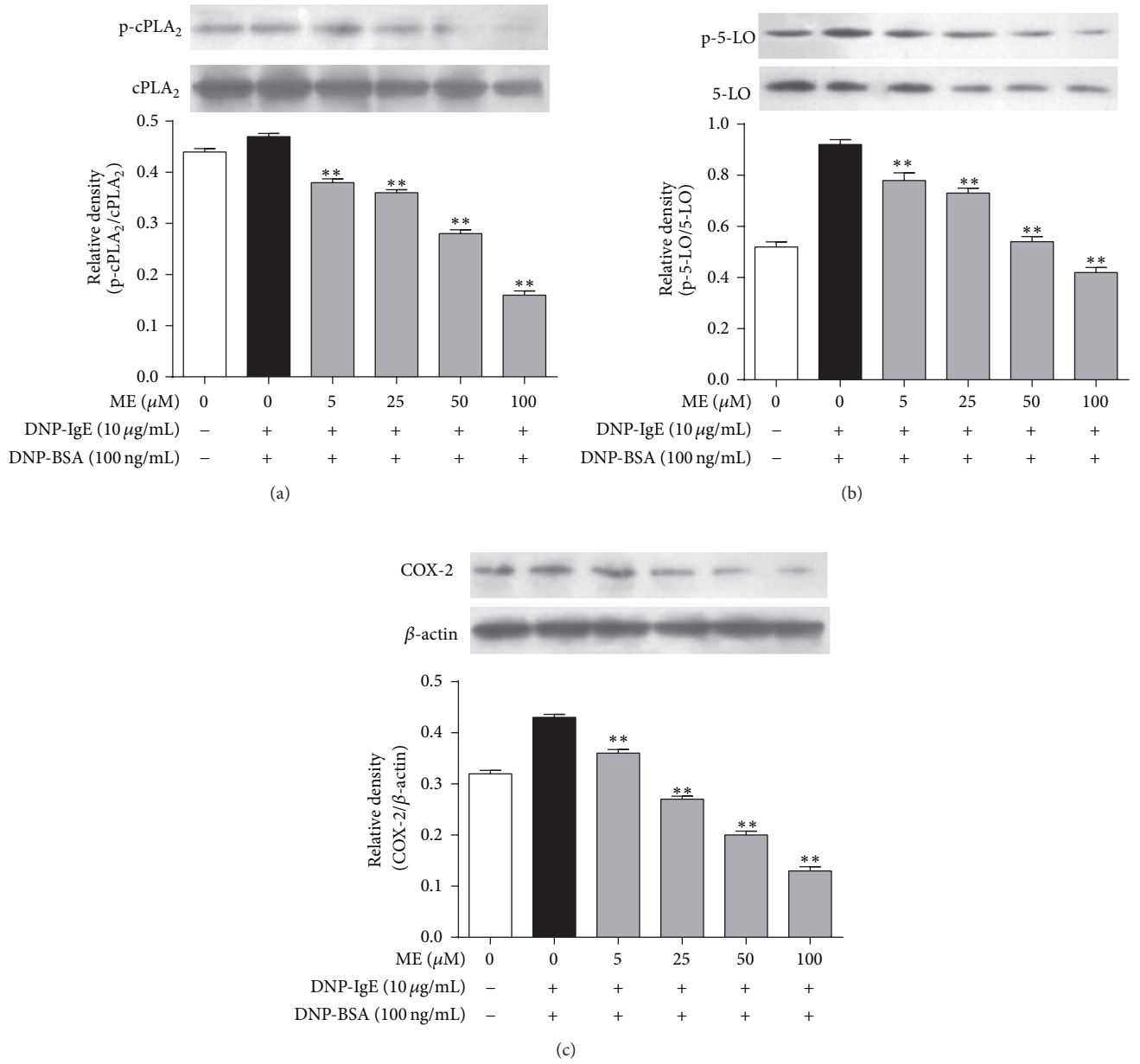

Figure 3: Effect of ME on a late stage of the FcεRI signal cascade in IgE-activated RBL-2H3 cells. RBL-2H3 cells were seeded on a 6-well plate in DMEM with 10% FBS at 37°C overnight, and then the cells were washed and further incubated with DNP-IgE for 24 h. The cells were incubated with ME (0–100 μM) for 1 h and then stimulated by DNP-BSA for 4 h. The cells were rinsed and lysed with a cell lysis buffer. The expression of p-cPLA$_2$, cPLA$_2$, p-5-LO, 5-LO, COX-2, and β-actin was determined as described in Section 2. Data represent the mean ± SD of three independent experiments and differences between mean values were assessed by one-way ANOVA. $^{*}P < 0.05$, $^{**}P < 0.01$ indicate significant differences compared with the DNP-BSA-treated group.

decreases the activation of several targets, including cPLA$_2$, 5-LO, and COX-2, suggesting that the antiallergic action of ME may be mediated by arachidonate cascade suppression.

3.4. Suppressive Effect of ME on FcεRI Signaling Pathway. Next, we investigated the mechanism of the antiallergic action of ME. Activation of the FcεRI receptor induces Lyn and Syk phosphorylation, mediating the degranulation of mast cells [22]. In this respect, ME may affect Lyn or Syk phosphorylation in the early phase of the FcεRI receptor cascade. When RBL-2H3 cells were preincubated with ME for 1 h before antigen challenge, and the incubation was extended an additional 10 min, the phosphorylation of Syk, but not Lyn, was inhibited in a dose-dependent manner (Figure 4). Notably, ME markedly reduced the expression and phosphorylation of ERK1/2 (Figure 5(a)). Thus, ME could reduce ERK1/2 function by directly suppressing ERK1/2 expression. Additionally, phosphorylation of MAP kinases,

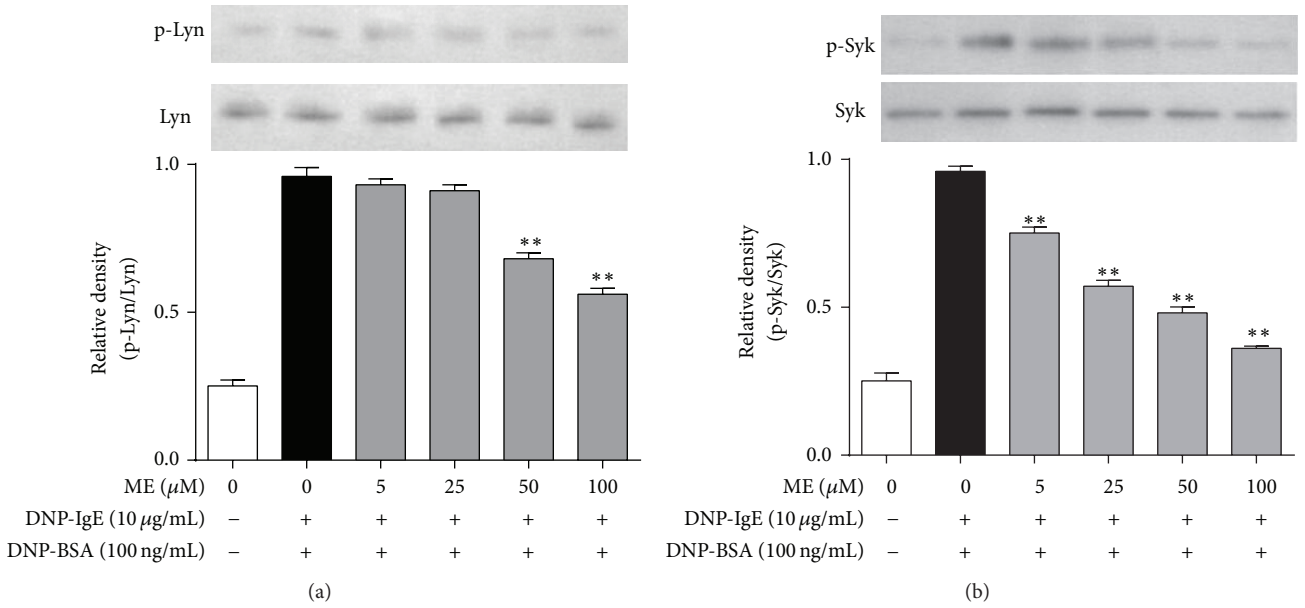

Figure 4: Effect of ME on early stage of FcεRI cascade in IgE-activated RBL-2H3 cells. IgE-sensitized RBL-2H3 cells were exposed to ME (0–100 μM) for 1 h and then stimulated by DNP-BSA (100 ng/mL) for 10 min. The cells were rinsed with 1× PBS and lysed with cell lysis buffer. The expression of p-Lyn, Lyn, p-Syk, and Syk was determined as described in Section 2. Data represent the mean ± SD of three independent experiments and differences between mean values were assessed by one-way ANOVA. $^{*}P < 0.05$, $^{**}P < 0.01$ indicate significant differences compared with the DNP-BSA-treated group.

such as p38 or JNK, was also suppressed by ME, although p38 phosphorylation was more sensitive to ME (Figures 5(b) and 5(c)).

4. Discussion

The essential oil of *Asiasari radix* has many beneficial health effects, exhibiting anti-inflammatory, antibacterial, and antiallergy properties, as well as affecting the respiratory and circulatory systems [25]. *Asiasari radix* essential oils contain a considerable number of chemical ingredients, including ME, asarylketone, cineol, safrole, limonene, and eucarvone [26]. Previously, ME was reported to have beneficial effects on inflammation, ischemia, anaphylaxis, and nociception. Our present data demonstrate that ME exerts antiallergic effects in IgE-activated RBL-2H3 cells. ME significantly suppresses degranulation and proinflammatory cytokine release in antigen-sensitized mast cells. Several cytokines play critical roles in allergic inflammation. For example, TNF-α, which is secreted from IgE-activated mast cells, plays an important role in allergic responses [27]. Therefore, the inhibitory effect of ME on TNF-α formation may indicate its added advantage as an antiallergy agent. During the pathogenesis of allergic disease, IL-4 is crucial for the induction of IgE synthesis and mast cell development [28]. IL-4 also modulates the inflammatory response, owing to its ability to affect adhesion molecule expression and cytokine production in endothelial cells, and promotes growth and activation of neutrophils, mast cells, T cells, and eosinophils [29]. These results suggest that ME significantly inhibits mast cell degranulation and proinflammatory cytokine release.

One possible mechanism of ME-induced antiallergic activity may be its effect on the FcεRI signal cascade. IgE-induced degranulation in mast cells is associated with activation of the FcεRI receptor, and this activation induces the release of various inflammatory mediators, including TNF-α, leukotrienes, and prostaglandins via phosphorylation of the Lyn/Syk pathway [23]. In turn, the activation of Syk increases intracellular Ca^{2+} and the activation of the MAP kinase family [23]. Thus, Lyn and Syk are important intracellular mediators in early signaling following FcεRI receptor activation. In the present study, Syk was markedly inhibited by ME, supporting the notion that it is a primary target of ME. In support of this observation, ME significantly reduced the phosphorylation of ERK1/2, p38, and JNK, which are downstream effectors of FcεRI [23].

In the present study, 100 μM ME obviously inhibited $cPLA_2$ and 5-LO phosphorylation and decreased the formation of the 5-LO products, LTB_4 and LTC_4. This effect may improve the antiallergy action of ME, because LTB_4 is a potent chemoattractant and activator of neutrophils and other immune cells in severe asthma [30, 31]. LTC_4 is a potent spasmogenic agent and an agonist of cysteinyl-LT receptors, which are known to induce chronic inflammatory reactions in allergic diseases [21]. Furthermore, ME also inhibited COX-2 expression and dramatically reduced the levels of the COX-2 products PGE_2 and PGD_2, which are enhanced in activated immune cells, including mast cells [20, 32]. The suppressive effects of ME on PGE_2 formation may contribute to its increased antiallergic activity, as PGE_2 may mediate asthma development and inflammation associated with IL-4 and IL-5, which are produced by helper T cells [32].

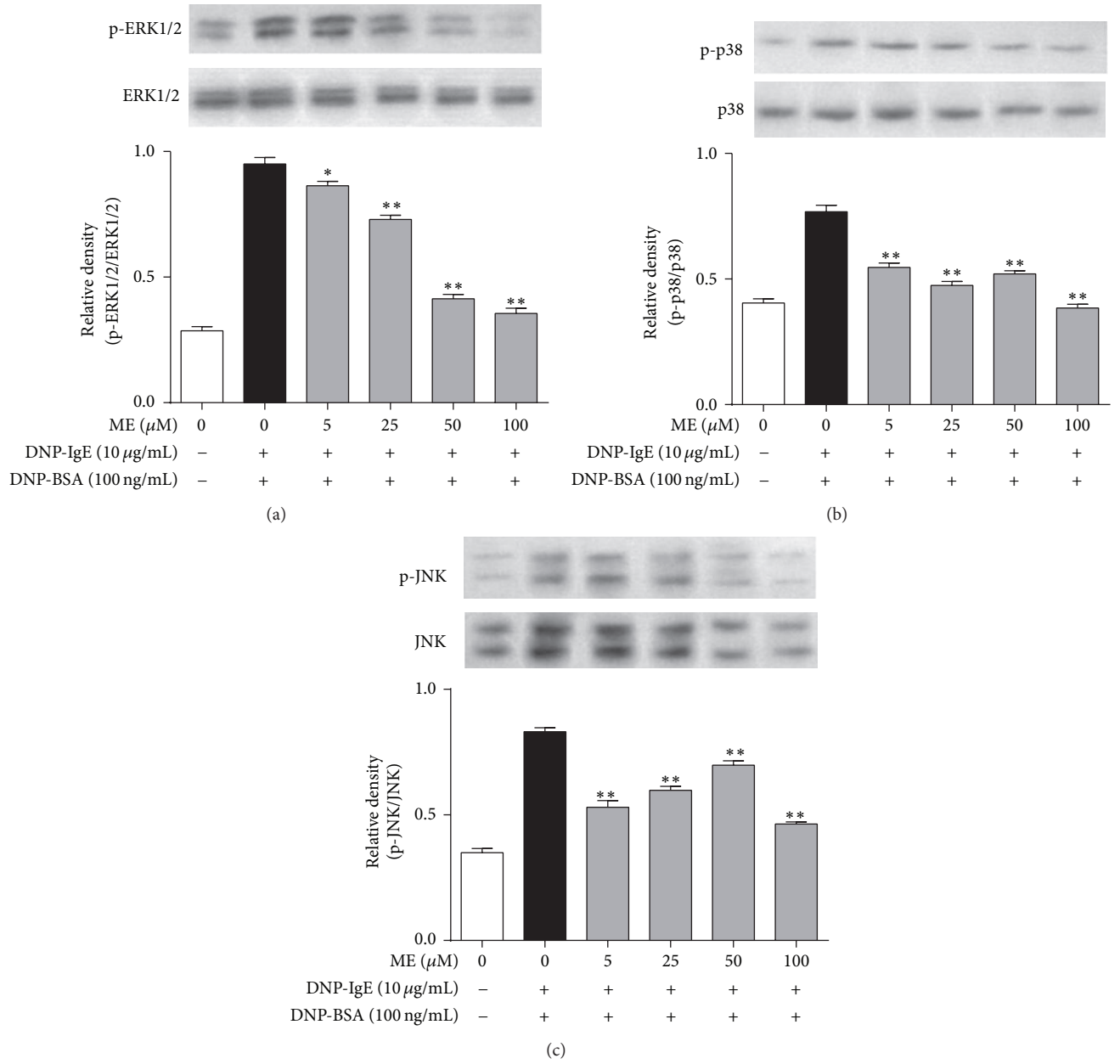

Figure 5: Effect of ME on MAP kinase pathway in IgE-activated RBL-2H3 cells. IgE-sensitized RBL-2H3 cells were exposed to ME (0–100μM) for 1 h and then stimulated by DNP-HSA (100 ng/mL) for 10 min. The cells were rinsed with 1× PBS and lysed with cell lysis buffer. The expression of p-ERK1/2, ERK1/2, p-p38, p38, p-JNK1/2, or JNK1/2 was determined as described in Section 2. Data represent the mean ± SD of three independent experiments and differences between mean values were assessed by one-way ANOVA. $^{*}P < 0.05$, $^{**}P < 0.01$ indicate significant differences compared with the DNP-BSA-treated group.

Moreover, the inhibitory effect of ME on PGD_2 formation may add to the antiallergic action, as PGD_2 is known to cause bronchoconstriction and vasodilation and increases capillary permeability and mucous production in asthma [20]. Collectively, these findings suggest that ME can reduce allergic reactions through suppression of $cPLA_2$ and 5-LO activation and through inhibition of COX-2 activity. Taken together, ME can inhibit allergic reaction by suppressing the activation of Syk, ERK1/2, p38, and JNK and reducing the activity of the enzymes responsible for the biosynthesis of PGD_2 and LTB_4. Further, these effects may be extended to anti-inflammatory effects on other cells or tissues. Additionally, the expression of TNF-α is associated with p38, JNK, and ERK1/2 activation in the FcεRI receptor cascade in IgE-activated mast cells [23]. Therefore, the reduction of TNF-α formation by ME may provide an additional advantage to ME as an antiallergic agent.

In conclusion, the present study demonstrates that ME has antiallergic effects in IgE-activated RBL-2H3 cells. The mechanisms responsible for its antiallergic effects may

involve multiple targets including Sky, ERK1/2, p38, JNK, $cPLA_2$, 5-LO, and COX-2. Such effects may provide further information for the application of ME as an antiallergic agent. Therefore, our future studies will focus on providing additional pharmacological evidence to demonstrate this possibility.

Conflict of Interests

The authors declare that they have no conflict of interests.

Acknowledgments

This research was supported by the Science and Technology Development Funding Foundation of Guangdong Province (Grant no. 2012A032400002), the Medical Scientific Research Foundation of Guangdong Province (B2013074), the National Natural Science Foundation of China (Grant no. 81202431), and the Natural Science Foundation of Guangdong Province (Grant no. S2012010009576).

References

[1] C. Flohr, R. J. Quinnell, and J. Britton, "Do helminth parasites protect against atopy and allergic disease?" *Clinical and Experimental Allergy*, vol. 39, no. 1, pp. 20–32, 2009.

[2] K. J. Erb, "Can helminths or helminth-derived products be used in humans to prevent or treat allergic diseases?" *Trends in Immunology*, vol. 30, no. 2, pp. 75–82, 2009.

[3] B. S. Bochner and R. P. Schleimer, "Mast cells, basophils, and eosinophils: distinct but overlapping pathways for recruitment," *Immunological Reviews*, vol. 179, pp. 5–15, 2001.

[4] S. J. Galli, "New concepts about the mast cell," *The New England Journal of Medicine*, vol. 328, no. 4, pp. 257–265, 1993.

[5] M. Nguyen, A. J. Pace, and B. H. Koller, "Age-induced reprogramming of mast cell degranulation," *Journal of Immunology*, vol. 175, no. 9, pp. 5701–5707, 2005.

[6] A. M. Gilfillan and C. Tkaczyk, "Integrated signalling pathways for mast-cell activation," *Nature Reviews Immunology*, vol. 6, no. 3, pp. 218–230, 2006.

[7] M. K. Church and F. Levi-Schaffer, "The human mast cell," *Journal of Allergy and Clinical Immunology*, vol. 99, no. 2, pp. 155–160, 1997.

[8] D. D. Metcalfe, M. Kaliner, and M. A. Donlon, "The mast cell," *Critical Reviews in Immunology*, vol. 3, no. 1, pp. 23–74, 1981.

[9] W. Duan and W. S. F. Wong, "Targeting mitogen-activated protein kinases for asthma," *Current Drug Targets*, vol. 7, no. 6, pp. 691–698, 2006.

[10] A. Lorentz, I. Klopp, T. Gebhardt, M. P. Manns, and S. C. Bischoff, "Role of activator protein 1, nuclear factor-kappaB, and nuclear factor of activated T cells in IgE receptor-mediated cytokine expression in mature human mast cells," *Journal of Allergy and Clinical Immunology*, vol. 111, no. 5, pp. 1062–1068, 2003.

[11] B. Frossi, J. Rivera, E. Hirsch, and C. Pucillo, "Selective activation of Fyn/PI3K and p38 MAPK regulates IL-4 production in BMMC under nontoxic stress condition," *The Journal of Immunology*, vol. 178, no. 4, pp. 2549–2555, 2007.

[12] Y. Kawakami, S. E. Hartman, P. M. Holland, J. A. Cooper, and T. Kawakami, "Multiple signaling pathways for the activation of JNK in mast cells: involvement of Bruton's tyrosine kinase, protein kinase C, and JNK kinases, SEK1 and MKK7," *Journal of Immunology*, vol. 161, no. 4, pp. 1795–1802, 1998.

[13] D. Hata, Y. Kawakami, N. Inagaki et al., "Involvement of Bruton's tyrosine kinase in FcepsilonRI-dependent mast cell degranulation and cytokine production," *Journal of Experimental Medicine*, vol. 187, no. 8, pp. 1235–1247, 1998.

[14] S. Yano, Y. Suzuki, M. Yuzurihara et al., "Antinociceptive effect of methyleugenol on formalin-induced hyperalgesia in mice," *European Journal of Pharmacology*, vol. 553, no. 1–3, pp. 99–103, 2006.

[15] K. Hashimoto, T. Yanagisawa, Y. Okui, Y. Ikeya, M. Maruno, and T. Fujita, "Studies on anti-allergic components in the roots of Asiasarum sieboldi," *Planta Medica*, vol. 60, no. 2, pp. 124–127, 1994.

[16] C. C. Lima, D. N. Criddle, A. N. Coelho-De-Souza, F. J. Q. Monte, M. Jaffar, and J. H. Leal-Cardoso, "Relaxant and antispasmodic actions of methyleugenol on guinea-pig isolated ileum," *Planta Medica*, vol. 66, no. 5, pp. 408–411, 2000.

[17] Y. K. Choi, G.-S. Cho, S. Hwang et al., "Methyleugenol reduces cerebral ischemic injury by suppression of oxidative injury and inflammation," *Free Radical Research*, vol. 44, no. 8, pp. 925–935, 2010.

[18] B. K. Shin, E. H. Lee, and H. M. Kim, "Suppression of L-histidine decarboxylase mRNA expression by methyleugenol," *Biochemical and Biophysical Research Communications*, vol. 232, no. 1, pp. 188–191, 1997.

[19] M. Ishiyama, H. Tominaga, M. Shiga, K. Sasamoto, Y. Ohkura, and K. Ueno, "A combined assay of cell viability and in vitro cytotoxicity with a highly water-soluble tetrazolium salt, neutral red and crystal violet," *Biological and Pharmaceutical Bulletin*, vol. 19, no. 11, pp. 1518–1520, 1996.

[20] M. Arima and T. Fukuda, "Prostaglandin D_2 and T_H2 inflammation in the pathogenesis of bronchial asthma," *The Korean Journal of Internal Medicine*, vol. 26, no. 1, pp. 8–18, 2011.

[21] E. Nettis, M. D'Erasmo, E. di Leo et al., "The employment of leukotriene antagonists in cutaneous diseases belonging to allergological field," *Mediators of Inflammation*, vol. 2010, Article ID 628171, 6 pages, 2010.

[22] Y. Kawakami, J. Kitaura, A. B. Satterthwaite et al., "Redundant and opposing functions of two tyrosine kinases, Btk and Lyn, in mast cell activation," *Journal of Immunology*, vol. 165, no. 3, pp. 1210–1219, 2000.

[23] K. Roth, W. M. Chen, and T. J. Lin, "Positive and negative regulatory mechanisms in high-affinity IgE receptor-mediated mast cell activation," *Archivum Immunologiae et Therapiae Experimentalis*, vol. 56, no. 6, pp. 385–399, 2008.

[24] Y. Kim, Y.-S. Lee, J.-H. Hahn et al., "Hyaluronic acid targets CD44 and inhibits FcεRI signaling involving PKCδ, Rac1, ROS, and MAPK to exert anti-allergic effect," *Molecular Immunology*, vol. 45, no. 9, pp. 2537–2547, 2008.

[25] Y. S. Wang, *Pharmacology and Application of Chinese Materia Medica*, People's Health Publisher, Beijing, China, 1983.

[26] R. H. Zhou, *Resource Science of Chinese Medicinal Materials*, China Medical & Pharmaceutical Sciences Press, Beijing, China, 1993.

[27] T. C. Theoharides and D. Kalogeromitros, "The critical role of mast cells in allergy and inflammation," *Annals of the New York Academy of Sciences*, vol. 1088, pp. 78–99, 2006.

[28] Y. Nabeshima, T. Hiragun, E. Morita, S. Mihara, Y. Kameyoshi, and M. Hide, "IL-4 modulates the histamine content of mast

cells in a mast cell/fibroblast co-culture through a Stat6 signaling pathway in fibroblasts," *FEBS Letters*, vol. 579, no. 29, pp. 6653–6658, 2005.

[29] J.-L. Boulay and W. E. Paul, "The interleukin-4 family of lymphokines," *Current Opinion in Immunology*, vol. 4, no. 3, pp. 294–298, 1992.

[30] A. W. Ford-Hutchinson, M. A. Bray, M. V. Doig, M. E. Shipley, and M. J. H. Smith, "Leukotriene B, a potent chemokinetic and aggregating substance released from polymorphonuclear leukocytes," *Nature*, vol. 286, no. 5770, pp. 264–265, 1980.

[31] A. M. Tager and A. D. Luster, "BLT1 and BLT2: the leukotriene B(4) receptors," *Prostaglandins Leukotrienes and Essential Fatty Acids*, vol. 69, no. 2-3, pp. 123–134, 2003.

[32] T. C. T. M. van der Pouw Kraan, L. C. M. Boeije, R. J. T. Smeenk, J. Wijdenes, and L. A. Aarden, "Prostaglandin-E2 is a potent inhibitor of human interleukin 12 production," *Journal of Experimental Medicine*, vol. 181, no. 2, pp. 775–779, 1995.

Hindawi Publishing Corporation
Mediators of Inflammation
Volume 2015, Article ID 460264, 11 pages
http://dx.doi.org/10.1155/2015/460264

Research Article

Construction, Expression, and Characterization of a Recombinant Immunotoxin Targeting EpCAM

Minghua Lv,[1] Feng Qiu,[2] Tingting Li,[3] Yuanjie Sun,[4] Chunmei Zhang,[4] Ping Zhu,[1] Xiaokun Qi,[2] Jun Wan,[3] Kun Yang,[4] and Kui Zhang[1,4]

[1]*Department of Clinical Immunology, Xijing Hospital, Fourth Military Medical University, Xi'an 710032, China*
[2]*Department of Neurology, Chinese Navy General Hospital, Beijing 100048, China*
[3]*Department of Geriatric Gastroenterology, Chinese People's Liberation Army General Hospital, Beijing 100853, China*
[4]*Department of Immunology, Fourth Military Medical University, Xi'an 710032, China*

Correspondence should be addressed to Xiaokun Qi; bjqxk@sina.com, Jun Wan; wanjun301@126.com, Kun Yang; yangkunkun@fmmu.edu.cn, and Kui Zhang; zhk100@fmmu.edu.cn

Received 17 October 2014; Accepted 4 December 2014

Academic Editor: Lijun Xin

Epithelial cell adhesion molecule (EpCAM) is a type I transmembrane glycoprotein overexpressed in human epithelioma but with relatively low expression in normal epithelial tissues. To exploit this differential expression pattern for targeted cancer therapy, an EpCAM-targeted immunotoxin was developed and its antitumor activity was investigated *in vitro*. An immunotoxin (scFv2A9-PE or APE) was constructed by genetically fusing a truncated form (PE38KDEL) of *Pseudomonas aeruginosa* exotoxin with an anti-EpCAM single-chain variable fragment (scFv). ELISA and flow cytometry were performed to verify immunotoxin (scFv2A9-PE or APE) antigen-binding activity with EpCAM. Cytotoxicity was measured by MTT assay. Confocal microscopy was used to observe its cellular localization. The results of ELISA and flow cytometry revealed that the immunotoxin efficiently recognized recombinant and natural EpCAM. Its antigen-binding activity was relatively lower than 2A9. MTT assay confirmed potent reduction in EpCAM-positive HHCC (human hepatocellular carcinoma) cell viability (IC_{50} 50 pM). Immunofluorescence revealed that the immunotoxin localized to endoplasmic reticulum 24 h later. In conclusion, we described the development of an EpCAM-targeted immunotoxin with potent activity against tumor cells, which may lay the foundation for future development of therapeutic antibody for the treatment of EpCAM-positive tumors.

1. Introduction

The most ideal outcomes for tumor targeted therapy are improved patient survival and minimal adverse effects on normal tissues. Drugs that can specifically home to a cancer cell based on a surface receptor have helped to address that goal with the advent of monoclonal antibody therapy [1]. Rituximab, directed against the CD20 antigen found on the surface of normal and malignant B cells, is the first monoclonal antibody approved by the US Food and Drug Administration for the treatment of B-cell non-Hodgkin's lymphoma [2]. Monoclonal antibodies have been developed and have been impressive, but they are limited by immunogenicity [3], thus, leading to the development of single-chain variable fragment (scFv) antibodies.

Researchers have designed and produced many scFvs since the 1980s. Recombinant scFvs are promising because they can target an effector molecule or a cell to a disease-related target structure [4, 5]. Immunotoxin, as one type of immunoconjugate, can be produced by genetically fusing scFv with toxin and this molecule can recognize target cells by scFv and kill them via its toxin. Many immunotoxins have undergone or are currently undergoing study in humans for leukemia treatment [6, 7]. Denileukin diftitox (Ontak) has been approved by the FDA for the treatment of cutaneous T-cell lymphoma in adults [8]. Thus, immunotoxins are promising therapeutics for targeted cancer therapy.

Epithelial cell adhesion molecule (EpCAM), also known as CD326, is a type I membrane glycoprotein of approximately 40 kDa. It participates in many biological processes,

Table 1: Sequences of the primers used in this study are listed as A to L.

Primers	Sequence
A	tgaggagacggtgaccgtggtcccttggccccag
B	aggtsmarctgcagsagtcwgg
C	gttagatctccagcttggtccc
D	gacattcagctgacccagtctcca
E	gc**ggatcc**gaggtgaagctrcagcagt
F	c**ggtcgac**tgaggagacrgtgaccgtkg
G	c**ggtcgac**ggtggtggtggttctggtggtggtggttctggtggtggtggttctgatgttgtgctgacccagtctccactcactttgt
H	gc**aagctt**gatctccagcttggtccctcc
I	gc**gaattc**ggtggtggtggttctggtggtggtggttctggtggtggtggttctgcggccgcttctggaggt
J	cgc**tcgag**tcacagttcgtctttcggcggtttg
K	gc**ggtacc**caggaagaatgtgtctgtg
L	cg**aagctt**accagcttttagaccctg

B and F were degenerate primers; the degenerate base codes are as follows: s:c/g; m:a/c; r:a/g; w:a/t; k:g/t.

such as cell adhesion, proliferation, and differentiation [9]. EpCAM is frequently highly expressed on most solid tumors, including carcinomas of the breast, ovarian, lung, colon, and pancreatic cancer and in squamous cell carcinoma of the head and neck, suggesting its potential as a therapeutic target [10, 11].

EpCAM-targeted antibody therapy has been studied frequently since the 1980s. MAb17-1A, a low affinity monoclonal antibody against EpCAM, is successfully used in Germany for breast and colon carcinoma therapy [12, 13] and CD3/17-1A, a bispecific scFv, is demonstrated to have cytotoxicity to EpCAM-positive tumor cells *in vitro* [14]. Finally, catumaxomab, a trifunctional anti-EpCAM/CD3 monoclonal antibody, has been approved in the European Union for the treatment of EpCAM-positive tumors in patients with malignant ascites [15]. Due to limited applications and adverse effects of these antibodies, researchers wish to exploit more effective and EpCAM antibodies with greater potential to treat carcinomas. In the past 20 years, fully humanized and bispecific scFv fusion proteins have been studied in preclinical and clinical trials [16, 17] and EpCAM targeted immunotoxins have been confirmed to have antitumor activity *in vitro* [18]. Simon made modification to an EpCAM-targeting fusion toxin by facile click PEGylation to increase its antitumor efficacy *in vitro* and *in vivo* [19]. All these investigations have increased the promise of EpCAM as a target for cancer therapy.

We prepared seven EpCAM monoclonal antibodies, FMU-EpCAM-2A9, FMU-EpCAM-2D7, FMU-EpCAM-4B11, FMU-EpCAM-4F11, FMU-EpCAM-4E4, FMU-EpCAM-4A11, and FMU-EpCAM-4F6. FMU-EpCAM-2A9 and FMU-EPCAM-2D7 are also named FMU-Ep1 and FMU-Ep3, respectively. In previous work, we reported that some of these antibodies (FMU-Ep1 and FMU-Ep3) can be used for immunohistochemical staining to identify normal and malignant colon tissue [20]. However, whether these are effective anticancer agents is uncertain. Thus, we report the construction, expression, and characterization of an immunotoxin, comprised of a single-chain variable fragment (scFv) of FMU-EpCAM-2A9 and a truncated form (PE38KDEL) of *Pseudomonas aeruginosa* exotoxin. The recombinant immunotoxin was successfully cloned and expressed and its antigen-binding ability and cytotoxicity were measured. This recombinant immunotoxin potently inhibited HHCC cell lines, which lays the foundation for further development of this agent as a possible cancer chemotherapeutic.

2. Materials and Methods

2.1. Materials. The recombinant plasmid PGEX-4T3-EpCAM and the monoclonal antibodies of EpCAM (FMU-EpCAM-2A9 and FMU-EpCAM-2D7) are all prepared in our lab. Fetal bovine serum and mRNA isolation kit are purchased from Gibco. FITC conjugated goat anti-mouse IgG is bought from Biolegend. Mouse anti-GST antibody, protein ultrafiltration centrifugal tube, and PVDF membrane are from Millipore. The primers used were synthesized by Shanghai Sangon Biotech Company. The sequences of the primers were listed in Table 1.

2.2. Organism. *Escherichia coli* DH5α and BL21 were used for cloning of the pMD-T18-2A9-V_H (or -V_L) plasmid and pGEX-4T1-scFv plasmid, respectively. *E. coli* M15 was used to express the extracellular domain of EpCAM (pQE30-EpCAM).

2.3. Cell Lines and Cultures. The hepatocellular carcinoma cell lines (HHCC and SMMC-7721), breast cancer cell line (SKBR3), and colon cancer cells (Colo205 and SW480) are all from ATCC. They were grown in RPMI 1640 medium supplemented with 10% fetal bovine serum (FBS) and 1% penicillin-streptomycin (100 units/mL penicillin and 100 μg/mL streptomycin) at 37°C and 5% CO_2 in a humidified incubator.

2.4. Cloning Light and Heavy Chain Variable Region of FMU-EpCAM-2A9 (FMU-Ep1). Hybridoma cells were cultured in

RPMI1640 medium supplemented with 10% fetal bovine serum. Cells were collected in the logarithmic phase and total RNA was extracted with Trizol according to the manufacturer's instructions. The sequences encoding the light and heavy chain variable regions (V_L and V_H) of 2A9 were amplified by RT-PCR. The V_H sequence was amplified using primers A and B, while the V_L sequence was amplified with primers C and D. After purification, PCR products were cloned into a pMD-T18 vector and transformed into *E. coli* DH5α. The positive colony (pMD-T18-2A9-V_H or pMD-T18-2A9-V_L) was identified by colony PCR and restriction enzyme analysis.

2.5. Construction of the pGEX-4T1-scFv2A9-PE Expression Vector. The sequence encoding the 2A9-V_H and 2A9-V_L was amplified by PCR from plasmids pMD-T18-2A9-V_H and pMD-T18-2A9-V_L, respectively, and inserted into the pGEX-4T1 expression vector in two steps. A special linker was added to the N terminal of V_L by forward primer. The peptide sequence of the linker was GGGGSGGGGSGGGGS. The 2A9-V_H sequence was amplified by primers E and F, whereas the 2A9-V_L sequence was amplified using primers G and H. After gel purification, the amplified V_H products were digested, purified, and ligated between the BamH I and Sal I sites of plasmid vector pGEX-4T1. After identification of the pGEX-4T1-V_H plasmid, the amplified V_L products were ligated between the Sal I and EcoR I sites of plasmid vector pGEX-4T1-V_H. The pGEX-4T1-V_H-V_L (pGEX-4T1-scFv2A9) vector was confirmed by restriction enzyme digestion and DNA sequencing. The sequence encoding a truncated form of *Pseudomonas* exotoxin (PE38KDEL) was amplified by PCR, and the template was kindly supplied by Professor Boquan Jin of the Fourth Military Medical University and cloned as an ~1,200 bp EcoR I-Xhol I fragment downstream of the scFv2A9 sequence present in the pGEX-4T1-based scFv2A9 expression vector. The primers used were I and J. The expression vector pGEX-4T1-scFv2A9-PE was identified by restriction enzyme digestion and DNA sequencing.

2.6. Protein Expression and Purification of the Immunotoxin against EpCAM. The pGEX-4T1-scFv2A9-PE plasmid was expressed in BL21 *E. coli* cells. Bacterial cultures were incubated at 37°C in LB growth medium containing 100 ng/mL ampicillin and grown until an early log phase (A600 nm = 0.6–0.8). Protein expression was induced for 7 h at 30°C by the addition of IPTG (final concentration 500 nM). Bacteria were harvested by centrifugation at 12,000 rpm for 20 min at 4°C. For purification, the pellet obtained from a 100 mL culture was resuspended in 10 mL 0.15 M PBS and pulse-sonicated for 30 × 1 min (1 s working and 1 s resting for a 1 min pulse and then cooled on ice for 1 min). The soluble and insoluble fractions were separated by centrifugation at 12,000 rpm for 20 min at 4°C. Then the soluble fraction was purified by using the Glutathione Resin GST Fusion Protein Purification Kit according to the manufacturer's instructions (Genscript cat. number L00206). The purified immunotoxin was labeled by biotin according to the manufacturer's instruction (Roche, Biotin Protein Labeling Kit).

2.7. Western Blotting Detection of the Immunotoxin against EpCAM. Purified protein samples were analyzed by electrophoresis on 10% SDS-PAGE under denaturing conditions and transferred to PVDF membrane. Western blot analysis was conducted using a mouse anti-GST antibody (the scFv was coexpressed with a GST tag) as the primary antibody (Millipore, 1 : 3000) and a horseradish peroxidase- (HRP-) labeled rabbit anti-mouse IgG as the secondary antibody, in accordance with the manufacturer's protocols.

2.8. Construction of the pQE30-EpCAM Plasmid. The sequence encoding the extracellular domain of EpCAM was amplified by PCR from plasmid pGEX-4T-3-EpCAM and cloned as a 750 bp Kpn I - Hind III fragment to the plasmid pQE30. The primers used were K and L.

2.9. Prokaryotic Expression of pQE30-EpCAM. The pQE30-EpCAM plasmid was used to express the extracellular domain of EpCAM in M15 *E. coli*. Cells were grown at 37°C in a shaking incubator (220 rpm) until the culture reached an OD_{600} of 0.6–0.8. Protein expression was induced for 7 h at 30°C by adding IPTG (Sigma) at a final concentration of 500 nM. The harvested pellet was ultrasonicated and analyzed via SDS-PAGE Coomassie Blue staining and Western blot. The protein from the supernatant was purified with a Nickel-affinity chromatography column, in accordance with the manufacturer's instruction (GE).

2.10. ELISA Detection of the Binding Ability of the Immunotoxin to EpCAM. The binding ability of the immunotoxin to EpCAM was detected by ELISA. Briefly, a 96-well plate was coated with 100 μL 5 μg/mL EpCAM-HIS recombinant protein overnight at 4°C in PBS. After incubation and washing, 100 μL 2A9 or immunotoxin was added to the wells at different concentrations (20, 2, 0.2, 0.02, and 0.002 μg/mL) and incubated for 1 h at 37°C. A mouse anti-GST primary antibody (1 : 500) and a HRP-labeled rabbit anti-mouse secondary antibody (1 : 2,500) were used to detect 2A9 or immunotoxin; the tetramethylbenzidine (TMB) was used to develop the ELISA results. All experiments were repeated three times.

2.11. Flow Cytometry Analysis. Colo205 and HHCC cells at 5 × 10^6 cells/mL were incubated with biotin labeled immunotoxin (20 μg/mL) or antibodies against EpCAM (20 μg/mL) for 40 minutes at 4°C. The cells were washed with PBS and then incubated with the FITC labeled avidin or antibodies for 30 minutes at 4°C. The fluorescence was examined by flow cytometry analysis using a FACScan flow cytometer (BD).

2.12. In Vitro Cytotoxicity Assay. Cytotoxic activity of the immunotoxin was measured with a standard MTT assay. Briefly, 4,000 HHCC cells were seeded in 96-well microplates in a total volume of 200 μL of culture medium/well. Immunotoxin (2–32.5 M) was added and cells were incubated for 72 h under standard cell culture conditions. Then, 20 μL of 5 mg/mL MTT solution was added to each well, and plates

were incubated for 4 h at 37°C. Cell lysis and formazan solubilization were achieved by the addition of 150 μL DMSO, and released formazan crystals were allowed to dissolve 10 min at 37°C. Absorption was quantified at 490 nm using a microplate reader. All experiments were measured in triplicate.

2.13. Immunofluorescence. Intracellular localization of the immunotoxin was observed by laser scanning confocal microscopy. Briefly, the HHCC cells were seeded in 24-well plates. After incubating for 8 h, biotin-labeled immunotoxin was added to the wells and incubated for different times. To localize the immunotoxin, cells were washed and fixed with 4% paraformaldehyde, and after blocking, cells were stained with primary antibody of the specific endoplasmic reticulum protein CRT (prepared in our laboratory). Fluorescence was measured by adding PE conjugated goat anti-mouse IgG and FITC-labeled avidin. Cell nuclei were stained with DAPI. After mounting, results were observed with laser scanning confocal microscopy.

2.14. Statistical Analysis. Differences between groups were determined using an unpaired two-tailed Student's t-test. Data analyses were performed using GraphPad Prism version 5.0 (GraphPad Software, San Diego, CA). For all tests, a P value less than 0.05 was considered significant.

3. Results

3.1. Screening Parental Antibody against EpCAM. To screen the parental antibody of scFv, we compared the binding activity of two EpCAM mAbs (FMU-2A9 and FMU-2D7) with EpCAM on the surface of EpCAM-positive cells (Colo205 and HHCC) and EpCAM-negative cells (Sw480) by flow cytometry. Sw480 cells were similar to isotype control antibody (data not shown). The results of Colo205 and HHCC are depicted in Figure 1. 2A9 had relatively higher binding ability than 2D7 with the natural EpCAM molecule on these two cell surfaces. Thus, we selected 2A9 as the parental antibody to construct the scFv.

3.2. Construction, Expression, and Purification of the Immunotoxin. After three rounds of PCR, the plasmid pGEX4T1-scFv2A9-PE was constructed. Three separate products generated an ~2,000 bp immunotoxin (Figures 2(a) and 2(b)). The sequence of the immunotoxin (APE) was further confirmed by DNA sequencing (Figure 3). APE was expressed in BL21 *E. coli*, after sonication and purification, and samples were analyzed. SDS-PAGE and Western blot results (Figures 2(c) and 2(d)) indicated that the expressed GST-immunotoxin was ~95 kDa, which was consistent with the predicted molecule weight. Immunotoxin mainly interacted with inclusion bodies. To analyze immunotoxin activity, the GST tag was cut with thrombin and removed by purification, and the true molecule mass of the immunotoxin was 67 kDa (Figure 2(e)).

3.3. Construction, Expression, and Purification of the Extracellular Domain of EpCAM. To analyze the binding ability of the immunotoxin, we constructed and expressed the recombinant protein HIS-EpCAM. The plasmid pQE30-EpCAM was identified by restriction enzyme analysis (Figure 4(a)) and DNA sequencing. The expression of HIS-EpCAM was induced with 500 nM IPTG at 30°C for 7 h. After sonication and centrifugation of the bacteria, total protein, supernatants, and inclusion bodies were separated with 10% SDS-PAGE under reducing conditions. As shown in Figure 4(b), the expression strain produced the recombinant protein in both soluble and inclusion bodies form. Western blot (Figure 4(c)) confirmed a novel band at the predicted molecular weight of 32 kDa. After purification and identification, proteins were stored at −80°C for ELISA.

3.4. Binding Ability of Immunotoxin to EpCAM. Immunotoxin was successfully prepared, and the binding ability of the immunotoxin to EpCAM was tested by flow cytometry and ELISA. Briefly, prepared His-EpCAM or BSA was coated on 96-well plates, and the immunotoxin or 2A9 was added to detect recognition to EpCAM. Data showed (Figure 5(a)) that 2A9 had relatively higher binding ability with recombinant His-EpCAM (2 μg/mL) (unpaired t-test, $P = 0.0071$). In fact, the binding activity of APE with His-EpCAM was weaker than 2A9 at other concentrations used (20, 0.2, 0.02, and 0.002 μg/mL, data not shown). Flow cytometry analysis (Figure 5(b)) demonstrated that the immunotoxin could efficiently recognize the EpCAM molecule on HHCC cells, although the binding ability was lower than 2A9. The mean fluorescent intensity of 2A9 was 25.02 ± 3.23, while the immunotoxin intensity was 10.03 ± 3.07.

3.5. Cytotoxicity Assay of Immunotoxin. The immunotoxin could bind to EpCAM in carcinoma cells, but whether it was cytotoxic to cancer cells requires more study. Cytotoxicity of the immunotoxin to EpCAM-positive (HHCC, Colo205, SMMC-7721, and SKBr3) and EpCAM-negative (Sw480) cells was tested by MTT assay. Data show (Figure 6(a)) that APE and PE both inhibited HHCC cell viability and had no other effect on other cells' survival (data not shown). The IC_{50} of the immunotoxin to HHCC cells was 50 pM, and the control toxin exceeded 5,000 pM. This indicates that the immunotoxin can efficiently recognize certain cancer cells and has anticancer activity.

The mechanism of cytotoxicity was studied by immunofluorescence. After staining, the localization of the immunotoxin was observed by laser scanning confocal microscopy. Data show that (Figure 6(b)) after 6 h of incubation, the immunotoxin internalized to the HHCC cells and colocalized with CRT protein in the endoplasmic reticulum where it diffused uniformly in the endoplasmic reticulum after 24 h of incubation.

4. Discussion

The challenging problem in cancer therapy is drug resistance and relapse. Thus, the development of novel drugs that target the specific antigen of carcinomas is greatly needed. EpCAM was reported to participate in the development and

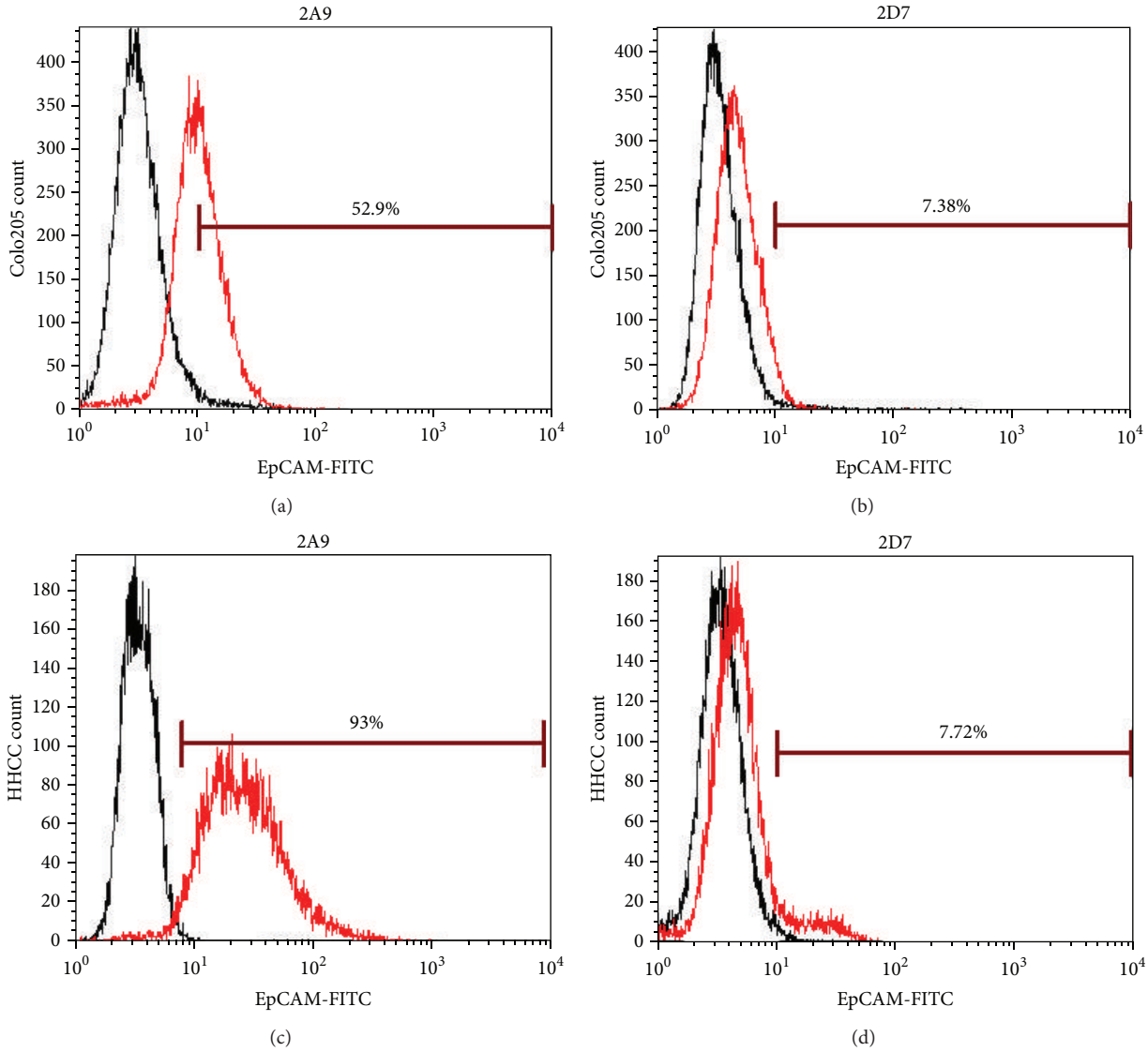

Figure 1: Binding ability of 2A9 and 2D7 to EpCAM was detected on Colo205 and HHCC cells by flow cytometry. Cells were incubated with biotin labeled EpCAM antibody (2A9 or 2D7, red histograms) or isotype control (black histograms) antibody (20 μg/mL) for 40 min at 4°C. Then cells were washed and stained with FITC-labeled secondary antibody and analyzed by flow cytometry.

progression of diverse carcinomas as well as serve as a marker of prognosis [21], which triggered the study of EpCAM-target immunotherapy. EpCAM-specific antibodies were designed and used to treat many cancers *in vitro* and *in vivo* [22, 23]. Several EpCAM-target antibodies have been used in the clinic to treat malignant ascites and squamous cell carcinomas of the head and neck [24, 25], as well. These results suggest that EpCAM-targeted immunotoxin might be used to treat cancers.

In the current study, we designed, produced, and characterized a recombinant immunotoxin APE, comprised of an EpCAM scFv and PE38KDEL. We prepared seven EpCAM monoclonal antibodies, and they were used to identify CD326 at the 8th International Conference on HLDA (Human Leucocyte Differentiation Antigens) [26]. The sequences encoding the light and heavy chain variable regions of four antibodies have been cloned and homology comparison and analysis of the nucleoside sequences of the four variable regions were performed using GenBank + EMBL + DDBJ + PDB databases. The DNASIS program was used to analyze the nucleotide sequence and deduce the amino acid sequence, which was "blasted" in nonredundant GenBank CDS translations + PDB + SwissProt + PIR + PRF protein databases. IMGT/V-QUEST was used to analyze the structure of variable region and determine the CDR region of the antibodies. Patents have been sought for these four sequences of variable regions (antibodies were FMU-EpCAM-2A9, FMU-EpCAM-2D7, FMU-EpCAM-4E4, and FMU-EpCAM-4F6). Our previous work indicated that all of the antibodies could be used to stain colon carcinoma tissues for immunohistochemistry [20], suggesting that they have the potential to become anticancer drugs. In this work,

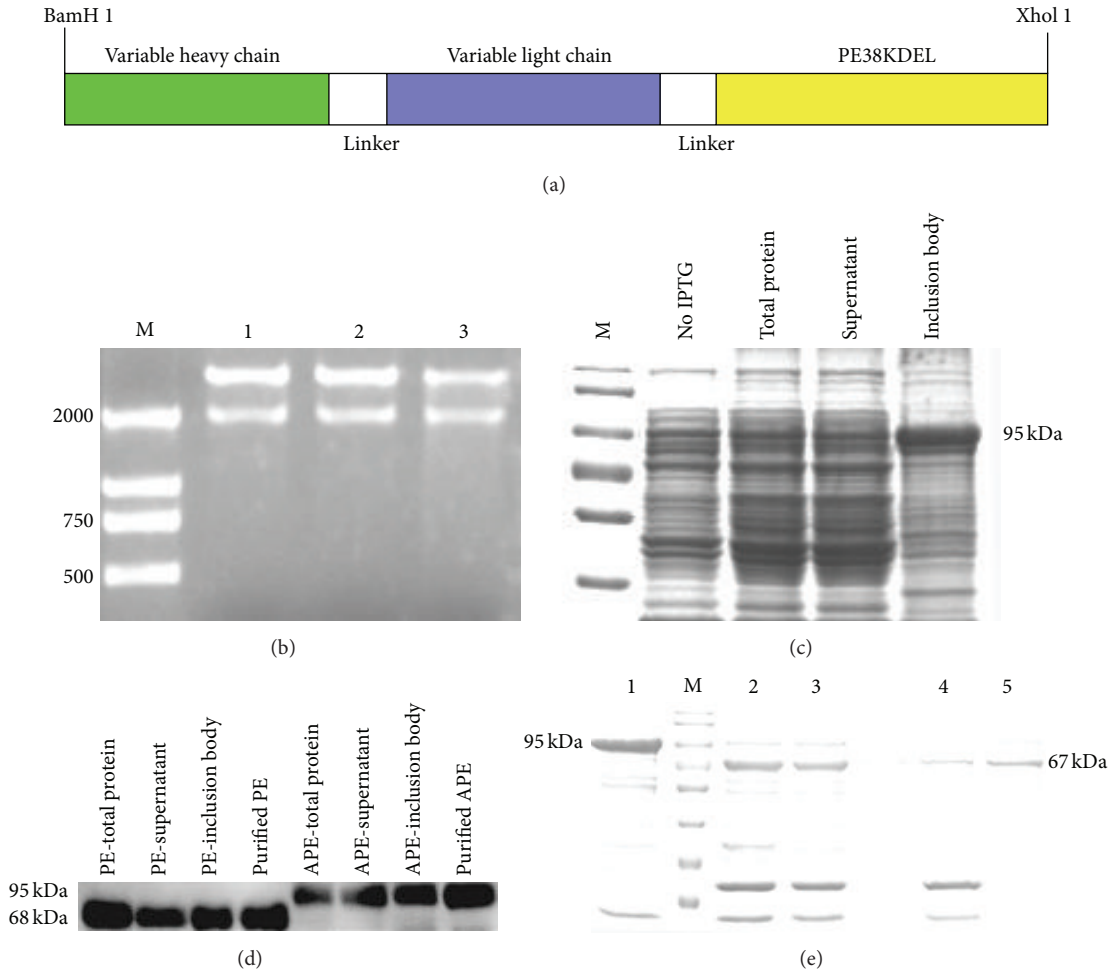

Figure 2: Construction, expression, and purification of immunotoxin. (a) Schematic representation of immunotoxin. (b) Restriction enzyme analysis of the expression plasmid (pGEX-4T1-scFv2A9-PE). Plasmids (lanes: 1–3) were digested with BamH-I and Xhol-I, and the 2,000 bp fragment was the recombinant immunotoxin. Lane: (M) LD2000 DNA ladder. (c) SDS-PAGE of recombinant protein. Protein from noninduced cells, IPTG induced cells, and supernatant and inclusion bodies were separated on 10% agarose gel and stained with Coomassie Brilliant Blue. Lane: (M) protein marker. (d) The recombinant protein was tested via Western blot. APE represents the immunotoxin; PE represents the empty control (pGEX-4T1-PE). (e) The purified recombinant protein was digested with thrombin. After removing the GST tag and thrombin, the immunotoxin was confirmed to be 67 kDa. Lanes: (1) purified APE protein; (M) protein marker; (2) APE after digestion with thrombin; (3) APE after digestion without thrombin; (4) APE without thrombin and GST protein; and (5) purified APE without the GST tag.

we used 2A9 and 2D7 as candidate antibodies to prepare scFv. FCM analysis showed that 2A9 had relatively higher binding ability to EpCAM on the surface of two EpCAM-positive cells. Similar results were observed in SMMC-7721 cells (data not shown). So we selected 2A9 as the parental antibody to construct scFv2A9. The constructed expression vector pGEX4T1-scFv2A9-PE was finally identified by DNA sequencing.

After purification and identification, we performed flow cytometry analysis and ELISA to measure immunotoxin activity. The original pGEX-4T3-EpCAM and the immunotoxin all have a GST tag and can be hardly distinguished by anti-GST antibody. To detect its antigen-binding activity, we expressed the recombinant protein HIS-EpCAM as an antigen. ELISA and flow cytometry analysis confirmed functionality, in which the APE can detect the EpCAM molecule as 2A9, though with relatively lower activity. This was consistent with flow cytometry results that 2A9 and APE can bind the natural EpCAM with different binding abilities. Characterization of the specificity and binding affinity of APE was also carried out with a competitive binding assay with the monoclonal 2A9 antibody and APE. To confirm that APE recognizes the same extracellular EpCAM epitope as the 2A9 mAb, APE was used to block the binding of the 2A9 monoclonal antibody. The results (data not shown) confirmed that APE could compete with 2A9 to certain extent, but incompletely. Previous studies demonstrated that high affinity anti-EpCAM antibodies could cause toxic effects (phase I trials) [27, 28], while antibodies with moderate affinity to EpCAM-positive cancers efficiently mediated both

GGATCC

GAGGTGAAGCTGCAGCAGTCAGGGACTGTGCTGGCAAGGCCTGGGACTTCCGTGAAGATGTCCTGCAGGGCTTCTGGCTACAGTTTTA

CCAGCTACTGGTTGCACTGGATAAAACAGAGGCCTGGACAGGGTCTAGAATGGGTTGGTGGTATCTATCCTGGAAATAGTGCTACTAGT

TACAAACAGAAGTTTAAGGACAAGGCCACACTGACTGCAGTCACATCCGCCAGTACTGCCTACATGGAACTCAGTAGCCTGACAAATGA

GGACTCTGCGGTCTATTACTGCATAAGAGGGGGGAACTACTGGGGCCAAGGGACCACGGTCACCGTCTCCTCA

GTCGAC

GGTGGTGGTGGTTCTGGTGGTGGTGGTTCTGGTGGTGGTGGTTCT

GATGTTGTGCTGACCCAGTCTCCACTCACTTTGTCGGTTACCATTGGACAACCAGCCTCCATCTCTTGCAAGTCAAGTCAGAGCCTCTTA

GATAGTGATGGAAAGACATATTTGAATTGGTTGTTCCAGAGGCCAGGCCAGTCTCCAAAGCGCCTGATCTATGTGGTGTCTAAACTGGA

CTCTGGAGTCCCTGACAGGTTCACTGGCAGTGGATCAGGGACAGATTTCACACTGAAAATCAGTAGAGTGGAGGCTGAGGATTTGGGAG

TTTATTATTGCTGGCAAGGTACACACTTTCCGTGGACGTTCGGTGGAGGGACCAAGCTGGAGATC

GAATTC

GGTGGTGGTGGTTCTGGTGGTGGTGGTTCTGGTGGTGGTGGTTCT

GCGGCCGCTTCTGGAGGTCCTGAGGGCGGCAGCCTGGCCGCGCTGACCGCGCATCAGGCCTGCCATCTGCCGCTGGAGACTTTCACCCGT

CATCGCCAGCCGCGCGGCTGGGAACAACTGGAGCAGTGCGGCTATCCGGTGCAGCGTCTGGTCGCCCTTTACCTGGCGGCGCGTCTGTCAT

GGAACCAGGTCGACCAGGTGATCCGCAACGCACTGGCAAGCCCTGGCAGCGGCGGCGACCTGGGCGAAGCGATCCGCGAGCAGCCGGAG

CAGGCACGTCTGGCACTGACCCTGGCAGCAGCAGAGAGCGAGCGCTTCGTCCGTCAGGGCACCGGCAACGACGAGGCAGGCGCGGCAAA

CGGCCCGGCGGACAGCGGCGACGCCCTGCTGGAGCGCAACTATCCTACTGGCGCGGAGTTCCTTGGCGACGGCGGCGACGTCAGCTTCAG

CACCCGCGGCACGCAGAACTGGACGGTGGAGCGTCTGCTTCAGGCGCATCGCCAACTGGAGGAGCGCGGCTATGTGTTCGTCGGCTACCA

TGGCACCTTCCTTGAAGCGGCGCAAAGCATCGTCTTCGGCGGGGTGCGCGCGCGCAGCCAGGACCTTGACGCGATCTGGCGCGGTTTCTAT

ATCGCCGGCGATCCGGCGCTGGCCTACGCCTACGCCCAGGACCAGGAACCTGACGCACGCGGCCGTATCCGCAACGGTGCCCTGCTGCGTG

TCTATGTGCCGCGCTCAAGCCTGCCGGGCTTCTACCGCACCAGCCTGACCCTGGCCGCGCCGGAGGCGGCGGGCGAGGTCGAACGTCTGATC

GGCCATCCGCTGCCGCTGCGCCTGGACGCCATCACCGGCCCTGAGGAGGAAGGCGGGCGCCTGGAGACCATTCTTGGCTGGCCGCTGGCCGA

GCGCACCGTGGTGATTCCTTCAGCGATCCCTACCGACCCGCGCAACGTCGGCGGCGACCTTGACCCGTCTAGCATCCCTGACAAGGAACAGG

CGATCAGCGCCCTGCCGGACTACGCCAGCCAGCCTGGCAAACCGCCGAAAGACGAACTGCAG

Figure 3: Sequence of immunotoxin. Black bold basic group represents restriction enzyme recognition site; red bold basic group represents the linker sequence.

antibody-dependent cellular cytotoxicity and complement-mediated cytotoxicity [29–31]. We must characterize the anticancer activity of the immunotoxin.

The immunotoxin can recognize EpCAM, and whether it is cytotoxic to EpCAM-positive tumor cells must be confirmed. MTT assay demonstrated that APE induced a 50% reduction of viability (IC_{50}) of HHCC cells at a concentration of 50 pM, compared to control PE (>5000 pM). These compounds did not affect other cancer cells. Previous work suggested that immunotoxin cytotoxicity was related to its cellular internalization [32]. The immunotoxin has a C-terminal KDEL motif, which can localize it to the endoplasmic reticulum [33]. We observed this localization in HHCC cells by immunofluorescence and this suggested that the immunotoxin might internalize to cells and transport to the endoplasmic reticulum to exert its function. This finding was consistent with a study on KDEL receptor [34]. In addition, the internalization of the immunotoxin to Colo205 was also observed by immunofluorescence, and the immunotoxin was not detectable in cells after 24 h of incubation (data not shown).

The recombinant protein was expressed in *E. coli* cells as soluble form and as an inclusion body form (mainly). The soluble form of the protein maintained the natural structure and function and it could be used for function analysis [35]. We purified the soluble protein from 4 L bacteria and 2 mg of purified APE was collected, a yield somewhat lower than previous reports [36, 37]. Because the inclusion body was the main form of the immunotoxin, in follow-up work, we will purify the protein from inclusion bodies [38].

Immunotoxin, comprised of scFv and toxin, has many advantages compared with other therapeutics, such as small molecular weight, fewer side effects, a simple preparation method, and low production cost. If the scFv used to construct an immunotoxin can be fully humanized, the therapeutic potential of the immunotoxin will be powerful.

In conclusion, we have successfully developed an immunotoxin made of a single-chain variable fragment (scFv), derived from EpCAM monoclonal antibody FMU-EpCAM-2A9 and PE38KDEL. Its antigen-binding ability and cytotoxicity have been confirmed *in vitro*. Future work will include optimization of protein production, further development and

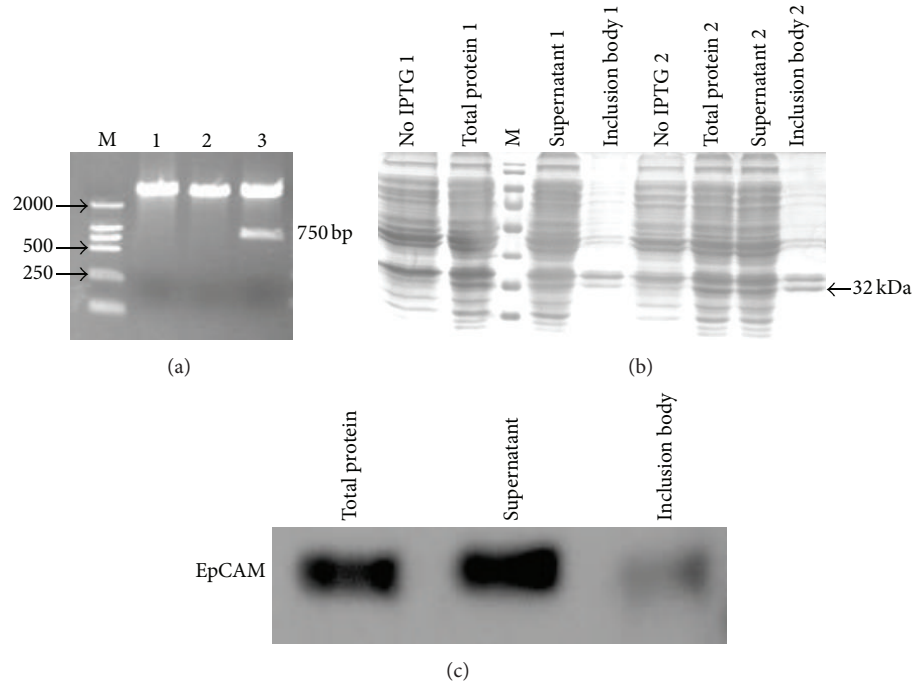

Figure 4: Restriction enzyme analysis, SDS-PAGE, and Western blot of recombinant EpCAM expressed in M15 *E. coli* cells. (a) The plasmid pQE30-EpCAM was digested with Kpn I and Hind III. Lanes: (M) LD2000 DNA marker; (1–3) digestion products 1 and 2 were negative colonies; 3 was the positive colony. (b) Proteins were separated by 10% SDS-PAGE and visualized by Coomassie Brilliant Blue R250 staining. Two colonies were induced to express protein. (c) Purified HIS-EpCAM was identified by Western blot.

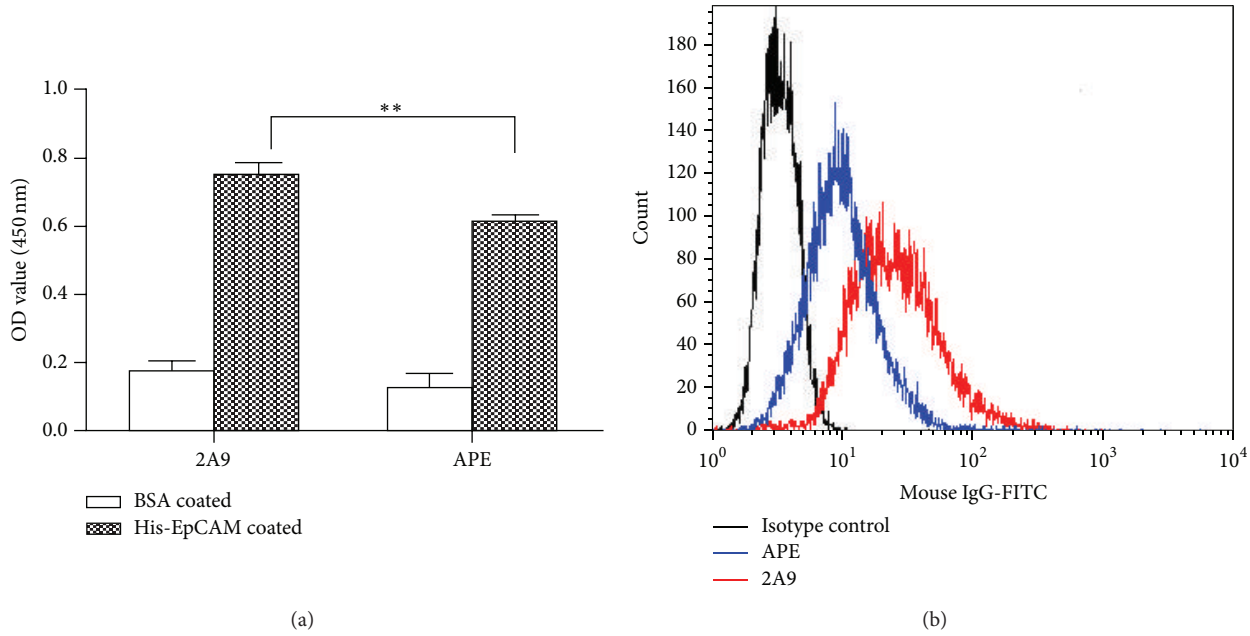

Figure 5: Binding ability of immunotoxin to recombinant His-EpCAM and natural EpCAM. (a) Recombinant HIS-EpCAM protein was coated on 96-well plates (5 μg/mL). The binding of the immunotoxin to His-EpCAM was detected by ELISA. The P value was analyzed by an unpaired Student's t-test. $^{**}P$ value was less than 0.05. (b) HHCC cells were collected and stained with primary antibody (biotin labeled immunotoxin, biotin labeled 2A9, or biotin labeled isotype control antibody) at a concentration of 5 μg/mL and FITC labeled avidin (1 : 50) as the secondary antibody. Fluorescence was detected by BD FACS Calibur. The mean fluorescent intensity was measured by FlowJo software.

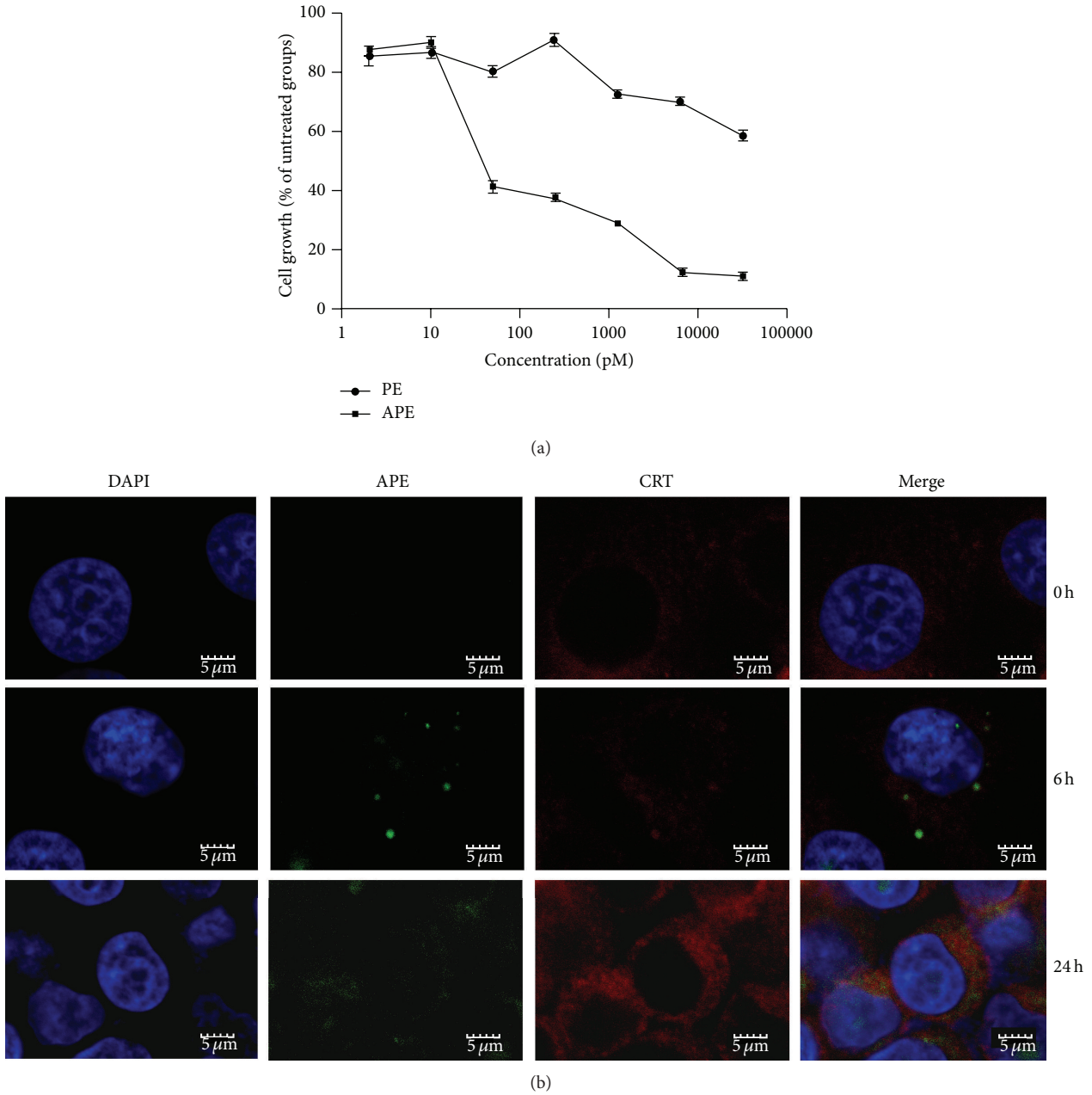

Figure 6: Cytotoxicity and localization of the immunotoxin. (a) HHCC cells were incubated with different concentrations (0.002, 0.01, 0.05, 0.25, 1.25, 6.5, and 32.5 nM) of the immunotoxin for 72 h, and cell growth was measured by MTT assay. (b) The localization of the immunotoxin was observed by laser scanning confocal microscopy at different incubation times (0, 6, and 24 h). DAPI indicates the cell nucleus; APE represents the immunotoxin; CRT is the calprotectin. All data are expressed as means ± standard deviations (SD).

testing of immunotoxin-based targeted therapies in animal models, and modification of the immunotoxin to decrease immunogenicity and toxicity.

Ethical Approval

The research was approved by Ethical Standards Committee of Xijing Hospital.

Conflict of Interests

The authors have no conflict of interests.

Authors' Contribution

Xiaokun Qi, Jun Wan, Kun Yang, and Kui Zhang contributed equally to this work. Minghua Lv, Feng Qiu, and Tingting Li are joint first authors.

Acknowledgments

This study was supported by Grants from the National Natural Science Foundation of China (no. 81401338), Natural Scientific Foundation of Beijing (Grant no. 7142148), and Capital Foundation for Medical Development and Research (Grant no. 2009-2054).

References

[1] J. G. Jurcic, D. A. Scheinberg, and A. N. Houghton, "Monoclonal antibody therapy of cancer.," *Cancer chemotherapy and biological response modifiers*, vol. 15, pp. 152–175, 1994.

[2] G. A. Leget and M. S. Czuczman, "Use of rituximab, the new FDA-approved antibody," *Current Opinion in Oncology*, vol. 10, no. 6, pp. 548–551, 1998.

[3] T. Yamaguchi and T. Takahashi, "Application of monoclonal antibody for cancer therapy," *Gan to Kagaku Ryoho*, vol. 21, no. 2, pp. 157–162, 1994.

[4] B. E. Bejcek, D. Wang, E. Berven et al., "Development and characterization of three recombinant single chain antibody fragments (scFvs) directed against the CD19 antigen," *Cancer Research*, vol. 55, no. 11, pp. 2346–2351, 1995.

[5] D. Flieger, P. Kufer, I. Beier, T. Sauerbruch, and I. G. H. Schmidt-Wolf, "A bispecific single-chain antibody directed against EpCAM/CD3 in combination with the cytokines interferon α and interleukin-2 efficiently retargets T and CD3+CD56+ natural-killer-like T lymphocytes to EpCAM-expressing tumor cells," *Cancer Immunology Immunotherapy*, vol. 49, no. 8, pp. 441–448, 2000.

[6] A. S. Wayne, R. J. Kreitman, H. W. Findley et al., "Anti-CD22 immunotoxin RFB4(dsFv)-PE38 (BL22) for CD22-positive hematologic malignancies of childhood: preclinical studies and phase I clinical trial," *Clinical Cancer Research*, vol. 16, no. 6, pp. 1894–1903, 2010.

[7] R. J. Kreitman, M. S. Tallman, T. Robak et al., "Phase I trial of anti-CD22 recombinant immunotoxin moxetumomab pasudotox (CAT-8015 or HA22) in patients with hairy cell leukemia," *Journal of Clinical Oncology*, vol. 30, no. 15, pp. 1822–1828, 2012.

[8] P. Piascik, "FDA approves fusion protein for treatment of lymphoma," *Journal of the American Pharmaceutical Association*, vol. 39, no. 4, pp. 571–572, 1999.

[9] U. Schnell, V. Cirulli, and B. N. G. Giepmans, "EpCAM: structure and function in health and disease," *Biochimica et Biophysica Acta*, vol. 1828, no. 8, pp. 1989–2001, 2013.

[10] P. A. Baeuerle and O. Gires, "EpCAM (CD326) finding its role in cancer," *British Journal of Cancer*, vol. 96, no. 3, pp. 417–423, 2007.

[11] P. Went, M. Vasei, L. Bubendorf et al., "Frequent high-level expression of the immunotherapeutic target Ep-CAM in colon, stomach, prostate and lung cancers," *British Journal of Cancer*, vol. 94, no. 1, pp. 128–135, 2006.

[12] G. Riethmüller, E. Holz, G. Schlimok et al., "Monoclonal antibody therapy for resected Dukes' C colerectal cancer: seven-year outcome of a multicenter randomized trial," *Journal of Clinical Oncology*, vol. 16, no. 5, pp. 1788–1794, 1998.

[13] E. M. Kirchner, R. Gerhards, and R. Voigtmann, "Sequential immunochemotherapy and edrecolomab in the adjuvant therapy of breast cancer: Reduction of 17-1A-positive disseminated tumour cells," *Annals of Oncology*, vol. 13, no. 7, pp. 1044–1048, 2002.

[14] M. Mack, G. Riethmuller, and P. Kufer, "A small bispecific antibody construct expressed as a functional single-chain molecule with high tumor cell cytotoxicity," *Proceedings of the National Academy of Sciences of the United States of America*, vol. 92, no. 15, pp. 7021–7025, 1995.

[15] A. Burges, P. Wimberger, C. Kümper et al., "Effective relief of malignant ascites in patients with advanced ovarian cancer by a trifunctional anti-EpCAM x anti-CD3 antibody: a phase I/II study," *Clinical Cancer Research*, vol. 13, no. 13, pp. 3899–3905, 2007.

[16] D. A. Vallera, B. Zhang, M. K. Gleason et al., "Heterodimeric bispecific single-chain variable-fragment antibodies against EpCAM and CD16 induce effective antibody-dependent cellular cytotoxicity against human carcinoma cells," *Cancer Biotherapy & Radiopharmaceuticals*, vol. 28, no. 4, pp. 274–282, 2013.

[17] N. Shirasu, H. Yamada, H. Shibaguchi, and M. Kuroki, "Molecular characterization of a fully human chimeric T-cell antigen receptor for tumor-associated antigen EpCAM," *Journal of Biomedicine and Biotechnology*, vol. 2012, Article ID 853879, 7 pages, 2012.

[18] C. Di Paolo, J. Willuda, S. Kubetzko et al., "A recombinant immunotoxin derived from a humanized epithelial cell adhesion molecule-specific single-chain antibody fragment has potent and selective antitumor activity," *Clinical Cancer Research*, vol. 9, no. 7, pp. 2837–2848, 2003.

[19] M. Simon, N. Stefan, L. Borsig, A. Pleuckthun, and U. Zangemeister-Wittke, "Increasing the antitumor effect of an EpCAM-targeting fusion toxin by facile click PEgylation," *Molecular Cancer Therapeutics*, vol. 13, no. 2, pp. 375–385, 2014.

[20] X. Xie, C. Y. Wang, Y. X. Cao et al., "Expression pattern of epithelial cell adhesion molecule on normal and malignant colon tissues," *World Journal of Gastroenterology*, vol. 11, no. 3, pp. 344–347, 2005.

[21] P. A. Baeuerle and O. Gires, "EpCAM (CD326) finding its role in cancer," *British Journal of Cancer*, vol. 96, no. 3, pp. 417–423, 2007.

[22] D. Seimetz, H. Lindhofer, and C. Bokemeyer, "Development and approval of the trifunctional antibody catumaxomab (anti-EpCAM×anti-CD3) as a targeted cancer immunotherapy," *Cancer Treatment Reviews*, vol. 36, no. 6, pp. 458–467, 2010.

[23] K. Ogawa, S. Tanaka, S. Matsumura et al., "EpCAM-targeted therapy for human hepatocellular carcinoma," *Annals of Surgical Oncology*, vol. 21, no. 4, pp. 1314–1322, 2014.

[24] C. Bokemeyer, "Catumaxomab trifunctional anti-EpCAM antibody used to treat malignant ascites," *Expert Opinion on Biological Therapy*, vol. 10, no. 8, pp. 1259–1269, 2010.

[25] A. Premsukh, J. M. Lavoie, J. Cizeau, J. Entwistle, and G. C. MacDonald, "Development of a GMP Phase III purification process for VB4-845, an immunotoxin expressed in *E. coli* using high cell density fermentation," *Protein Expression and Purification*, vol. 78, no. 1, pp. 27–37, 2011.

[26] H. Zola and B. Swart, "The human leucocyte differentiation antigens (HLDA) workshops: the evolving role of antibodies in research, diagnosis and therapy," *Cell Research*, vol. 15, no. 9, pp. 691–694, 2005.

[27] J. Posey, M. Khazaeli, and M. Saleh, "Phase I trial testing multiple doses of humanized monoclonal antibody (Mab) 3622W94," *ASCO Annual Meeting*, vol. 17, p. 436, 1998.

[28] J. S. de Bono, A. W. Tolcher, A. Forero et al., "ING-1, a monoclonal antibody targeting Ep-CAM in patients with advanced adenocarcinomas," *Clinical Cancer Research*, vol. 10, no. 22, pp. 7555–7565, 2004.

[29] S. Naundorf, S. Preithner, P. Mayer et al., "*In vitro* and *in vivo* activity of MT201, a fully human monoclonal antibody for pancarcinoma treatment," *International Journal of Cancer*, vol. 100, no. 1, pp. 101–110, 2002.

[30] W. Xiang, P. Wimberger, T. Dreier et al., "Cytotoxic activity of novel human monoclonal antibody MT201 against primary ovarian tumor cells," *Journal of Cancer Research and Clinical Oncology*, vol. 129, no. 6, pp. 341–348, 2003.

[31] N. Prang, S. Preithner, K. Brischwein et al., "Cellular and complement-dependent cytotoxicity of Ep-CAM-specific monoclonal antibody MT201 against breast cancer cell lines," *British Journal of Cancer*, vol. 92, no. 2, pp. 342–349, 2005.

[32] U. C. Wargalla and R. A. Reisfeld, "Rate of internalization of an immunotoxin correlates with cytotoxic activity against human tumor cells," *Proceedings of the National Academy of Sciences of the United States of America*, vol. 86, no. 13, pp. 5146–5150, 1989.

[33] K. Yamamoto, H. Hamada, H. Shinkai, Y. Kohno, H. Koseki, and T. Aoe, "The KDEL receptor modulates the endoplasmic reticulum stress response through mitogen-activated protein kinase signaling cascades," *Journal of Biological Chemistry*, vol. 278, no. 36, pp. 34525–34532, 2003.

[34] M. Capitani and M. Sallese, "The KDEL receptor: new functions for an old protein," *FEBS Letters*, vol. 583, no. 23, pp. 3863–3871, 2009.

[35] S. Song, J. Xue, K. Fan et al., "Preparation and characterization of fusion protein truncated *Pseudomonas* Exotoxin A (PE38KDEL) in *Escherichia coli*," *Protein Expression and Purification*, vol. 44, no. 1, pp. 52–57, 2005.

[36] L. M. Thomas, P. J. Huntington, L. J. Mead, D. L. Wingate, B. A. Rogerson, and A. M. Lew, "A soluble recombinant fusion protein of the transmembrane envelop protein of equine infectious anaemia virus for ELISA," *Veterinary Microbiology*, vol. 31, no. 2-3, pp. 127–137, 1992.

[37] Y.-Q. Luo, L.-H. Wang, Q. Yi, and B.-H. Jiao, "Expression of soluble, biologically active recombinant human tumstatin in *Escherichia coli*," *Clinical and Experimental Medicine*, vol. 8, no. 1, pp. 37–42, 2008.

[38] H. Wang, J. Dai, B. Li et al., "Expression, purification, and characterization of an immunotoxin containing a humanized anti-CD25 single-chain fragment variable antibody fused to a modified truncated *Pseudomonas* exotoxin A," *Protein Expression and Purification*, vol. 58, no. 1, pp. 140–147, 2008.